The Dissertation Committee for Omkar Ashok Namjoshi Certifies that this is the approved version of the following dissertation:

Thermal Degradation of PZ-Promoted Tertiary Amines for CO$_2$ Capture

Committee:

Gary Rochelle, Supervisor

Lydia Contreras

J. Tim Cullinane

Danny Reible

C. Grant Willson

Thermal Degradation of PZ-Promoted Tertiary Amines for CO$_2$ Capture

by

Omkar Ashok Namjoshi, B.S.ChE.

Dissertation

Presented to the Faculty of the Graduate School of

The University of Texas at Austin

in Partial Fulfillment

of the Requirements

for the Degree of

Doctor of Philosophy

The University of Texas at Austin

May 2015

Dedication

To the Giants whose shoulders I have stood on

And to the Giants who stand on mine

Acknowledgements

I would like to thank my research advisor, Gary Rochelle, for his mentorship, encouragement, and patience throughout my tenure at UT-Austin. GTR, as he is also known, always has his door open, always made time to answer all of my questions, and taught me at least one new thing during each of our weekly meetings. His demeanor, humility, sense of values, and approach to solving research problems helped smooth the transition from the "real world" to the "ivory tower." With the benefit of hindsight, I'd gladly choose him again as an advisor if I were to restart the graduate program. I also would like to thank Lydia Contreras, Tim Cullinane, Danny Reible, and Grant Willson for serving on my supervising committee and for their feedback on this project.

I'd like to thank everyone in our research group who was a member during my time at UT. It has been a privilege learning from and with you during our discussions inside and outside of lab, joint projects, and your presentations during our weekly group meetings. Former group members include Stephanie Freeman, Fred Closmann, Humera Rafique, David Van Wagener, Xi Chen, Qing Xu, Jorge Plaza, Mandana Ashouripashaki, Stuart Cohen, Alex Voice, Thu Nguyen, Tarun Madan, and Peter Frailie. Current group members and recent graduates include Chao Wang, Lynn Li, Steven Fulk, Nathan Fine, Darshan Sachde, Brent Sherman, Yang Du, Paul Nielsen, Matt Walters, Di Song, Yu-Jeng Lin, Yue Zhang, Junyuan Ding, Kent Fischer, Matt Beaudry, and Ye Yuan.

A special thank you goes to Michael Baldea, Bruce Eldridge, Nico de Munck, Richard Trepagnier, and Brian Roberts – faculty from UT-Austin and colleagues from ExxonMobil – who all answered technical questions I had and also gave me objective feedback regarding my research. I greatly appreciate the time you took from your busy

schedules to see "alpha" versions of my analysis in PowerPoint form, read draft copies of my preliminary, or discuss experimental plans, procedures, and observations.

A very special thank you goes to my undergraduate research assistants Mark Goldman, Hanbi Liu, and Daniel Hatchell. Without your support, I probably would've taken six years to graduate with only half as much data to present and none of my sanity intact. I'm extremely proud of and humbled by your accomplishments in the lab, and I'm confident you'll find success in the future no matter where this game of life takes you.

A big thank you goes to Maeve Cooney for your help with scheduling, travel and conference planning, and most importantly, for editing our research bulletins and manuscripts. Although you might disagree, I think I've become a (somewhat) better technical writer thanks to your feedback. I also wish to thank other staff members for their help with administrative matters concerning graduate school, purchasing, computer and equipment support, and lab safety: T Stockman, Kate Baird, Eddie Ibarra, Tammie McDade, Teri Sahba, Randy Rife, Jason Barborka, Patrick Danielewski, Kevin Haynes, Jim Smitherman, Butch Cunningham, and Shak McDonald.

Last, but not least, a huge thank you goes to my friends, coworkers, and especially my family for your incredible unconditional moral and emotional support throughout this journey; to Bee Yap, for "encouraging" me to pursue an educational leave of absence; and to John Kovich, for convincing the powers-that-be to make that leave happen. I didn't have the guts to leave a good career at the peak of the economic crisis to earn a research degree, but you made it possible for me to follow my dreams without having to make significant sacrifices. I hope I've made you proud.

Thermal Degradation of PZ-Promoted Tertiary Amines for CO_2 Capture

Omkar Ashok Namjoshi, Ph.D.

The University of Texas at Austin, 2015

Supervisor: Gary Rochelle

The thermal degradation of piperazine (PZ)-promoted tertiary amine solvents for CO_2-capture has been investigated and quantified in this study, which takes place in the high temperature (>100 °C) section of the capture plant. PZ-promoted tertiary amine solvents possess comparable energy performance to concentrated PZ, considered a benchmark solvent for CO_2 capture from flue gas without its solid solubility limits that hinder operational performance.

PZ-promoted aliphatic tertiary amine solvents with at least one methyl group, such as methyldiethanolamine (MDEA), were found to be the least stable solvents and can be regenerated in the desorber between 120 and 130 °C. PZ-promoted tertiary amine solvents with no methyl groups, such as ethyldiethanolamine (EDEA), were found to have an intermediate stability and can be regenerated in the desorber between 130 and 140 °C. PZ-promoted tertiary morpholines, such as hydroxyethylmorpholine (HEM), were found to be stable above 150 °C. Tertiary amines with at least one hydroxyethyl or hydroxyisopropyl functional group form intermediate byproducts that can accelerate the degradation rate of the promoter by a factor from 1.5 to 2.3. Tertiary amines with 3-carbon and 5-carbon functional groups, such as dimethylaminopropanol or

dimethylaminoethoxyethanol, form stable intermediate byproducts that do not readily react with the promoter.

A degradation model for PZ-promoted MDEA that can be used for process design calculations using acidified solvent degradation to model the initial degradation rate over a range of CO_2 loading and initial amine concentration was developed. Thermal degradation was modeled using second-order kinetics as a function of free amine and protonated amine. The degradation kinetics, along with the observed degradation products, suggest that the dominant pathway is by free PZ attack on a methyl substituent group of protonated MDEA to form diethanolamine (DEA) and 1-methylpiperazine (1-MPZ). The model predicts total amine loss from experimental CO_2 degradation rate measurements within 20%. The modeling work was extended to other PZ-promoted tertiary amine solvents with bulkier substituent groups. PZ attack on ethyl or hydroxyethyl groups was 17% and 4% as fast, respectively, as attack on methyl groups.

Table of Contents

List of Tables

xviii

List of Figures

xxvi

xxxii

Chapter 1: Introduction

1.1   MOTIVATION FOR IMPLEMENTING CO_2 CAPTURE

Concerns about the effects of climate change have spurred several industrialized countries to propose regulatory frameworks to manage CO_2 emissions from industrial sources and power plants. In 2012, 32% of all CO_2 emitted in the United States was from power plants and 20% from industrial sources (EPA 2014).

In 2007, the United States Supreme Court ruled that CO_2 can be considered to be a pollutant under the Clean Air Act, giving the executive branch of the U.S. government the authority to regulate CO_2 emissions without requiring authorization from Congress (Talley 2009). The U.S. Environmental Protection Agency is planning to issue rules regulating the amount of CO_2 emissions per megawatt of electricity generated for new and existing power plant facilities in 2015, and it is likely that similar rules affecting other industrial facilities will be enacted in the near future (EPA 2015). Other industrialized countries and states have launched cap-and-trade programs that place a hard limit on the total amount of CO_2 emissions per year (Lazo 2014).

About 67% of all electrical generating capacity in the U.S. is sourced from fossil fuels (EIA 2015). Analysts from the International Energy Agency and the Energy Information Administration have predicted that fossil energy resources will remain the dominant source of energy until the 2030's (IEA 2010). Alternatives to fossil energy, such as solar and wind energy, cannot provide continuous sources of energy unless coupled to energy storage mechanisms (The Economist 2012). Second-generation carbon-neutral biofuels that do not compete with food production have yet to be developed (Inderwildi 2009). Carbon capture and storage thus offers one means to use

1

existing fossil energy resources and infrastructure while reducing CO_2 emissions. On a high level, the capture process captures the CO_2 from a gas source, such as the flue gas from power plants, compresses the CO_2, and sequesters it into a geological formation or depleted oil and gas reservoir where it is trapped.

In the absence of a regulatory framework, captured CO_2 from point sources can be injected into unproductive oil and gas fields, displacing trapped hydrocarbons and boosting oil and gas production. This process is called Enhanced Oil Recovery, or EOR (Herzog 2004). About 25 billion kg of CO_2 was sequestered in 2014 for use in EOR, with about 95% of the CO_2 sourced from natural gas or synthesis gas processing facilities (Global CCS Institute 2014). The first major post-combustion capture plant, located in Canada, started operations in October 2014. The plant is designed to capture 1 billion kg of CO_2 annually from a 120 MWe coal-fired power unit operated by SaskPower for EOR (Saskpower 2015). In 2014, construction work commenced on a CO_2-capture unit on a 240 MWe coal-fired power unit operated by NRG Energy in Thompsons, Texas to inject 2 billion kg of CO_2 annually in a depleted oil reservoir to extract 15,000 barrels of oil/day (NRG Energy 2014). The total investment cost for each plant was about $1 billion (Fountain 2014, Smith 2014).

1.2 AMINE-BASED SCRUBBING

Aqueous amine solvents were first proposed for use in the early 1930's to selectively remove H_2S, CO_2, COS, and other acidic gases from gas streams (Bottoms 1933). An aqueous ethanolamine mixture consisting of triethanolamine with small amounts of diethanolamine and monoethanolamine was used as the amine solvent in these early processes. Processes using amine-based treating methods remain the

dominant technology to remove acid gas from untreated natural gas (Kohl 1960, White 2010).

This process concept can be applied to remove CO_2 from flue gas, such as the exhaust gas from power plants. Compared to alternative technologies, such as oxycombustion, physical adsorption, and membrane separation, amine scrubbing for flue gas CO_2 capture is considered to be the furthest along in development and energy efficiency (Rochelle 2009, Rochelle 2012) and can be retrofitted to existing power plants. The energy required to run a CO_2 capture facility can represent anywhere from 20 to 30% of the power plant output (Cohen 2012), and implementing amine scrubbing processes on existing fossil-fueled facilities is expected to double the absolute price of electricity (Fisher 2007). If capital costs, fuel costs, and other operating costs are considered, natural gas-fueled power plants with carbon capture are cheaper than solar power plants and offshore wind power plants and are competitive with conventional wind power plants (EIA 2013).

Amines, being bases, can react reversibly and exothermically with acidic gases and bind them to solution. The acidic gas can be desorbed from the solution with the application of heat. At low temperature and high acid gas partial pressure, the equilibrium favors the amine-acid gas complex, and at high temperature and low acid gas partial pressure the equilibrium favors free amine and unbound acid gas. These phenomena are identical to the phenomena observed in gas absorption and stripping without reaction. A detailed description of amine-based absorption chemistry is presented in Section 2.2.

Figure 1.1 shows a simplified flowsheet of a typical amine-scrubbing process for CO_2 capture from flue gas. The feed gas is fed at the bottom of the absorber, where it contacts and reversibly reacts with the amine solution circulating in the absorber; most

3

absorbers are designed to capture 90% of the CO_2 in the feed gas. The scrubbed gas from the absorber is fed to a water wash column to remove traces of volatile amine before being discharged to the atmosphere. The CO_2-rich amine solution exiting from the absorber is heated and then fed to a reboiled stripping column or a series of heated flash vessels to desorb the CO_2 from the amine, regenerating the amine and generating a high-purity CO_2 stream. The regenerated CO_2-lean amine is recycled back to the absorber and a cross exchanger is used to cool the regenerated amine by heating the CO_2-rich amine. Reclaimer units are sometimes added downstream of the reboiler to remove degradation products from the amine solvent; the flow through the reclaimer is a small fraction of the total amine solvent circulation rate (Kohl 1960). The high-purity CO_2 stream is then compressed to about 150 bar (Rochelle 2009) and sequestered or used for EOR.

The process flowsheet for CO_2 and H_2S removal from natural gas and synthesis gas is not significantly different from flue-gas removal. The absorption column typically operates at much higher pressure and in an anerobic environment, and the amount of acid gas removal is generally set by downstream processing requirements. The H_2S might have to be separated from the CO_2 in the gas steam from the amine stripper depending on the disposal location.
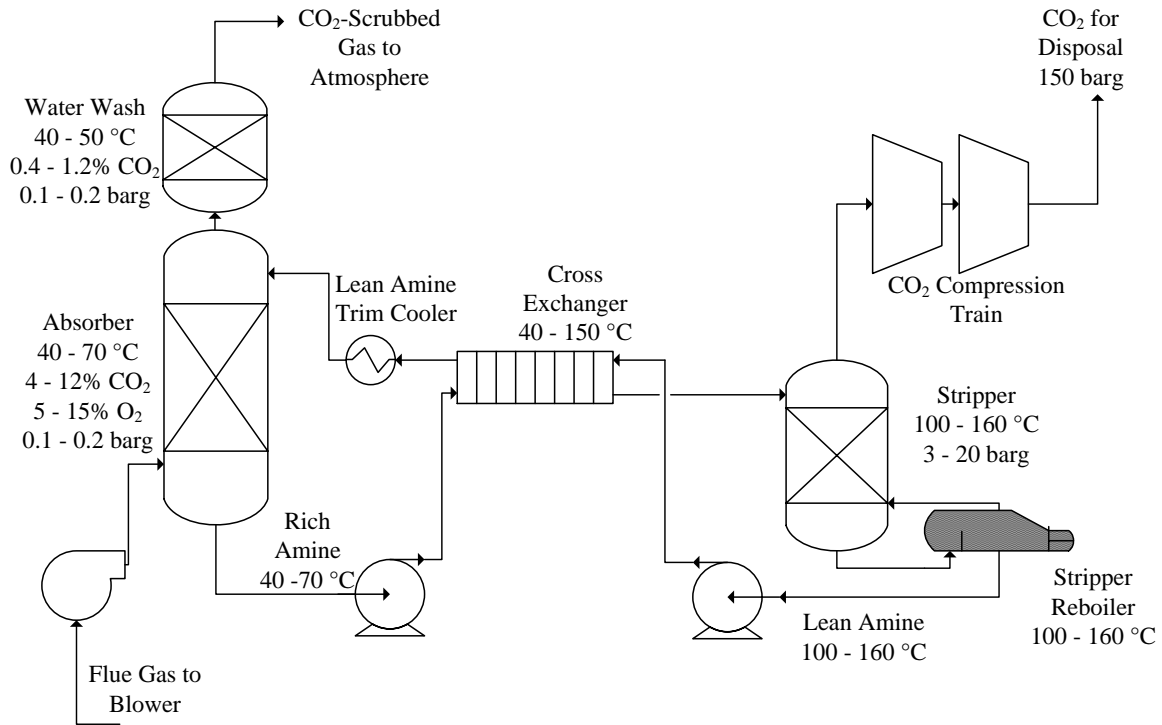
Figure 1.1: Process flow diagram of CO$_2$ Capture from flue gas with major unit operations and relevant process conditions shown

Regardless of application, amine solvents must have good cyclic acid gas capacity, a fast absorption rate, low volatility, resistance to thermal degradation, and resistance to reaction and interaction with other compounds in the feed gas, such as SO$_X$ and NO$_X$. Solvents used in aerobic service, such as CO$_2$-capture from flue gas, should also be resistant to oxidation and have extremely low volatility due to the intrinsically low absorber pressure, which typically is around $0.1 - 0.2$ bar gauge.

1.3   ROLE OF THERMAL DEGRADATION AND RESEARCH CONTEXT

Thermal degradation is considered to be the "greatest contributor to solvent loss" (Kohl 1960) in natural gas treating and synthesis gas treating applications. It is a secondary contributor to amine loss in flue-gas capture applications and is estimated to represent between 20 and 30% of the total amine loss in applications capturing CO$_2$ from

coal-fired applications. Oxidative degradation is the dominant mechanism of solvent degradation in flue-gas capture applications (IEAGHG 2014). In all applications, thermal degradation sets the maximum regeneration temperature of the solvent and can affect the process design of the stripper reboiler to minimize the temperature delta between the reboiler skin and the bulk amine solution circulating in the reboiler (Dutchover 2005).

Van Wagener (2011) simulated regenerating the amine solvent at higher temperature in capture applications from coal-derived flue gas with CO_2 compression to 150 bar. These results indicated that the net equivalent work of separating and compressing CO_2 is reduced due to an increase in the stripping pressure. The reduction in compressor work is sufficient to offset an increase in the reboiler duty and can potentially decrease the size and the number of stages of the CO_2 compressor, reducing capital costs. Increasing the regeneration temperature from 100 to 120 °C of 35 wt% monoethanolamine (MEA), a first-generation solvent proposed for use in CO_2 capture, can reduce the equivalent work by up to 6%. Increasing the temperature of 40 wt% piperazine (PZ) from 120 to 150 °C, a second-generation solvent proposed for CO_2 capture, can reduce the equivalent work of the process anywhere from 2% to 8% depending on the complexity of the stripper configuration. Pilot data showed that 40 wt% PZ had a 10% lower energy requirement when regenerated at 155 °C than 125 °C (Cousins 2014).

Fine (2013) and Rochelle (2013) reported that a stripper regeneration temperature of 150 °C or greater can destroy nitrosamines and nitramines, carcinogenic byproducts formed from the reaction of NO_X from flue gas or produced as an oxidation byproduct with secondary or primary amine, respectively, in the circulating solvent. The presence of nitrosamine in the solvent "can represent a risk of contaminating airsheds and drinking water supplies (Wagner 2014)."

Previous work on the thermal degradation of MEA (Davis 2009) and PZ (Freeman 2011) indicated that these solvents were stable up to 121 and 163 °C, respectively. At higher regeneration temperature, these solvents thermally degrade at a rate where amine makeup costs can become uneconomic. MEA cannot be economically regenerated at the temperature required to control nitrosamine and nitramine concentration in the circulating solvent and thus would require other methods for their control, adding to capital cost.

Thermal degradation is expected to account for an operating cost of anywhere from 0.06 – 0.26 $ per 1000 kg of captured CO_2 from flue gas (IEA 2014) depending on the solvent type and application. Applying these pricing data to the proposed NRG CO_2 capture facility represents a potential annual operating cost of 100 k$ - 500 k$ to make up amine lost from thermal degradation.

Understanding the thermal degradation rate of amine solvents is important to set process operating and design parameters to maximize energy performance, minimize solvent loss, and manage the capital cost in all applications and is also important for nitrosamine and nitramine control in CO_2 capture from flue gas. In this work, the thermal degradation of tertiary amine solvents promoted with PZ, a secondary amine, is studied.

As a process concept, tertiary amine solvents promoted with either a primary or secondary amine have high cyclic capacity and fast absorption rate when compared to primary or secondary amine solvents, which is discussed in detail in Section 2.2. One example of a promoted tertiary amine solvent is PZ-promoted methyldiethanolamine (MDEA). This solvent has been used successfully and extensively in gas treating applications. In CO_2-capture from flue gas, PZ-promoted MDEA has a comparable energy performance to concentrated PZ but does not precipitate at or near the operating range of the solvent. The latter has impacted reliability of concentrated PZ capture plants

at the pilot scale, especially those operating under cold weather (Chen 2014). Because of their proven performance in gas treating applications and promise in CO_2 capture applications from flue gas, promoted tertiary solvents merit additional study.

Davis (2009) and Freeman (2011) conducted extensive and exhaustive studies of MEA and PZ thermal degradation, respectively. MEA was considered to be a state-of-the-art solvent for flue gas CO_2 capture before the concentrated PZ solvent concept was first developed in 2008 (Rochelle 2011a). The thermal degradation studies of both Freeman and Davis helped to refine the MEA and concentrated PZ capture processes, especially in setting operational envelopes for processes using these solvents.

Several studies have investigated the degradation of promoted MDEA solvents (Dawodu 1996, Closmann 2011, Burfiend 2015). These studies focused on identification of thermal degradation products and/or identifying potential degradation pathways based on the degradation products seen. Kinetic degradation studies of MDEA using MEA, DEA, PZ, and morpholine as rate promoters have been conducted, but they have not validated the proposed degradation pathway. As a result, their use in process modeling and optimization is limited. Some work on single-point degradation of unpromoted tertiary amine solvents has been published (Lichtfers 2007, Eide-Hagumo 2011, Lepaumier 2009, Lepaumier 2010). Although these data are helpful in understanding the relative rate of degradation of one solvent to another, kinetic data cannot be extracted from these measurements. These data also cannot be used to estimate the rate loss of tertiary amine in the presence of PZ due to the ability of PZ to react with intermediate products present in degraded solution. An overview of previous studies of thermal degradation of promoted and unpromoted tertiary amine solvents is presented in Section 2.3.

In this work, the proposed initial degradation pathway of PZ-promoted MDEA has been validated using second-order kinetics. The kinetic measurements can be used to model the initial loss of amine in PZ-promoted MDEA capture over a range of concentration and CO_2 loading and can be applied to process design cases for optimization. Kinetic rate data for a range of PZ-promoted tertiary amine solvents has been measured as a function of tertiary amine structure and other process parameters, such as concentration, loading, and temperature. The results from these rate measurements can be used to identify thermally stable tertiary amines and structural features of tertiary amines that can enhance thermal stability.

1.4   RESEARCH OBJECTIVES

- Quantify thermal degradation of tertiary amine and promoted tertiary amine solvents over a range of temperature, concentration, and loading to better understand the effect of process parameters and amine structure on degradation rate. These results are presented in Chapters 4 and 7.

- Enhance understanding of thermal degradation byproduct formation in PZ-promoted tertiary amine solvents, especially major and intermediate byproduct formation as well as intermediate byproduct reaction with PZ. These results are presented in Chapters 4, 5, and 6.

- Understand the effect of physical solvents capable of physically absorbing CO_2 and H_2S at high pressure on the degradation behavior of PZ-promoted MDEA. These results are presented in Chapter 7.

- Validate the degradation mechanisms postulated in previous studies of PZ-promoted methyldiethanolamine (MDEA) and quantify thermal degradation kinetics as a function of tertiary amine structure in piperazine (PZ)-promoted tertiary amine solvent systems using rate models consistent with proposed degradation mechanisms. These results are presented in Chapters 5 and 6.

- Develop a model that can be used to account for thermal degradation as a function of amine lean loading for use in process design. The model data are presented in Chapter 5.

Chapter 2: Literature Review

2.1   INTRODUCTION & SCOPE

In this chapter, the development of MDEA and promoted MDEA solvents is discussed, and a review of thermal degradation studies of tertiary amine and promoted tertiary amine solvents is presented. Key conclusions and limitations of prior studies are discussed. All reactions shown in this chapter and in all subsequent chapters take place in aqueous solution.

2.2   DEVELOPMENT AND PROCESS CONCEPT OF MDEA AND PZ-PROMOTED MDEA SOLVENTS

Methyldiethanolamine, or MDEA, was first documented by Frazier (1950) as a solvent capable of selectively removing H_2S in the presence of CO_2 in the lab scale.

MDEA, like all amines, can absorb H_2S as shown in Figure 2.1:

Figure 2.1: MDEA reaction with H_2S to form protonated MDEA and bisulfide in aqueous solution

This exothermic reaction functions as a proton-transfer process to generate a protonated amine and bisulfide ion, which can be treated as an instantaneous reaction. For the majority of amines the absorption of H_2S is gas-film controlled in most process designs (Lagas 2000).

The reaction between MDEA and CO_2 is shown in Figure 2.2:

Figure 2.2: MDEA reaction with CO_2 to form protonated MDEA and bicarbonate in aqueous solution

The exothermic reaction between MDEA and CO_2 is significantly slower than the reaction between MDEA and H_2S, hence its original use for selective H_2S removal in the presence of CO_2. MDEA does not form a carbamate like primary and secondary amines, which is several orders of magnitude faster in rate than bicarbonate formation (Vaiyda 2007). The carbamate-forming reaction is shown in Figure 2.3 using piperazine (PZ), a secondary amine. Hindered amines, such as 2-amino-2-methyl-1-propanol (AMP), form an unstable carbamate due to the steric hindrance of the amine, favoring the bicarbonate pathway shown in Figure 2.2 (Sartori 1983).
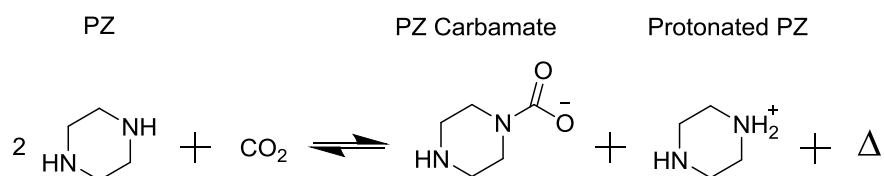
Figure 2.3: PZ reaction with CO_2 to form amine carbamate and protonated amine in aqueous solution

An advantage that MDEA, other tertiary amines, and hindered amines have over amines forming stable carbamate is their significantly greater capacity: only one equivalent of amine is used to react with one equivalent of CO_2, whereas unhindered primary and secondary amines consume two equivalents of amine with reaction of CO_2.

Tertiary amines promoted with secondary or primary amines thus can combine characteristics of both solvents: fast reaction with a large cyclic capacity. The primary or secondary amine can also react with CO_2 to produce the carbamate and have the tertiary amine function as a proton sink and is shown in Figure 2.4 with PZ used as the rate promoter and MDEA as the tertiary amine. The presence of the primary or secondary amine at small quantities at the gas-liquid interface ensures that a relatively high absorption rate is maintained throughout the loading range (Frailie 2011).
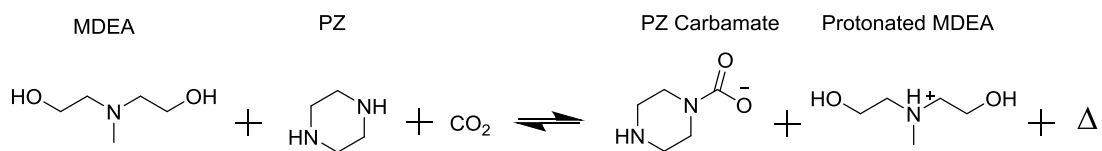
Figure 2.4: PZ reaction with CO_2 to form amine carbamate and protonated amine in aqueous solution

As discussed in Chapter 1, the thermodynamic equilibrium favors the carbamate and protonated amine at low temperature, and at high temperature the equilibrium favors free amine and unbound acid gas. Because of these phenomena, absorption occurs at low temperature whereas stripping occurs at high temperature. Stripping at higher temperature can generate CO_2 at a higher pressure and reduce compressor work. This is shown in Figure 2.5, which plots the equilibrium CO_2 partial pressure corresponding to a given solvent loading. The solvent loading is defined as mol CO_2 in the solvent per mol of amino functions, or alkalinity, in the solvent capable of absorbing CO_2.

The ethanolamine mixture for gas treating patented by Bottoms (1933) could be viewed as a promoted tertiary amine solvent system, albeit one that was used inadvertently due to the inability or unwillingness to separate monoethanolamine, a primary amine, and diethanolamine, a secondary amine, from triethanolamine, a tertiary

amine, at the time. BASF AG (Bartholome 1970) patented the first "true" promoted MDEA solvent, using methylaminoethanol, or MAE, as a rate promoter added in small quantities (0.1 to 0.4 mol/kg) to a concentrated aqueous MDEA solution. This solvent was specifically designed to remove about 99% of CO_2 and virtually all of the H_2S from high-pressure syngas with a CO_2 concentration up to 10 vol% and a H_2S concentration up to 5 vol% in the feed syngas. The H_2S content in the treated gas was claimed to be less than 4 ppmv. BASF AG then patented another process that replaced MAE with PZ at a concentration of 0.05 − 0.8 mole PZ/liter solution. PZ was found to have a significantly faster reaction rate than MAE and other primary or secondary amines (Appl 1982, Bishnoi 2000, Derks 2006). The PZ-promoted MDEA solvent is widely used in industry and has been considered one of the "most cost-effective" solutions (Mokhatab 2006) and "a benchmark for other solvent systems" (Mokhatab 2012) for bulk acid gas removal from natural gas.
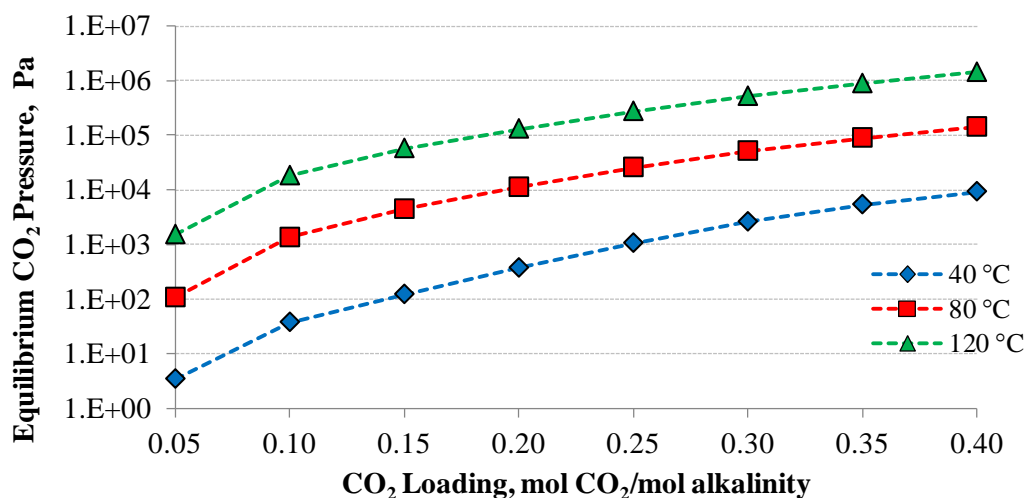
Figure 2.5: Equilibrium CO_2 Pressure and Solvent Loading for 21 wt% PZ / 29 wt% MDEA over 40 °C – 120 °C (Model from Frailie (2014))

14

Derivative PZ-promoted MDEA solvents were patented after the expiration of the original BASF patent. Union Carbide (Schubert 2000) patented a PZ-promoted MDEA solvent mixture with a minimum concentration of 1 mol/liter solution of PZ and a similar MDEA concentration range as was claimed in the BASF patent in order to boost cyclic capacity and reduce amine circulation rate. PZ-promoted MDEA in the presence of sulfolane, a physical solvent selective to acid gas, was patented by Royal Dutch Shell (Brok 2003) for use in gas treating applications whose feed gas has a high concentration of acid gas and whose treated gas specification typically calls for a partial pressure of 100 – 500 μbar (Song 2010) of acid gas. Several other derivative patents (Grossman 2004, Just 2010, Rochelle 2014) have claimed the use of other aliphatic tertiary amines, cyclic tertiary amines, and/or PZ-based rate promoters to improve process performance over PZ-promoted MDEA.

PZ-promoted MDEA was explored as a potential amine solvent to capture CO_2 from flue-gas derived solvent as early as 1995 (Erga). Numerous publications (Bishnoi 2002, Böttinger 2008, Muhammad 2009, Nguyen 2010, Chen 2011, Kim 2011) investigated its mass transfer and thermodynamic properties at conditions relevant to flue-gas CO_2 capture, and a rate-based process model for PZ-promoted MDEA using this data as well as others was developed by Frailie (2014) in the Aspen Plus process simulator (AspenTech). These data indicated that PZ-promoted MDEA has comparable CO_2 cyclic capacity, CO_2 absorption rate, and heat of absorption to concentrated PZ, which is considered to be a leading solvent for use in CO_2 capture applications (Rochelle 2011b), thus giving it a comparable energy performance to concentrated PZ. Concentrated PZ is also thermally stable to 160 °C and oxidatively stable, which has been demonstrated in the lab and pilot scale (Freeman 2011, Nielsen 2013). Some of these data are summarized in Table 2.1. Concentrated PZ, however, has a limited solid

solubility range and can precipitate at low temperature and low CO_2 loading as well as at rich loading at typical absorber temperature, limiting its operating range and requiring good control of the process and/or the use of process heat tracing. Appl (1982) noted that this prevents PZ from being used as a high pressure gas treating solvent by itself. PZ-promoted MDEA does not suffer as severely from this problem (Frailie 2014). Solid solubility data for concentrated PZ and PZ-promoted MDEA solvents (Du, personal communication, 2015) at low CO_2 loading, which is representative of the lean amine feed to the absorber, is presented in Figure 2.6. For these reasons, PZ-promoted MDEA as well as promoted tertiary amines have been successfully used high-pressure gas treating applications and show promise for low-pressure CO_2 capture applications.

Table 2.1: Capacities, Absorption Rates, and Heats of CO_2 Absorption of Various CO_2 Capture Solvents at Coal Conditions

Amine	Absorption Rate (kg') $mol*m^{-2}*Pa^{-1}*s^{-1}*10^7$	Solvent Capacity mol CO_2/kg solvent	Heat of CO_2 Absorption kJ/mol CO_2
41 wt% PZ[1]	8.5	0.79	64
30 wt% PZ[1]	11.3	0.63	64
21 wt% PZ[2] 29 wt% MDEA	8.3	0.98	69
9 wt% PZ[2] 42 wt% MDEA	6.9	0.80	68
11 wt% PZ[3] 23 wt% AMP	8.3	0.77	73
30 wt% MEA[1]	4.3	0.50	71
42 wt% DEA[3]	4.9	0.80	73

[1] Dugas (2009); [2] Chen (2011); [3] Li (2014)
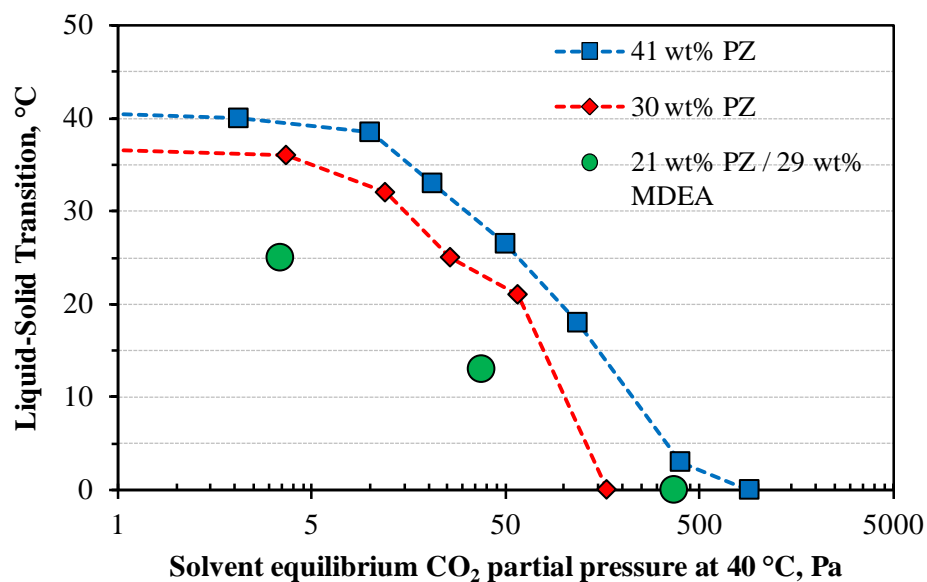
Figure 2.6: Solid Solubility of 41 wt% PZ, 30 wt% PZ, and 21 wt% PZ / 29 wt% MDEA at lean conditions (Du, personal communication, 2015)

2.3 REVIEW OF MDEA, PROMOTED MDEA, AND TERTIARY AMINE DEGRADATION

2.3.1. Early Thermal Degradation Studies (pre-2000)

Chakma (Chakma 1987, Chakma 1997) published the first study of MDEA degradation. Chakma degraded MDEA in a stirred 500 ml autoclave initially charged with 250 to 350 ml of aqueous MDEA solution and blanketed with a headspace of CO_2 over a range of initial operating pressure, temperature, and concentration and analyzed for products using a coupled gas chromatograph-mass spectrometer, or GC-MS. Chakma noted that changing the amount of headspace from 100 to 400 ml and changing agitation speed had no effect on the measured degradation rate.

Chakma found that the presence of CO_2 is necessary for the solution to degrade; MDEA showed negligible degradation in the presence of N_2. Higher CO_2 pressures led

to an increased rate of degradation, and temperatures above 200 °C led to the formation of volatile degradation products.

Chakma identified diethanolamine (DEA) as a degradation product, and also identified products corresponding to DEA degradation products (Kohl 1960, Kennard 1985, Hsu 1985) in the degraded MDEA solution. Based on the degradation products observed, Chakma proposed the following initial step for MDEA degradation, shown in Figure 2.7:
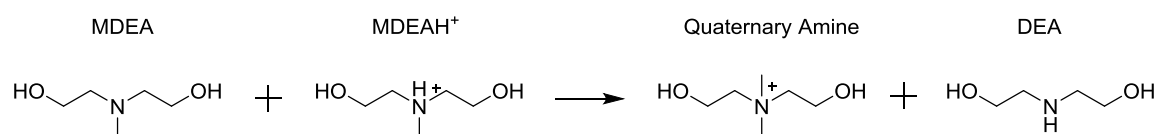
Figure 2.7: Initial thermal degradation step of MDEA (Chakma 1987)

The mechanism shown in Figure 2.7 is consistent with Chakma's observation that the degradation of MDEA is accelerated at increased CO_2 partial pressure and negligible at experimental conditions in a N_2 environment. Greater quantities of protonated amine will exist in solution at increased CO_2 partial pressure, which will increase the net forward degradation rate.

Chakma proposed that the dihydroxyethanolammonium (DMDEAm), the quaternary amine, would decompose to form dimethylaminoethanol, another tertiary amine, and ethylene oxide, which could be hydrolyzed to form ethylene glycol. The DEA would then degrade by pathways proposed by Kim (1984), Hsu (1985), and Kennard (1985). The pathway of DEA degradation, which is initiated by the presence of DEA carbamate, forms hydroxyethyloxazolidone (HEOD). DEA was not found to degrade in solutions loaded with H_2S and thus the DEA carbamate as opposed to protonated DEA is required to initiate degradation (Kim 1984). The pathway to produce

18

HEOD is analogous to the fourth step in Bucherer-Bergs synthesis in which the carbamate undergoes an internal ring closing to form an oxazolidone (Li 2006). HEOD can then react with DEA to form a polyamine. This is shown in Figure 2.8.

Conjugate acid of DEA Carbamate   Hydroxyethyloxazolidone (HEOD)

Tris(hydroxyethyl)ethylenediamine (THEED)
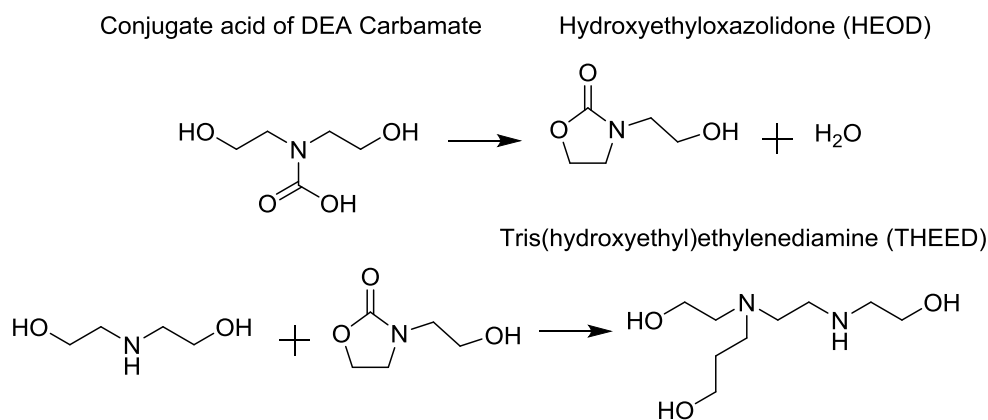
Figure 2.8: Degradation of DEA (Adapted from Hsu (1985) and Kennard (1985))

Chakma developed a thermal degradation model of MDEA as well as the formation and consumption of byproducts. The model was overall first-order and was able to predict MDEA loss at experimental conditions reasonably well. The reaction order used in the model is not consistent with the degradation pathway shown in Figure 2.7, which is overall second-order and first-order in free MDEA concentration and first-order in protonated MDEA concentration.

Other early work on promoted MDEA solvents investigated the effects of PZ, morpholine (Mor), monoethanolamine (MEA), and DEA as on thermal degradation. All of the experiments were conducted in autoclaves blanketed with CO_2 with or without stirring and with varying amount of headspace.

Daptardar (1994) noted that the degradation of PZ-promoted MDEA was proportional to the amount of PZ added as a rate promoter and to the headspace CO_2

partial pressure, which sets solvent loading. Daptardar also noted that Mor was a more stable rate promoter than PZ in promoted MDEA and that PZ-promoted triethanolamine (TEA) showed an overall greater stability than PZ-promoted MDEA. These results are consistent when considering promoter and tertiary amine pKa: Mor and TEA have lower pKa values than PZ and MDEA, respectively. These data are shown in Table 2.2.

Table 2.2: pKa1 values of PZ, MDEA, Morpholine, and Triethanolamine

Amine	pKa1 (25 °C)
PZ[1]	9.7
MDEA[2]	8.5
Mor[3]	8.5
TEA[3]	7.8

[1] Khalili 2009
[2] Simond, 2012
[3] Haynes, Ed. 2014

Replacing PZ with Mor as a rate promoter and MDEA with TEA as the tertiary amine would reduce the concentration of protonated species, reducing the intrinsic rate of degradation. However, Daptardar found that Mor-promoted TEA had the highest rate of degradation, which is inconsistent with data from Davis (2009) that indicated that PZ and Mor had a comparable thermal degradation rate when blended with other solvents.

Dawodu (1996) investigated the degradation of MEA and DEA promoted MDEA solvents. Dawodu noted that the observed rate of degradation of DEA was greater than MEA and that the observed rate of MDEA degradation was the same regardless of the promoter used and that no degradation occurred in solutions degraded in a pure N_2 headspace. The degradation products that Dawodu observed in DEA-promoted MDEA were the same as MDEA and is consistent with Chakma's observation that DEA is an intermediate degradation product of MDEA degradation. Products associated with MEA-promoted MDEA degradation were identical to MDEA and DEA-promoted degradation;

however, degradation products associated with MEA and MAE degradation that were found by Polderman (Kohl 1960), Davis (2009), and Lepaumier (2011) were also observed in MEA-promoted MDEA.

Lepaumier (2011) noted that MAE was significantly more unstable than MEA, which implies that the MAE-promoted MDEA solvent developed by BASF would be thermally unstable. Huntsman Chemical (Critchfield 1999) proposed a solvent using 2-aminoethoxyethanol as the MDEA rate promoter and cited that the use of 2-aminoethoxyethanol instead of MAE would avoid the thermal degradation seen in MAE-promoted MDEA.

2.3.2. Later Thermal Degradation Studies (post-2000)

Lepaumier (Lepaumier 2009, Lepaumier 2010) addressed the formation of degradation products of a range of amine solvents and proposed generalized degradation mechanisms based on the presence of major degradation products. The degradation was conducted in stirred autoclaves at 140 °C and with a constant CO_2 headspace pressure of 2 MPa with initial amine concentration set at 4 M. Degraded amine samples were analyzed using GC-MS. Only one sample was drawn per amine degraded, limiting the study's ability to extract thermal degradation kinetics from each experiment.

Lepaumier degraded the tertiary amines dimethylaminoethanol (DMAE), MDEA, and N,N,N'N'-tetramethylethylenediamine (TMEDA) in addition to a range of other primary and secondary amines, such as MAE, MEA, and DEA, used as promoters or found as degradation products in promoted tertiary amine solutions. Several other substituted tertiary amines as well as secondary amines were found as degradation products in the tertiary amine solvents, and glycol was observed in the degradation of tertiary alkanolamines. Primary and secondary alkanolamine solvents with two or three

carbons between the amine and hydroxyl functions followed the same pathway as DEA (Kohl 1960, Hsu 1985, Kennard 1985). A summary of the proposed degradation pathways for these molecules is summarized in Figures 2.9 and 2.10.

Bedell (Bedell 2010, Bedell 2011) identified quaternary amines in degraded MDEA solution. Quaternary amines were also found in degraded solutions of other tertiary amines, such as TEA and DMAE. These experiments were run in autoclaves without any CO_2 loading and under a N_2 blanket, and only about 1% of amine was degraded. Bedell used ion chromatography to analyze for degraded samples.
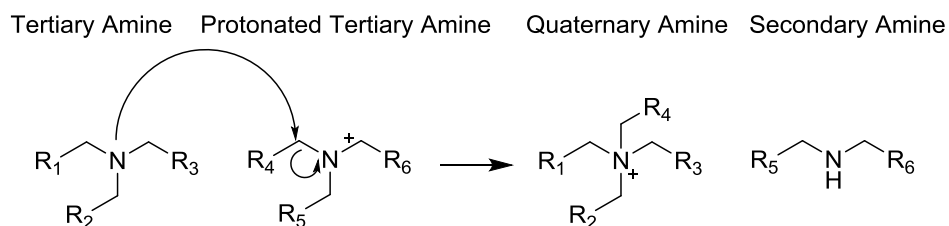
Figure 2.9: Generic degradation pathway of tertiary amines (adapted from Lepaumier 2009)
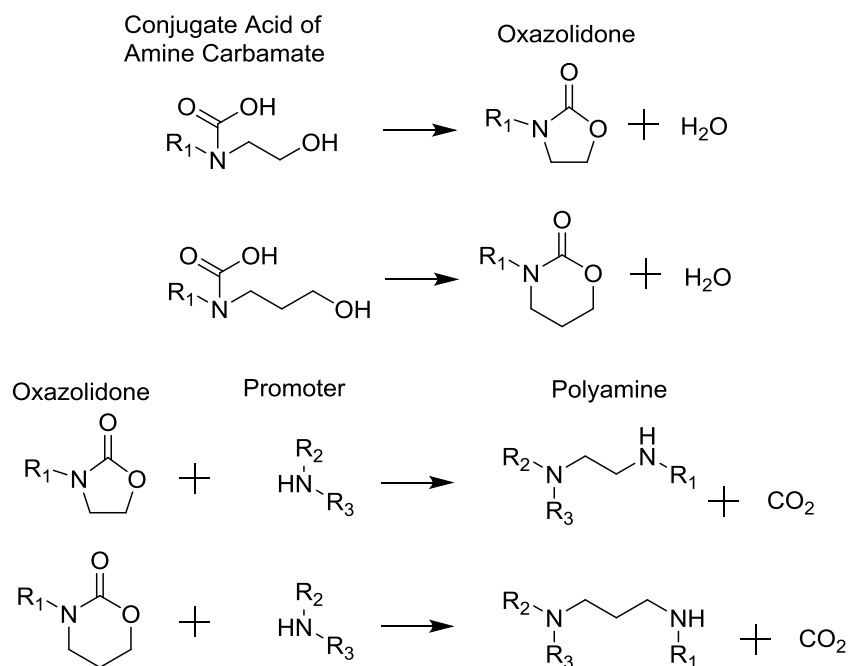
Figure 2.10: Generic degradation pathway of alkanolamines via carbamate polymerization (adapted from Lepaumier 2009)

Closmann (2011) extended Bedell's work to address PZ-promoted MDEA degradation in the presence of CO_2 at an initial concentration of 42 wt% MDEA and 9 wt% PZ. These experiments were run in sealed Swagelok® stainless-steel cylinders, whose construction and operation is documented in Chapter 3 and in Appendix A, with CO_2-loaded amine solution up to 150 °C. Consistent with other researchers, Closmann found that increased CO_2 concentration led to an increased rate of thermal degradation and noted that the degradation rate of PZ was greater than the rate of MDEA. Burfiend (2015) varied PZ concentration at constant MDEA and CO_2 concentration and found that a reduced PZ concentration led to a decrease in the observed degradation rate. Addtionally, Closmann developed a thermal degradation model was developed for PZ-promoted MDEA, which was first-order in amine concentration but did not explicitly account for protonated amine concentration.

Closmann found that the primary degradation products of PZ-promoted MDEA were DEA, 1-methylpiperazine (1-MPZ), and 1,4-dimethylpiperazine (1,4-DMPZ), and that PZ would react with DEA to form substituted polyamines, consistent with the generalized degradation mechanism proposed by Lepaumier. This would explain why the rate of PZ loss was greater than MDEA loss. MAE and 1-hydroxyethylpiperazine (1-HePZ) were identified as minor degradation products and suggested that the reaction with bulkier substituent groups, such as hydroxyethyl groups, was slow. Based on the degradation product slate, Closmann proposed the following initial degradation mechanisms of PZ-promoted MDEA degradation, shown in Figures 2.11 and 2.12. The end products of either mechanism would predict the major degradation products observed by Closmann.

BASF (Lichtfers 2007) disclosed that tertiary amines without methyl groups in the absence of a rate promoter were more stable to thermal degradation than tertiary amines with methyl groups based on single-point experiments. These experiments were conducted using autoclaves and used GC to quantify the amount of parent amine left after degradation. At 163 °C and a CO_2 pressure of 6.3 bar, tertiary amines such as diethylaminoethanol (DEAE), ethyldiethanolamine (EDEA), and dimethylaminopropanol (DMAP) showed negligible degradation, whereas MDEA and dimethylaminoethanol (DMAE) degraded by 4% and 6%, respectively. These results were confirmed by Eide-Hagumo (2011), who noted that DMAE and MDEA degraded by about 30-40% whereas DEAE and TEA degraded by about 10-15% at an initial concentration of about 2-4 M amine, 0.5 mol CO_2/alkalinity solvent loading, and 135 °C. Eide-Hagumo analyzed samples using liquid chromatography and used an experimental setup similar to Closmann.
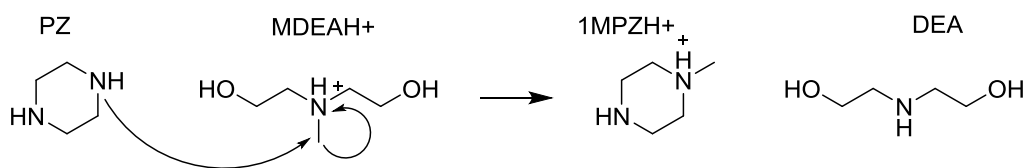
Figure 2.11: Degradation pathway of PZ-promoted MDEA, via PZ direct substitution, to form 1-MPZ and DEA (adapted from Closmann 2011)
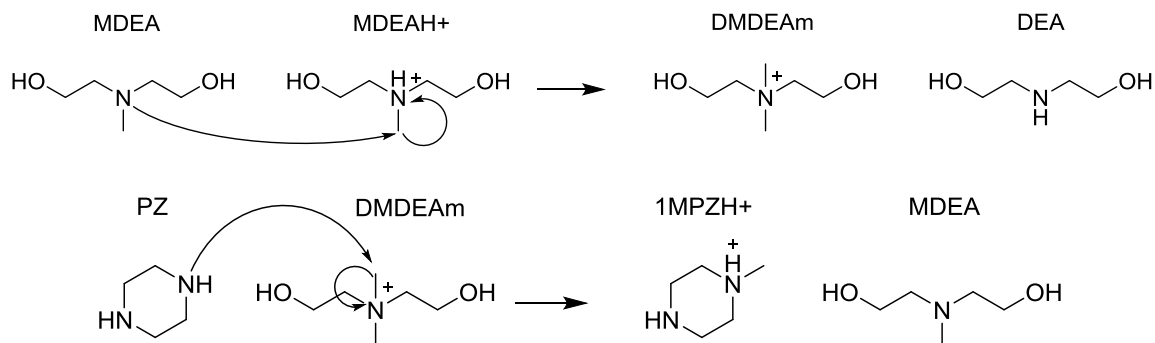
Figure 2.12: Degradation pathway of PZ-promoted MDEA, via quaternary amine intermediate, to form 1-MPZ and DEA (adapted from Closmann 2011)

2.3.3. Oxidative Degradation and Amine Volatility of PZ-Promoted MDEA

Some data exists on the oxidative degradation of PZ-promoted MDEA and the volatility of PZ-promoted MDEA at conditions relevant to flue-gas CO_2 capture. Voice (2013a) and Closmann (2011) studied the oxidative degradation of PZ-promoted MDEA in a cycling apparatus in which the solvent is degraded in the presence of air or pure oxygen at a 1.5 to 2 kPa equilibrium CO_2 partial pressure in an oxidation reactor at low temperature, degassed, and then subsequently degraded at high temperature in a set of heated exchangers before being returned to the oxidation reactor. Voice found that the oxidation rate of unpromoted MDEA is anywhere from 0-50% greater than concentrated PZ when MDEA is oxidized at 55 °C and PZ is oxidized at 40 °C; both solvents were cycled to 120 °C. Closmann noted that a solution of PZ-promoted MDEA oxidizes at

25

about the same rate as MDEA in the cycling apparatus, and Voice noted that the degradation rate of MDEA is less than MEA in MEA-promoted MDEA and MEA solvents. Based on these data, the oxidative rate loss of PZ-promoted MDEA is expected to be at most 50% greater than concentrated PZ. Nguyen (2013) studied the relative volatility of MDEA in PZ-promoted MDEA solutions and found that MDEA was about as volatile as PZ. Other tertiary amines with only two hydrophilic groups, such as dimethylaminoethanol (DMAE), were found to be two orders of magnitude more volatile than MDEA. Their high volatility would require a water wash column capable of removing volatile amine from the treated gas, especially in flue-gas CO_2 capture process designs operating at low absorber pressure.

2.4 THERMAL DEGRADATION OF OTHER AMINE SOLVENTS AND CONNECTIONS TO PROMOTED TERTIARY AMINE DEGRADATION

2.4.1 Degradation of MEA: Carbamate Polymerization and Urea Formation

Davis (2009) degraded solutions of monoethanolamine (MEA). Davis noted that MEA degrades via the carbamate polymerization pathway, shown in Figure 2.10, to produce 2-oxazolidone (2OZD). 2OZD can react with MEA to form hydroxyethylethylenediamine (HEEDA), a diamine. This pathway is shown in Figure 2.13 and is analogous to the pathway of DEA with HEOD to form THEED.
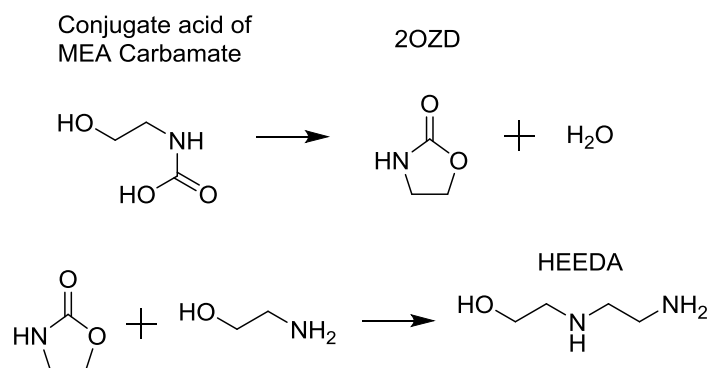
Figure 2.13: Formation of HEEDA from MEA (Davis 2009)

HEEDA can then undergo degradation via the carbamate polymerization pathway or form a cyclic urea or imidazolidone. The cyclic urea formation is analogous to oxazolidone formation and only happens in the presence of CO_2. The amino functions of ureas have low pKa values and cannot participate in reaction between CO_2 or H_2S. Their presence reduces solution alkalinity and thus cyclic capacity. Amines with two or three carbons between two primary or secondary amino functions can undergo this degradation pathway. The degradation of HEEDA to form hydroxyethylimidazolidone (HEIA) is shown in Figure 2.14.
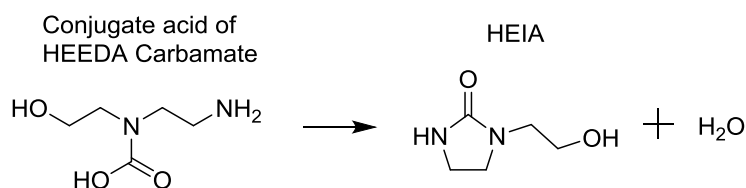
Figure 2.14: Formation of HEIA from HEEDA

Linear ureas, such dihydroxyethylurea (DHU), were observed in MEA degradation (Davis 2009). Freeman (2011) identified similar products in concentrated PZ degradation and ethylenediamine degradation. Gouedard (2011) suggested that the linear

urea formation occurs via a condensation step, which is analogous to the formation of urea from ammonium carbamate used in the Bosch-Meisen process (Krase 1922, Bosch 1922, Bruckner 2002). This pathway can occur between a protonated primary or secondary amine and amine carbamate and is shown in Figure 2.15.
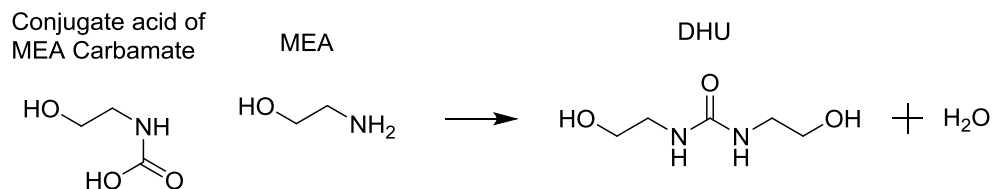
Figure 2.15: Formation of DHU from MEA and MEA carbamate (adapted from Gouedard 2011)

Both cyclic ureas and linear ureas likely exist in degraded PZ-promoted tertiary amine solutions due to the presence of intermediate degradation products, such as DEA, that degrade via similar routes to MEA. The presence of ureas can be indirectly measured by quantifying solution alkalinity, which can determine the amount of amino groups present in solution capable of reaction with CO_2.

Davis studied the degradation of MEA analogues by increasing chain length and steric hindrance and found that increased chain length and increased steric hindrance decrease the rate of oxazolidone formation. Alkanolamines with four carbons between the amino function and hydroxyl function would ring close in a condensation reaction, whereas alkanolamines with five or more carbons were relatively stable and did not readily ring close. Lepaumier (2010) and Hatchell (2014) identified analogous trends and mechanisms in diamine degradation in which the diamine would undergo an internal ring closing to form ammonia and a secondary or tertiary monoamine. Diamines with four carbons between their amino functions were the most susceptible to this degradation

pathway, whereas diamines with five or six carbons between their amino functions did not readily ring close.

2.4.2   Degradation of PZ: Ring-Opening and Formate Production

Freeman (2011) thermally degraded concentrated PZ solutions and noted that PZ by itself is more stable than PZ-promoted MDEA by more than an order of magnitude. PZ was proposed to degrade via a ring-opening step to form aminoethylaminoethylpiperazine (AEAEPZ), shown in Figure 2.16, with a free PZ interacting with the carbon alpha to a protonated amino function on another PZ molecule. AEAEPZ can then form a cyclic urea like HEEDA.
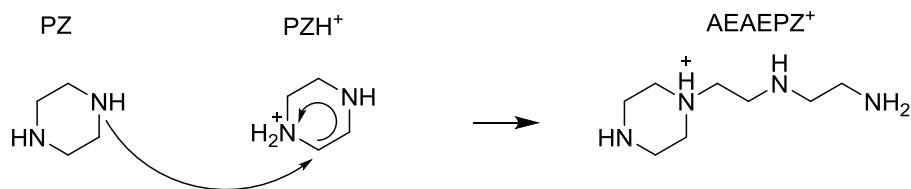
Figure 2.16: Initial degradation step of PZ when used by itself as a CO$_2$ Capture Solvent (Freeman 2011)

This pathway is conceptually similar to the proposed pathway of PZ-promoted MDEA degradation, which involves a free PZ interacting with the alpha carbon of a functional group attached to the protonated amine of MDEA.

Above 165 °C, n-formyl piperazine was found to be the dominant degradation product in PZ degradation, representing about 30% of the amine lost at 165 °C and 150 days. NMR studies indicated that it was formed from the PZ carbamate (Freeman 2011). The formyl amide of PZ is shown in Figure 2.17.

Piperazine
Carbamate

n-Formyl
Piperazine
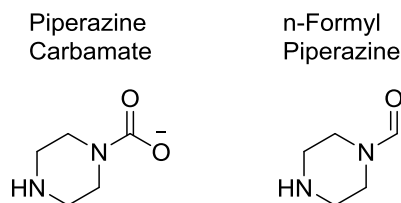
Figure 2.17: PZ Carbamate [a] and n-Formyl Piperazine [b], a formyl amide of PZ

Degraded samples containing formyl amides can be hydrolyzed using concentrated base to form the parent amine and formate ion (Sexton 2008) and is similar to reclaiming the amine using caustic or sodium carbonate solution (Kohl 1960). Closmann reported that n-formyl piperazine and formate derivatives represented 0.3% to 2.6% of the product lost in PZ-promoted MDEA at 150 °C after 22 days.

2.4.3 Connecting MEA and PZ Degradation to Promoted Tertiary Amine Degradation

PZ degradation through the pathways Freeman (2011) described is likely not significant at conditions tested in this work unless the tertiary amine is as stable as PZ in the PZ-promoted solution. The results from Closmann show that formate and formyl amide production in PZ-promoted solvents represents a minor degradation pathway at experimental conditions.

The results from Davis (2009) can be used to identify structural features of promoted tertiary amines that impart thermal stability, such as the length and/or the steric hindrance of the hydroxyalkyl functional group attached to the tertiary amino function.

30

2.5   SUMMARY OF LITERATURE REVIEW

The prior studies emphasize identification of thermal degradation products and propose degradation pathways based on the degradation product slate of tertiary amine and promoted tertiary amine solutions. The thermal degradation rate of MDEA, PZ-promoted MDEA, MEA-promoted MDEA, DEA-promoted MDEA, and PZ-promoted MDEA has been quantified. Single-point thermal degradation data exists on other unpromoted tertiary amine solvents degraded in the presence of CO_2 to understand the relative loss of amine over a set period of time. These data, however, cannot be effectively used to extract degradation kinetics.

The vast majority of studies, with the exception of Bedell, Closmann, and Eide-Hagumo, have used GC to analyze and quantify products in degraded amine solution. The gas chromatograph generally operates at high temperatures, typically above 200 °C (Lepaumier 2011), and it is possible that samples can encounter additional degradation during analysis. Davis (2009) attempted to quantify the degradation of PZ using GC; the GC analysis indicated that the sample was degraded when ion chromatography, amine titration analysis, and C_{13} nuclear magnetic resonance spectroscopy indicated that the sample did not degrade. Liquid chromatography and ion chromatography run close to ambient temperatures (30 °C to 40 °C) where amine will not degrade.

The effect of protonated amines, which are included in the initial degradation step proposed by all of the researchers, have not been explicitly accounted for in degradation models by Chakma and Closmann. Although these models are able to predict experimental data reasonably well, they cannot be extended to conditions beyond what has been measured experimentally and thus limits their use in the process design of CO_2 capture and gas treating plants. Due to the presence of CO_2, several other polyamines are formed and present in the degradation. Therefore, it is difficult to estimate the

31

concentration of free and protonated species in the absence of thermodynamic data or standards available for byproducts in degraded solution. Performing degradation in acidified solution, which has protonated amine but no CO_2 and thus no amine carbamate present, is necessary to understand the initial rate of degradation as a function of protonated and free amine species as standards and thermodynamic data are available for the major degradation products initially seen. The initial rate of degradation will set operating envelopes, such as the maximum operating temperature, of the capture plant.

This work builds upon the foundation of others, principally in understanding the rate of degradation of a range of PZ-promoted tertiary amines as a function of structure and process parameters, validating the MDEA and PZ-promoted MDEA degradation omodel for PZ-promoted MDEA that can be applied to process design, expanding the fundamental mechanistic studies to include other PZ-promoted tertiary amines, and understanding structural features of amines that increase thermal stability.

Chapter 3: Experimental Methods

3.1 INTRODUCTION & SCOPE

In this chapter, relevant terms and definitions, experimental techniques, and analytical methods will be discussed. In a broad sense, the methods presented in this chapter are identical to those of Freeman (2011), Voice (2013a), Davis (2009), and Closmann (2011).

3.2 RELEVANT TERMS & DEFINITIONS

Specific terms used throughout the rest of the dissertation are explained in this section.

Solution or Solvent Amine Concentration is generally reported in either $mol*kg^{-1}$, $mmol*kg^{-1}$, or as molality. Molality, defined with the symbol m, is defined in Equation 3.1:

$$1 \text{ molal amine} = 1 \text{ m amine} = \frac{1 \text{ mol amine}}{1 \text{ kg H}_2\text{O}} \qquad \text{Eq. 3.1}$$

Molality is used purely out of convenience from a solvent preparation standpoint and 1 kg water uses a basis of 1 kg water. For example, a solution comprising 5 m piperazine (PZ) / 5 m methyldiethanolamine (MDEA) consists of 5 mol PZ, 5 mol MDEA, and 1 kg water. A smaller batch of solution with an identical molality would use 250 g water, 1.25 mol PZ, and 1.25 mol MDEA.

Solvent or Solution Alkalinity is defined as the sum of amino functions capable of reaction with CO_2 to form either amine carbamate or bicarbonate and are reported as $mol*kg^{-1}$, $mmol*kg^{-1}$, or as molality. One mole of PZ has two moles of alkalinity because PZ is a diamine, and one mole of MDEA has one mole of alkalinity because MDEA is a monoamine. For example, 5 m PZ / 5 m MDEA would have an alkalinity of 15 m, and 5 m MDEA would have an alkalinity of 5 m.

Solvent or Solution Loading is defined as mol CO_2/mol alkalinity or as mol H^+/mol alkalinity depending on whether CO_2 or a concentrated acid is used to load the solution. For example, 5 m PZ / 5 m MDEA prepared using 1 kg water, would have an absolute alkalinity of 15 mol. To load this solution to 0.2 mol CO_2/mol alkalinity, 3 mol CO_2 would have to be added into the solution. 5 m PZ / 5 m MDEA, prepared using 250 g water, would have an absolute alkalinity of 3.75 mol, and 0.75 mol CO_2 would have to be added to the solution prepared using 250 g water to obtain a loading of 0.2 mol CO_2/mol alkalinity.

Lean Loading, Conditions, or Amine and ***Rich Loading, Conditions, or Amine*** are used to denote the CO_2 loading of the solvent at the absorber inlet and the absorber outlet. In this work, the lean and rich loading corresponds to the equilibrium loading of the amine solvent at a CO_2 partial pressure of 500 Pa and 5000 Pa, respectively, which is used as a baseline for absorber design for flue gas capture from coal-fired power plants. The amine loading in the stripper is generally the same as the lean loading; thus, the lean loading corresponds to the conditions encountered in thermal degradation.

3.3   SOLVENT PREPARATION

All solvents are prepared gravimetrically using a scale with an accuracy of 0.1 g. Several sovlents were solids at room temperature. Piperazine was available as a solid flake and could be directly added to water. Solvents that were not solid in amorphous or crystalline form, such as hexamethylenediamine and triisopropanolamine, had to be heated to their melting temperature in a hot water bath before they could be added to solution. Amine-water solutions that were solid or partially solid at room temperature had to be heated using a water bath to about 50 °C prior to loading with CO_2. Adding CO_2 to solution increases the solid solubility of the solvent, and virtually all solvents, when loaded to their target loading, were present as a homogeneous liquid at room temperature.

Solvents are loaded with CO_2 by first placing the unloaded solvent in a gas washing bottle. The gas washing bottle with the amine is weighed and given the mass M_1. The cylinder is then placed onto a scale in a fume hood with an accuracy of 0.1 g and connected to a CO_2 gas line with a supply pressure between 3 to 5 bar gauge. The scale in the fume hood is zeroed. CO_2 is then sparged into the gas-washing bottle. The rate of CO_2 addition is set to be slow enough to minimize flashing of water; the addition of CO_2 to the amine is exothermic with a heat of reaction of about 60- 80 kJ/mol CO_2. Once the desired amount of CO_2 has been added, the gas line is shut and then disconnected from the gas-washing bottle. The bottle with the amine is weighed again and given the mass M_2. The difference between M_2 and M_1 represents the gravimetric addition of CO_2 to the solution. A schematic of the loading apparatus is shown in Figure 3.1.

CO₂ inlet (via polymer tubing)

Outlet to Vent

Gas Washing Bottle with Removable Stopper Assembly, loaded with amine (Wilmad LabGlass)

Scale (0.1 g accuracy)
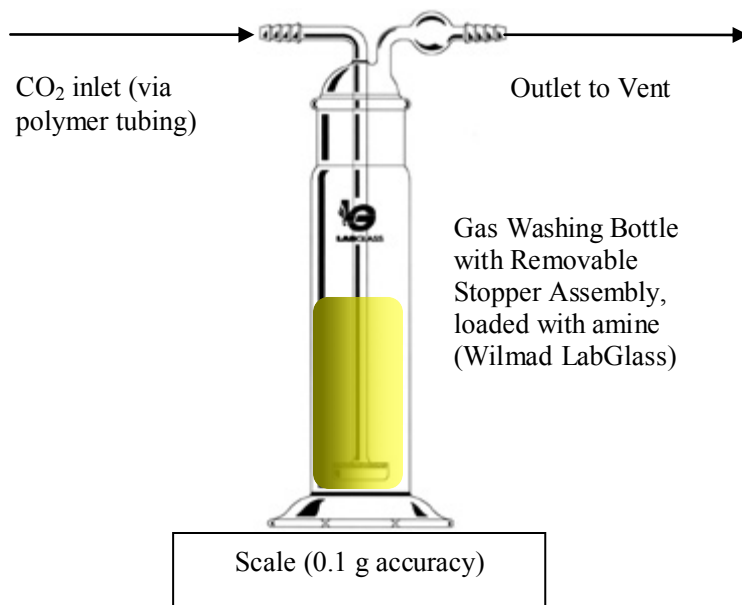
Figure 3.1: CO$_2$ loading apparatus used to add CO$_2$ to amine solution

In general, it takes about 30 minutes to load 5 m PZ / 5 m MDEA to a loading of about 0.23 mol CO$_2$/mol alkalinity.

Solution loading can be reduced by adding fresh amine to the loaded solution, and amine concentration, but not loading, can be diluted by adding water to the solution. For example, a solution of 5 m PZ loaded to 0.35 mol CO$_2$/mol alkalinity using 1 kg of water can be made into a solution of 5 m PZ / 5 m MDEA loaded to 0.23 mol CO$_2$/mol alkalinity by adding 5 moles of MDEA to the loaded PZ solution.

Acid loaded solutions were prepared by adding sulfuric or hydrochloric acid to an unloaded aqueous solution with some amine present. Dilute acid was used for the majority of the experiments because of the intrinsic safety of working with dilute acid instead of concentrated acid. As is the case with the CO$_2$-loaded solutions, acid loading

can be reduced by adding fresh amine to the acid-loaded solution and amine concentration can be diluted by addition of water.

3.4 THERMAL DEGRADATION SETUP

Swagelok® 316L stainless steel cylinders rated up to 130 barg pressure were used as degradation reactors and placed inside Lab-Line Imperial V convection ovens vented to a fume hood and equipped with Eurotherm 2100-series digital temperature controls. The heater is able to maintain a uniform temperature throughout the oven with a temperature variation of about 0.1 to 0.2 °C. An image of the degradation reactor is shown in Figure 3.2. A standard operating procedure that discusses reactor preparation, cleaning, and setup is provided in Appendix A-1. In addition to Davis (2009), Voice (2013a), Freeman (2011), and Closmann (2011), similar setups have been used by other researchers (Huang 2014, da Silva 2009, Fine 2014, Goldman 2013, Lepaumier 2011) who have studied amine degradation as well as nitrosamine formation in amine solutions.

Two different kinds of Swagelok® reactors were used. Very early studies of piperazine reaction with oxazolidone-forming amines, presented in Section 4.4, were conducted using first-generation reactors used by Davis (2009), Freeman (2011), Closmann (2011), and Voice (2013a). The first-generation reactors were made from 316L stainless steel, had a tube diameter of 1.25 cm, a tube length of 10 cm, and a volume of about 10 ml. Second-generation reactors, used for all other experiments, were made from 316L stainless steel, had a tube diameter of 0.95 cm, a tube length of 10 cm, and a volume of about 4.5 ml. Both reactors had a maximum pressure rating above 130 barg. Freeman (2011) reported that the seals of a third to a half of first-generation reactors would fail at 175 °C. In a failed reactor, amine solution would leak from the

cylinder and volatilize in the oven, leaving behind a nonvolatile dark residue on the exterior of the cylinder. The second-generation reactors had no such failures, even at experiments run at 175 °C, and is likely due to the smaller diameter that can permit intrinsically better sealing and higher pressure than the larger diameter.

(A)   (B)   (C)

10 cm

0.95 cm
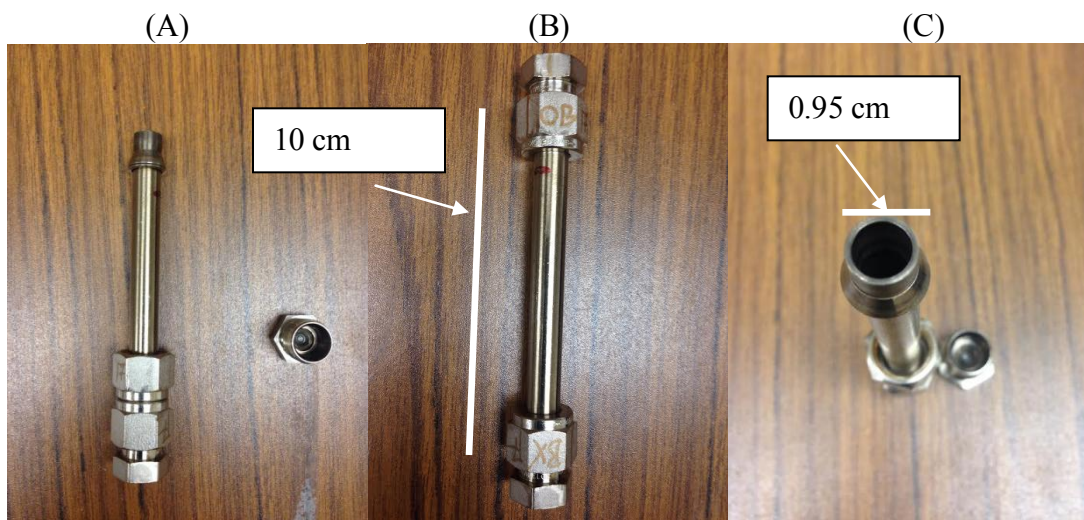
Figure 3.2: Second-generation Swagelok® stainless cylinders used for thermal degradation experiments; (A) open view, (B) closed view, (C) detail of reactor opening

Amine solution was loaded into the cylinder, which was then hand-tightened and weighed. About 4 ml of CO_2-loaded solution was added to the second-generation reactor and 7 ml of solution was added to the first-generation reactor, leaving a small headspace in the reactor. The headspace was left to minimize the chance of cylinder failure due to over-pressurization and liquid expansion. About 4.4 ml of H^+-loaded solution was added to the second-generation reactor for acid-loaded experiments. A smaller headspace can be used for acid-loaded experiments because the acid-loaded solutions do not contain CO_2, which becomes more volatile as temperature is increased. At 150 °C, the equilibrium CO_2 partial pressure is on the order of 10 bar gauge (Xu 2011).

38

The cylinder was then sealed by turning the end cap of the cylinder a quarter-turn past hand-tight using a wrench, placed inside the convection oven at the temperature setpoint, and was removed at a set interval. The cylinders were not agitated; the long experiment time, which is on the order of several days, is sufficiently slow enough for the degradation reactions to be kinetically controlled (Davis 2009). After removal, the cylinder was weighed again; samples with a deviation of 0.3 g, or about 7%, of their masses were discarded and not used in the analysis. The sealed cylinder was placed inside a chemical fridge for preservation and was decanted from the cylinder immediately before the solutions were analyzed.

Corrosion from metals leaching from the cylinder walls as well as the presence of oxygen in the headspace of the cylinder are not expected to be significant contributors to the measured degradation of the amine. Freeman (2011) degraded a set of cylinders that were loaded and hand-tightened in a pure-nitrogen environment and saw no difference in the measured degradation rate of concentrated PZ loaded in a nitrogen environment versus without.

Freeman (2011) degraded concentrated PZ in specially-prepared cylinders with glass liners to avoid contact with metals. The use of the liner increased the headspace of the cylinder by about 30%. The results from Freeman showed that the degraded solution in the glass-lined cylinder had no metals content and an identical amine loss to the solution degraded in cylinders without the glass liner. Da Silva (2009) also reported similar results for the thermal degradation of monoethanolamine solutions, which are known to be significantly more corrosive and more susceptible to oxidative degradation than PZ. Lepaumier (2011) found no difference in the degradation rate of CO_2-loaded MAE in glass-lined cylinders compared to cylinders without a glass liner.

3.5   ANALYTICAL METHODS

Cation chromatography, low-resolution mass spectrometry (LCMS), and total alkalinity measurements were used to determine the concentration of parent amine and amine byproducts.   Cation chromatography and total alkalinity measurements were conducted internally whereas the LCMS analysis was a turnkey service provided by the Chemistry Department at UT-Austin.

3.5.1   Cation Chromatography

Cation Chromatography System Overview

Cation chromatography was used to analyze for the concentration of parent amines as well as amine byproducts present in solution. A process flow diagram of the cation chromatograph, along with operating parameters and units, is shown in Figure 3.3. The methods employed in this work are similar to those of Voice (2013a), Freeman (2011), Closmann (2011), and Davis (2009).

A Dionex™ ICS-2100 chromatograph with an autosampler was used to conduct the analysis and Dionex Chromeleon™ 6.8 software was used to control the chromatograph. 18.2 μmho deionized water is pumped through the unit and is used as the mobile phase. A gradient of methylsulfonic acid, or MSA, varying anywhere from 0-100 mM MSA, is added to the mobile phase, which is then filtered to remove any trace contaminants, such as potassium and sodium, using a trap column. The mobile phase is then degassed to remove any dissolved gases present in solution.   25 μl of sample, consisting of an amine sample diluted to approximately 30 - 60 ppmw total amine concentration, is injected into an injection valve and mixed with the mobile phase; the sample, mixed with the mobile phase, is then fed into the guard and analytical columns.

The columns are held at a constant 30 °C temperature, the lowest controllable temperature allowed by the unit.
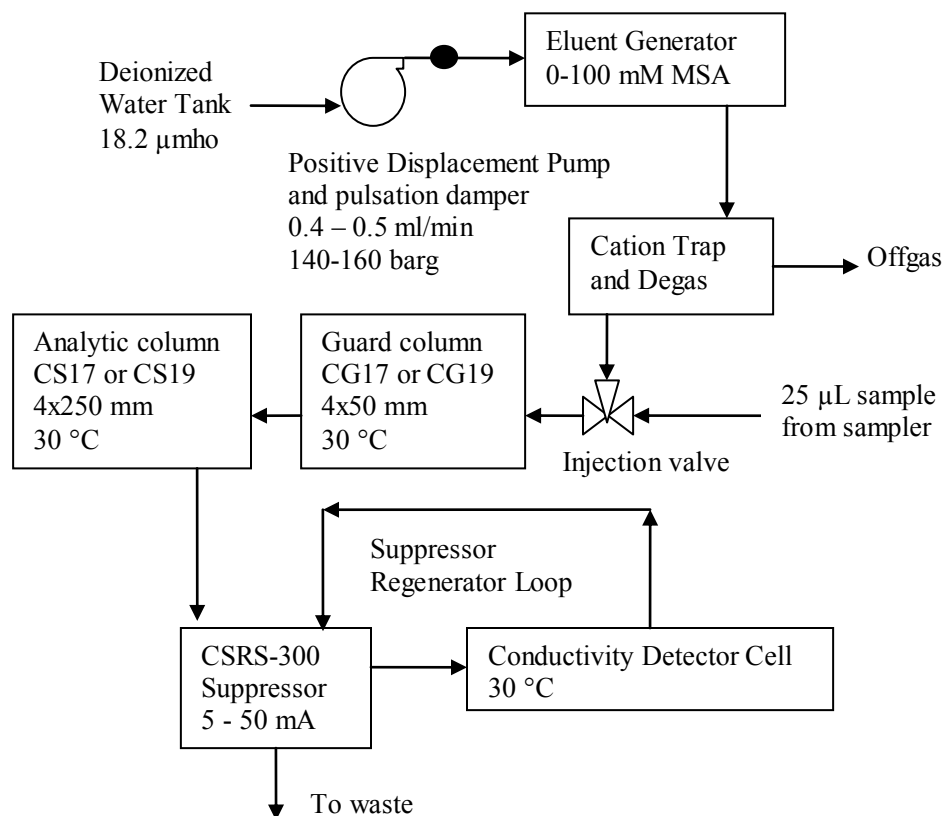
Figure 3.3: Process flow diagram of the cation chromatograph (Dionex ICS-2100)

The analytical column, either a 4 mm x 250 mm Dionex CS17 or CS19 column, consists of a densely-packed ion exchange resin that can selectively adsorb cations and is referred to as the stationary phase. The Dionex CS17 4 mm x 50 mm guard column consists of the same ion exchange resin as the CS17 column, and the Dionex CG19 4 mm x 50 mm guard column consists of a densely-packed material that can filter out solids that could otherwise damage the analytical column. The CG17 guard and CS17 analytic

columns were used for routine analyses for the majority of experiments; the CG19 guard and CS19 analytic columns, which have a greater total packing density than the CG17 and CS17 columns, were used to separate compounds that would otherwise be difficult to separate using the CG17 and CS17 columns.

The amine in the mobile phase is adsorbed onto the stationary phase and moves through the column much more slowly than the mobile phase. The amine can elute more quickly at high values of acid concentration. A regenerating suppressor is used to neutralize any excess MSA downstream of the column before it is analyzed by the conductivity detector and permits the use of variable, steadily increasing acid concentration through the sample run. The effluent from the conductivity detector is then used to regenerate the suppressor before being sent to waste.

A sequence is set in the Chromeleon™ software to analyze samples. The first two samples in the sequence consist of deionized water blanks; the first injection of deionized water equilibrates the system, and the second injection is used to determine the baseline. The remainder of the samples is then run on the instrument. This process, including unit shutdown, is fully automated.

Methods and Chromatograms – CG17/CS17

Routine analyses were conducted using the CG17 guard column and the CS17 analytical column. Early work used the "Stephanie_3_Auto_AS" program developed by Freeman. A new program, "Argonaut-R0," was later developed and used; it is identical to the program made by Freeman (2011) but uses a reduced suppressor current to extend suppressor lifetime. The program parameters and a plot showing the acid gradient are shown in Table 3.1 and Figure 3.4. A sample chromatogram is shown in Figure 3.5. The code for the full "Argonaut-R0" program is included in the Appendix.

Table 3.1: Program Parameters for Cation Chromatography Analysis Using the CG17 and CS17 Columns

Setting	"Stephanie3_Auto_AS"	"Argonaut_R0"
Flowrate	0.5 ml/min	0.5 ml/min
Column Temperature	30 °C	30 °C
Cell Temperature	30 °C	30 °C
Eluent Concentration	5.5 – 38.5 mM	5.5 – 38.5 mM
Suppressor Current	77 mA	50 mA
Program Length	50 min	50 min
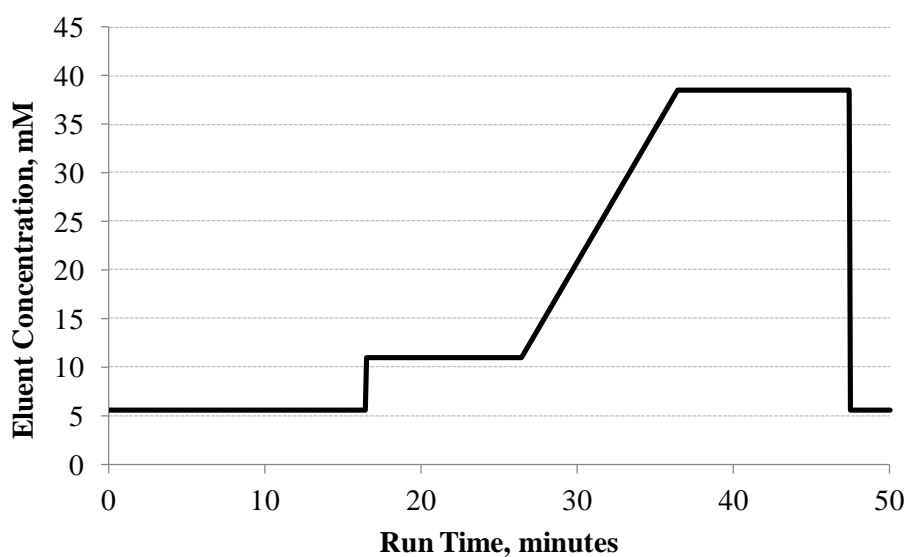
Figure 3.4: MSA Gradient Ramp for "Stephanie_3_Auto_AS" and "Argonaut_R0" chromatography programs
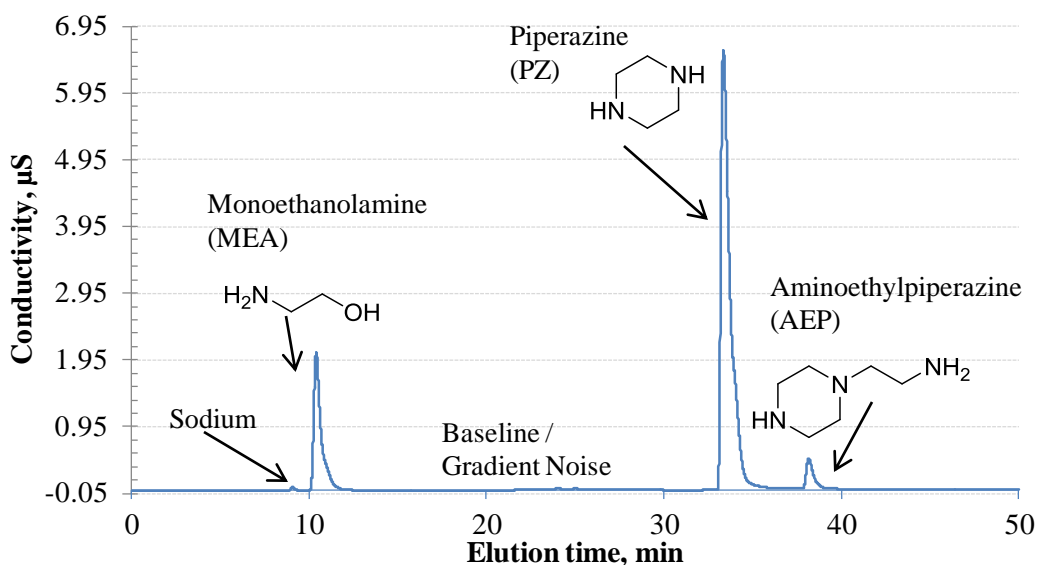
Figure 3.5: Chromatogram of degraded 7 m PZ / 2 m MEA solution using the "Stephanie_3_Auto_AS" program

In Figure 3.5, monoethanolamine (MEA) elutes at approximately 10.5 minutes; piperazine (PZ), a diamine, elutes at 33.5 minutes, and aminoethylpiperazine (AEP), a triamine, elutes approximately at 38.5 minutes. In general, monoamines elute anywhere between 10 and 20 minutes, diamines elute anywhere between 28 and 36 minutes, triamines elute anywhere between 36 and 40 minutes, and tetramines and larger polyamines elute after 40 minutes using either "Stephanie_3_Auto_AS" or "Argonaut_R0." Tertiary amines generally elute after secondary amines, which elute after primary amines. Understanding the time at which a particular amine elutes is helpful in understanding the byproduct slate. Suspected degradation products can be assigned peaks based on elution times, especially if a product predicted by a pathway is suspected to exist in MS spectra.

Methods and Chromatograms – CG19/CS19

The CG19 guard column and the CS19 analytical column were used to separate analytes that would elute at the same time with the CG17/CS17 column. This method was used to understand the formation of methylaminoethanol (MAE) and diethanolamine (DEA), degradation products of PZ-promoted MDEA that had identical elution times. A new set of programs, dubbed "Nautilus," was created to separate the two compounds. The programs are run sequentially: the sample is injected to run the first program ("Nautilus_DEAMAE"), and then a deionized water blank is injected and the second program ("Nautilus_DEAMAE_Flush_R1") is used to remove bulkier monoamines and heavier polyamines from the column from the injection of the first sample. The program parameters are shown in Table 3.2. The "Nautilus_DEAME" uses a constant acid concentration; the "Nautilus-DEAMAE_Flush_R1" uses a MSA concentration of 40 mM for the first 45 minutes to remove polyamines and a MSA concentration 1 mM for the last 12.5 minutes to equilibrate the column prior to sample injection. Sample chromatograms are shown in Figure 3.6 and 3.7. The code for the "Nautilus" programs is included in the Appendix.

Table 3.2: Program Parameters for Cation Chromatography Analysis Using the CG19 and CS19 Columns

Setting	"Nautilus_DEAMAE"	"Nautilus_DEAMAE_Flush_R1"
Flowrate	0.4 ml/min	0.4 ml/min
Column Temperature	30 °C	30 °C
Cell Temperature	30 °C	30 °C
Eluent Concentration	1 mM	40 mM, 0-45 min
		1 mM, 45-57.5 min
Suppressor Current	5 mA	48 mA
Program Length	90 min	57.5 min
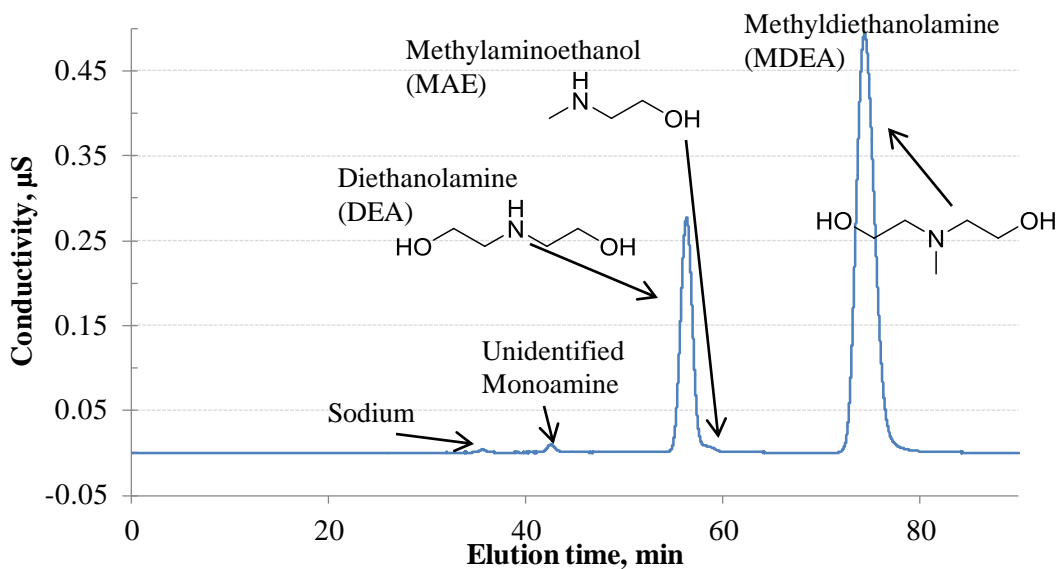
Figure 3.6: Chromatogram of degraded 2.5 m PZ / 2.5 m MDEA at a loading of 0.14 mol H+/mol alkalinity using the "Nautilus_DEAMAE" program
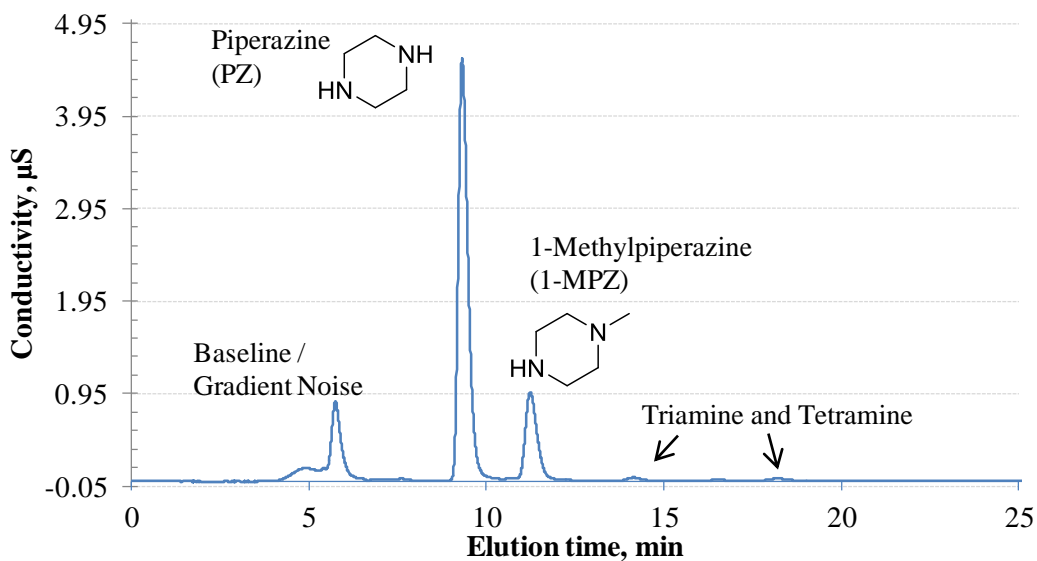
Figure 3.7: Chromatogram of degraded 2.5 m PZ / 2.5 m MDEA at a loading of 0.14 mol H+/mol alkalinity using the "Nautilus_DEAMAE_Flush_R1" program; length cropped to 25 minutes from 57.5 minutes

Standards and Product Identification

Standard curves of parent amines as well as degradation products had to be made to quantify the amount of amine present. Because suppressed ion chromatography was used, a quadratic fit was used to generate most standard curves. A linear calibration curve was able to be used on positively-charged quaternary amines. Standard curves will, in general, overlap if the standard is determined using a mole basis and if the amine species are structurally similar to one another. This can be used to obtain an estimate of the concentration of amines that are suspected to exist but cannot be quantified due to commercial standards being unavailable and was used by Davis (2009) to estimate the concentration of polyamines found in monoethanolamine (MEA) thermal degradation. An example is shown in Figure 3.8.
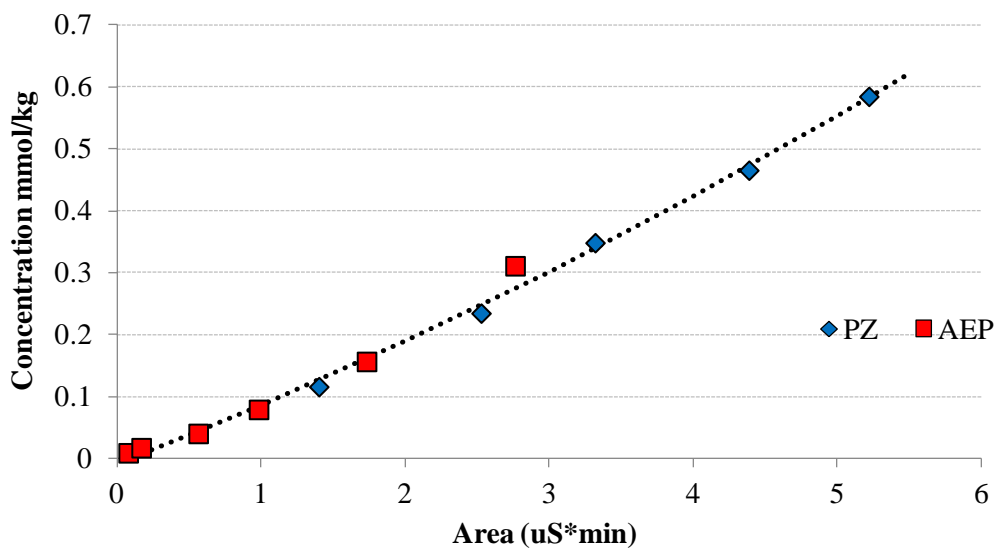
Figure 3.8: Standard curve of PZ and AEP on a mole basis using cation chromatography

Products were identified using a combination of retention-time matching for major products if standards were available. A separate low resolution LC-MS analysis was used to match suspected products predicted by mechanisms and cation chromatography elution times based on molecular weight. A coupled IC-MS analysis was not available due to the MS not being designed for the corrosive eluent used in ion chromatography.

Sample Preparation for Cation Analysis

Amine samples were diluted by a factor of about 5000 to 10000 in 18.2 μmho deionized water to generate a diluted sample of about 30 to 60 ppmw total amine for analysis. The maximum concentration of amine that the unit can accept is about 100 ppmw; higher concentrations will saturate the stationary phase and give non-representative results. A Mettler-Toledo analytic lab balance with an accuracy of 0.1 mg was used to record the mass of amine and water used in the dilutions. Samples were diluted serially in autosampler vials. The concentrated amine sample is first diluted by a factor of 70 to 100 in a 1.5 ml borosilicate glass vial by adding 15 to 20 mg of sample in 1.485 g deionized water; the diluted sample is then vortexed to mix the amine and water. This sample is referred to as the "100X" sample. The "100X" sample is then diluted again by a factor of 70 to 100 in a 1.5 ml polypropylene vial, vortexed, and then analyzed by cation chromatography. This is referred to as the "10000X" sample.

Borosilicate glass can slowly leach sodium ions, which can also elute on the cation chromatograph, and is the reason why the glass vials were not used to make the final dilution used in the cation analysis. They are, however, hard to confuse with plastic vials, reducing the chance that a "100X" sample is used instead of the "10000X" sample.

The "100X" samples are disposed of as chemical waste after being used to make the "10000X" samples.

Davis, Freeman, and Closmann used large 10 ml vials or beakers to dilute the samples and reduce the error from mass measurements to about zero; Voice and this work used 1.5 ml autosampler vials to dilute the samples. The use of autosampler vials to leads to an error propagation of up to 1.5% based on the mass of sample used and the accuracy of the analytic balance. The autosampler vials are single-use only; reusing and washing glass vials for dilution introduces sodium, potassium, and other ion species that can interfere with amine peaks present in solution and affect the results.

3.5.2   Low-resolution LC-MS

The low-resolution LC-MS analysis was a turnkey service provided by UT-Austin's Chemistry Department. Degraded PZ-promoted tertiary amine samples under acidified conditions were analyzed using this technique. A Dionex Ultimate 3000 HPLC with a Phenomenex Kinetex C18 2.1x50 mm column was used to carry out the separation. The mobile phase consisted of 0.7 ml/min of 98% H_2O / 2% MeOH linearly ramped to 98% MeOH / 2% H2O over 8 minutes. A ThermoFinnigan TSQ Quantum was used as the detector and was run under positive electrospray ionization mode. Samples were diluted to about 50 ppmw amine.

The chromatogram indicates that all of the amines eluted at one point and, as a result, the LCMS analysis effectively functioned like a direct-injection mass spectrometry analysis. A sample chromatogram from the LC-MS along with the mass spectra of PZ-promoted dimethylaminoethoxyethanol (DMAEE) is shown in Figure 3.9 and 3.10.

In Figure 3.9, the peak corresponding to a retention time of 0.15 min is the amine and includes PZ, DMAEE, and amine-based degradation products. The amine products were not able to be separated using the LC-MS separation technique.

The mass spectrum shown in Figure 3.10 corresponds to the peak with the retention time of 0.15 min. The peaks corresponding to m/z ratios of 87 and 134 correspond to PZ and DMAEE, respectively, and the peaks corresponding to m/z ratios of 101 and 120 are major degradation products 1-MPZ and methylaminoethoxyethanol, respectively, of PZ-promoted DMAEE.
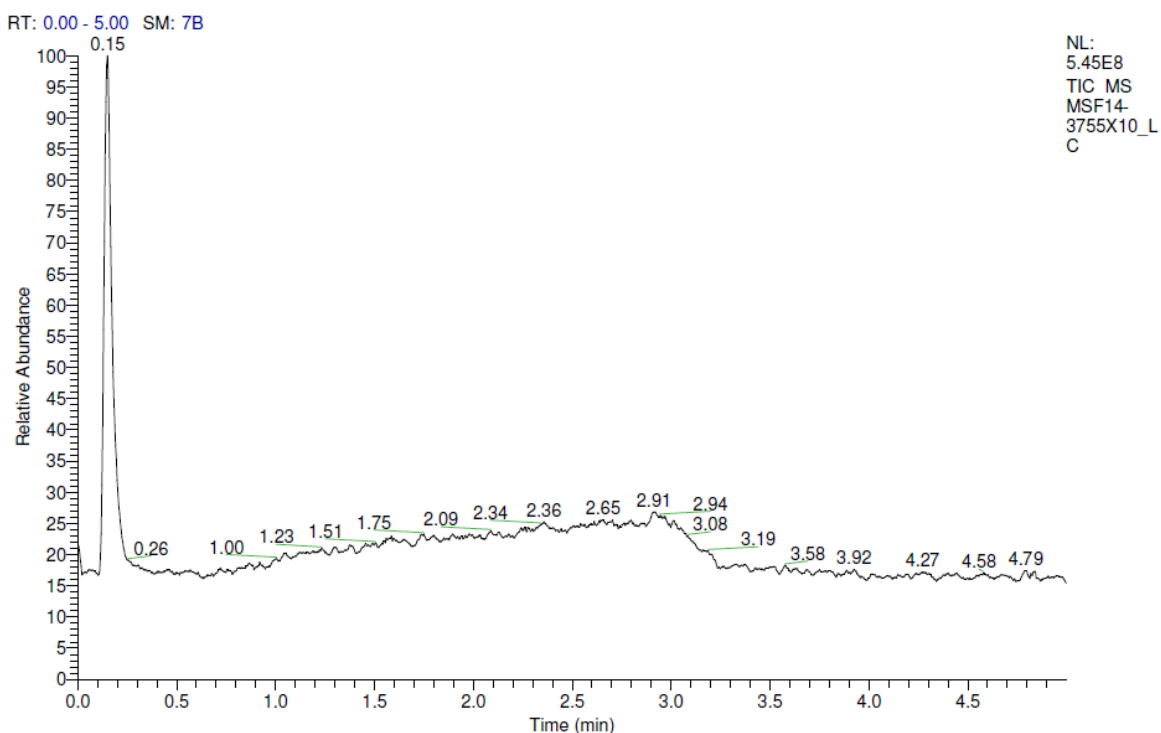
Figure 3.9: LC-MS chromatogram of degraded PZ-promoted DMAEE
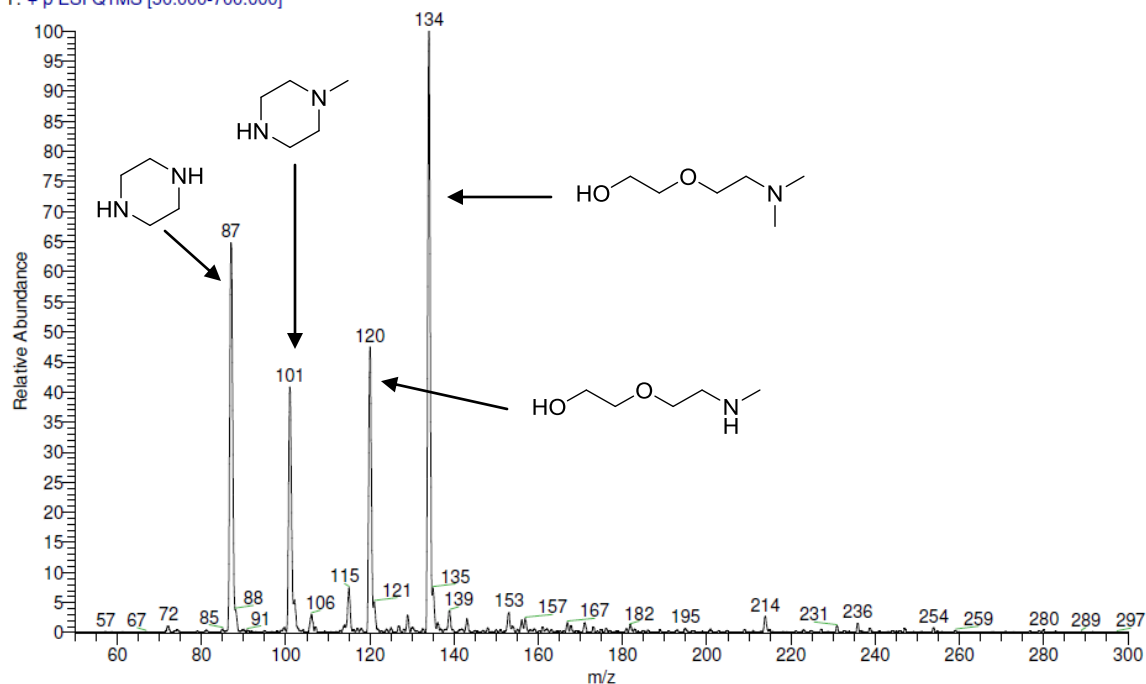
Figure 3.10: Mass spectrum of degraded PZ-promoted DMAEE at a retention time of 0.15 minutes

3.5.3 Total Alkalinity

The total alkalinity measurement was used to determine the alkalinity of degraded solutions and used to quantify the concentration of amine groups in degraded solvents that were still capable of reaction with CO_2. In this work, alkalinity measurements were used as a proxy to estimate amine degradation in systems that are not constrained by rate or mass transfer but are constrained by capacity. The methods used are identical to those used by Freeman (2011), Davis (2009), and Chen (2011).

A Metrohm 830 automatic titrator with a Metrohm 801 stir plate was used to conduct the titration analysis using 0.1 molar sulfuric acid as the titrant. 0.2 g of amine solution was added to 60 g deionized water in a beaker with a magnetic stirring rod. Metrohm PC-Control software was used to control the titrator, and the method used was

51

capable of automatically detecting the endpoint in which all amine groups present in solution were protonated with the titrant. Several endpoints were commonly seen in degraded solution; all amine solvents tested had a calculated final endpoint at a pH value anywhere from 3.9 to 4.4, and the volume of acid added to solution at that endpoint was used to calculate the alkalinity of the solution.

3.6 REPRODUCIBILITY

Standard Curve Evolution

The standard curves used on the cation instrument can shift over time as the internals of the column are degraded. A set of calibration standards of PZ and MDEA taken over 1.5 years are shown as examples in Figures 3.11 and 3.12, and the average values, standard deviation, and relative standard deviation of both calibration curves is summarized in Table 3.3.
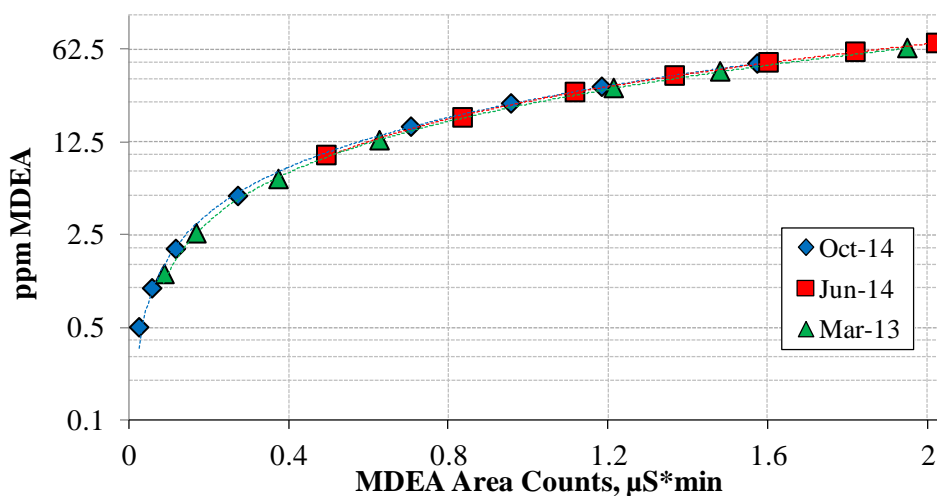
Figure 3.11: Evolution of MDEA standard curves on the cation chromatograph
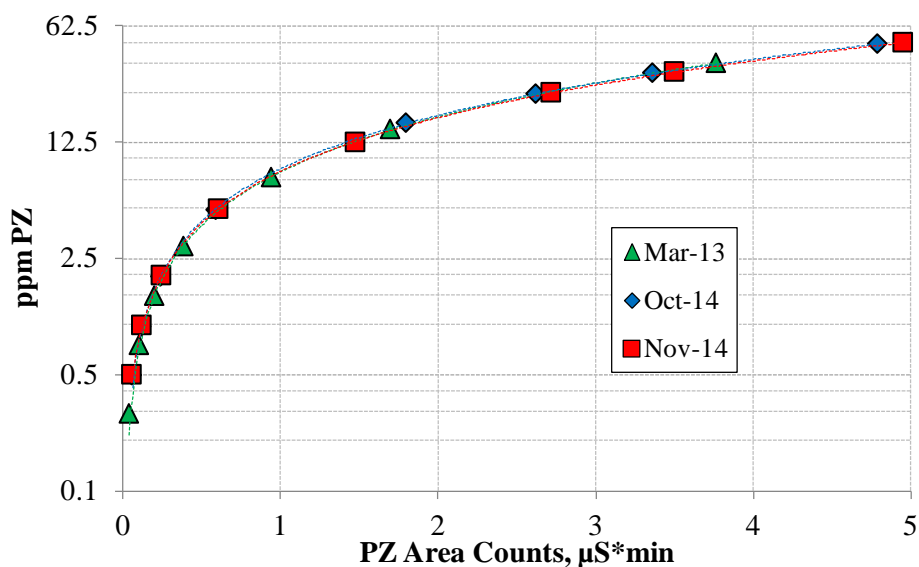
Figure 3.12: Evolution of PZ standard curves on the cation chromatograph

Table 3.3: Average Concentration, Standard Deviation, and Relative Standard Deviation of Calibration Curves of PZ and MDEA

Amine	Average Concentration (ppm) at 1.2 µS	Standard Deviation (ppm)	Relative Standard Deviation
PZ	10.29	0.24	2.37 %
MDEA	32.95	1.45	4.40 %

Combined Expected Dilution, Cylinder, and Instrument Error

Samples of PZ-promoted Dimethylaminopropanol (DMAP) at a loading of 0.23 mol CO_2/mol alkalinity were degraded for approximately 115 hours using the second-generation stainless steel cylinders. Three cylinders were degraded for each solvent, each cylinder was diluted six separate times, and each diluted sample, of which there were 18, was analyzed using cation chromatography. These results are shown in Table 3.4.

Table 3.4: Average Concentration, Standard Deviation, and Relative Standard Deviation of Calibration Curves of PZ and DMAP

Cylinder #	PZ Average Concentration (mmol*kg^{-1})	PZ Standard Deviation (mmol*kg^{-1})	PZ Relative Standard Deviation	DMAP Average Concentration (mmol*kg^{-1})	DMAP Standard Deviation (mmol*kg^{-1})	DMAP Relative Standard Deviation
1	1993	31	1.57%	2051	25	1.24%
2	1998	34	1.68%	2054	28	1.36%
3	2013	34	1.67%	2066	28	1.35%
Average (Cylinders 1, 2, and 3)	2001	10	0.51%	2057	8	0.40%

The error propagation for the experiment due to variation in the cation analysis, dilution, and experimental values can be estimated using Eq. 3.2 (Lindberg 2000):

$$\text{Propagation (\%)} = \sqrt{\sum_{i=1}^{n} (\text{RSD}_i)^2} \qquad\qquad \text{Eq. 3.2}$$

In Eq. 3.2, RSD represents the relative standard deviation for each component i of the experiment and/or analysis. If the relative standard deviation from each cylinder is assumed to be ±0.5%, the relative standard deviation for each dilution and instrument measurement is assumed to be ±1.5%, and the relative standard deviation from calibration assumed to be ±4%, the error propagation for each discrete point is ±4.3% (Lindberg 2000) and is consistent with Freeman's observation that the propagated error is about ±5% (Freeman 2011).

Replicate Experiments

Two different solutions of 5 m PZ / 5 m MDEA solution initially at about 0.23 mol CO_2/alkalinity were degraded and the degradation rate of PZ and MDEA was estimated using a first-order rate model; the modeling technique is described in Chapter 4. The two solutions, whose raw data can be found in Tables B.1.13 and B.4.5 in the appendix, were prepared separately and used different calibration curves to estimate the concentration present in degraded and undegraded solution. The results are shown in Table 3.5.

A statistical test was used to determine whether degradation rate constants of PZ and MDEA degradation from both experiments were statistically identical at a significance level of 0.05, corresponding to a confidence interval of 95%. The method used in this work is exactly the same method used by Freeman (2011).

In Table 3.5, S_X^2 is the variance of the x-variable or experiment time, $S_{P,Y/X}^2$ is the pooled estimate of variance for the two experiments and is computed from the mean-square error, or $S_{Y/X}^2$, of the experiment. These two values are then used to compute the absolute value of the *T*-statistic; the computed value of *T* can be compared to the student's t-value. If the absolute value of *T* is less than the student's t-value for the corresponding degrees of freedom, the rate constants can be considered to be statistically similar. These data are summarized in Table 3.5 and are calculated using Equations 3.3 to 3.6, which have been adapted from Freeman (2011).

$$S_X^2 = \frac{1}{n-1}\sum_{i=1}^{n}\left(x_i - \bar{x}\right)^2 \qquad\qquad \text{Eq. 3.3}$$

$$S_{Y/X}^2 = \frac{1}{n-2}\sum_{i=1}^{n}\left(y_i - y_{i,\text{Regressed}}\right)^2 \qquad\qquad \text{Eq. 3.4}$$

$$S_{P,Y/X}^2 = \frac{(n_1 - 2) * S_{Y/X,1}^2 + (n_2 - 2) * S_{Y/X,2}^2}{n_1 + n_2 - 4}$$

Eq. 3.5

$$T = \frac{|m_1 - m_2|}{\sqrt{S_{P,Y/X}^2 * \left[\frac{1}{(n_1 - 1) * S_{X,1}^2} + \frac{1}{(n_2 - 1) * S_{X,2}^2}\right]}}$$

Eq. 3.6

In these equations, numeric subscripts on all variables indicate the experiment replicate. The values of m correspond to the regressed value of the first-order rate constant. x corresponds to experiment time, and y corresponds to the natural logarithm of the amine concentration. n denotes the number of experimental points used in the analysis for a given experiment.

Table 3.5: Statistical data of two different experiments to compare significance of degradation constants of PZ-promoted MDEA

Parameter	MDEA		PZ	
	Expt 1	Expt 2	Expt 1	Expt 2
n	11	10	11	10
m $(hr^{-1}*10^3)$	-1.17	-1.07	-2.76	-2.89
S_X^2	82200	91400	82200	91400
$S_{Y/X}^2$	0.00239	0.00110	0.00313	0.00256
$S_{P,Y/X}^2$	0.00178		0.00286	
T	1.52		1.56	
Student's t-value^	2.11		2.11	

^ t-value computed with DOF of 17 and significance of 0.05

The preceding analysis indicates that the rate constants for both experiments are not statistically different from each other at the given significance level. These data in linearized form are shown in Figure 3.13.
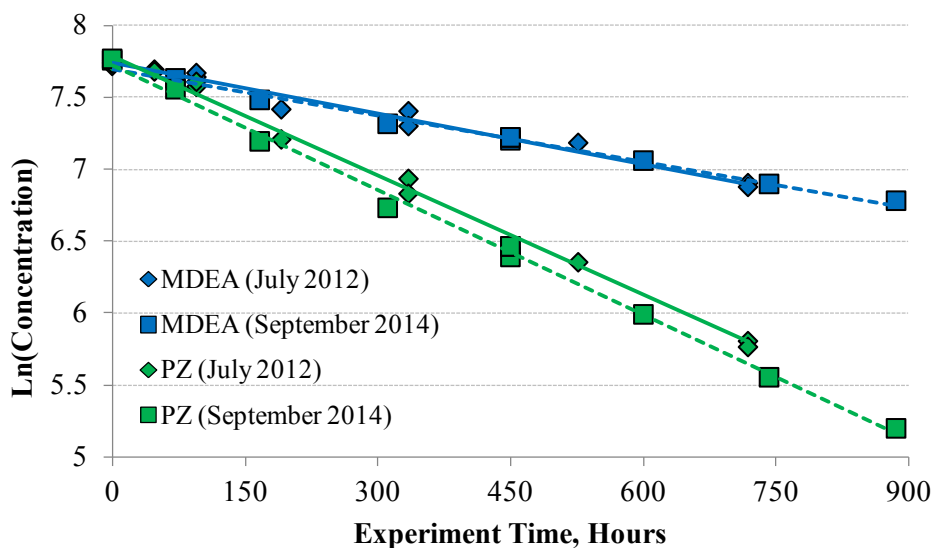
Figure 3.13: Comparison of degradation rate of PZ-promoted MDEA initially at 5 m PZ, 5 m MDEA, and 0.23 mol CO₂/mol alkalinity at 150 °C

Chapter 4: Degradation of Piperazine (PZ)-Promoted Tertiary Amines in CO$_2$-Loaded Solvents

4.1 INTRODUCTION & SCOPE

Practical results of the degradation of CO$_2$-loaded PZ-promoted tertiary amine solvents as well as MDEA solvents with other rate promoters are presented in this chapter. The rate of PZ reaction with oxazolidone-forming amines is also presented in this chapter. These results are helpful in understanding the effects of structure on the degradation rate, to a lesser extent, the effects of amine concentration, loading, and temperature on the degradation rate. The data are then interpreted to generate a maximum stripping temperature (T$_{MAX}$) value, which can be used to set a process envelope on the regeneration temperature of a process plant. These results and analysis do not explicitly account for amine speciation and other properties, such as tertiary amine pKa, to model thermal degradation; these data are presented in Chapters 5 and 6. Table 4.1 gives the tertiary amines and rate promoters that were tested. Raw data for all experiments in this chapter is presented in Appendix B.1.

Table 4.1:Amines Tested

Amine Promoters

Amine	Abbreviation / CAS#	MW	Supplier / Purity (wt%)
Piperazine	PZ 110-85-0	86.1	Sigma-Aldrich 99%
Bis(aminoethyl)ether	BAE 2752-17-2	104.2	Huntsman Chemical 95.5%
Hexamethylenediamine	HMDA 124-9-4	116.2	Sigma-Aldrich 98%
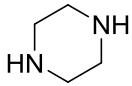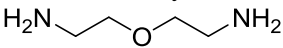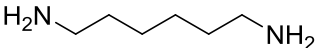
Table 4.1: Amines Tested (continued)

Tertiary Amines

Amine	Abbreviation / CAS#	MW	Supplier / Purity (wt%)
Methyldiethanolamine	MDEA 105-59-9	119.2	Acros Organics 99%
Dimethylaminoethanol	DMAE 108-1-0	89.1	Sigma-Aldrich 99.5%
Dimethylaminopropanol	DMAP 3179-63-3	103.2	Sigma-Aldrich 99%
Dimethylamino-isopropanol	DMAIP 108-16-7	103.2	Sigma-Aldrich 99%
Dimethylaminobutanol	DMAB 13330-96-6	117.2	Tokyo Chemical Industry 98%
Dimethylaminoethoxy-ethanol	DMAEE 1704-62-2	133.2	Sigma-Aldrich 98%
Ethyldiethanolamine	EDEA 139-87-7	133.2	Sigma-Aldrich 98%
n-Butyldiethanolamine	nBuDEA 102-79-4	161.2	Sigma-Aldrich 98.6%
tert-Butyldiethanolamine	tBuDEA	161.2	Sigma-Aldrich 97%
Diethylaminoethanol	DEAE 100-37-8	117.2	Sigma-Aldrich 99.5%
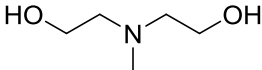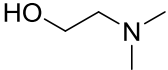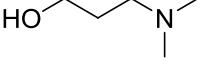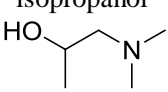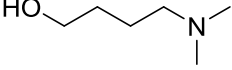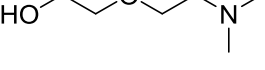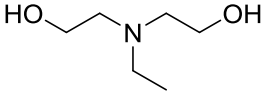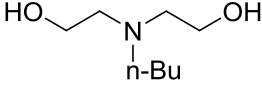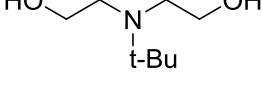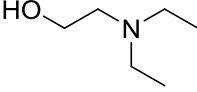
Table 4.1: Amines Tested (continued)

Tertiary Amines (continued)

Amine	Abbreviation / CAS#	MW	Supplier / Purity (wt%)
Triisopropanolamine	TIPA 122-20-3	191.3	Sigma-Aldrich 95%
Hydroxyethyl-morpholine	HEM 622-40-2	131.2	Acros Organics 99%
Hyroxypropyl-morpholine	HPM 4441-30-9	145.2	Tokyo Chemical Industry 98%
Hydroxyisopropyl-morpholine	HIPM 2109-66-2	145.2	Tokyo Chemical Industry 98%
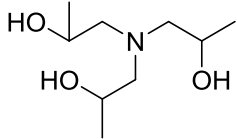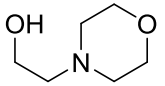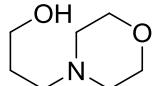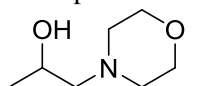
Oxazolidone-forming Amines

Amine	Abbreviation / CAS#	MW	Supplier / Purity (wt%)
Monoethanolamine	MEA 141-43-5	61.1	Acros Organics 99%
Monoisopropanolamine	MIPA 78-96-6	75.1	Sigma-Aldrich 93%
2-Amino-2-Methyl-1-Propanol	AMP 124-68-5	89.1	Acros Organics 99%
Methylaminoethanol	MAE 109-83-1	75.1	Acros Organics 99%
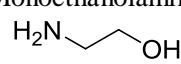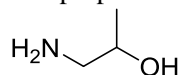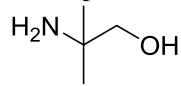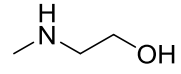
Table 4.1: List of Amines Tested (continued)

Oxazolidone-forming Amines (continued)

Amine	Abbreviation / CAS#	MW	Supplier / Purity (wt%)
Ethylaminoethanol	EAE 110-73-6	89.1	Sigma-Aldrich 98%
Diethanolamine	DEA 111-42-2	105.1	Acros Organics 99%
Monopropanolamine	nBuDEA 156-87-6	75.1	Acros Organics 99%
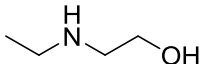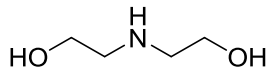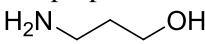
4.2 MODELING DEGRADATION OF CO_2-LOADED PZ-PROMOTED TERTIARY AMINE SOLVENTS

Pseudo first-order rate models with respect to the parent amine concentrations were used to estimate degradation rate constants for promoted tertiary amines degraded in the presence of CO_2. These models show reasonable agreement with the experimental data for the initial amine loss rate, can be used to compare the effects of tertiary amine structure on the thermal degradation rate, and have been used to model degradation of various amine solvent systems (Davis 2009, Freeman 2011, Huang 2014) in the literature. Equations 4.1 and 4.2 were used to determine the rate constants k for the tertiary amine, denoted as TA, and PZ, respectively. Their integrated forms are shown in Equations 4.3 and 4.4. A plot showing the degradation of PZ-promoted MDEA and DMAP using these models is shown in Figure 4.1.

$$\frac{dC_{PZ}}{dt} = k_{1,PZ} * C_{PZ} \qquad \text{Eq. 4.1}$$

$$\frac{dC_{TA}}{dt} = k_{1,TA} * C_{TA} \qquad \text{Eq. 4.2}$$

$$\ln(C_{PZ}) = k_{1,PZ} * t \qquad\qquad\qquad\qquad \text{Eq. 4.3}$$

$$\ln(C_{TA}) = k_{1,TA} * t \qquad\qquad\qquad\qquad \text{Eq. 4.4}$$

In Eq. 4.1 to 4.4, $k_{1,PZ}$ and $k_{1,TA}$ are the first-order degradation rate constants for PZ and the tertiary amine in $\sec^{-1}$. t is the experimental time in seconds, and C_{PZ} and C_{TA} represent the concentration of PZ and tertiary amine in mol/kg.
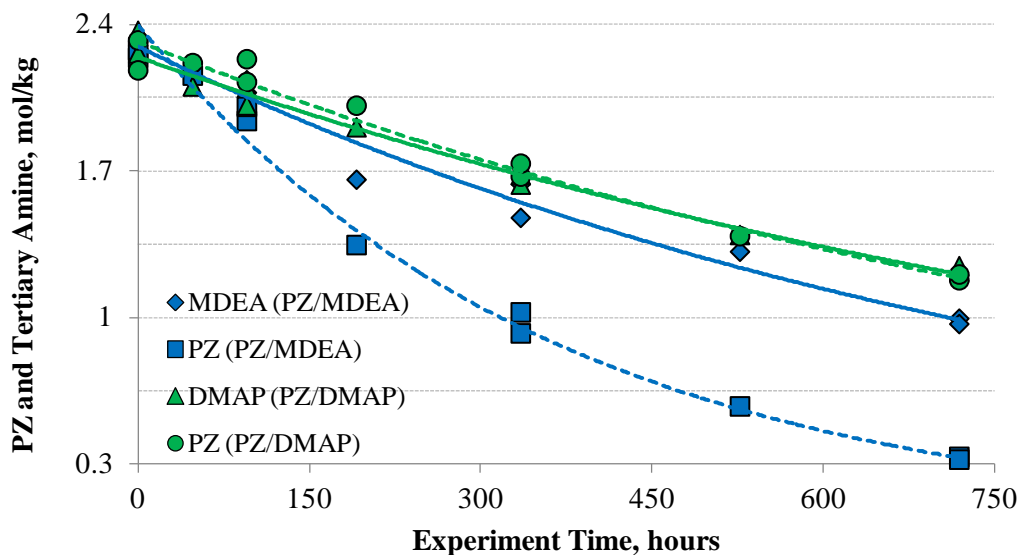
Figure 4.1: Fit of first-order rate models modeling PZ-promoted MDEA (Blue) and PZ-promoted DMAP (Green) thermal degradation. Initial conditions: 5 m PZ / 5 m tertiary amine, 0.23 mol CO_2/mol alkalinity, 150 °C

The primary initial degradation pathway of PZ-promoted tertiary amine solvents proposed by Closmann (2011), shown in Figures 4.2 and 4.3, suggests that the degradation of the tertiary amine follows overall second-order kinetics with free PZ participating in a S_N2 substitution with a protonated tertiary amine to form 1-methylpiperazine (1-MPZ) and diethanolamine (DEA).

This pathway indicates that the initial rate constant of PZ degradation and MDEA degradation should be similar. However, PZ is free to interact with other degradation

products present, such as oxazolidone-forming amines. DEA, in the presence of CO_2, can degrade via the carbamate polymerization pathway to form hydroxyethyloxazolidone (HEOD) (Kohl 1960) from DEA carbamate (DEACOO⁻). HEOD can then rapidly react with PZ, forming a hydroxyethylaminoethylpiperazine (HeAEtPZ), which is a polyamine byproduct (Davis, 2009) that can continue to react with PZ via the carbamate polymerization pathway due to the presence of the hydroxyethyl functional group attached to a secondary amino group. These reactions are shown in Figure 4.3.
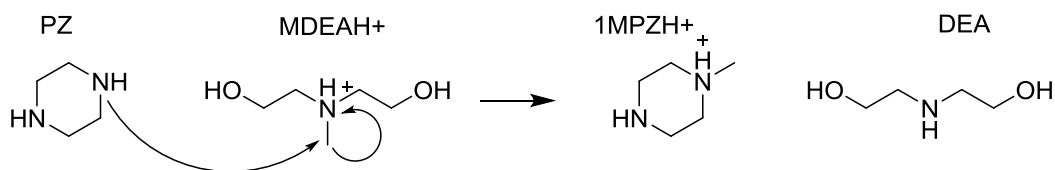
Figure 4.2: Proposed initial degradation step to form protonated 1-methylpiperazine (1MPZ) and diethanolamine (DEA) from PZ and protonated MDEA (Closmann 2011)
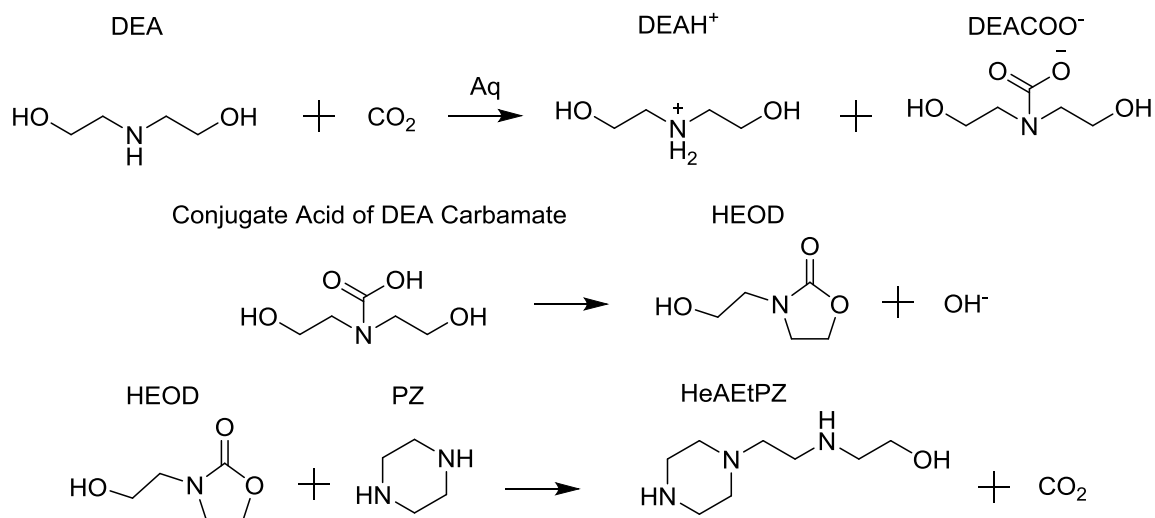
Figure 4.3: Proposed degradation pathway of PZ and intermediate byproducts of PZ-promoted MDEA degradation: hydroxyethyloxazolidone formation and PZ reaction with HEOD to form polyamines (summarized from Closmann (2011))

63

A proposed, generalized pathway that covers the degradation route of promoted tertiary aliphatic amines is presented in Figure 4.4 and is similar to the proposed pathway of PZ-promoted MDEA degradation shown in Figure 4.2.
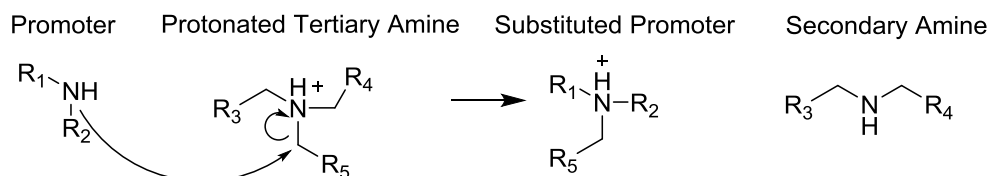
Figure 4.4: Generalized initial degradation step of promoted tertiary amine degradation, forming a substituted promoter and a secondary amine byproduct. R denotes either hydrogen or another functional group

Davis (2009) noted that primary and secondary amines that have hydroxyethyl or hydroxypropyl functions attached to the amino group are all capable of reacting with strong nucleophiles, such as PZ, through the same pathway shown in Figures 4.3 and in the presence of CO_2 and is shown in Figure 4.5.

Based on the initial degradation pathway shown in Figures 4.2 and 4.4, a second-order model was used to fit the data for PZ-promoted MDEA and PZ-promoted DMAP. This model is shown in Equation 4.5. The rate of degradation was estimated using a finite difference method, shown in Equation 4.6 (Fogler 2005), and also using Euler's method (Billo 2001, van Riel 2014). The initial starting point for calculating the rate using Euler's method, which was not varied, was set to be equal to experimental data. These data are shown in Figures 4.6 and 4.7 as well as Table 4.2. The rate constants predicted by Euler's method and by the method of estimating rate using finite differences, such as in Eq. 4.6, are virtually identical. Finite difference methods to calculate rate constants are extensively used in Chapters 5 and 6, and their calculation procedure is presented in Appendix A.3.

64
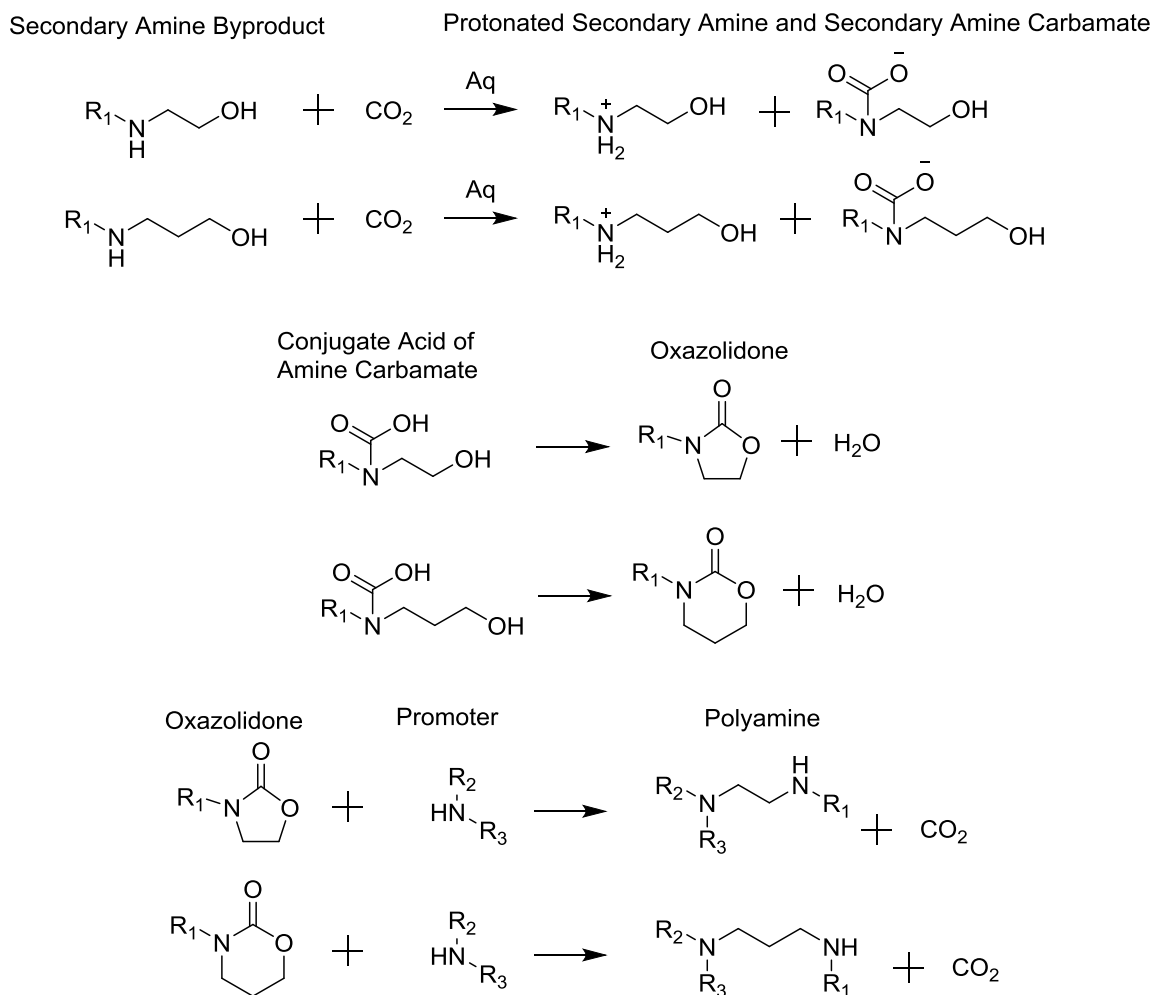
Figure 4.5: Proposed degradation pathway of rate promoter and intermediate secondary amine byproduct of promoted tertiary amine degradation. R denotes either hydrogen or another functional group (summarized from Lepaumier (2009))

$$\frac{dC_{PZ}}{dt} = \frac{dC_{TA}}{dt} = k_2 * C_{PZ} * C_{TA}$$

Eq. 4.5

$$\frac{d(C)}{dt}\bigg|_i \approx \frac{C_{i-1} - C_{i+1}}{2*(t_i - t_{i-1})}$$

Eq. 4.6

In Eq. 4.5 and 4.6, k_2 is the second-order degradation rate constant in $kg*mol^{-1}*sec^{-1}$. t is the experimental time in seconds, C_{PZ} and C_{TA} represent the concentration of PZ and tertiary amine in mol/kg, and i represents the ith experimental point.

Table 4.2: Comparison of 2nd-Order Rate Parameters for PZ-promoted MDEA and PZ-promoted DMAP initially at 5 m PZ / 5 m tertiary amine, 0.23 mol CO$_2$/mol alkalinity, and 150 °C

PZ-promoted DMAP		PZ-promoted MDEA	
k_2, Finite Difference, $kg*mol^{-1}*sec^{-1}*10^9$	k_2, Euler's Method, $kg*mol^{-1}*sec^{-1}*10^9$	k_2, Finite Difference, $kg*mol^{-1}*sec^{-1}*10^9$	k_2, Euler's Method, $kg*mol^{-1}*sec^{-1}*10^9$
140±36	138	322±137	310
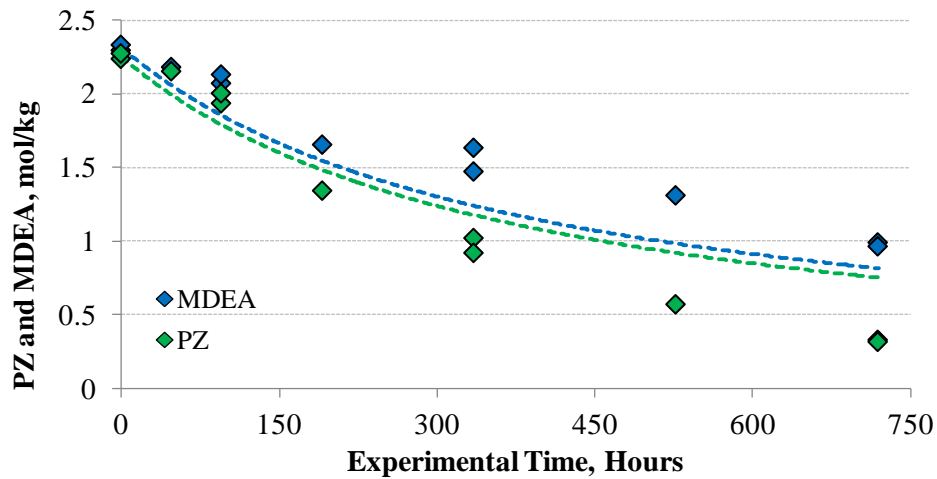
Figure 4.6: 2nd-order rate model fit of PZ-promoted MDEA, initially at 5 m PZ / 5 m MDEA, 0.23 mol CO$_2$/mol alkalinity, and 150 °C
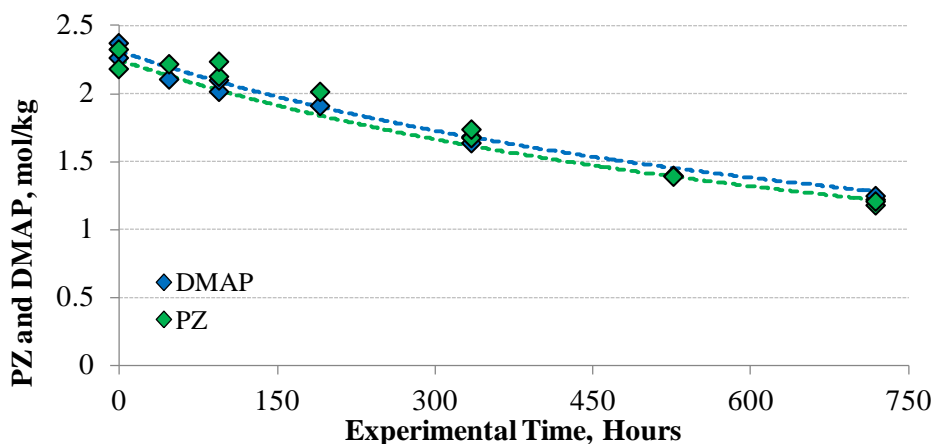
Figure 4.7: 2nd-order rate model fit of PZ-promoted DMAP, initially at 5 m PZ / 5 m MDEA, 0.23 mol CO2/mol alkalinity, and 150 °C

At nearly identical initial amine concentration, DMAP and PZ in PZ-promoted DMAP degrade at a nearly identical rate, whereas PZ in PZ-promoted MDEA degrades at a greater rate than MDEA. These trends are reflected in the behavior of the second-order model. PZ-promoted DMAP is able to be modeled relatively well using a 2nd-order fit, whereas PZ-promoted MDEA is not: the model overpredicts MDEA degradation and underpredicts PZ degradation. This discrepancy can be best described by the ability of PZ to interact with DEA to form intermediate byproducts, which the model does not account for; the intermediate degradation product of PZ-promoted DMAP is not susceptible to degradation as evidenced by the nearly identical degradation rate of PZ and DMAP. The degradation rate will also vary as the concentration of protonated and free amine changes, which can occur as amine byproducts with different pKa values are generated. Fundamental modeling of PZ-promoted tertiary amine degradation that explores these phenomena is presented in Chapters 5 and 6.

67

4.3   DEGRADATION OF CO₂-LOADED PZ-PROMOTED TERTIARY AMINE SOLVENTS AS A FUNCTION OF AMINE STRUCTURE

The following sections summarize rate results of promoted tertiary amines. The initial concentration, temperature, and amine loading were held constant so the effect of amine structure on degradation could be understood. The loading of about 0.23 mol CO_2/mol alkalinity used for these experiments corresponds to the operational lean loading of 5 m PZ / 5 m MDEA when used to capture CO_2 from coal-fired power plants.

4.3.1   Degradation of PZ-Promoted Tertiary Amine Solvents with at Least One Methyl Group

Tertiary amines with at least one methyl group, compared to other tertiary amine solvents, have the greatest rate of degradation. The degradation rate of PZ-promoted tertiary methylamines at 150 °C and initially at 5 m PZ / 5 m Tertiary Amine and about 0.23 mol CO_2/mol alkalinity is shown in Table 4.3 and Figures 4.8 and 4.9.

The rate of PZ degradation was about 2.3 times, 1.5 times, and 1.4 times as great as the tertiary amine degradation rate in PZ-promoted MDEA, DMAE, and DMAIP Both MDEA and DMAE have at least one hydroxyethyl functional group; their intermediate products, DEA and MAE, can readily form oxazolidones in the presence of CO_2 that can readily react with strong nucleophiles like PZ. Hydroxyisopropyl functional groups can also readily form oxazolidones (Davis, 2009) and can react with PZ. Thus, up to 2 equivalents of PZ are initially lost with each equivalent of tertiary amine for PZ-promoted DMAE, MDEA, and DMAIP. The intermediate formed from PZ and HEOD, the oxazolidone formed from DEA carbamate, can also form an oxazolidone, indicating that up to 3 equivalents of PZ can be lost with each equivalent of MDEA lost in severely-degraded solutions of PZ-promoted MDEA.

The degradation rate of PZ in PZ-promoted DMAEE and DMAP is statistically similar to the tertiary amine and suggests that PZ does not readily react with the intermediate secondary amine degradation product in these solvents.

DEA, MAE, and Methylaminopropanol (MAP), which are the initial secondary monoamine degradation products of MDEA, DMAE, and DMAP, respectively, were quantified in degraded solutions and are shown in Figure 4.10 and Table 4.4. These data indicate that DEA and MAE act as reactive intermediates whereas MAP accumulates in degraded solutions. DEA, MAE, and MAP all degrade through the carbamate
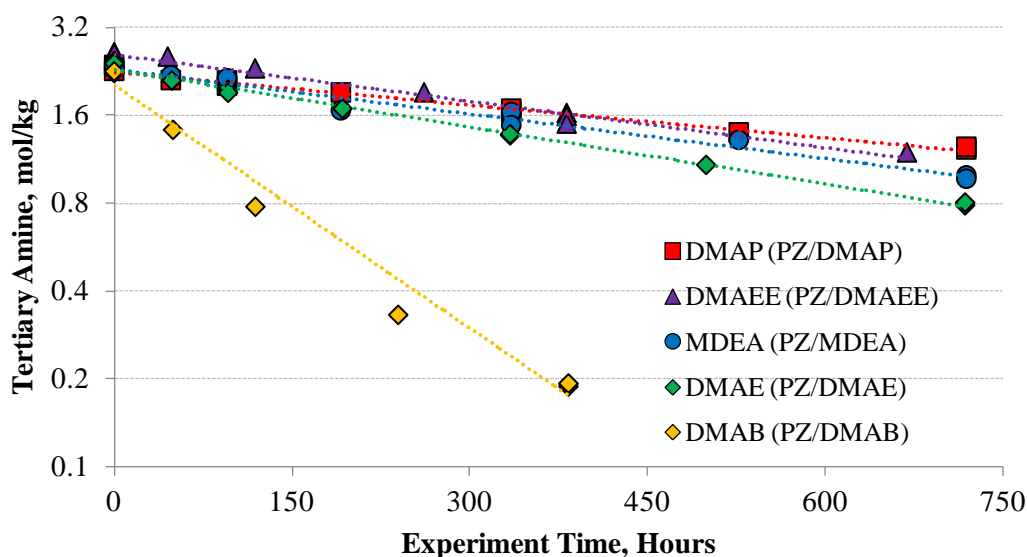
Figure 4.8: First-order rate model fit of tertiary amine loss in degradation of PZ-promoted tertiary amine solvents with at least one methyl group, initially at 5 m PZ / 5 m tertiary amine, 0.23 mol CO_2/mol alkalinity, and 150 °C

69
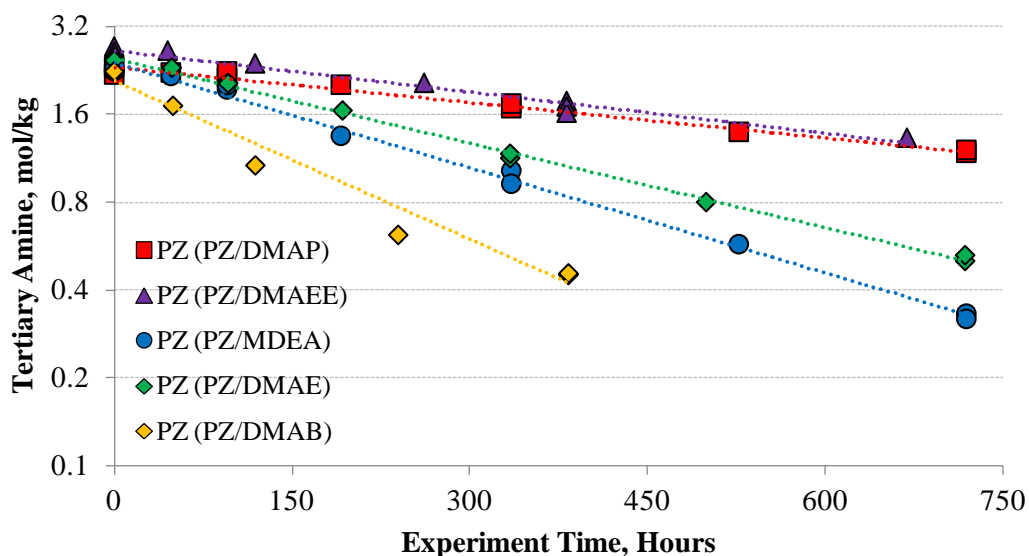
Figure 4.9: First-order rate model fit of PZ loss in degradation of PZ-promoted tertiary amine solvents with at least one methyl group, initially at 5 m PZ / 5 m tertiary amine, 0.23 mol CO_2/mol alkalinity, and 150 °C

polymerization pathway, with their oxazolidones reacting with PZ to form polyamines. The MAP carbamate would form a six-membered oxazolidone versus a five-membered oxazolidone. These data are consistent with the data of Davis (2009), who indicated that alkanolamines with three carbons between the amino and hydroxyl groups degrade at a reduced rate to the alkanolamines with two carbons between the amino and hydroxyl groups at identical CO_2 loading.

Table 4.3: Comparison of First-Order Rate Parameters for Thermal Degradation of PZ-promoted Tertiary Amines with at Least One Methyl Group. Conditions: 5 m PZ / 5 m TA initially, 150 °C

Tertiary Amine	Initial CO_2 Loading mol CO_2/mol alk	k_1, TA s-1*10^9	k_1, PZ s-1*10^9	$\frac{k_1, PZ}{k_1, TA}$
DMAB	0.23	1780±210	1150±160	0.7
DMAE	0.23	417±24	617±20	1.5
DMAEE	0.23	339±40	302±41	0.9
MDEA	0.24	325±36	766±41	2.4
DMAP	0.23	240±20	258±23	1.1
DMAIP	0.22	202±12	278±11	1.4

Table 4.4: Intermediate Secondary Amine Byproducts of Thermal Degradation in 5 m PZ / 5 m Tertiary Amine Solvents

Tertiary Amine	Secondary Monoamine Byproduct	Secondary Monoamine Byproduct Structure
Methyldiethanolamine MDEA	Diethanolamine DEA	
Dimethylaminoethanol DMAE	Methylaminoethanol MAE	
Dimethylaminopropanol DMAP	Methylaminopropanol MAP	
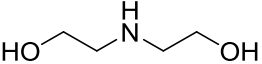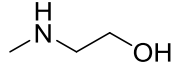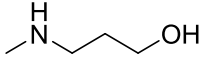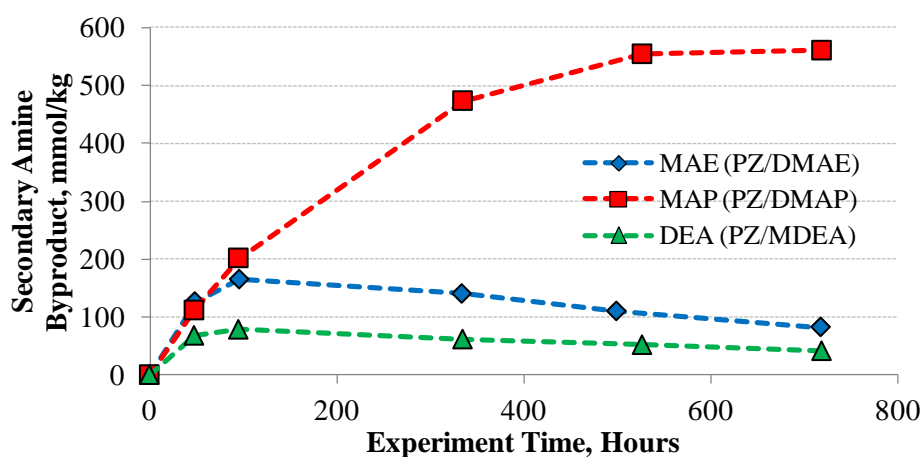
Figure 4.10: Evolution of secondary amine byproducts in PZ-promoted tertiary amine solvents with at least one methyl group. Conditions: 5 m PZ / 5 m tertiary amine and 0.23 mol CO_2/mol alkalinity initially, 150 °C

The rate of DMAB degradation is significantly higher than the degradation of other tertiary amines. It is possible that the DMAB, which has a four-membered chain between the amino group and terminal hydroxyl group, undergoes a ring-closing dehydrolysis, forming a hydroxide ion and a quaternary pyrrolodine. Molecules consistent with the molecular weights of dimethylpyrrolodine and methylpyrrolodine were observed in low-resolution mass spectra of PZ-promoted DMAB in acidified solutions, described in Chapter 6. This is shown in Figure 4.11. These observations are consistent with the degradation of putrescine (Hatchell, 2014), 4-amino-1-butanol (Davis, 2009), and tetramethylbutyldiamine (Lepaumier, 2010), amines with four-membered chains between their amino group and terminal hydroxyl or amino group, all of which formed pyrrolodine or substituted pyrrolodine as thermal degradation byproducts. The quaternary amine can then rapidly react with PZ or other nucleophiles. Hatchell (2014) and Davis (2009) also observed that amines with a five-membered chain between the amino group and the terminal hydroxyl or amino group do not readily ring close and is consistent with the rate observations in this study that suggest that PZ-promoted DMAEE initially degrades the same as PZ-promoted MDEA.
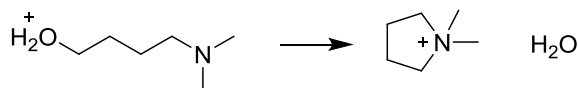
Figure 4.11: Ring-closing dehydration of DMAB to form substituted pyrrolodine

4.3.2 Degradation of PZ-Promoted Tertiary Amine Solvents with no Methyl Groups

Tertiary amines with no methyl groups, with the exception of tBuDEA, degrade more slowly than the tertiary amines with at least one methyl group. The rate of degradation is shown in Table 4.5 and Figures 4.12 and 4.13.

Table 4.5: Comparison of First-Order Rate Parameters for Degradation of PZ-promoted Tertiary Amines with no Methyl Groups. Conditions: 5 m PZ / 5 m TA initially, 150 °C

Tertiary Amine	Initial CO_2 Loading mol CO_2/mol alk	k_1, TA s-1*10^9	k_1, PZ s-1*10^9	$\frac{k_1, PZ}{k_1, TA}$
tBuDEA	0.22	1220±95	1180±170	1.0
EDEA	0.23	199±12	333±21	1.7
nBuDEA	0.23	177±21	291±26	1.6
DEAE	0.23	168±11	257±5	1.5
TEA	0.22	161±27	277±26	1.7
TIPA	0.22	58±7	129±11	2.2

The observed rate of DEAE thermal degradation is 40% as fast as DMAE and the observed rate of EDEA thermal degradation is 70% as fast as MDEA. These data are shown in Figure 4.14. With the exception of PZ-promoted tBuDEA, this data is consistent with data in the literature that also suggest that S_N2 reactions with bulkier substituent groups react slower than methyl substituent groups (Anslyn 2006). A more fundamental study that explores the initial second-order rate constant of thermal degradation between methyl, ethyl, and hydroxyethyl functional groups is presented in Chapter 6.

All of the PZ-promoted tertiary amines without methyl groups in this study had at least one hydroxyethyl or hydroxyisopropyl group present. Data shown in Section 4.3.1 indicated that the presence of these functional groups increased the rate of PZ degradation relative to tertiary amine degradation due to PZ reaction with the

intermediate degradation product formed from the initial degradation step through the mechanisms shown in Figures 4.4 and 4.5. With the exception of PZ-promoted tBuDEA, the results presented in Table 4.5 are consistent with the analysis presented in Section 4.3.1.
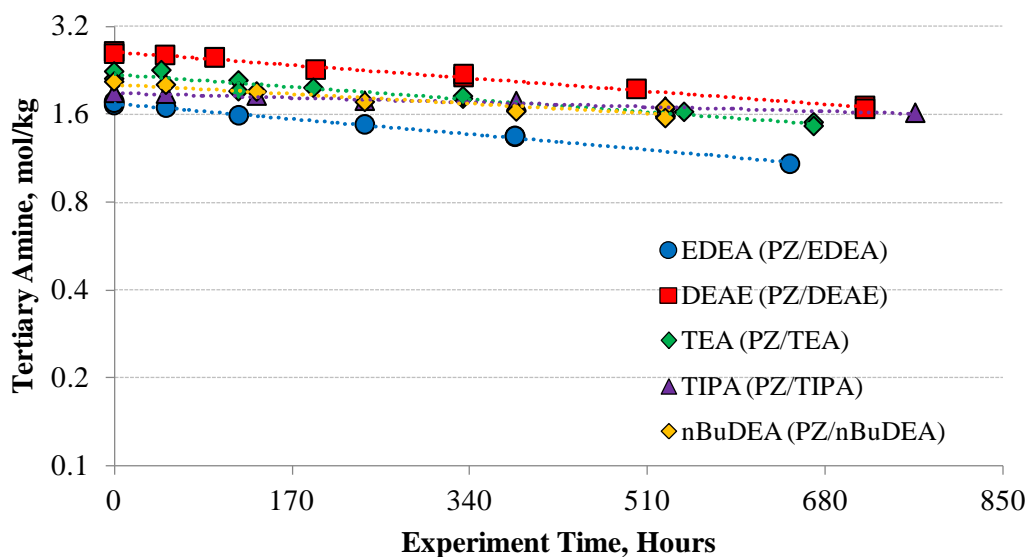
Figure 4.12: First-order rate model fit of tertiary amine loss in degradation of PZ-promoted tertiary amine solvents with no methyl groups, initially at 5 m PZ / 5 m tertiary amine, 0.23 mol CO$_2$/mol alkalinity, and 150 °C
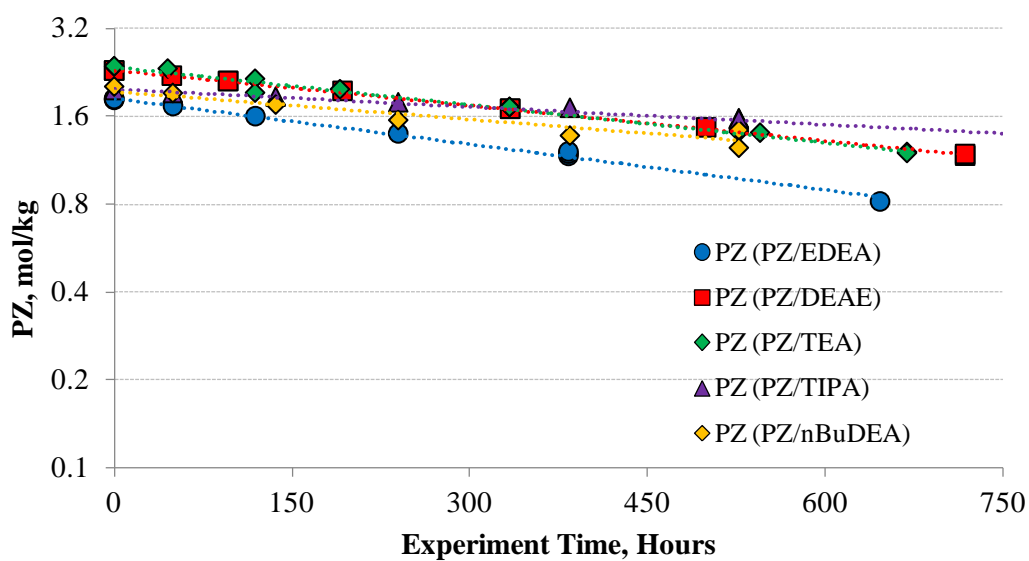
Figure 4.13: First-order rate model fit of PZ loss in degradation of PZ-promoted tertiary amine solvents with no methyl groups, initially at 5 m PZ / 5 m tertiary amine, 0.23 mol CO_2/mol alkalinity, and 150 °C
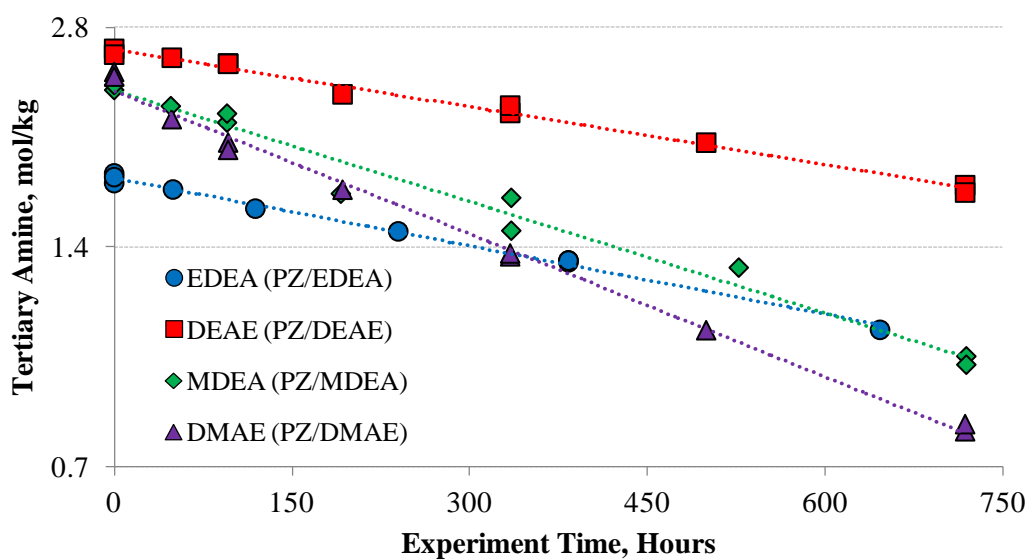
Figure 4.14: Comparison of degradation of tertiary amine in PZ-promoted tertiary amine solvents with and without methyl groups, initially at 5 m PZ / 5 m tertiary amine, 0.23 mol CO_2/mol alkalinity, and 150 °C

tBuDEA degraded at a significantly greater rate than many of the other tertiary amines tested; PZ degraded at the same rate as tBuDEA. DEA was present as an intermediate steady-state byproduct and rapidly reacted with PZ. Cylinders containing degraded samples of PZ-promoted tBuDEA were pressurized and had a gasoline-like odor, suggesting that tBuDEA undergoes elimination to form isobutylene and DEA, which was present at steady-state concentrations and was able to react with PZ present in solution. These data are shown in Figure 4.15. A proposed degradation pathway is shown in Figure 4.16.
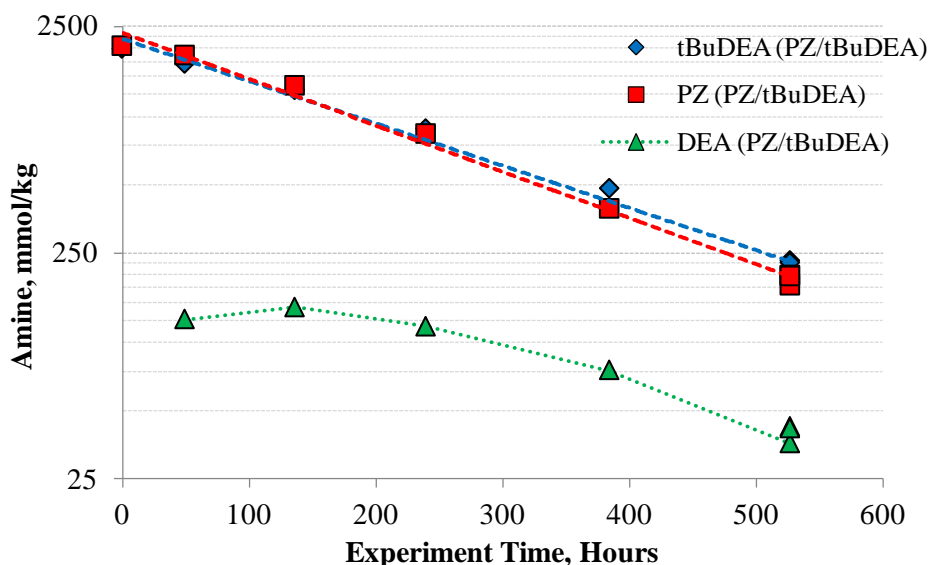
Figure 4.15: Degradation of PZ-promoted tBuDEA initially at 5 m PZ / 5 m tBuDEA, 0.23 mol CO_2/mol alkalinity, and 150 °C
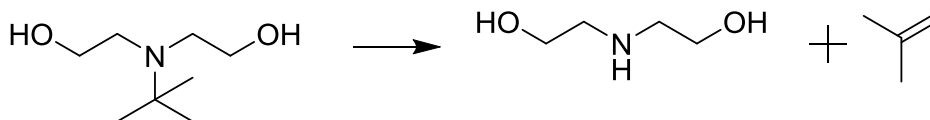
Figure 4.16: Proposed degradation path of tBuDEA to form DEA and isobutylene

4.3.3 Degradation of PZ-Promoted Tertiary Morpholines

PZ-promoted tertiary morpholines degrade one to two orders of magnitude more slowly than the tertiary aliphatic amines. The rate of degradation is shown in Table 4.6. Morpholine, a degradation product consistent with the degradation scheme shown in Figure 4.4, was detected in degraded solutions but represented less than 10% of the degradation of the tertiary morpholine. The calculated first-order degradation constants of PZ and tertiary morpholine are not statistically different from each other.

Table 4.6: Comparison of First-Order Rate Parameters for Degradation of PZ-promoted Tertiary Morpholine Solvents. Conditions: 5 m PZ / 5 m TA initially, 150 °C

Tertiary Amine	Initial CO_2 Loading mol CO_2/mol alk	k_1, TA $s^{-1}*10^9$	k_1, PZ $s^{-1}*10^9$	$\dfrac{k_1, PZ}{k_1, TA}$
HIPM	0.22	11±18	14±4	1.3
HEM	0.22	11±6	17±7	1.6
HPM	0.22	5±6	10±4	2.0

PZ, morpholine, and PZ derivatives were found to be some of the most thermally stable amines by Davis (2009) and Freeman (2011). Freeman indicated that the initial step of PZ degradation is initiated by free PZ reacting via S_N2 substitution on a carbon alpha to a protonated amino function on another PZ molecule, opening the PZ ring and creating aminoethylaminoethylpiperazine (AEAEPZ). It is possible that the PZ-promoted tertiary morpholine solvents degrade similarly, and additional work should be undertaken to fundamentally understand why this solvent system is stable and is discussed in Chapter 8.

4.3.4 Degradation Comparison of PZ, HMDA, and BAE promoted MDEA solvents

Hexamethylenediamine (HMDA) and Bisaminoethylether (BAE), two primary diamines, were used as rate promoters and degraded with MDEA initially at 5 m promoter / 5 m MDEA and 0.23 mol CO_2/mol alkalinity. The results are shown in Table 4.7.

Table 4.7: Comparison of First-Order Rate Parameters for Degradation of promoted MDEA solvents. Conditions: 5 m promoter / 5 m MDEA initially, 150 °C.

MDEA Promoter	Initial CO_2 Loading mol CO_2/mol alk	pKa$_1$ pKa$_2$ (25 °C)*	k_1, TA s^{-1}*10^9	k_1, Promoter s^{-1}*10^9	$\frac{k_1, \text{Promter}}{k_1, \text{TA}}$
HMDA	0.24	10.93 9.83	81±17	195±40	2.4
BAE	0.23	9.75 9.14	173±11	301±38	1.7
PZ	0.24	9.73 5.35	325±36	766±41	2.4

* pKa data for HMDA and PZ from Perrin (1964) and Khalili (2009), respectively. pKa data for BAE estimated using MarvinSketch/Chemicalize (ChemAxon)

HMDA was found to be the most stable promoter, followed by BAE, and then by PZ. The more stable promoters have higher pKa values, which runs counter to observations that nucleophiles with higher pKa values have a higher rate of reaction (Anslyn 2006, Rochelle 2001). At identical loading, greater quantities of HMDA and BAE will be complexed with the CO_2, reducing the amount of protonated tertiary amine and free promoter to participate in the degradation and leading to a reduced observed rate of thermal degradation.

4.4 INTERACTION BETWEEN PZ AND OXAZOLIDONE-FORMING PRIMARY AND SECONDARY AMINES IN THE PRESENCE OF CO_2

Oxazolidone-forming amines frequently are encountered as intermediate degradation products in the thermal degradation between PZ and a tertiary amine with at least one hydroxyl group present with two or three carbons between the hydroxyl group and the amino group. Since PZ is a strong nucleophile, it can rapidly react with an oxazolidone-forming amine via the carbamate polymerization pathway, and thus the presence of oxazolidone-forming amine intermediate byproducts increases the rate of PZ degradation relative to the rate of tertiary amine degradation.

The reactions between the oxazolidone-forming amines and PZ were tested at 7 m PZ/2 m oxazolidone-forming amine at an initial loading of about 0.3 mol CO_2/mol alkalinity and 150 °C. A first-order rate model, shown in Equation 4.7, was used to model the loss of the oxazolidone-forming amine; these models give reasonable agreement with experimental data and are shown in Figure 4.17 and summarized in Table 4.8.

$$\frac{dC_{OZD}}{dt} = k_{1,OZD} * C_{OZD} \qquad \text{Eq. 4.7}$$

In Eq. 4.7, $k_{1,OZD}$ is the first-order constant in sec^{-1} that is used to estimate the loss of the oxazolidone-forming amine, C_{OZD} is the concentration of the oxazolidone-forming amine in mol/kg, and t is time in seconds.
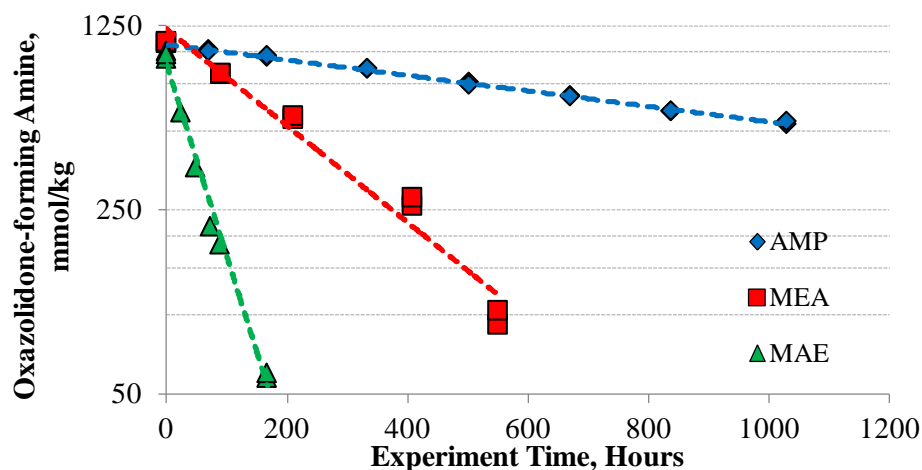
Figure 4.17: First-order model fit of loss of oxazolidone-forming amine in presence of PZ. Conditions: 7 m PZ / 2 m oxazolidone-forming amine, 0.3 mol CO_2/mol alkalinity, 150 °C

As described in previous sections, oxazolidone-forming amines frequently are encountered as intermediate degradation products in the thermal degradation between PZ and a tertiary amine with at least one hydroxyl group present with two or three carbons between the hydroxyl group and the amino group. Since PZ is a strong nucleophile, it can rapidly react with an oxazolidone-forming amine via the carbamate polymerization pathway, and thus the presence of oxazolidone-forming amine intermediate byproducts increases the rate of PZ degradation relative to the rate of tertiary amine degradation.

Table 4.8: Comparison of Loss of Oxazolidone-forming Amines in Presence of PZ. Conditions: 7 m PZ / 2 m Oxazolidone-forming amine initially, 150 °C.

Oxazolidinone-forming Amine	CO_2 Loading mol CO_2/mol alk	k, loss of OZD former $s^{-1}*10^9$
MEA	0.29	1170±172
MIPA	0.31	242±25
AMP	0.30	187±6
MPA	0.31	337±31
MAE	0.30	4660±391
EAE	0.31	2490±354
DEA	0.31	8400±511

The results indicate that increased chain length from two to three carbons or hindrance of either the hydroxyl or amino group leads to a decreased rate of degradation of the oxazolidone-forming amine. Secondary oxazolidone-forming amines react more rapidly with PZ than primary amines; however, increasing chain length on a substituent group incapable of participating in the carbamate polymerization pathway on the secondary oxazolidone-forming amine decreases the overall rate of reaction. DEA has the greatest rate of reaction of the secondary amines due to its ability to form an oxazolidone with either of its hydroxyl groups. These results are consistent with the observations of Davis who found that oxazolidone-forming amines, when degraded in the presence of CO_2 and without PZ, have lower rates of degradation with increasing chain length or steric hindrance (Davis 2009) and also with the results shown in Section 4.3.1.

4.5 DEGRADATION OF CO_2-LOADED PZ-PROMOTED TERTIARY AMINE SOLVENTS AS A FUNCTION OF CO_2 LOADING, AMINE CONCENTRATION, AND TEMPERATURE

4.5.1 Effect of Amine Concentration

The degradation rates of PZ-promoted tertiary amines at 150 °C with 2 m PZ / 7 m Tertiary Amine and about 0.13 mol CO_2/mol alkalinity are summarized in Table 4.9 and shown in Figures 4.18 and 4.19. This loading corrresponds to the operational lean loading of 2 m PZ / 7 m MDEA when used to capture CO_2 from coal-fired power plants.

Table 4.9: Comparison of First-Order Rate Parameters for Thermal Degradation of PZ-promoted Tertiary Amines at Lean Loading. Conditions: 2 m PZ / 7 m TA initially, 150 °C

Tertiary Amine	CO_2 Loading mol CO_2/mol alk	k_1, TA $s^{-1}*10^9$	k_1, PZ $s^{-1}*10^9$
DMAE	0.13	193±46	1370±56
MDEA	0.13	177±21	291±26
DMAP	0.14	134±26	534±27
TEA	0.13	124±61	433±60
DEAE	0.12	90.2±10	419±32

The rate data can be normalized by concentration by multiplying the rate constant of MDEA and PZ by the initial concentration of MDEA and PZ, respectively to give an estimate of the initial rate, shown in Equation 4.8. The initial rate data are summarized in Table 4.10.

$$r_{initial} = k_1 * C_{initial} \qquad \text{Eq. 4.7}$$

In Eq. 4.7, k_1 is the measured rate constant extracted from the first-order rate analysis, $C_{initial}$ is the initial concentration of either PZ or the tertiary amine in mol/kg, and $r_{initial}$ is the initial rate in mol*kg^{-1}*s^{-1}.
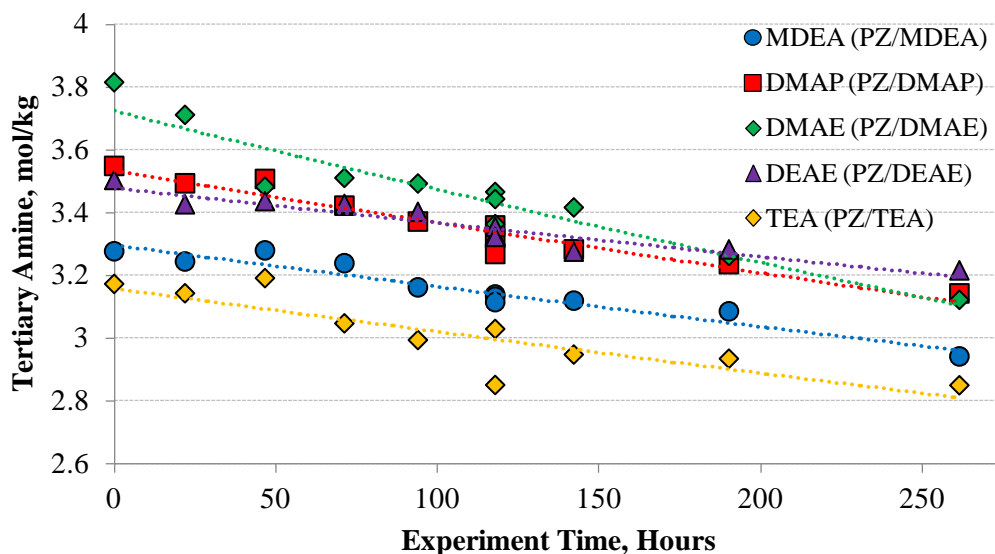
Figure 4.18: First-order rate model fit of tertiary amine loss in degradation of PZ-promoted tertiary amine solvents initially at 2 m PZ / 7 m tertiary amine, 0.13 mol CO_2/mol alkalinity, and 150 °C
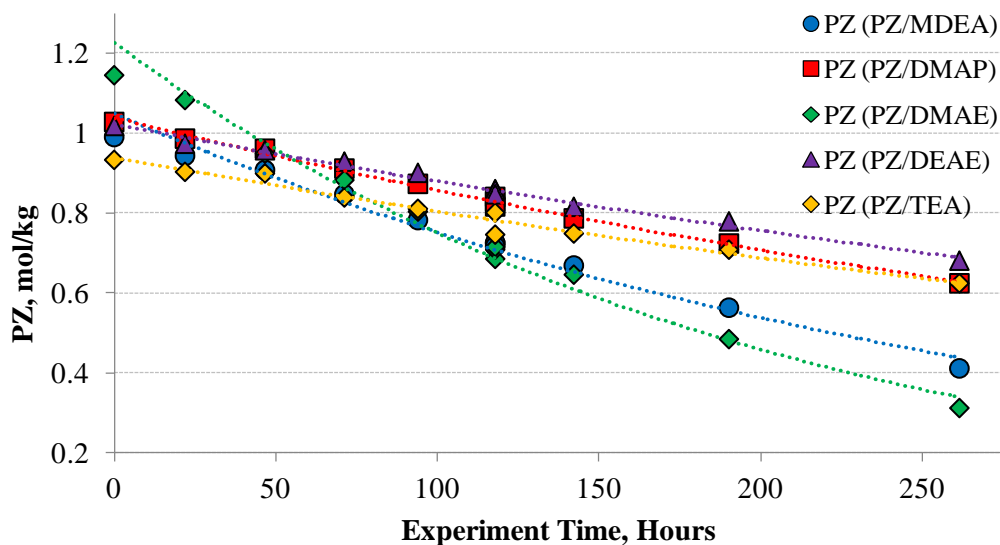
Figure 4.19: First-order rate model fit of PZ loss in degradation of PZ-promoted tertiary amine solvents initially at 2 m PZ / 7 m tertiary amine, 0.13 mol CO_2/mol alkalinity, and 150 °C

Table 4.10: Initial Degradation Rate of PZ-promoted Tertiary Amine at Lean Loading

Tertiary Amine	Tertiary Amine Initial Rate mol/kg/s*10^9		Piperazine Initial Rate mol/kg/s*10^9	
	5 m PZ / 5 m TA	2 m PZ / 7 m TA	5 m PZ / 5 m TA	2 m PZ / 7 m TA
DMAE	1010	736	1510	1570
DMAP	554	447	581	548
MDEA	752	374	1730	918
DEAE	435	369	587	427
TEA	350	393	652	403

The initial rate at 7 m tertiary amine and 2 m PZ and at lean loading follows the trends observed with amine solvents at 5 m tertiary amine and 5 m PZ. The initial rate loss is lower with a lower concentration of PZ, leading to a reduced initial rate of reaction. PZ in the presence of MDEA, DEAE, or DMAE degrades more rapidly than the tertiary amine; DMAP has an initial degradation rate similar to PZ. The stoichiometric loss of PZ is nearly equivalent to that of TEA at 2 m PZ / 7 m TA. This is believed to be due to speciation effects: because TEA has a lower pKa of 7.7 at 25 °C (Haynes, Ed. 2014), a relatively greater amount of CO_2 and H^+ are bound to the PZ relative to the TEA at lean loading, reducing the observed degradation rate of TEA by reducing the amount of free PZ available to react with TEA and intermediate byproducts.

4.5.2 Effect of CO_2 Loading

The degradation rate constant as well as the initial degradation rate of PZ-promoted tertiary amines at 150 °C and 2 m PZ / 7 m Tertiary Amine and about 0.25 mol CO_2/mol alkalinity is shown in Table 4.11 and Figures 4.20 and 4.21. This loading corresponds to the rich loading of 7 m MDEA / 2 m PZ in applications that capture CO_2 from coal-derived flue gas. All of the tertiary amine solvents, with the exception of PZ/DMAP, have significantly greater thermal degradation rates at rich conditions than at lean conditions.
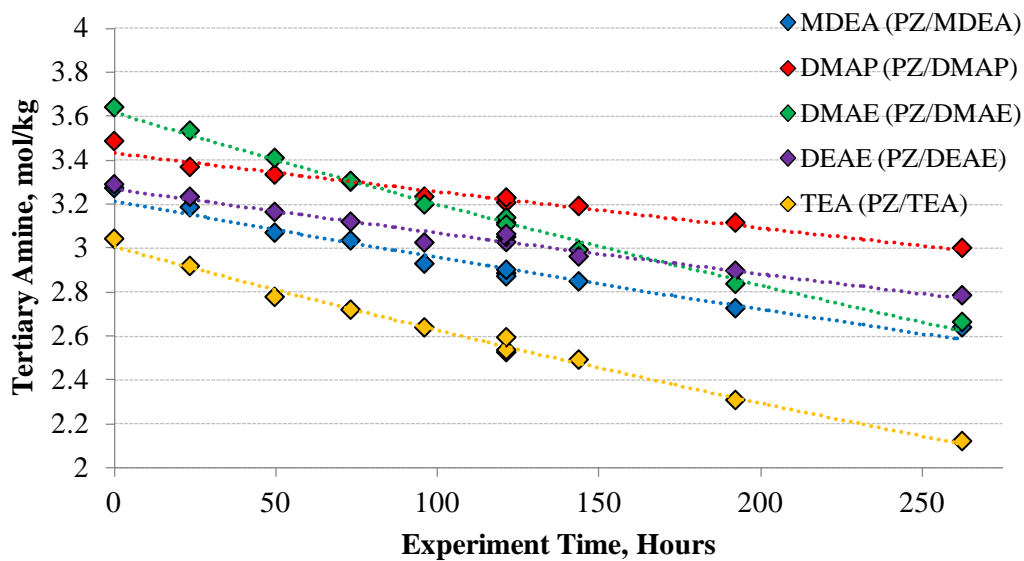
Figure 4.20: First-order rate model fit of tertiary amine loss in degradation of PZ-promoted tertiary amine solvents initially at 2 m PZ / 7 m tertiary amine, 0.26 mol CO_2/mol alkalinity, and 150 °C
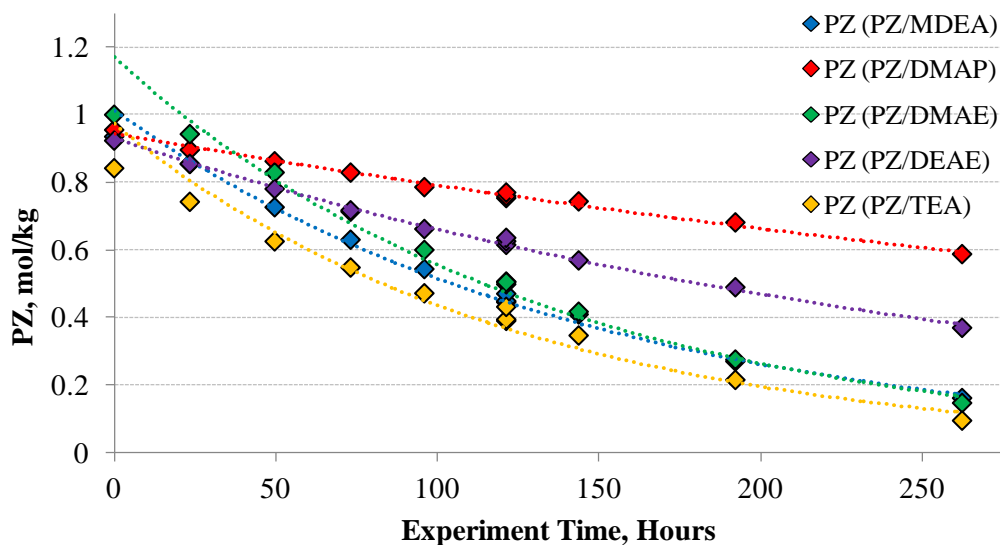
Figure 4.21: First-order rate model fit of PZ loss in degradation of PZ-promoted tertiary amine solvents initially at 2 m PZ / 7 m tertiary amine, 0.26 mol CO_2/mol alkalinity, and 150 °C

At rich loading, greater quantities of the tertiary amine are complexed with H^+ than at lean loading and are more susceptible to attack by PZ. Intermediate amine byproducts, such as DEA, will be complexed with carbamate at higher concentrations due to the higher concentration of CO_2 present in the rich solvent than the lean solvent. This leads to an increased overall rate of oxazolidone formation and thus a higher rate of reaction with PZ, increasing PZ loss.

Table 4.11: Comparison of First-Order Rate Parameters for Thermal Degradation of PZ-promoted Tertiary Amines at Rich Loading. Conditions: 2 m PZ / 7 m TA initially, 150 °C

Tertiary Amine	CO_2 Loading mol CO_2/mol alk	k_1, TA $s^{-1}*10^9$	k_1, PZ $s^{-1}*10^9$
DMAE	0.26	340±22	2070±214
MDEA	0.26	231±31	1880±122
DMAP	0.25	146±18	491±31
TEA	0.26	375±24	2230±321
DEAE	0.28	175±22	950±46

The degradation rate of PZ/DMAP at rich conditions is not statistically different from the degradation rate at lean conditions at 2 m PZ / 7 m TA. The intermediate amine product in PZ/DMAP, MAP, was found to accumulate in degraded solutions at rich conditions, and does not readily react with PZ. This is shown in Figure 4.22.
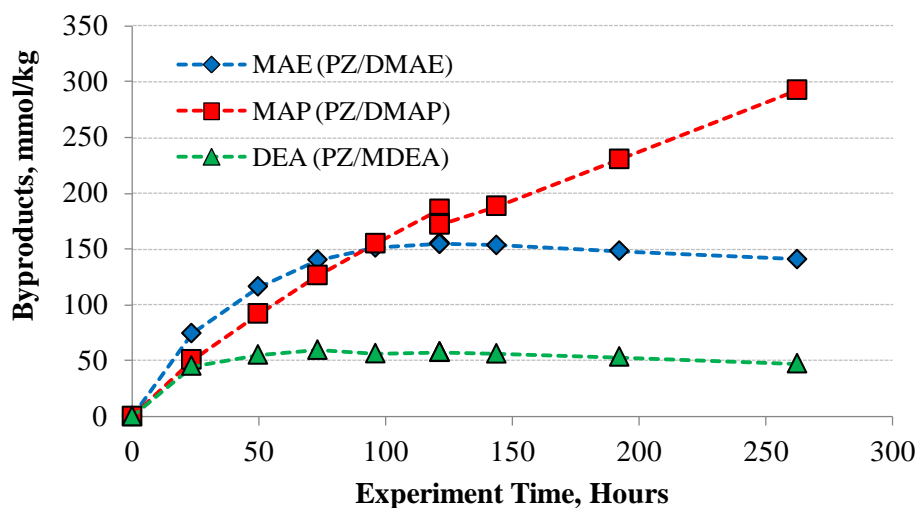
Figure 4.22: Evolution of secondary amine byproducts in PZ-promoted tertiary amine solvents. Conditions: 2 m PZ / 7 m tertiary amine and 0.26 mol CO_2/mol alkalinity initially, 150 °C

4.5.3 Effect of Temperature

Higher temperature leads to higher rates of thermal degradation. The effect of temperature on the degradation of amine loss can be shown using an Arrhenius relationship, shown in Equation 4.8.

$$k = A * \exp(\frac{-E_A}{R*T})$$
Eq. 4.8

In Eq. 4.8, k is the rate constant, A is a preexponential factor with the same units as the rate constant, R is the gas constant, T is the absolute temperature, and E_A is the activation energy in J/mol. A higher E_A value indicates that the reaction is more sensitive to the effects of temperature, whereas a lower E_A value indicates that the reaction is not as sensitive to temperature.

87

An Arrhenius plot of the degradation of PZ/MDEA and PZ/DEAE is shown in Figure 4.23, and the activation energies derived from the Arrhenius plots are presented in Table 4.12. The activation energies appear to be correlated with the type of tertiary amine present in solutions at lean loading. PZ-activated tertiary amine solutions whose tertiary amine has at least two methyl groups present, such as DMAE and DMAP, have the lowest activation energies, and amines without methyl groups, such as DEAE and TEA, have relatively higher activation energies. The solutions which have the highest activation energies have tertiary amines that degrade the slowest. At rich loading, the activation energies appear to converge to around 140 to 150 kJ/mol for all solvents, likely due to speciation effects.
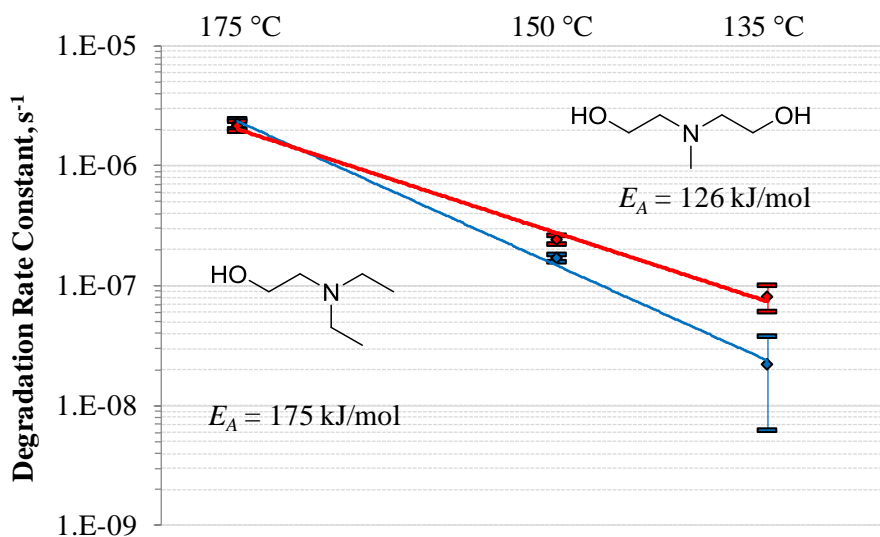
Figure 4.22: Activation energy of thermal degradation of PZ-promoted DEAE and MDEA, initially at 5 m PZ / 5 m TA and 0.23 mol CO_2/mol alkalinity

Table 4.12: Activation Energies of Thermal Degradation of PZ-promoted Tertiary Amine Solvents

Tertiary Amine	5 m PZ / 5 m TA 0.23 mol CO_2 / mol alkalinity		2 m PZ / 7 m TA 0.10 mol CO_2 / mol alkalinity		2 m PZ / 7 m TA 0.25 mol CO_2 / mol alkalinity	
	E_A TA kJ/mol	E_A PZ kJ/mol	E_A TA kJ/mol	E_A PZ kJ/mol	E_A TA kJ/mol	E_A PZ kJ/mol
DMAE	134	126	125	133	128	141
DMAP	126	131	136	134	147	157
MDEA	140	139	140	146	140	140
DEAE	175	168	177	193	141	152
TEA	169	190	137	154	142	155

4.6 MAXIMUM STRIPPING TEMPERATURES (T_{MAX}) OF PZ-PROMOTED TERTIARY AMINES AT LEAN LOADING

The data presented in preceding sections can be used to set operational parameters, such as the maximum stripping temperature (T_{MAX}), in the regeneration section of the CO_2 capture plant.

Davis determined that the stripping temperature that balances solvent degradation and capture plant energy performance for 30 wt% MEA was 121 °C, which corresponds to a first-order batch thermal degradation rate constant of 2%/week or $2.91*10^{-8}$ s^{-1} (Davis 2009). Freeman extended this analysis to other solvents to determine the temperature at which their thermal degradation rate constants are equal to $2.91*10^{-8}$ s^{-1} (Freeman 2011). Based on this analysis, Freeman found that the optimum stripping temperature for concentrated piperazine was 163 °C. Literature data indicates that pilot units using MEA operate the reboiler between 110 and 120 °C (Knudsen 2007, Moser 2011, Artanto 2012, Cousins 2014) and that pilot units using concentrated PZ operate the reboiler between 150 and 155 °C (Nielsen 2013, Cousins 2014), validating Freeman's methodology.

A first-order thermal degradation rate constant was recalculated for all amine solvents studied with respect to total amine concentration. This is shown in Equation 4.9.

$$\frac{dC_{\text{Total Amine}}}{dt} = k_1 * C_{\text{Total Amine}} \hspace{5cm} \text{Eq. 4.9}$$

In Eq. 4.9, $C_{\text{Total Amine}}$ is the sum of concentration of the parent amines in solution. In promoted tertiary amine systems, this would be equivalent to the sum of the promoter and tertiary amine. k_1 is the first-order rate constant in s^{-1} and t is the experiment time in seconds.

The degradation rate for all solvent systems tested was recalculated using Eq. 4.9. Activation energies of thermal degradation for PZ/MDEA, PZ/DMAP, PZ/DMAE, PZ/DEAE, and PZ/TEA were recalculated using Eq. 4.8 using the first-order rate constant calculated from Eq. 4.9. Many of the solvents in this study were tested only at 150 °C, and the activation energies of these solvents were assumed to be equivalent to MDEA, DMAP/DMAE, DEAE, TEA, or concentrated PZ based on the structure and degradation rate of the tertiary amine. The activation energy and the measured degradation rate at 150 °C were used to extract the pre-exponential factor A using Eq. 4.8. This calculated value of A was used to calculate the temperature at which the degradation rate of the amine is equal to $2.91*10^{-8}$ s^{-1} using Eq. 4.8. These data are summarized in Table 4.13.

PZ-promoted tertiary morpholine solvents can be run at the greatest regeneration temperatures, followed by aliphatic tertiary amines with no methyl groups, aliphatic tertiary amines with methyl groups, and finally by aliphatic tertiary amines that have an additional pathway of degradation in which the tertiary amine attacks itself. Solvents

with a reduced promoter/tertiary amine concentration ratio can be regenerated at a higher temperature than solvents with greater promoter/tertiary amine concentration ratio.

Table 4.13: Maximum Stripping Temperature of Promoted Tertiary Amine Solvents

Tertiary Amine / Promoter	Concentration molal TA / molal promoter	Loading mol CO_2/mol alk	Activation Energy kJ/mol	T_{MAX} °C
HPM/PZ	5/5	0.22	180[1]	161
HIPM/PZ	5/5	0.22	180[1]	157
HEM/PZ	5/5	0.22	180[1]	156
TIPA/PZ	5/5	0.22	190[2]	140
DEAE/PZ	7/2	0.12	180	137
MDEA/HMDA	5/5	0.24	140	135
TEA/PZ	5/5	0.22	140	134
DEAE/PZ	5/5	0.23	170	134
nBuDEA/PZ	5/5	0.22	170[3]	133
EDEA/PZ	5/5	0.23	170[3]	132
TEA/PZ	7/2	0.13	190	131
MDEA/BAE	5/5	0.23	140[5]	129
DMAP/PZ	7/2	0.14	130	128
DMAIP/PZ	5/5	0.22	130[4]	127
DMAP/PZ	5/5	0.23	130	127
MDEA/PZ	7/2	0.13	130	127
DMAEE/PZ	5/5	0.23	130[4]	124
MDEA/PZ	5/5	0.24	140	122
DMAE/PZ	7/2	0.13	120	121
DMAE/PZ	5/5	0.23	130	120
tBuDEA/PZ	5/5	0.22	130[4]	111
DMAB/PZ	5/5	0.23	130[4]	108

[1]: E_A of 8 m PZ (Freeman 2011)
[2]: E_A of 5 m TEA/5 m PZ
[3]: E_A of 7 m DEAE/2 m PZ
[4]: E_A of 5 m DMAE/5 m PZ and 5 m DMAP/5 m PZ
[5]: E_A of 5 m MDEA/5 m PZ

The PZ-promoted tertiary morpholines have a stability temperature greater than 150 °C, which would promote the thermal destruction of nitrosamines in the stripper with adequate residence time (Fine 2014). PZ-promoted tertiary amines that have at least one methyl group, such as PZ/MDEA, are as thermally stable as MEA (Davis 2009).

4.7   CONCLUSIONS

- First-order rate models represent the degradation of PZ-promoted tertiary amines in environments in which speciation changes and the promoter has substantial interaction with other amine byproducts. In other cases, second-order rate models consistent with proposed degradation pathways can model degradation reasonably well.

- PZ-promoted tertiary amines with at least one methyl group are the least stable solvents tested and have a maximum stripping temperature between 120 and 130 °C, which is comparable to MEA.

- PZ-promoted tertiary amines with no methyl groups present have an intermediate stability and have a maximum stripping temperature between 130 and 140 °C.

- PZ-promoted tertiary morpholine solvents are the most stable amine solvents tested and have a maximum stripping temperature above 150 °C, which is comparable to concentrated PZ.

- Tertiary amines with at least one hydroxyethyl or hydroxyisopropyl functional group can form intermediate byproducts that degrade via the carbamate polymerization pathway. PZ-promoted tertiary amine solvents with these functional groups have a PZ degradation rate that is 40 to 130% greater than the tertiary amine degradation rate.

- Tertiary amines with a hydroxypropyl functional group or a five-membered functional group do not form intermediate byproducts that degrade via the carbamate polymerization pathway; in these solvent systems, PZ loss is comparable to the tertiary amine loss.

- DMAB likely degrades by a ring-closing dehydration mechanism and tBuDEA likely degrades by elimination of the t-butyl functional group. These amines do not feature PZ as a part of their initial degradation mechanism and thus degrade more quickly than other tertiary amines and at the same rate as PZ.

- On a stoichometric basis and at lean loading, PZ solvents at 7 m TA / 2 m PZ degrade at a slower rate than PZ solvents at 5 m TA / 5 m PZ, likely due to the lower concentration of PZ that leads to a lower initial rate of degradation.

- Increased loading leads to significantly higher rates of degradation for most tertiary amines with at least one hydroxyethyl or hydroxyisopropyl group with the exception of PZ-promoted DMAP. This is due to a higher concentration of protonated tertiary amine present in rich-loaded solutions, which increases the initial rate of degradation. The increased concentration of CO_2 in solution leads to greater PZ loss due to an increased rate of oxazolidone formation via the carbamate polymerization pathway.

- The activation energy of thermal degradation of PZ-promoted tertiary amine is correlated with the degradation rate. More stable amines have higher activation energies than less stable amines.

Chapter 5: Modeling of Piperazine (PZ)-Promoted Methyldiethanolamine (MDEA) Thermal Degradation

5.1   INTRODUCTION & SCOPE

In Chapter 4, the thermal degradation of tertiary amines in the presence of CO_2 was presented. The data presented in Chapter 4 are helpful in understanding the effects of CO_2 loading, amine concentration, and especially the amine structure on the rate of degradation on a practical level; however, they do not explicitly account for amine speciation as a function of degradation. Because of this limitation, the data presented in Chapter 4 cannot be effectively used to model and predict the rate of degradation as amine concentration, lean loading, and amine speciation are varied.

The thermal degradation of PZ-promoted MDEA in the presence of H^+ is modeled as a function of protonated and free amine species. Prior thermal degradation studies in have not explicitly accounted for the presence of protonated species in degradation. This is representative of the initial degradation rate of PZ-promoted MDEA as it is initiated by a free amine attacking a protonated amine. A degradation pathway is proposed based on the product degradation slate and validated using rate measurements and fitting kinetic parameters to proposed rate laws. Degradation under acidified conditions is compared to degradation in the presence of CO_2 and used to model degradation based on the design initial concentration and lean CO_2 loading from a process design perspective.

Raw data, chromatograms, and mass spectra for the experiments discussed in this chapter are presented in Appendix B.2. The procedure to determine free and protonated amine concentration based on total amine and proton concentration is outlined in Appendix A.4.

5.2   ACIDIFIED SOLVENT DEGRADATION OVERVIEW

Degrading solvents in the presence of H^+ instead of CO_2 can help in understanding the role that CO_2 plays in the degradation mechanism and can be used to model the initial rate of degradation if the degradation is initiated by a free amine species attacking a protonated amine species.

Sulfuric acid is used to protonate the amines. Hydrochloric acid can cause stress-corrosion cracking of the stainless steel degradation cylinders, and nitric acid is an oxidizer and would generate degradation products that are not representative of thermal degradation. Hydrochloric acid was used only in one experiment to understand the effect on degradation rate of using a monovalent acid instead of a divalent acid.

Closmann (2011) degraded solutions of PZ-promoted MDEA under acidified conditions using methylsulfonic acid. This study established diethanolamine (DEA) and methypiperazine (1-MPZ) as major byproducts of thermal degradation of PZ-promoted MDEA. Closmann also noted that the absolute loss rate of PZ and MDEA was similar, suggesting that both PZ and MDEA participate in the degradation pathway. Based on these data, Closmann proposed two different degradation pathways for PZ-promoted MDEA, which are shown in Figures 5.1 through 5.3.
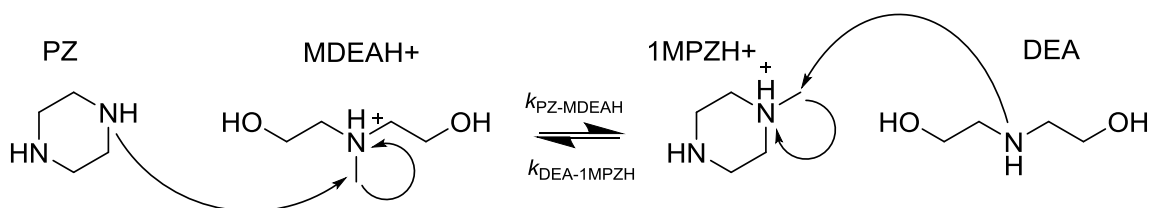
Figure 5.1: Proposed net degradation pathway of PZ-promoted MDEA to form DEA and 1-MPZ

95
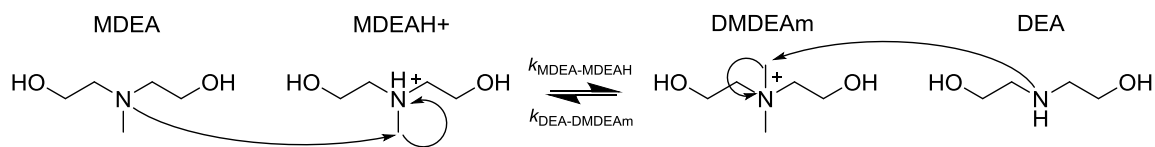
Figure 5.2: Proposed net degradation pathway of MDEA to form DEA and DMDEAm
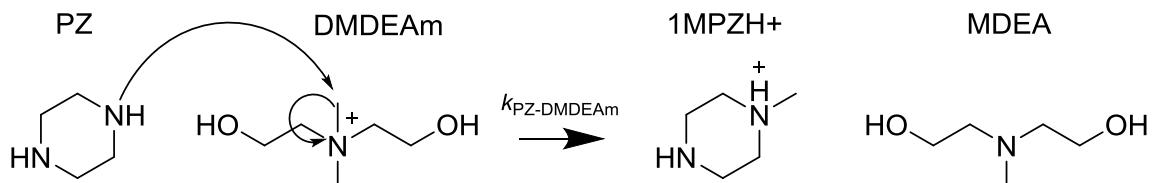
Figure 5.3: Attack of DMDEAm by PZ to form 1-MPZ and regenerate MDEA

In the first pathway, shown in Figure 5.1, free PZ can attack protonated MDEA (MDEAH+), forming DEA and 1-MPZ. In the second pathway, shown in Figure 5.2, free MDEA can attack MDEAH+ to form DEA and dimethyldiethanolammonium (DMDEAm), a quaternary amine. DMDEAm can then rapidly react with free PZ to form 1-MPZ and regenerate MDEA, shown in Figure 5.3. Both reaction mechanisms are supported by the product slate seen and by observations that quaternary amines are present in the degradation of tertiary amines (Bedell, 2010)

5.3   PRODUCTS OBSERVED IN DEGRADATION

5.3.1   Products Seen in PZ-Promoted MDEA

The degradation products of both PZ-promoted MDEA and MDEA are shown in Tables 5.1 through 5.3, and the evolution of degradation products is shown in Figures 5.3 and 5.4. Since PZ is a much stronger nucleophile than MDEA, a different product slate is observed in PZ-promoted MDEA and MDEA degradation.

96

Table 5.1: Products Observed in Degradation of PZ-Promoted MDEA

Structure	Name Abbreviation	Molecular Weight	Quantification & Identification
HO⌒N(CH₃)⌒OH	Methyldiethanolamine MDEA	119.2	Quantified – IC
Piperazine	Piperazine PZ	86.1	Quantified – IC
HO⌒NH⌒OH	Diethanolamine DEA	105.1	Quantified – IC
1-Methylpiperazine	1-Methylpiperazine 1-MPZ	100.2	Quantified – IC
1,4-Dimethylpiperazine	1,4-Dimethylpiperazine 1,4-DMPZ	114.2	Quantified – IC
HO⌒N⁺(CH₃)⌒OH	Dimethyldiethanolammonium DMDEAm	134.2	Quantified – IC*
CH₃NH⌒OH	Methylaminoethanol MAE	75.1	Identified – IC
1-Hydroxyethylpiperazine	1-Hydroxyethylpiperazine 1-HePZ	131.2	Identified – IC
HeMAEtPZ structure	2-(methyl(2-(piperazin-1-yl)ethyl)amino)ethan-1-ol (HeMAEtPZ)	187	Estimated – IC Suspected – LCMS and based on IC elution times
HeMAEtMPZ structure	2-(methyl(2-(4-methylpiperazin-1-yl)ethyl)amino)ethan-1-ol (HeMAEtMPZ)	201	Estimated – IC* Suspected based on IC elution times
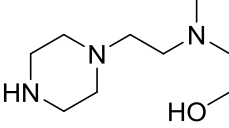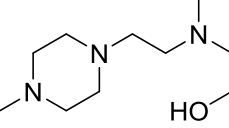
*Only quantified and identified for 7 m MDEA / 0.75 m PZ. Other experiments did not show quantifiable amounts of these compounds

97

Table 5.2: Mass Balance, PZ-Promoted MDEA, initially at 2.5 m PZ / 2.5 m MDEA and 0.14 mol H+/mol alkalinity at 150 °C after 865 hours

Amine	Concentration formed (lost) mol/kg	Mol/kg N	Mol/kg C
Parent Amines			
MDEA	(0.41)	(0.41)	(2.05)
PZ	(0.40)	(0.8)	(1.60)
Total Lost		(1.21)	(3.65)
Major Degradation Products			
DEA	0.41	0.41	1.64
1-MPZ	0.32	0.64	1.60
Total from Major Degradation Products		1.05 87%	3.24 89%
Other Degradation Products			
1,4-DMPZ	0.02	0.04	0.12
HeMAEtPZ	0.03	0.09	0.21
Total Material Balance		1.18 98%	3.57 98%
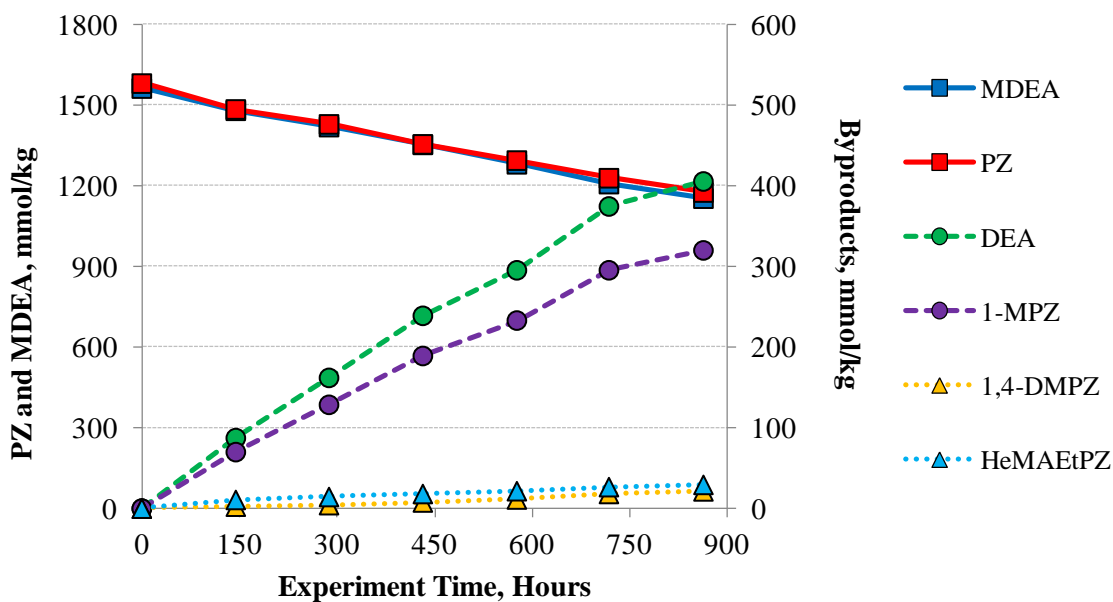
Figure 5.3: Degradation Products and Parent Amines of PZ-Promoted MDEA initially at 2.5 m PZ / 2.5 m MDEA and 0.14 mol H+/mol alkalinity at 150 °C.

Table 5.3: Mass Balance, PZ-Promoted MDEA, initially at 0.75 m PZ / 7 m MDEA and 0.11 mol H+/mol alkalinity at 165 °C after 187 hours

Amine Name	Concentration formed (lost) mol/kg	Mol/kg N	Mol/kg C
Parent Amines			
MDEA	(0.50)	(0.50)	(2.48)
PZ	(0.33)	(0.66)	(1.31)
Total Lost		(1.16)	(3.79)
Major Degradation Products			
DEA	0.42	0.42	1.66
1-MPZ	0.13	0.27	0.67
Total from Major Degradation Products		0.69 59%	2.33 61%
Other Degradation Products			
DMDEAm	0.01	0.01	0.04
1,4-DMPZ	0.07	0.14	0.41
HeMAEtPZ	0.05	0.15	0.34
HeMAEtMPZ	0.03	0.08	0.22
Total Material Balance		1.07 92%	3.34 88%
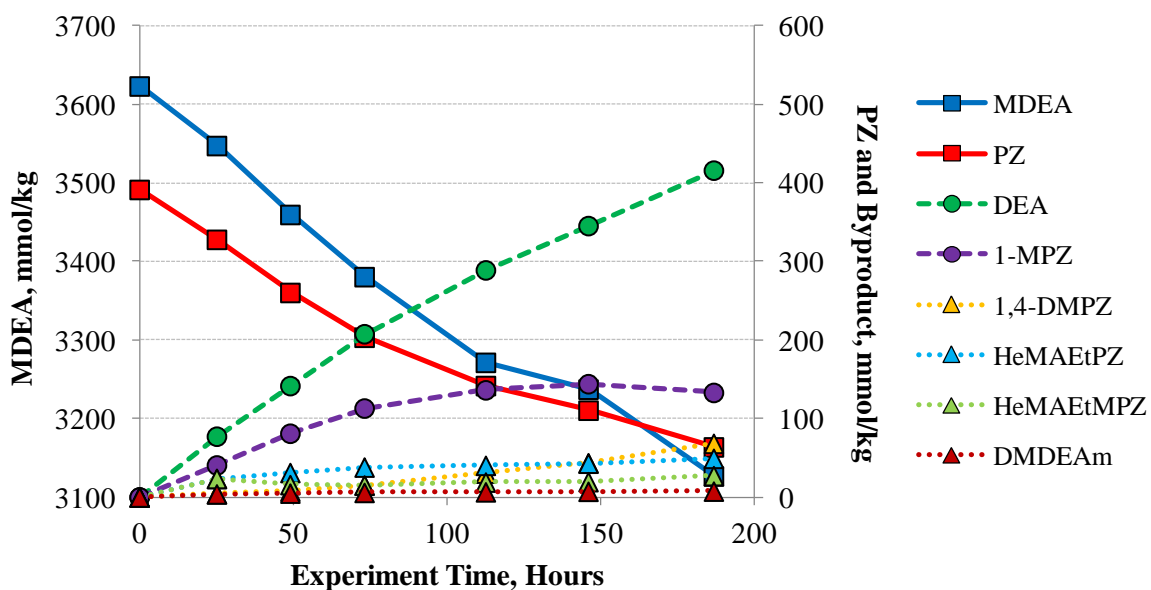
Figure 5.4: Degradation Products and Parent Amines of 0.75 m PZ / 7 m MDEA and 0.11 mol H+/mol alkalinity at 150 °C

The data from this study confirm Closmann's findings that DEA and 1-MPZ are the dominant degradation products of acidified PZ-promoted MDEA. These data strongly suggest that the interaction between the PZ and methyl groups on the tertiary amine is dominant. Additionally, the interaction between PZ and the carbon alpha to the hydroxyl group is minor. The quaternary amine was only able to be detected using MS and quantified using cation chromatography in experiments with an initial molar ratio of MDEA to PZ greater than 9. Other minor degradation products, such as dimethylpiperazine (1,4-DMPZ), were detected using cation chromatography and MS in the small quantities quantified. Minor PZ derivatives, such as 2-(methyl(2-(piperazin-1-yl)ethyl)amino)ethan-1-ol (MAHeEtPZ) were detected using MS and their concentration was estimated based on their elution times using cation chromatography (IC) and the calibration curve of PZ, respectively. The formation of these products is consistent with free PZ attacking a carbon alpha to the hydroxyl function of MDEA. Their observed relative rates of formation are slower than the formation of DEA and 1-MPZ. An analog of MAHEtPZ, 2-(methyl(2-(4-methylpiperazin-1-yl)ethyl)amino)ethan-1-ol, or MAHEtMPZ, was suspected to be present in solution. The method to quantify MAHEtPZ is similar to the one used by Davis (2009) to estimate the concentration of byproducts for which standards are unavailable.

Closmann (2011) discussed the possibility of PZ attacking the hydroxyethyl group of MDEAH+ to form 1-hydroxyethylpiperazine (1-HePZ) and methylaminoethanol (MAE). Both of these compounds were detected using cation chromatography and MS, but their concentration was too low to be quantified. 1-HePZ had a concentration less than 0.01 mol/kg in degraded PZ-promoted MDEA initially at 2.5 m PZ / 2.5 m MDEA and 0.14 mol H+/mol alkalinity after 650 hours at 150 °C. The peak area ratio between DEA and MAE was approximately 34:1 in the same experiment. These results strongly

suggest that the rate at which bulkier substituent groups are attacked by nucleophiles is significantly less than methyl groups. These observations have been suggested in the literature (Lichtfers 2007, Anslyn 2006) and will be expanded upon in Chapter 6.

The identified and quantified degradation products account for 98% of the lost amine in PZ-promoted MDEA at 2.5 m PZ / 2.5 m MDEA and 0.14 mol H+/mol alkalinity at 150 °C and for 90% in PZ-promoted MDEA at 0.75 m PZ / 7 m MDEA and 0.11 mol H+/mol alkalinity at 165 °C. The exclusion of MAE and 1-HePZ, other minor degradation products such as higher polyamines formed by S_N2 substitution with the – OH group, as well as inaccuracies in the quantification of MHEtPZ and MHEtMPZ might represent the nitrogen and carbon that was unable to be quantified.

5.3.2   Products of MDEA Degradation

Tables 5.4 and 5.5 summarize the degradation products and material balance with in acidified MDEA degradation; these data are plotted in Figure 5.5. DEA and DMDEAm were the dominant degradation products and appeared to reach a thermodynamic equilibrium after about 500 hours of experiment time. Several other tertiary amines and their associated quaternary amines were detected using mass spectrometry and cation chromatography. The elution times of the tertiary amines were nearly the same as MDEA and thus could not be accurately quantified. The peak area ratio between DEA and MAE was 60:1, and the peak area ratio between MDEA and DMAE was 200:1. Low resolution MS indicated that the relative abundance of TEA and THeMAm was an order of magnitude less than DMAE and choline. Additional products whose elution times were consistent with diamines were detected using cation chromatography, suggesting that MDEA and/or its degradation products participated in amine attack on carbons alpha to hydroxyl groups to form diamines.

101

Table 5.4: Products observed in MDEA Degradation
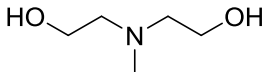
Structure	Name Abbreviation	Molecular Weight	Quantification & Identification
	Methyldiethanolamine MDEA	119.2	Quantified – IC
	Dimethyldiethanolammonium DMDEAm	134.2	Quantified – IC
	Diethanolamine DEA	105.1	Quantified – IC
	Dimethylaminoethanol DMAE	89.1	Identified – IC
	Methylaminoethanol MAE	75.1	Identified – IC
	Choline TMHeAm	104.2	Identified – IC
	Triethanolamine TEA	149.1	Suspected – LCMS
	Tris(hydroxyethyl)methylammonium THeMAm	164	Suspected – LCMS
	2,2'-(ethane-1,2-diylbis(methylazanediyl))-bis(ethan-1-ol) HeMAEtAHeM	176	Suspected – LCMS
	2,2'-((2-((2-hydroxyethyl)(methyl)amino)ethyl)-azanediyl)bis(ethan-1-ol) HeMAEtABHe	206	Suspected – LCMS
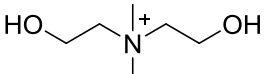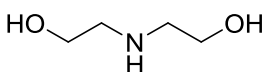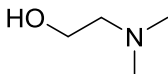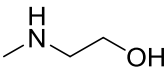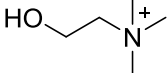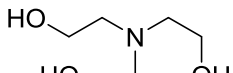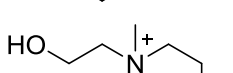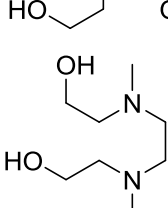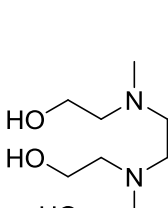
Table 5.5: Mass Balance, MDEA, initially at 5 m MDEA and 0.20 mol H+/mol alkalinity at 150 °C

Amine Name	After 143 hours			After 647 hours		
	Concentration formed (lost) mol/kg	Mol/kg N	Mol/kg C	Concentration formed (lost) mol/kg	Mol/kg N	Mol/kg C
Parent Amines						
MDEA	(0.18)	(0.18)	(0.90)	(0.40)	(0.40)	(2.00)
Total Lost		(0.18)	(0.90)		(0.40)	(2.00)
Major Degradation Products						
DEA	0.08	0.08	0.32	0.12	0.12	0.49
DMDEAm	0.08	0.08	0.46	0.15	0.15	0.87
Total from Major Degradation Products		0.15	0.78		0.27	1.36
		88%	87%		68%	68%
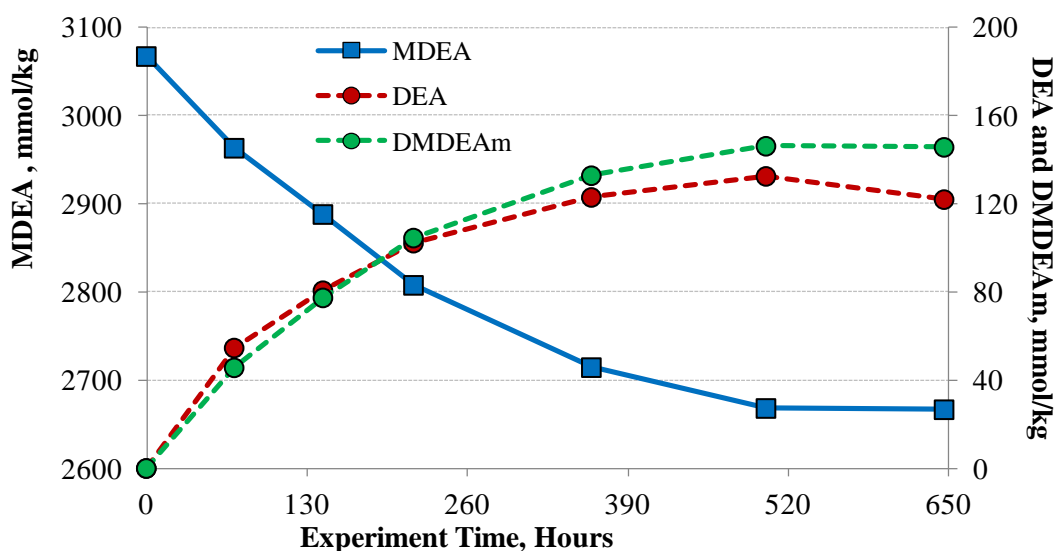
Figure 5.5: Parent Amine and Degradation Products of MDEA initially at 5 m MDEA and 0.2 mol H+/mol alkalinity at 150 °C

DMDEAm was proposed as an intermediate degradation product by Chakma (Chakma 1987) but was not found in degraded solutions by both Chakma and Lepaumier (Lepaumier 2010). Ethylene glycol, a product that Lepaumier and Chakma both identified in MDEA degradation, was not detected using mass spectrometry in this study.

103

Lepaumier and Chakma both used a gas chromatograph to analyze for degradation compounds. Quaternary amines with at least one hydroxyl group will, upon boiling, decompose to form a tertiary amine and the corresponding glycol from the hydroxyl group (Mathews 1916). If DMDEAm were to be boiled, DMAE and ethylene glycol will be formed, and it is likely that this is what was observed in previous studies of MDEA degradation.

5.4 MODELING KINETICS OF PZ-PROMOTED MDEA AND MDEA DEGRADATION

5.4.1 Methodology

Degradation is modeled using the mechanisms shown in Figures 5.1 through 5.3, all of which involve reactions between free and charged amine species. A pKa model was developed in Matlab (The Mathworks) to determine the ratio between protonated amine and free amine species based on the concentration of total amine measured on the ion chromatograph and the concentration of acid measured gravimetrically. This model assumes that the species form an ideal solution with an activity coefficient equal to 1; any nonidealities in solution are embedded within the regressed rate constants.

pKa data were available for MDEA, PZ, DEA, 1-MPZ, and 1,4-DMPZ; the data were regressed and extrapolated from 135 to 165 °C (Khalili 2009, Simond 2012). pKa data were not readily available for MHEtPZ and MHEtMPZ and were estimated computationally using MarvinSketch/Chemicalize (ChemAxon). Only the first and second pKa values were used to estimate protonated amine concentration for diamines and triamines, respectively, as the solution pH is sufficiently high that the diprotonated diamines and triprotonated triamines are negligible. This assumption has been made in numerous thermodynamic models (Frailie 2014, AspenTech 2011) that model CO_2 absorption processes. The regressed values of the pKa are shown in Table 5.6.

Table 5.6: Regressed pKa values used to estimate concentration of free and protonated amine species
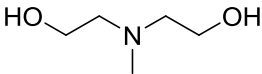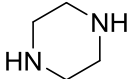
Structure Abbreviation	pKa 25 °C	pKa 135 °C	pKa 150 °C	pKa 165 °C
MDEA	8.53	6.9	6.74	6.59
PZ	pKa1: 9.73 pKa2: 5.35	7.73	7.54	7.36
DEA	8.88	6.89	6.70	6.53
1-MPZ	pKa1: 9.14 pKa2: 4.63	7.43	7.27	7.11
1,4-DMPZ	pKa1: 8.38 pKa2: 3.81	6.51	6.33	6.16
HeMAEtPZ	pKa1: 9.44 pKa2: 8.62 pKa3: 1.50	pKa1: 7.44 pKa2: 6.98	pKa1: 7.25 pKa2: 6.82	pKa1: 7.07 pKa2: 6.68
HeMAEtMPZ	pKa1: 9.02 pKa2: 8.00 pKa3: 0.03	pKa1: 7.38 pKa2: 6.29	pKa1: 7.22 pKa2: 6.13	pKa1: 7.07 pKa2: 5.97
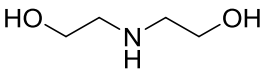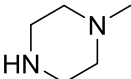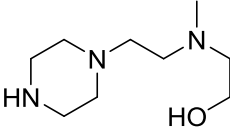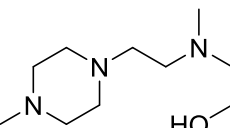
Note: pKa1 and pKa2 for HeMAEtPZ were assumed to vary the same as PZ and MDEA, respectively, and pKa1 and pKa2 for HeMAEtMPZ were assumed to vary the same as MDEA and 1-MPZ, respectively, as data were extrapolated to higher temperatures.

The rate loss of total amine was numerically estimated using a finite difference method (Fogler 2005). This allowed rate constants and activation energies to be estimated by regressing the rate data with the concentration data using a nonlinear regression solver. The XLSTAT nonlinear solver package (AddInSoft 2014) was used to regress the kinetic parameters.

The following equations were used to model the degradation of PZ-promoted MDEA and MDEA. The units of each amine species is in mol/kg.

$$\frac{d[\text{PZ}_{\text{total}}]}{dt} = -k_{\text{PZ−MDEAH}} * [\text{PZ}_{\text{free}}] * [\text{MDEAH}^+]..$$
$$+ k_{\text{DEA−1MPZH}} * [\text{DEA}_{\text{free}}] * [\text{1MPZH}^+] - k_{\text{PZ−DMDEAm}} * [\text{PZ}_{\text{free}}]$$

Eq. 5.1

$$\frac{d[\text{MDEA}_{\text{total}}]}{dt} = -k_{\text{PZ−MDEAH}} * [\text{PZ}_{\text{free}}] * [\text{MDEAH}^+]..$$
$$- k_{\text{MDEA−MDEAH}} * [\text{MDEA}_{\text{free}}] * [\text{MDEAH}^+] + k_{\text{DEA−1MPZH}} * [\text{DEA}_{\text{free}}] * [\text{1MPZH}^+]..$$
$$+ k_{\text{DEA−DMDEAm}} * [\text{DMDEAm}] * [\text{DEA}_{\text{free}}] + k_{\text{PZ−DMDEAm}} * [\text{PZ}_{\text{free}}]$$

Eq. 5.2

Each rate is assumed to follow Arrhenius behavior, which is shown in Eq. 5.3.

$$k = A * \exp\left(\frac{-E_A}{R*T}\right)$$

Eq. 5.3

In Eq. 5.1, $k_{\text{PZ-MDEAH}}$ and $k_{\text{DEA-1MPZH}}$ are the forward and reverse rates of PZ attacking protonated MDEA, which is depicted in Figure 5.1. $k_{\text{PZ-DMDEAm}}$ is the pseudo first-order rate constant where free PZ attacks DMDEAm. The inability to quantify DMDEAm in the majority of the degraded PZ-promoted MDEA solutions does not preclude its presence in small quantities.

Eq. 5.2 is the same as Eq. 5.1 with the addition of two additional terms: $k_{MDEA\text{-}MDEAH}$ and $k_{DEA\text{-}DMDEAm}$ are the forward and reverse rates of free MDEA attacking a protonated MDEA, which is depicted in Figure 5.2. $k_{PZ\text{-}DMDEAm}$ is the pseudo first-order rate constant in which free PZ attacks DMDEAm and is positive because it leads to MDEA formation.

In Eq. 5.3, A is the pre-exponential factor, E_A is the activation energy in J/mol, R is the gas constant and is equal to 8.314 J/(mol*K), and T is the temperature in Kelvin. The model regressed A and E_A for each rate. The model rate constants were evaluated using Eq. 5.3.

Interactions between free and protonated PZ and free and protonated 1-MPZ were neglected. Data from Freeman (2011) indicated that concentrated PZ as well as a blend of 1-MPZ / PZ were found to be an order of magnitude more stable than PZ-promoted MDEA in the presence of CO_2; as a result, any S_N2 interactions between the two species will be significantly slower than the interactions between PZ and MDEA.

5.4.2 Modeling Results: PZ-Promoted MDEA Degradation

Table 5.7 shows the regressed values of the kinetic rate constants from the model. Data from three different regression cases are presented. In Case A, only $k_{PZ\text{-}MDEAH}$ was considered and only for experiments whose initial PZ concentration was equal to the MDEA concentration. Cases B and C used data from all PZ-promoted MDEA experiments. Case B only considered the forward rates $k_{PZ\text{-}MDEAH}$ and $k_{MDEA\text{-}MDEAH}$, whereas Case C considered all forward and reverse rates. The regression results from Case C are shown in Figure 5.8 as a parity plot.

The acid loading of each experiment was chosen to approximate the operational lean loading from plants designed to remove CO_2 from coal-derived flue gas, and total

parent amine degradation was kept to a maximum of 25% loss to ensure that the initial degradation rate would be modeled with reasonable accuracy.

Table 5.7: Regressed Kinetic Parameters for PZ-Promoted MDEA

	Case A	Case B	Case C
Conditions:	1.6 mol/kg PZ 1.6 mol/kg MDEA 0.14 mol H+/mol alk 135 °C – 165 °C	0.4 - 1.6 mol/kg PZ 1.6 – 3.6 mol/kg MDEA 0.09 - 0.14 mol H+/mol alk 135 °C – 165 °C	
Data Points	15	35	
Second-Order Rate Constant at 150 °C kg mol^{-1} s^{-1}*10^6			
$k_{PZ\text{-}MDEAH}$	1.64	1.48	1.48
$k_{MDEA\text{-}MDEAH}$	--	0.12	0.12
$k_{DEA\text{-}1MPZH}$	--	--	0
$k_{DEA\text{-}DMDEAm}$	--	--	0
$k_{PZ\text{-}DMDEAm}$ (s^{-1})	--	--	0.02
Activation Energy kJ mol^{-1}			
$E_{A,PZ\text{-}MDEAH}$	131	143	141
$E_{A,MDEA\text{-}MDEAH}$	--	124	128
$E_{A,DEA\text{-}1MPZH}$	--	--	n/a
$E_{A,DEA\text{-}DMDEAm}$	--	--	n/a
$E_{A,PZ\text{-}DMDEAm}$	--	--	128
Correlation Coefficient	0.95	0.71	0.72

The regression results suggest that free PZ attacking a protonated MDEA is the dominant degradation route in PZ-promoted MDEA degradation. The MDEA-MDEAH degradation pathway is not as dominant and is an order of magnitude slower than the PZ pathway. Addition of the additional forward and reverse reactions does not appreciably change $k_{PZ\text{-}MDEAH}$; it varies by about 15% as additional rate parameters and experimental conditions are added to the model, and the correlation coefficient of the model improves only slightly. The model overpredicts the degradation of PZ at low ratios of PZ / MDEA.

This is due to the estimation and extrapolation of the concentration and pKa of the triamine products, which comprised 20% of the degradation product balance at an initial concentration of 0.4 mol/kg PZ and 1.6 mol/kg MDEA, and to the different activity coefficients of MDEA and PZ at low ratios of PZ / MDEA than at equimolar ratios of PZ / MDEA.

The reverse reactions are inconsequential in determining reaction rates at all experimental conditions. The reaction between 1-MPZ and DEA is almost zero because the concentration of 1-MPZ whose tertiary amino function is protonated is small. The tertiary amino function of 1-MPZ has a lower pKa value than the secondary amino function of 1-MPZ. The reaction between DEA and DMDEAm was considered only at high concentration of MDEA over PZ and is effectively zero because PZ is a much stronger nucleophile than DEA (Bedell 2010).

The ratio between $k_{PZ\text{-}MDEAH}$ and $k_{MDEA\text{-}MDEAH}$ was found to be between 12 and 13. Bedell (2010) investigated the rate of tetramethylammonium chloride (TMACl) disappearance using PZ and MDEA as nucleophiles; Bedell found that the ratio of the second-order rate constants between PZ and TMACl and MDEA and TMACl was 14 and is close to the ratio observed in this study.

The regression results from Case C were used to estimate the rate of another experiment whose data set was not used to regress the parameters of the kinetic model. The experiment was run at an initial condition of 2.5 m PZ / 2.5 m MDEA and 0.14 mol H+/mol alk at 165 °C. The data are shown in Figure 5.9. Data for another experiment at an initial condition of 2.5 m PZ / 2.5 m MDEA and 0.15 mol H+/mol alk added as hydrochloric acid, a monovalent strong acid, instead of sulfuric acid as the proton source is shown in Figure 5.10. The model prediction assumes that only DEA and 1-MPZ are present as byproducts.
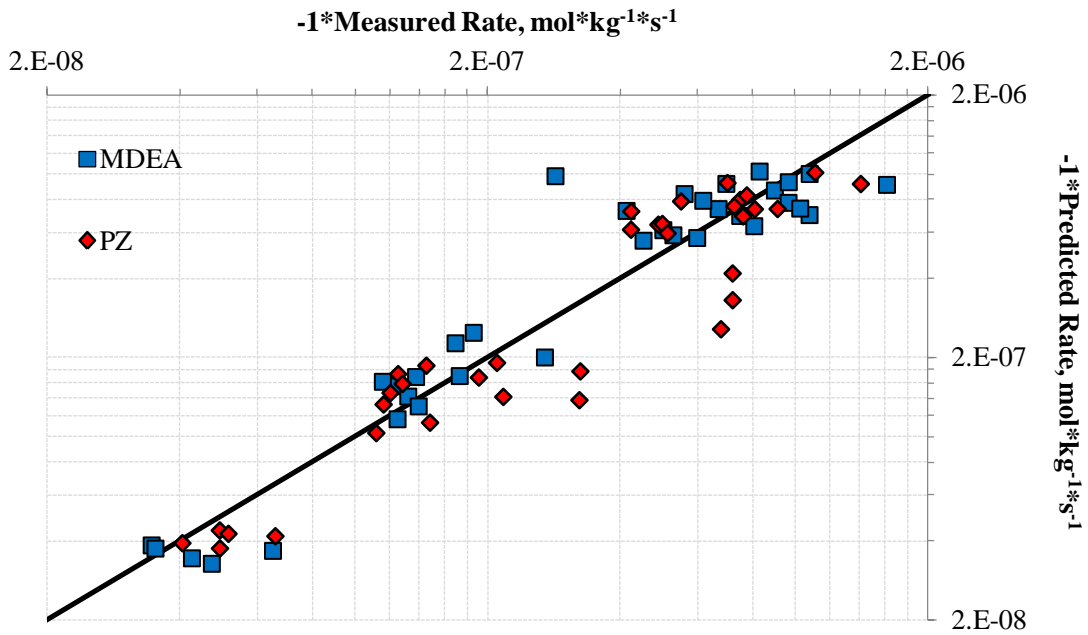
Figure 5.8: Parity Plot Showing Regression Results for Case C
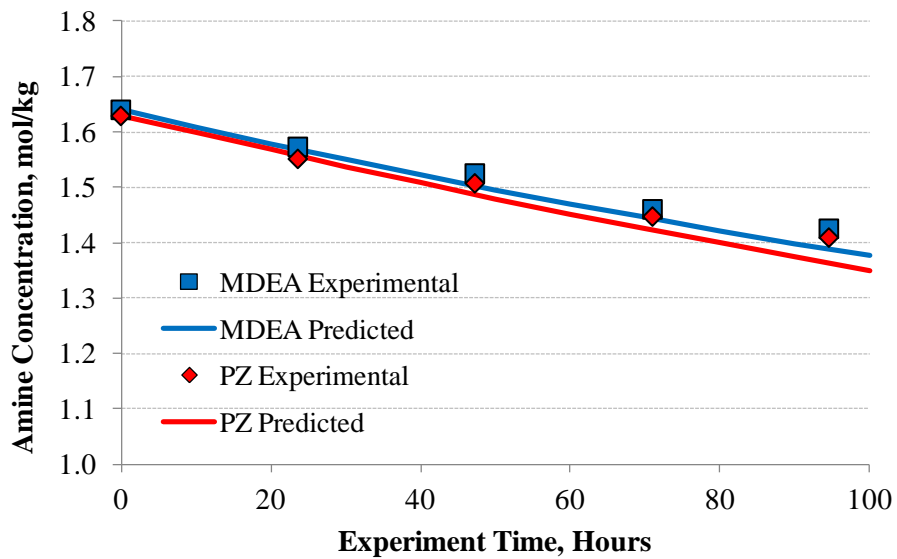
Figure 5.9: Model Prediction and experimental data for the degradation of 2.5 m PZ / 2.5 m MDEA with 0.14 mol H+/mol alk as H$_2$SO$_4$ at 165 °C
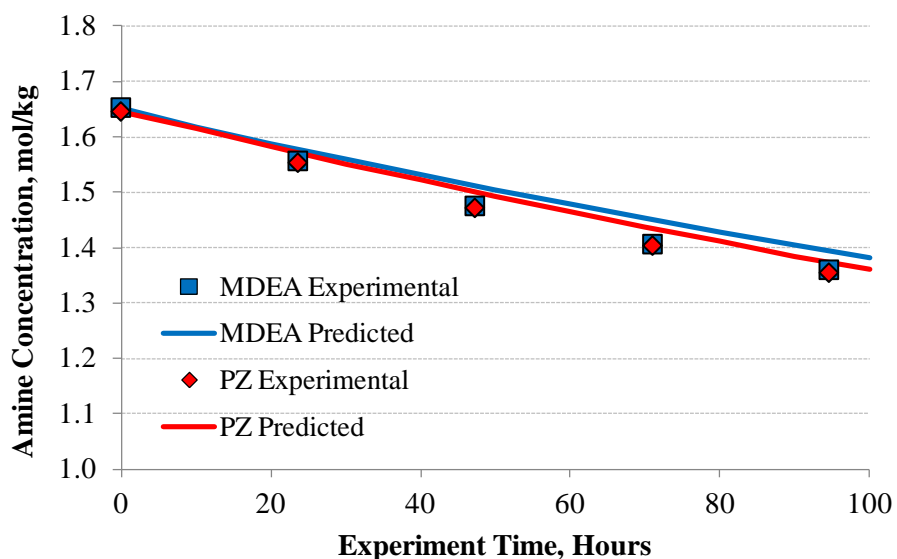
Figure 5.10: Model Prediction and experimental data for the degradation of 2.5 m PZ / 2.5 m MDEA with 0.14 mol H+/mol alk as HCl at 165 °C

The kinetic model overpredicts the degradation rate for 2.5 m PZ / 2.5 m MDEA and 0.14 mol H+/mol alkalinity at 165 °C by about 20% and underpredicts degradation for 2.5 m PZ / 2.5 m MDEA and 0.15 mol H+/mol alkalinity added as hydrochloric acid at 165 °C by about 25%. The measured concentration of PZ and MDEA is within 5% of the predicted model values for both sets of data. The model begins to deviate from the experimental results as the total degradation increases and is likely due to the omission of minor degradation products present in solution in the model and the exclusion of other interactions between PZ, MDEA, and other degradation products. The model prediction also indicates that the acid counterion does not appreciably change the solution activity to affect rate.

111

5.4.3 Modeling Results: MDEA Degradation

Table 5.8 shows the rate constants of the regressed data set for MDEA degradation. Eq. 5.2 was used to regress kinetic parameters for these experiments. Figure 5.11 shows the results as a parity plot.

Table 5.8: Regressed Kinetic Parameters for MDEA

Conditions:	3.0 mol/kg MDEA 0.20 mol H+/mol alk 135 °C – 165 °C
Data Points	15
Second-Order Rate Constant at 150 °C kg mol^{-1} s^{-1}*10^6	
$k_{MDEA-MDEAH}$	0.30
$k_{MDEA-DMDEAm}$	12
Activation Energy kJ mol^{-1}	
E_{A1}	117
E_{A2}	121
Correlation Coefficient	0.93
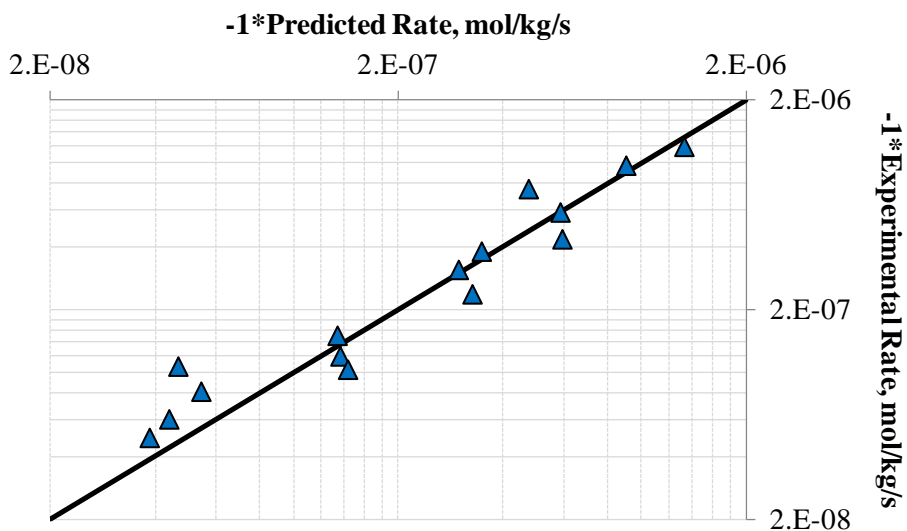
Figure 5.11: Parity Plot of MDEA Degradation Results

The forward rate parameter $k_{MDEA-MDEAH}$ is about two and a half times greater in MDEA solutions than the parameter regressed with the PZ-promoted MDEA experiments. The MDEA degradation experiments were run at a higher acid loading (0.2 mol H+/mol alkalinity) than the PZ-promoted MDEA experiments. It is possible that the higher solvent loading, lower concentration of free amino groups, and lack of PZ made the MDEA solvent more aprotic than PZ-promoted MDEA at experimental conditions; increased solvent aproticity can lead to greater S_N2 reaction rate. The reverse rate parameter $k_{DEA-DMDEAm}$ is about 40 times as fast as $k_{MDEA-MDEAH}$. DEA is known to be a weaker nucleophile than PZ due to its lower pKa value, and the high ratio of $k_{DEA-DMDEAm}$ to $k_{MDEA-MDEAH}$ indicates that the quaternary amine is a better leaving group than protonated tertiary amines.

5.4.4 Comparison of Initial Rates of PZ-Promoted MDEA Degradation in H+ Loaded Solutions and CO$_2$-Loaded Solutions

The acid-loaded experiments are useful in validating the initial degradation pathway of PZ-promoted MDEA and understanding the degradation rate as a function of amine speciation. However, the data need to be compared and reconciled against degradation of CO$_2$-loaded PZ-promoted MDEA to be used to model thermal degradation from a process design perspective.

Table 5.9 lists the activation energy of thermal degradation of PZ-promoted MDEA loaded either with H+ or CO$_2$ at conditions approximating operating lean loading.

Table 5.9: Activation Energy of Thermal Degradation of PZ-Promoted MDEA Solvents at Lean Loading

Solvent Composition	E_A PZ kJ/mol	E_A MDEA kJ/mol
0.75 – 2.5 m PZ 2.5 – 7 m MDEA 0.11 – 0.14 mol H+/mol alk	141 (Case C, E_{A1})	
2 m PZ 7 m MDEA 0.12 mol CO_2/mol alk	147	140
5 m PZ 5 m MDEA 0.24 mol CO_2/mol alk	139	140

The data indicate that the activation energy of thermal degradation predicted by the model is generally similar to the observed activation energy of thermal degradation in CO_2-loaded degradation and shows good agreement with each other.

Table 5.10 shows the speciation of major species present in CO_2-loaded PZ-promoted MDEA solvents at the temperature encountered in the amine desorber. The "Independence" (Frailie 2014) thermodynamic framework, regressed using AspenPlus 7.3 (AspenTech 2011), was used to determine the concentration and quantity of free amine, protonated amine, and amine carbamate at the given solvent loading. The speciation data from the model are presented in Table 5.10.

Table 5.10: Concentration (mol/kg) of Species Present in Loaded CO_2 Solutions at 150 °C with a Lean Loading Corresponding to 500 Pa CO_2 at 40 °C

Structure	Name	7 m MDEA 2 m PZ	5 m MDEA 5 m PZ
	MDEA	3.15	2.02
	MDEAH+	0.23	0.28
	PZ	0.62	0.56
	PZH+	0.19	0.53
	PZ Carbamate	0.20	0.54
	PZ Zwitterion	0.27	0.64
	PZ Dicarbamate	0.01	0.02
HCO_3^-	Bicarbonate	0.19	0.21
CO_3^{2-}	Carbonate	0.01	0.01
CO_2	Physically Absorbed CO_2	0.03	0.03
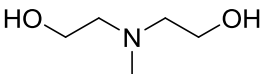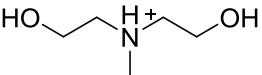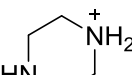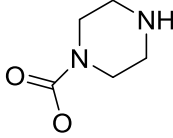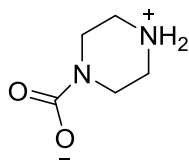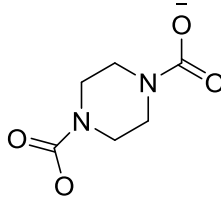
The speciation data indicate that, in addition to free PZ, protonated PZ, and PZ-carbamate, the dicarbamate salt as well as the PZ zwitterion is present. This suggests that the PZ carbamate salt can function as a nucleophile and thus participate in the degradation pathway. The pKa of the PZ carbamate was found by Bishnoi (Bishnoi 2000) to be about 9.15. This value is between that of PZ and morpholine, which has a pKa of about 8.50 (Haynes, Ed. 2014). Davis (2009) found that morpholine functioned as a strong nucleophile and has a similar degradation rate to PZ in the degradation of CO_2-loaded monoethanolamine (MEA) blended either with PZ or morpholine.

Both of the mechanisms shown in Figures 5.1 and 5.2 include DEA as a degradation product. DEA can form a carbamate and then form an oxazolidinone via the carbamate polymerization pathway. The oxazolidinone can then react with PZ. Data shown in Chapter 4 indicate that DEA concentration is nearly constant in CO_2-loaded degradation and behaves as a reactive steady-state intermediate. Data shown in Section 5.4.3 indicate that the quaternary amine salt is much more reactive than other protonated amine species, and thus it too can behave as a steady state intermediate.

The initial acid rate measurements need to consider these phenomena to properly account for the initial degradation rate in systems loaded with CO_2. The free PZ concentration in Eq. 5.1 and Eq. 5.2 can been modified to reflect the sum of PZ and PZ carbamate. The initial rate of PZ degradation can be assumed to be twice as fast as MDEA degradation because one equivalent of MDEA can, if byproducts are accounted for, react with two equivalents of PZ. Initial zeroth-order rate measurements of PZ-promoted MDEA under CO_2-loaded conditions up to 450 hours at 135 °C and 120 hours at 150 °C indicated that this ratio was about 1.7. Thus, the initial rate of PZ-promoted MDEA degradation can be corrected using the following two terms:

$$\frac{d[\text{MDEA}_{\text{total}}]}{dt} = -k_{\text{PZ-MDEAH}} * [\text{PZ}_{\text{free}} + \text{PZCOO}^-] * [\text{MDEAH}^+] ..$$
$$- k_{\text{MDEA-MDEAH}} * [\text{MDEA}_{\text{free}}] * [\text{MDEAH}^+]$$

Eq. 5.4

$$\frac{d[\text{PZ}_{\text{total}}]}{dt} = 2 * \frac{d[\text{MDEA}_{\text{total}}]}{dt}$$

Eq. 5.5

The initial amine loss rate of PZ-promoted MDEA in CO_2-loaded solution approximated using 0th order kinetics, whose average rate was taken over 100-120 hours, is compared with the initial rates predicted by the kinetic model at 150 °C. These data are shown in Table 5.11.

Table 5.11: Comparison of Corrected Model Results to Experimental CO_2-Loaded Degradation Data at 150 °C

Solvent Composition	PZ loss mol/kg/h*10^{-3} Model	PZ loss mol/kg/h*10^{-3} Experimental	MDEA loss mol/kg/h*10^{-3} Model	MDEA loss mol/kg/h*10^{-3} Experimental
2 m PZ 7 m MDEA 0.12 mol CO_2/mol alk	2.2	2.3±0.2	1.1	1.4±0.6
5 m PZ 5 m MDEA 0.24 mol CO_2/mol alk	3.6	3.0±1	1.8	2.2±1

With the corrections added, the kinetic model does a reasonable job predicting the initial loss rate of both MDEA and PZ to ±20%. The predicted values are within the 95% confidence limit of the regressed 0th order rate.

5.5 PROCESS DESIGN MODELING

If the corrections presented in Section 5.4.4 are incorporated into the kinetic model, the data from the model can be extended and used in process design problems to predict the thermal degradation rate as a function of design lean loading, design starting

amine concentration, and design stripping temperature. These predictions are helpful in setting process envelopes, such as the maximum stripping temperature, based on the plant design specifications for all CO_2 capture and removal processes. Oxidative degradation will have to be taken into account to understand the net overall degradation rate for CO_2 removal from sources with oxygen present such as the flue gas from power plants. The thermal degradation rate, however, can serve as a representative overall degradation rate for processes that remove CO_2 and H_2S from high pressure streams, such as liquefied natural gas and synthesis gas treating, due to the absence of other dominating degradation pathways from these sources.

The "Independence" framework (Frailie 2014) was used to determine the concentration of free amine, protonated amine, and PZ carbamate as a function of lean loading, starting concentration, and stripping temperature. The process design specifications used for the model in this study are presented in Table 5.12.

Table 5.12: Process Design Specifications Used in Model

Parameter	Value
Equilibrium CO_2 Pressure at Absorber Inlet	100 Pa CO_2 500 Pa CO_2 (at 40 °C)
Equilibrium CO_2 Pressure at Absorber Outlet	5000 Pa CO_2 (at 40 °C)
Residence Time	30 minutes
Residence Time in Sump (treated as CSTR)	10 minutes
Stripping Temperature	105 °C, 120 °C, 135 °C
Weight Percent Amine in solvent, CO_2-free basis	45%

Figure 5.12 shows the predicted total degradation rate in grams amine/tonne CO_2 captured as a function of PZ weight fraction of total amine, temperature, and lean loading, CO_2 capacity at a lean loading of 100 and 500 Pa CO_2, and CO_2 capacity corrected for viscosity at 500 Pa CO_2. The model predictions are compared to estimated degradation rate data extracted from the maximum stripping temperature analysis presented in Chapter 4.

Overall, the model is able to predict the degradation rate to within 20% of amine lost from experimental data from the T_{MAX} analysis. The T_{MAX} analysis takes into account the rate throughout the entire degradation and not just the initial rate, which can account for the discrepancy between the experimental and modeled results. The CO_2-loaded experiments also might have slightly different solution activities and solvation properties that might slow down the S_N2 reactions in the CO_2-loaded solution compared to the acid-loaded solution which can further increase the discrepency.
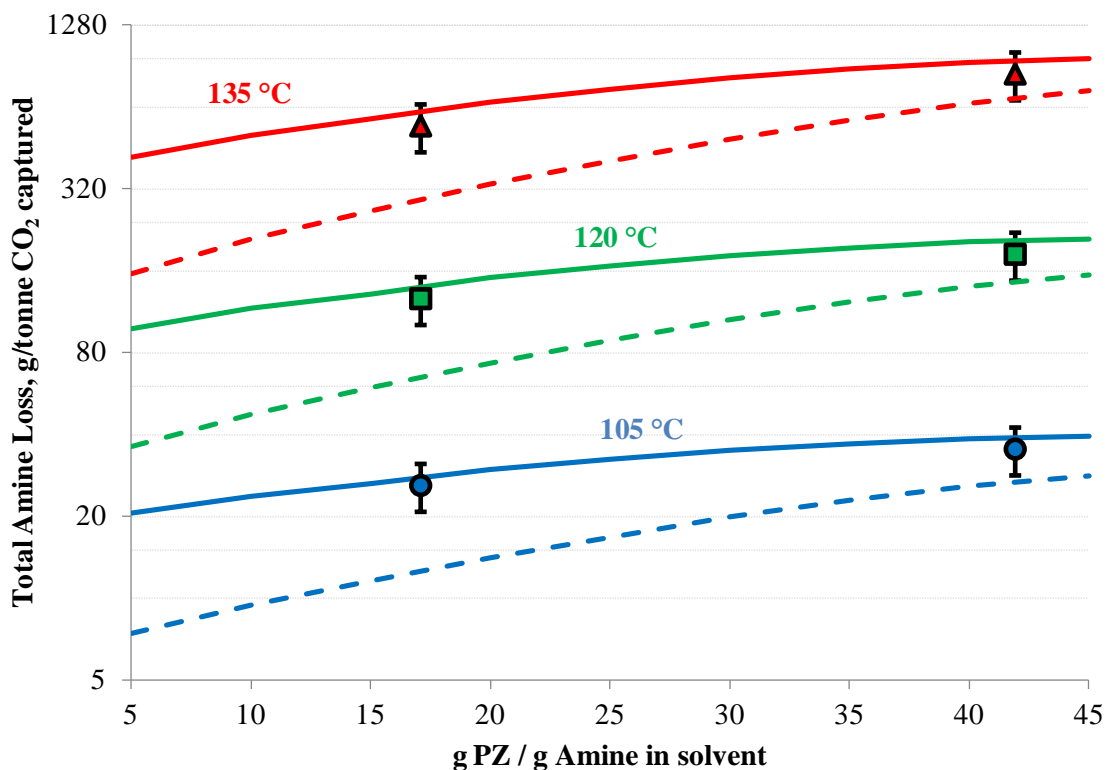
Figure 5.12: Process Design Model for Predicting Degradation Losses. Solid lines represent amine loss at a lean loading of 500 Pa CO_2. Thick dashed lines represent amine loss at a lean loading of 100 Pa CO_2. Points represent predictions from experimental data based on the T_{MAX} analysis presented in Chapter 4; error bars denote ±20% deviation from measurements.

The degradation rate as predicted by the model is significantly less with a lean loading of 100 Pa CO_2 and low PZ concentration than at higher lean loading and higher PZ concentration. As PZ concentration increases, the amount of CO_2 in solution increases to maintain the equilibrium CO_2 partial pressure and, as a result, the concentration of protonated MDEA also increases to a point where the net initial forward rate at a lean loading of 100 Pa CO_2 is greater than at a lean loading of 500 Pa CO_2. These data are shown in Figure 5.13. The overall degradation rate, however, is reduced due to the higher intrinsic capacity of running a solvent with lower lean loading. In real

120

systems, however, the intrinsic degradation rate will likely be somewhat less than the predicted rate at a lean loading of 100 Pa CO_2. At lower loading, the relative amount of DEA complexed with CO_2 will be less than at richer loading, reducing the stoichometric factor between MDEA and PZ and thus the overall degradation rate.
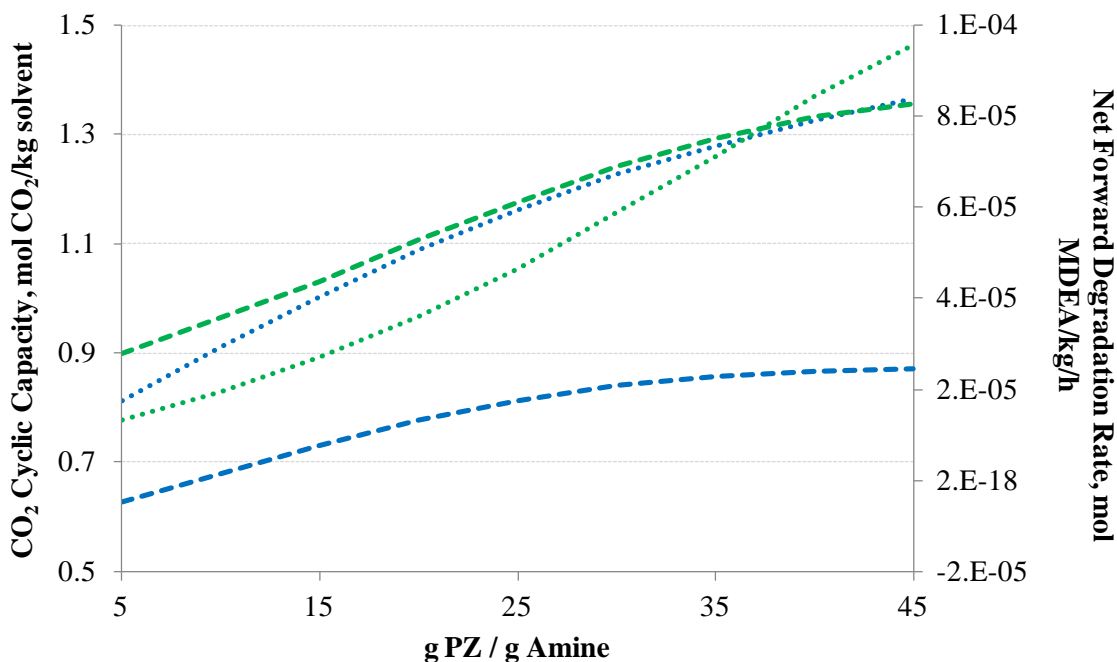
Figure 5.13: Intrinsic predicted MDEA loss (green lines) and CO$_2$ cyclic capacity (blue lines) at lean loadings of 100 Pa CO$_2$ (dotted lines) and 500 Pa CO$_2$ (dashed lines) at a concentration of 45 wt% amine and 120 °C.

Based on these data, it is possible to consider running at a lower lean loading and higher stripping temperature. A higher stripping temperature increases the desorption pressure of CO_2 in the stripper, reducing CO_2 compression costs, and can also serve to control the steady-state concentration of nitrosamine, which is a carcinogenic byproduct formed from the reaction of NOx in the flue gas with secondary amines, in solution (Fine, 2013). A lower lean loading will also increase the driving forces in the absorber,

121

reducing its size, and will also require smaller heat exchange equipment throughout the plant due to the lower circulation rate, reducing capital costs of the plant.

Assuming a price of \$3/kg for the amine, an average of \$0.2 can be saved per tonne of CO_2 captured at a lean loading of 100 Pa CO_2 versus 500 Pa CO_2 at 120 °C. At 135 °C, an average of \$0.9 can be saved from running at the leaner loading. Regardless of temperature, the costs from the expected additional energy required to strip the solvent to a lean loading to 100 Pa CO_2 instead of 500 Pa CO_2 is about \$1.1 per tonne of CO_2 if an electricity price of \$100/MW*h is used (Lin, personal communication, 2014). Therefore, it is not cost effective to run at a lower lean loading strictly from the viewpoint of thermal degradation and plant efficiency at conditions encountered in capture from coal-derived flue gas.

5.6 CONCLUSIONS

- Degradation of PZ-promoted MDEA is initiated by a S_N2 substitution involving free and protonated amine.

- The dominant initial degradation pathway involves free PZ attacking the methyl group of protonated MDEA, forming 1-MPZ and DEA. These happen to be the dominant degradation products in PZ-promoted MDEA and can account at least 60% of the mass lost by PZ and MDEA.

- MAE and 1-HePZ were observed in PZ-promoted MDEA degradation; however, their estimated concentration was more than an order of magnitude less than DEA and 1-MPZ and indicates that attack on a hydroxyethyl chain is not favored.

- Minor degradation products include 1,4-DMPZ and triamines whose structures suggest PZ attacking carbons alpha to the hydroxyl function of the MDEA and can account from 10 to 30% of the mass lost.

- The less dominant pathway involves MDEA attacking protonated MDEA, forming the quaternary amine salt DMDEAm and DEA. This pathway is the principal degradation pathway for MDEA degradation in the absence of PZ.

- DEA and DMDEAm can account for about 90% of the amine loss initially and eventually begin to approach equilibrium in MDEA degradation.

- Other tertiary amines, such as DMAE and TEA, and quaternary amine salts, such as THEMAm and choline, were detected on MS but were not quantified using the IC. Diamines consistent with MDEA attack on the carbon alpha to the hydroxyl were observed on MS in MDEA degradation experiments.

- The second-order rate constants predicted by the kinetic model indicate that the rate constant of PZ attacking MDEAH+ is $1.5*10^{-6}$ kg/mol/s at 150 °C and MDEA attacking MDEAH+ is $0.12*10^{-6}$ kg/mol/s in the presence of PZ. The rate of the reverse reactions to regenerate MDEA and PZ is not a significant contributor to modeling the amine losses initially.

- In the absence of PZ, the rate constant of MDEA attacking MDEAH+ is about $0.3*10^{-6}$ kg/mol/s and the reverse rate reaction to regenerate MDEA from DEA and DMDEAm is 40 times as fast as the forward reaction.

- The kinetic model is able to predict initial rates within 20% of the experimental CO_2 amine loss rates after making corrections to the kinetic model to account for additional PZ loss in the presence of CO_2 and the reactivity of the PZ carbamate. The activation energy of degradation predicted by the model is about 140 kJ/mol and is similar to the activation

energy of degradation observed in CO_2-loaded experiments which ranged from 140-147 kJ/mol.

- The kinetic model, when applied to process design conditions, is able to predict initial degradation rates that match reasonably (within 20%) to the results predicted by the T_{MAX} analysis presented in Chapter 4 as initial starting conditions and amine concentration are varied.

- At lower lean loading, net overall degradation is reduced due to the significantly higher working capacity of the solvent (as predicted by the model). The additional energy cost to strip to a lean loading of 100 Pa CO_2 incurs a cost penalty 5.5 times greater than the savings from achieving a reduced degradation rate at 120 °C.

Chapter 6: Thermal Degradation of Other Piperazine (PZ)-Promoted Tertiary Amines under Acidified Conditions

6.1 INTRODUCTION & SCOPE

Rigorous modeling of PZ-promoted MDEA thermal degradation was presented in Chapter 5. A key finding is that the dominant rate mechanism of PZ-promoted MDEA degradation is by PZ attack of protonated MDEA. These results are extended in this chapter to cover the acidified degradation of other tertiary amines with sulfuric acid used to supply H^+. The tertiary amines were systematically varied by changing structure and functional groups. The degradation of PZ-promoted dimethylaminoethanol (DMAE) and dimethylaminopropanol (DMAP) is modeled as rigorously as PZ-promoted MDEA and is presented, and the initial second-order reaction rate of PZ attack of methyl, ethyl, and hydroxyethyl groups as a function of secondary amine byproduct formation is presented. Finally, practical results that model degradation rate as a function of structure and not as a function of species are presented. The tertiary amines tested in this study are presented in Table 6.1. Raw data, chromatograms, and mass spectra for the experiments discussed in this chapter are presented in Appendix B.3.

6.2 MODELING OF PZ-PROMOTED DMAP AND DMAE

DMAP and DMAE are, like MDEA, tertiary aliphatic alkanolamines. They differ from MDEA in that DMAP and DMAE have two methyl groups rather than one and only one hydroxyl functional group rather than two as on MDEA. DMAP has a hydroxypropyl group which is longer by one carbon than the hydroxyethyl groups present in DMAE and MDEA. Figures 6.1 and 6.2 show the degradation pathway of PZ-promoted DMAE and DMAP, respectively.

Table 6.1: Tertiary Amines Tested

Amine	Name / Abbreviation	MW	Supplier / Purity (wt%)
	MDEA 105-59-9	119.2	Acros Organics 99%
	DMAE 108-01-0	89.1	Sigma-Aldrich 99.5%
	DMAP 3179-63-3	103.2	Sigma-Aldrich 99%
	DMAIP 108-16-7	103.2	Sigma-Aldrich 99%
	DMAB 13330-96-6	117.2	Tokyo Chemical Industry 98%
	DMAEE 1704-62-2	133.2	Sigma-Aldrich 98%
	EDEA 139-87-7	133.2	Sigma-Aldrich 98%
	nBuDEA 102-79-4	161.2	Sigma-Aldrich 98.6%
	DEAE 100-37-8	117.2	Sigma-Aldrich 99.5%
	TEA 102-71-6	149.2	Fisher Scientific 99.6%
	TIPA 122-20-3	191.3	Sigma-Aldrich 95%
	HEM 622-40-2	131.2	Acros Organics 99%
	HPM 4441-30-9	145.2	Tokyo Chemical Industry 98%
	HIPM 2109-66-2	145.2	Tokyo Chemical Industry 98%
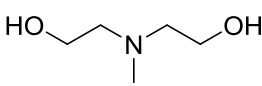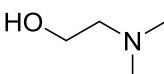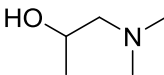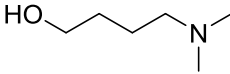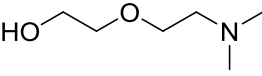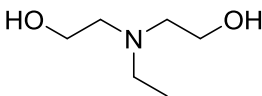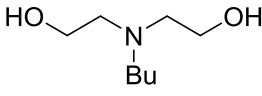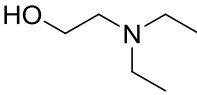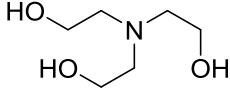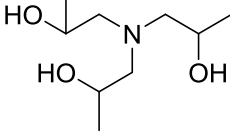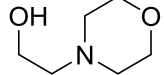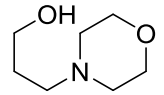
126
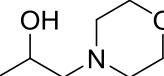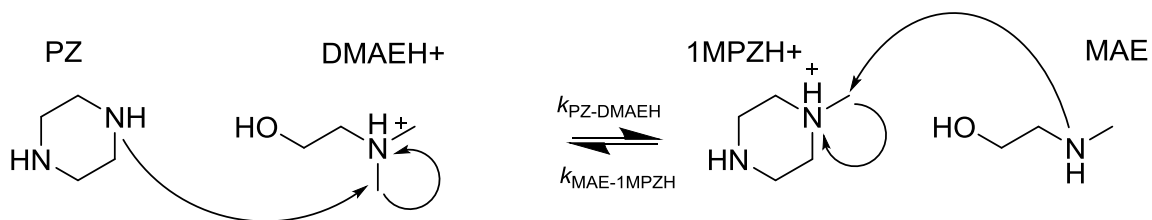
Figure 6.1: Proposed Degradation Pathway of PZ attack on protonated DMAE to form 1-MPZ and MAE
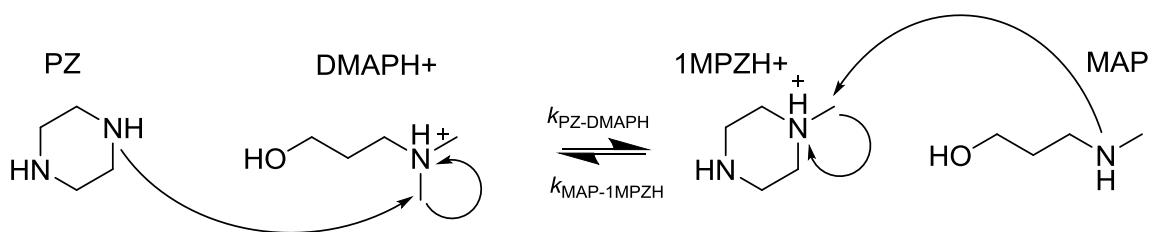
Figure 6.2: Proposed Degradation Pathway of PZ attack on protonated DMAP to form 1-MPZ and MAP

6.2.1 Products Observed / Material Balance in Degraded PZ-Promoted DMAP and DMAE solutions

Tables 6.2 through 6.5 list the degradation products present in degraded solution and the mass balance closure of PZ-promoted DMAE and DMAP, and Figures 6.3 and 6.4 show the evolution of degradation products in degraded solutions of PZ-promoted DMAE and PZ-promoted DMAP, respectively.

127

Table 6.2: Products Observed in Degradation of PZ-Promoted DMAE
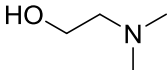
Structure	Name Abbreviation	Molecular Weight	Quantification & Identification
	Dimethylaminoethanol DMAE	89.1	Quantified – IC
	Piperazine PZ	86.1	Quantified – IC
	Methylaminoethanol MAE	75.1	Quantified – IC
	1-Methylpiperazine 1-MPZ	100.2	Quantified – IC
	1,4-Dimethylpiperazine 1,4-DMPZ	114.2	Quantified – IC
	Ethanolamine MEA	61.1	Identified – IC
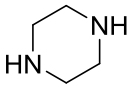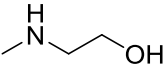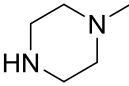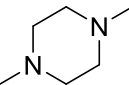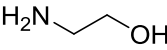
Table 6.3: Mass Balance, PZ-Promoted DMAE, initially at 2.5 m PZ / 2.5 m DMAE and 0.14 mol H+/mol alkalinity at 150 °C after 865 hours

Amine	Concentration formed (lost) mol/kg	Mol/kg N	Mol/kg C
Parent Amines			
DMAE	(0.44)	(0.44)	(1.75)
PZ	(0.45)	(0.90)	(1.81)
Total Lost		(1.34)	(3.56)
Major Degradation Products			
MAE	0.44	0.44	1.33
1-MPZ	0.41	0.82	2.10
1,4-DMPZ	0.03	0.06	0.17
Total Material		1.32	3.60
Balance		99%	101%

Table 6.4: Products Observed in Degradation of PZ-Promoted DMAP
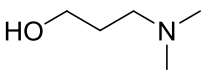
Structure	Name Abbreviation	Molecular Weight	Quantification & Identification
HO~~~N (dimethyl)	Dimethylaminopropanol DMAP	103.2	Quantified – IC
piperazine (HN, NH)	Piperazine PZ	86.1	Quantified – IC
methylamino-propanol structure	Methylaminopropanol MAP	89.1	Quantified – IC
1-methylpiperazine structure	1-Methylpiperazine 1-MPZ	100.2	Quantified – IC
1,4-dimethylpiperazine structure	1,4-Dimethylpiperazine 1,4-DMPZ	114.2	Quantified – IC
H_2N~~~OH	Propanolamine MPA	75.1	Identified – IC
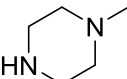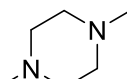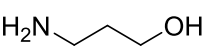
Table 6.5: Mass Balance, PZ-Promoted DMAP, initially at 2.5 m PZ / 2.5 m DMAP and 0.14 mol H+/mol alkalinity at 150 °C after 865 hours

Amine	Concentration formed (lost) mol/kg	Mol/kg N	Mol/kg C
Parent Amines			
DMAP	(0.44)	(0.44)	(2.18)
PZ	(0.45)	(0.90)	(1.81)
Total Lost		(1.34)	(3.56)
Major Degradation Products			
MAP	0.39	0.39	1.16
1-MPZ	0.40	0.81	2.02
1,4-DMPZ	0.03	0.05	0.16
Total Material		1.25	3.60
Balance		93%	94%
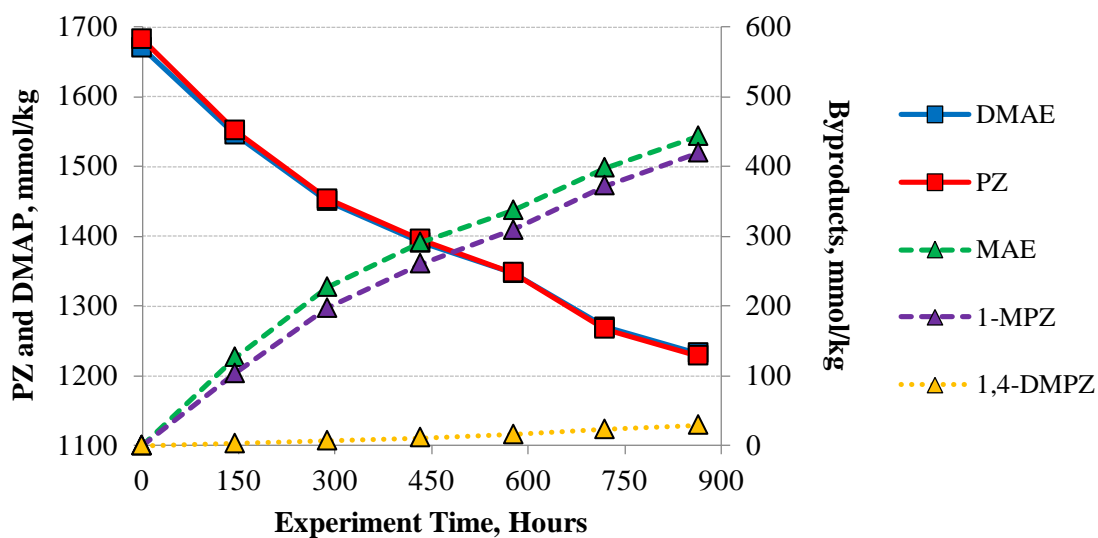
Figure 6.3: **Degradation Products and Parent Amines of PZ-Promoted DMAE initially at 2.5 m PZ / 2.5 m MDEA and 0.14 mol H+/mol alkalinity at 150 °C.**
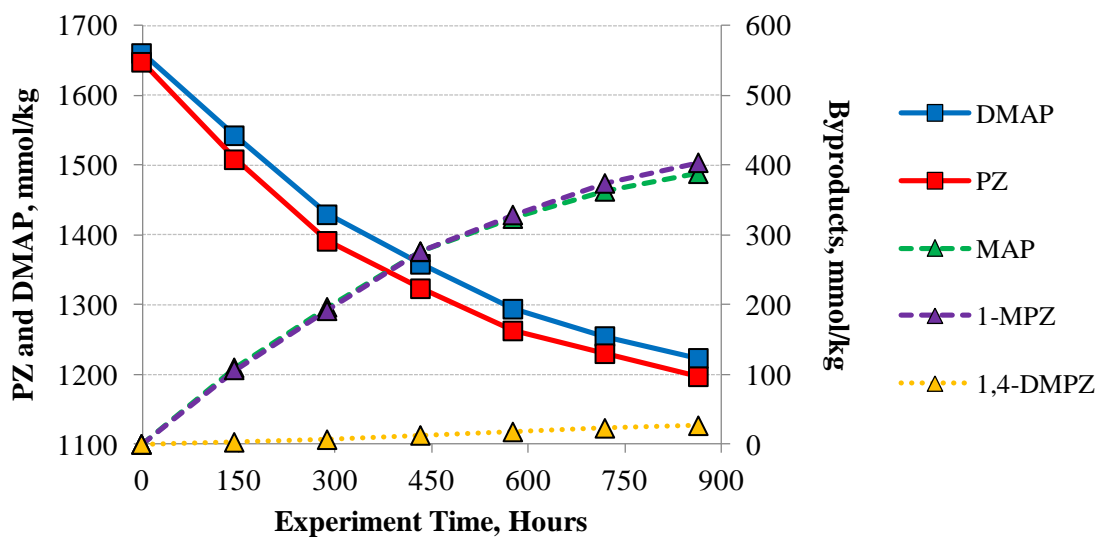
Figure 6.4: **Degradation Products and Parent Amines of PZ-Promoted DMAP initially at 2.5 m PZ / 2.5 m MDEA and 0.14 mol H+/mol alkalinity at 150 °C.**

The degradation product slate of PZ-promoted DMAE and PZ-promoted DMAP is largely identical to PZ-promoted MDEA. 1-MPZ and secondary monoamine byproducts are dominant, with 1,4-DMPZ serving as a minor degradation product. Ethanolamine and propanolamine were detected, but not quantified, in degraded solutions of PZ-promoted DMAE and DMAP, respectively. This suggests that PZ or other amines can interact with functional groups on secondary amines, especially reactive functional groups such as methyl groups.

6.2.2   Kinetic Modeling: Degradation of PZ-Promoted DMAP and DMAE

The rate modeling of both solvents assumes that the dominant degradation pathway is by PZ attack on the protonated tertiary amine with a negligible rate of reverse reaction. This was found in Chapter 5 to be the dominant degradation pathway in PZ-promoted MDEA degradation especially at a higher concentration of PZ relative to tertiary amine.

The pKa of the parent amines and degradation products was regressed using experimental data (Hamborg 2009, Khalili 2009, Simond 2012). The pKa values for DMAE, DMAP, MAP, and MAE are shown in Table 6.6. Experimental pKa data were not available for MAP. The pKa for MAP was estimated using MarvinSketch/Chemicalize (ChemAxon) at 25 °C. It was found to vary as a function of temperature using the following relationship, shown in Eq. 6.1:

$$\frac{\Delta_r H_{m,\text{MAP}}}{R} = \frac{d\ln(K)}{d(1/T)}_{\text{MAP}} = \frac{\Delta_r H_{m,\text{MAE}}}{R} * \frac{\Delta_r H_{m,\text{DMAP}}}{\Delta_r H_{m,\text{DMAE}}} \qquad \text{Eq. 6.1}$$

In Equation 6.1, R is the gas constant, $\Delta_r H_m$ is the standard change of enthalpy of reaction, T is the temperature, and K is the equilibrium constant between the protonated amine and free amine.

Table 6.6: Predicted pKa values of DMAE, MAE, DMAP, and MAP
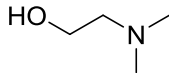
Structure Abbreviation	pKa 25 °C	pKa 135 °C	pKa 150 °C	pKa 165 °C
DMAE	9.19	7.46	7.29	7.13
MAE	9.85	7.64	7.42	7.23
DMAP	9.49	8.11	7.98	7.85
MAP	10.0	8.22	8.05	7.90
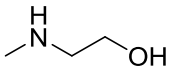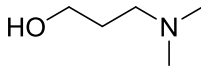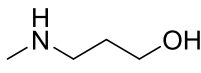
Equations 6.2 and 6.3 show the rate and the linearized rate expressions used to model the kinetics of the reactions. In these expressions, dC_{PZ}/dt and dC_{TA}/dt represents the loss of total PZ and total tertiary amine, respectively, estimated using finite-difference methods described in Eq. 5.1. A represents the preexponential factor, E_A represents the activation energy in J/mol, [TA$^+$] represents the concentration of protonated tertiary amine in mol/kg, and [PZ] represents the concentration of PZ in mol/kg.

$$\frac{dC_{PZ}}{dt} = \frac{dC_{TA}}{dt} = -r = -A * \exp(\frac{-E_A}{R*T}) * \left[TA^+\right] * \left[PZ_{free}\right] \qquad \text{Eq. 6.2}$$

$$\ln(-r) = \ln(-A) + (\frac{-E_A}{R*T}) + \ln([TA^+]) + \ln([PZ_{free}]) \qquad \text{Eq. 6.3}$$

The rate parameters of the forward rate expression were regressed using Microsoft Excel simultaneously using Equation 6.2. This routine was also used to reregress the parameters of PZ-promoted MDEA degradation; the parameters estimated from the linearized rate were not statistically different from the parameters predicted by the XLSTAT (AddInSoft 2014) nonlinear regression tool and are shown in Table 6.7.

Table 6.7: Regressed Kinetic Parameters for PZ-Promoted DMAE, PZ-Promoted MDEA, and PZ-Promoted DMAP

	PZ/MDEA	PZ/DMAE	PZ/DMAP
Conditions:	1.6 mol/kg PZ		
	1.6 mol/kg Tertiary Amine		
	0.14 mol H+/mol alk		
	135 °C – 165 °C		
Data Points	15	15	15
Second-Order Rate Constant at 150 °C kg mol^{-1} s^{-1}*10^6			
$k_{PZ\text{-Tertiary Amine}}$	1.57	0.83	0.32
Activation Energy kJ/mol			
$E_{A,\ PZ\text{-Tertiary Amine}}$	127±10	113±15	125±13
Preexponential Factor s^{-1}*10^{-8}			
$A_{,\ PZ\text{-Tertiary Amine}}$	67.7	0.767	9.25
Upper CI, $A_{,\ PZ\text{-Tertiary Amine}}$	944	57.2	379
Lower CI, $A_{,\ PZ\text{-Tertiary Amine}}$	4.86	0.01	0.23
Correlation Coefficient	0.97	0.89	0.93

PZ-promoted DMAE, PZ-promoted MDEA, and PZ-promoted DMAP are modeled well using this method, and the regressed value of the activation energy using second-order kinetics is similar to the activation energy of thermal degradation in CO_2-loaded solvents.

These data can be fit using a Brønsted Relationship, shown in Equation 6.4 (Anslyn 2006) and Figure 6.5.

$$\log(k) = \beta_{LG} * pKa_{LG} + \log(C)$$
<div align="right">Eq. 6.4</div>

In Eq. 6.4, k denotes the second-order rate constant between PZ and the tertiary amine. pKa_{LG} is the pKa value of the leaving group of the tertiary amine and corresponds to the secondary amine byproduct formed by thermal degradation. $\log(C)$ represents the intercept and is used as a fitting parameter that has no physical significance (Anslyn 2006). The slope, β_{LG}, correlates the "sensitivity of the reaction to the acidity of the conjugate acid of the leaving group" (Anslyn 2006) and also can give insight into the transition state of the reactants (Purich 2000). This analysis has been used to understand a range of reactions in organic chemistry and biochemistry, including olefin metathesis (Keitz 2011) and ribosome self-cleavage (Shih 2001). β_{LG} is negative: in S_N2 reactions, better leaving groups are weak bases, have lower pKa values, and are associated with a greater reaction rate (Loudon 2002).
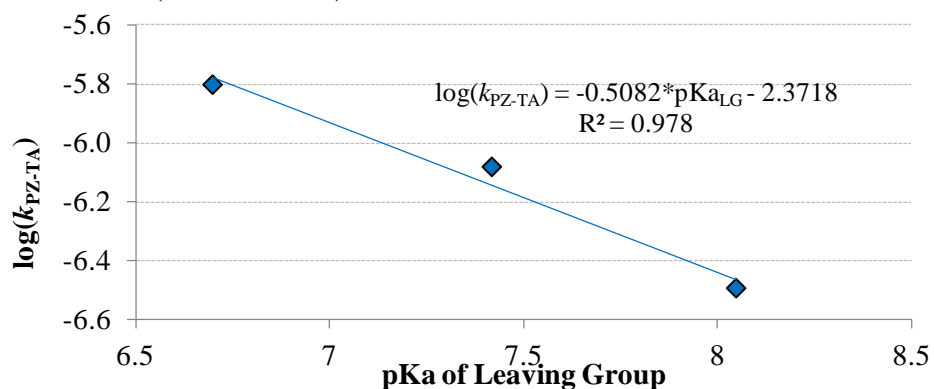
Figure 6.5: Brønsted plot of PZ-promoted tertiary amine degradation with at least one methyl group at 150 °C, 2.5 m PZ / 2.5 m TA, 0.14 mol H⁺/mol alk

The Brønsted relationship fits the data well and gives a β_{LG} value of about -0.5, suggesting that the structure of the S_N2 transition state of the tertiary amine-piperazine complex is intermediate between the reactants and the products (Purich 2000).

6.3 MODELING OF INITIAL SECOND-ORDER THERMAL DEGRADATION RATE CONSTANTS OF PZ-PROMOTED TERTIARY AMINE SOLVENTS

The effects of methyl, ethyl, and hydroxyethyl functional groups on the second-order thermal degradation rate is compared in this section. The initial secondary amine byproduct was able to be quantified for PZ-promoted DMAP, DMAE, MDEA, TEA, EDEA, and DEAE, and the rate of formation of the byproduct is used to determine the second-order rate constant of PZ attack on the carbon alpha to the nitrogen of the methyl, ethyl, or hydroxyethyl functional groups on protonated tertiary amines. A generalized degradation pathway is shown in Figure 6.8. This method is not as accurate as the method presented in Chapter 5 and in Section 6.2. However, this method does not require complete closure of the material balance; chromatograms of PZ-promoted solvents with tertiary amines without methyl groups suggested that triamine byproducts were present, implying that PZ reaction with the carbon alpha to the hydroxyl group takes place. The material balance of PZ-promoted DEAE and EDEA is shown in Table 6.9. The rate of formation of the secondary amine product was assumed to be constant and estimated using pseudo zeroth-order kinetics, shown in Equation 6.5, over the first 450 hours of degradation and is shown in Figures 6.6 and 6.7 as well as Table 6.8.

$$[\text{Secondary Amine Byproduct}] = k_0 * t + C \qquad \text{Eq. 6.5}$$

In Eq. 6.5, k_0 is the zeroth-order rate constant in mol*kg^{-1}*s^{-1}, [Secondary Amine Byproduct] denotes the concentration of the secondary amine, and t is the degradation time. C is the predicted concentration of secondary amine initially; PZ-promoted EDEA and TEA had quantities of the secondary amine byproduct present in undegraded solutions. The equivalent PZ byproduct was not found in the undegraded solution, and it is probable that the secondary amine is an impurity present in the tertiary amines.
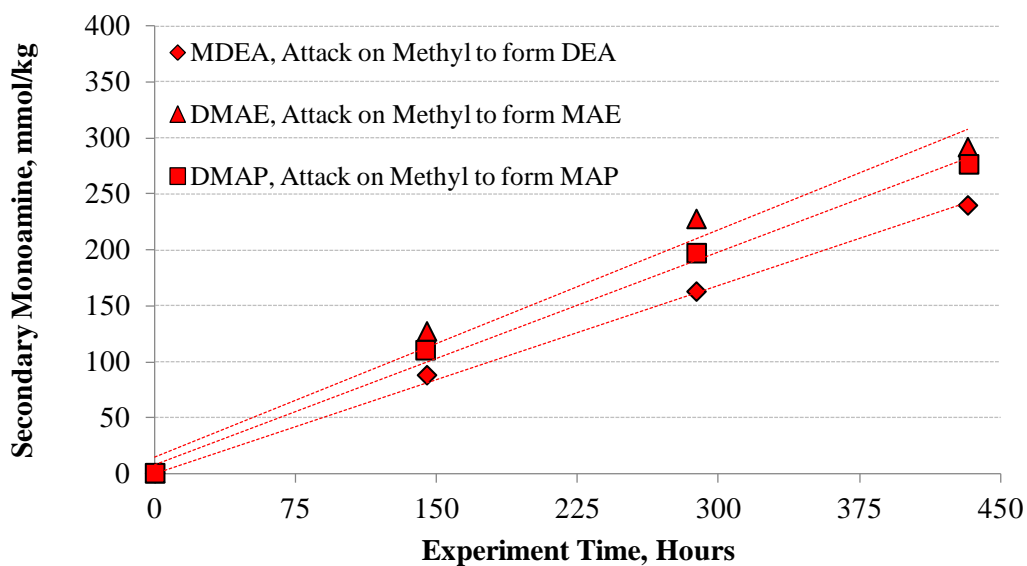
Figure 6.6: Formation of Secondary Monoamine Byproducts on PZ-promoted MDEA, PZ-promoted DMAE, and PZ-promoted DMAP. Conditions: 2.5 m PZ / 2.5 m Tertiary Amine, 0.14 mol H$^+$/mol alkalinity, 150 °C
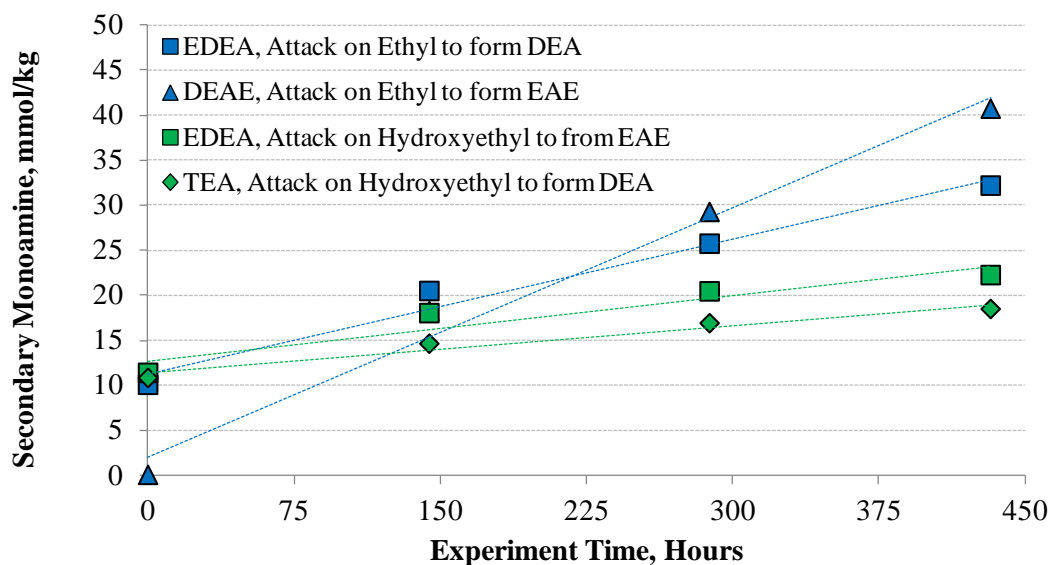
Figure 6.7: Formation of Secondary Monoamine Byproducts on PZ-promoted EDEA, PZ-promoted DEAE, and PZ-promoted TEA. Conditions: 2.5 m PZ / 2.5 m Tertiary Amine, 0.14 mol H⁺/mol alkalinity, 150 °C
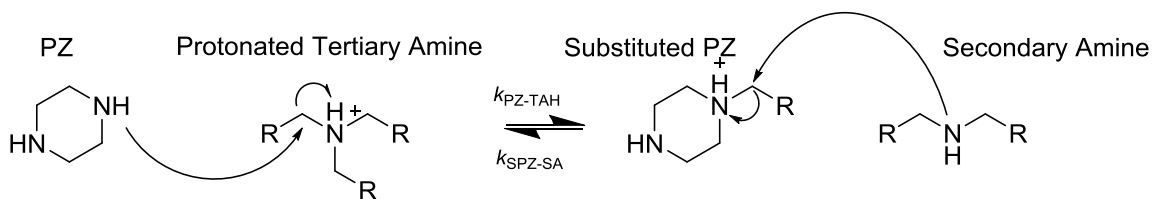
Figure 6.8: Generalized Proposed Degradation Pathway of PZ Attack on Alpha Carbon to Protonated Nitrogen of a Generic Functional Group

Table 6.8: Secondary Monoamine Byproduct Formation Rates. Conditions: 2.5 m PZ / 2.5 m Tertiary Amine, 0.14 mol H$^+$/mol alkalinity, 150 °C

Tertiary Amine Abbreviation	Secondary Amine Byproduct Abbreviation	Formation Rate k_0 mol*kg^{-1}*s^{-1}*10^9
MDEA	DEA	153±16
DMAE	DMAP	188±82
DMAP	DMAP	176±42
DEAE	EAE	26±10
EDEA	DEA	14±6
EDEA	EAE	7±7
TEA	DEA	5±3
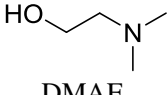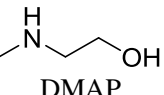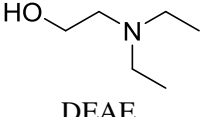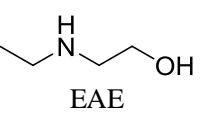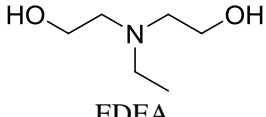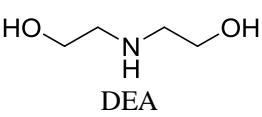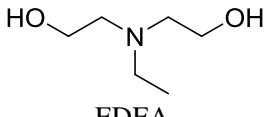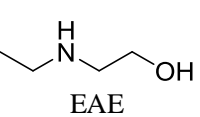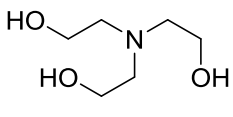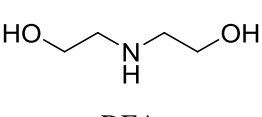
**Table 6.9: Material Balance, PZ-Promoted DEAE and PZ-Promoted DMAP.
Conditions: 2.5 m PZ / 2.5 m Tertiary Amine, 0.14 mol H⁺/mol
alkalinity, 150 °C**

Amine	PZ/DEAE Concentration formed (lost) mol/kg	Mol/kg N	Mol/kg C	PZ/EDEA Concentration formed (lost) mol/kg	Mol/kg N	Mol/kg C
Parent Amines						
DEAE	(0.08)	(0.08)	(0.49)	--	--	--
EDEA	--	--	--	(0.13)	(0.13)	(0.78)
PZ	(0.09)	(0.18)	(0.36)	(0.14)	(0.29)	(0.58)
Total Lost		(0.26)	(0.85)		(0.42)	(1.36)
Degradation Products						
DEA	--	--	--	0.04	0.04	0.15
EAE	0.07	0.07	0.26	0.02	0.02	0.07
1-Ethylpiperazine	0.06	0.12	0.37	0.04	0.08	0.24
1-HePZ	--	--	--	0.01	0.02	0.05
Total Material Balance		0.19	0.63		0.16	0.51
		73%	74%		38%	38%

Assuming that the rate of formation of the secondary amine byproduct is constant, a second-order rate constant can then be extracted using Equations 6.6 and 6.7:

$$k_0 = r_{initial} = k_2 * \left[\text{TAH}^+\right]_{t=0} * \left[\text{PZ}_{free}\right]_{t=0} \qquad \text{Eq. 6.6}$$

$$k_2° = \frac{k_2}{\text{Equivalent Functional Groups}} \qquad \text{Eq. 6.7}$$

In this equation, k_2 is the second-order rate constant in kg*mol^{-1}*s^{-1}, $[\text{TAH}^+]_{t=0}$ is the initial concentration of the protonated tertiary amine, and $[\text{PZ}_{free}]_{t=0}$ is the initial concentration of free PZ. $[\text{TAH}^+]$ and $[\text{PZ}_{free}]$ were calculated by extrapolating available pKa data (Hamborg 2009, Khalili 2009, Simond 2012, Rayer 2014) to 150 °C. Another rate parameter, $k_2°$, can be calculated by dividing k_2 by the number of equivalent

functional groups on the tertiary amine. As an example, for PZ attack on a methyl group, DMAE, with two methyl groups, will have the "equivalent functional group" term set to 2 whereas MDEA, with only one methyl group, will have the term set to 1. These data are shown in Figure 6.11 and Table 6.10.

The second-order rate constant decreases as the pKa of the tertiary amine and, by extension, the secondary amine byproduct, increases, and is consistent with lower reaction rate with higher pKa values of the leaving group (Anslyn, 2006). At 150 °C, DMAE and EDEA have similar pKa values, and the rate of attack between PZ and the alpha carbons of methyl, ethyl, and hydroxyethyl groups of the tertiary amine can be directly compared. Hydroxyethyl and ethyl groups were, respectively, found to be 4% and 17% as reactive as methyl groups. This is consistent with data that suggests that the S_N2 reaction rate decreases as substituent groups become bulkier and more sterically hindered (Anslyn 2006).

Table 6.10: Second-Order Initial Rate Constants of the Formation of Secondary Amine Byproducts. Conditions: 2.5 m PZ / 2.5 m Tertiary Amine, 0.14 mol H^+/mol alkalinity, 150 °C

Tertiary Amine	Functional Group Attacked Secondary Amine Formed	Tertiary Amine pKa (at 150 °C)	$[TA^+]_{t=0}$	$[PZ_{free}]_{t=0}$	Equivalent Functional Groups	$k_2°$ kg*mol^{-1}*s^{-1}*10^{-9}
MDEA	Methyl DEA	6.74	0.119	1.035	1	1240
DMAE	Methyl MAE	7.29	0.270	1.253	2	277
DMAP	Methyl MAP	7.98	0.472	1.438	2	130
EDEA	Ethyl DEA	7.29	0.253	1.160	1	47
DEAE	Ethyl EAE	7.64	0.362	1.275	2	28
TEA	Hydroxyethyl DEA	5.82	0.021	0.902	3	88
EDEA	Hydroxyethyl EAE	7.29	0.253	1.160	2	11
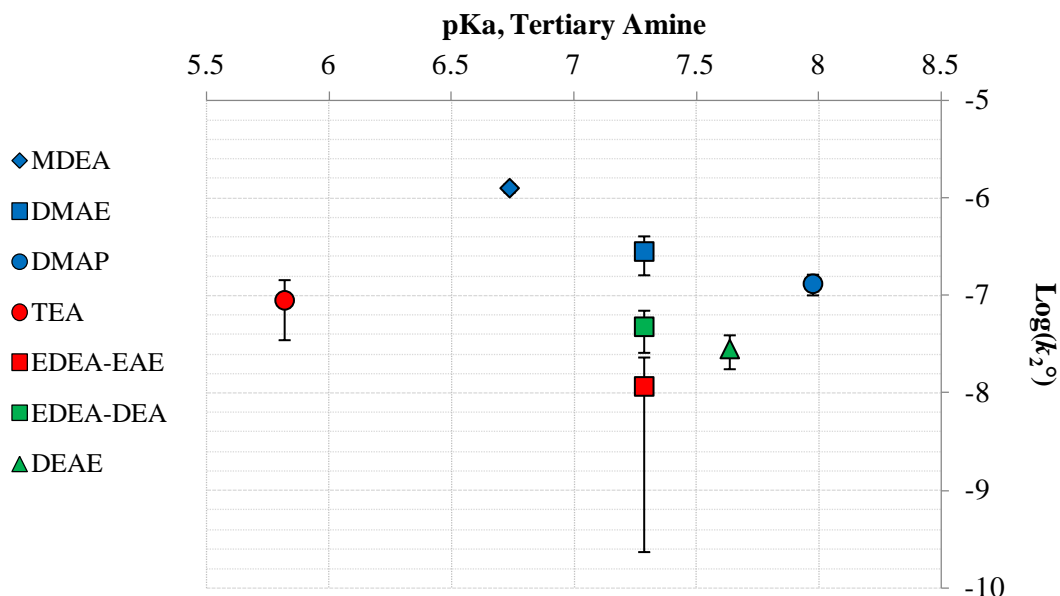
Figure 6.11: Formation of secondary amine byproducts as a function of tertiary amine pKa at 2.5 m PZ / 2.5 m TA, 0.14 mol H+/mol alk, and 150 °C. Blue points denote PZ attack on methyl groups, red points denote PZ attack on hydroxyethyl groups, and green points denote PZ attack on ethyl groups. Error bars indicate 95% confidence intervals.

6.4 SURVEY OF DEGRADATION RATES OF PZ-PROMOTED TERTIARY AMINE SOLVENTS USING PSUEDO ZEROTH-ORDER KINETICS

Practical results modeling degradation of PZ-promoted tertiary amines in acidified solutions is presented in this section and can be used to compare degradation rates as a function of amine structure. The zeroth-order rate model, shown in Eq. 6.7 and Figure 6.12, can be used to approximate the loss of both the tertiary amine and PZ reasonably well, especially in the absence of complete material balances or thermodynamic data that are necessary to determine the speciation of the parent amines and their degradation products.

$$[\text{Parent Amine}] = -k_0 * t + C$$

Eq. 6.7

In Eq. 6.7, [Parent Amine] represents the concentration of either the tertiary amine or PZ, k_0 is the zeroth-order rate constant in mol*kg^{-1}*s^{-1}, t is the experiment time in seconds, and C is the predicted initial concentration in mol/kg.
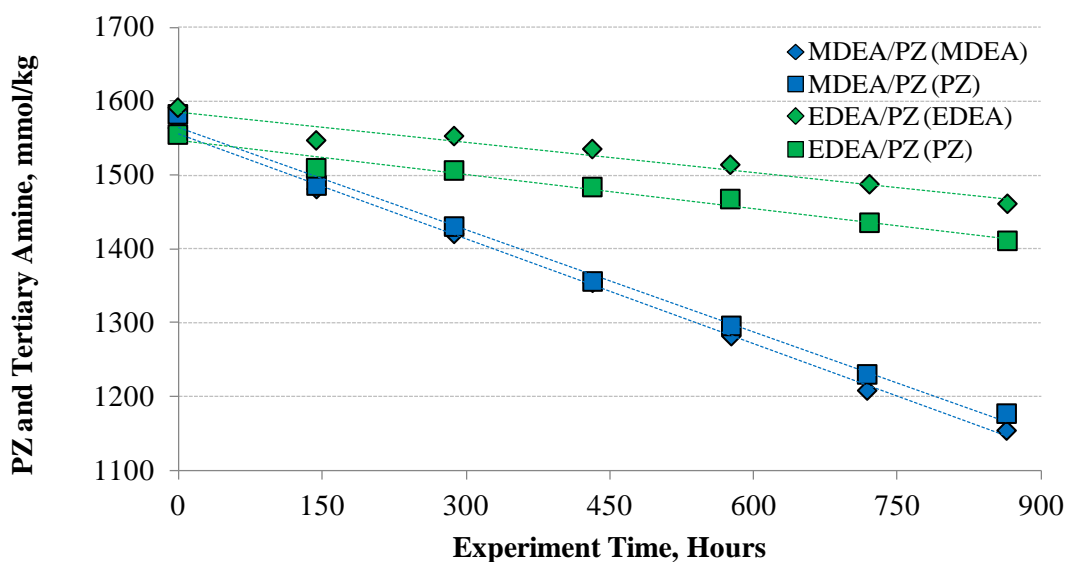
Figure 6.12: Pseudo Zeroth-Order Rate Models Applied to Thermal Degradation of 2.5 m PZ / 2.5 m TA at 0.14 mol H+/mol alkalinity and 150 °C

6.4.1 Degradation of PZ-Promoted Aliphatic Tertiary Amine Solvents with One Methyl Group

The degradation of PZ-promoted aliphatic tertiary amines with methyl groups is shown in Table 6.11. Most tertiary amines have identical rates of degradation, with PZ-promoted DMAEE and DMAIP having slightly higher rates of amine loss than the other tertiary amines. This could be attributed to pKa effects. The ratio of tertiary amine loss to PZ loss for many of the tertiary amines tested is close to 1 for the acidified degradation experiments. This is a strong indicator that the additional rate of PZ loss seen in the CO_2-loaded experiments is likely due to PZ-interaction with products formed from the carbamate species of the intermediate secondary monoamine formed between the reaction

142

of PZ and tertiary amine; this reaction cannot take place in the acidified solvent due to the lack of CO_2 in solution. PZ-promoted DMAB had a significantly higher loss rate than the other tertiary amines, suggesting that DMAB might degrade via other pathways than the ones proposed in Chapters 5 and 6. Work by Hatchell (Hatchell 2014) and Lepaumier (Lepaumier 2010) have suggested that amines with four carbons between the amino function and an electron withdrawing group can ring close, and MS analysis of degraded PZ-promoted DMAB indicated that a compound consistent with the molecular weight of 1-methylpyrrolodine, was present. This product is representative of DMAB ring closing.

Table 6.11: Degradation of PZ-promoted Tertiary Amines with at least one methyl group. Conditions: 2.5 m PZ / 2.5 m Tertiary Amine, 0.14 mol H^+/mol alkalinity, 150 °C

Tertiary Amine	Tertiary Amine Loss Rate mol*kg^{-1}*s^{-1}*10^9	PZ Loss Rate mol*kg^{-1}*s^{-1}*10^9	Tertiary Amine Loss / PZ Loss
DMAB	297±85	267±78	1.1
DMAEE	182±20	180±22	1.0
DMAIP	161±24	163±25	1.0
DMAP	139±37	140±45	1.0
DMAE	136±29	140±29	1.0
MDEA	132±6	128±11	1.0

6.4.2 Degradation of PZ-Promoted Aliphatic Tertiary Amine Solvents with No Methyl Groups

The degradation of PZ-promoted aliphatic tertiary amines with no methyl groups is shown in Table 6.12. These solvents degrade at a much slower rate than tertiary amines with at least one methyl group; PZ was found to degrade at nearly the same rate as the tertiary amine. These results are also consistent with the CO_2-loaded thermal degradation experiments presented in Chapter 4 in which the tertiary aliphatic amines without methyl groups were universally found to be more stable than tertiary aliphatic amines with at least one methyl group.

Table 6.12: Degradation of PZ-promoted Tertiary Amines with at least one methyl group. Conditions: 2.5 m PZ / 2.5 m Tertiary Amine, 0.14 mol H$^+$/mol alkalinity, 150 °C

Tertiary Amine	Tertiary Amine Loss Rate mol*kg^{-1}*s^{-1}*10^9	PZ Loss Rate mol*kg^{-1}*s^{-1}*10^9	Tertiary Amine Loss / PZ Loss
DEAE	41±37	41±34	1.00
EDEA	38±10	42±9	0.9
TIPA	37±29	27±10	1.4
TEA	28±24	29±11	1.0
nBuDEA	20±8	21±8	1.0

6.4.3   Degradation of PZ-Promoted Tertiary Morpholine Solvents

The degradation of PZ-promoted aliphatic tertiary morpholines is shown in Table 6.13.   The acidified degradation results are consistent with the CO_2-loaded thermal degradation results presented in Chapter 4 which indicated that the promoted tertiary morpholine solvents were more stable than all of the promoted aliphatic tertiary amine solvents.

Table 6.13: Degradation of PZ-promoted Tertiary Amines with at least one methyl group. Conditions: 2.5 m PZ / 2.5 m Tertiary Amine, 0.14 mol H$^+$/mol alkalinity, 150 °C

Tertiary Amine	Tertiary Amine Loss Rate mol*kg^{-1}*s^{-1}*10^9	PZ Loss Rate mol*kg^{-1}*s^{-1}*10^9	Tertiary Amine Loss / PZ Loss
HEM	3±20	4±14	0.8
HIPM	11±13	13±10	0.8
HPM	0.1±14	0.3±10	0.3

6.4.4 Activation Energy of Thermal Degradation

The activation energy of thermal degradation of PZ-promoted MDEA, DMAE, DMAP, EDEA, and TEA under acidified and CO_2-loaded conditions is shown in Table 6.14. The activation energies were estimated using the Arrhenius relationship and are similar to and consistent with the activation energy of thermal degradation of CO_2-loaded solvents suggesting that, like the degradation of PZ-promoted MDEA, the degradation of PZ-promoted tertiary amine solvents is initiated by protonated and free amine species and does not require CO_2.

Table 6.14: Degradation of PZ-promoted Tertiary Amines with at least one methyl group. Conditions: 2.5 m PZ / 2.5 m Tertiary Amine, 0.14 mol H^+/mol alkalinity, 150 °C

Tertiary Amine	E_A (kJ/mol) 5 m PZ / 5 m TA 0.23 mol CO_2/mol alk		E_A (kJ/mol) 2.5 m PZ / 2.5 m TA 0.14 mol H+/mol alk	
	TA	PZ	TA	PZ
TEA	169	190	179	166
DEAE	175	168	179	162
MDEA	140	139	143	138
DMAE	134	126	123	126
DMAP	126	131	140	141

6.5 CONCLUSIONS

- In PZ-promoted tertiary amines, the second-order degradation rate decreases with increased tertiary amine pKa.
- In PZ-promoted tertiary amines, the ethyl and hydroxyethyl groups are 17% and 4% as reactive as methyl groups when PZ is the nucleophile.

- Zeroth-order modeling of a range of PZ-promoted tertiary amine solvents under acidified conditions indicates that the rate of PZ loss is comparable to tertiary amine loss for the majority of the experiments.

- The stability of PZ-promoted solvents under acidified conditions is similar to solvents under CO_2-loaded conditions despite the additional interaction between PZ and intermediate amine byproducts in the CO_2-loaded experiments. Solvents with PZ-promoted aliphatic tertiary amines with at least one methyl group are the least stable, followed by PZ-promoted aliphatic tertiary amines with no methyl groups, and finally by PZ-promoted tertiary morpholine solvents.

- The activation energy of thermal degradation of PZ-promoted tertiary amine solvents under acidified conditions is similar to the activation energy seen in CO_2-loaded conditions, indicating that the initial degradation step does not involve CO_2 and involves PZ interacting with the tertiary amine.

Chapter 7: Thermal Degradation Topics Relevant to Gas Treating

7.1 INTRODUCTION & SCOPE

The majority of the results presented in Chapters 4, 5, and 6 were interpreted in the context of using the PZ-promoted tertiary amine solvents in low-pressure CO_2 capture applications such as capture from fossil-fueled power plants. In this chapter, data relating the maximum stripping temperature as a function of alkalinity loss of PZ-promoted tertiary amine solvents, amine loss of PZ-promoted MDEA in the presence of physical solvents, and amine loss of acidified non-promoted tertiary amine solvents is presented. These topics are relevant to understanding degradation of amine-based solvents used in industrial gas treating units. Raw data and selected chromatograms for the experiments discussed in this chapter are presented in Appendix B.4.

7.2 MAXIMUM STRIPPING TEMPERATURE AS A FUNCTION OF SOLVENT ALKALINITY

Alkalinity loss can be best described as the loss of amino groups capable of absorbing or desorbing CO_2 or H_2S and is a useful measurement to understand the theoretical CO_2 or H_2S capacity of the solvent. Amine byproducts observed in PZ-promoted tertiary amine degradation, such as DEA, MAE, and 1-MPZ, can still be used to absorb and desorb CO_2 or H_2S from the gas stream, albeit at different CO_2 absorption rate and CO_2/H_2S selectivity. Some of the amines present as byproducts have been used commercially, in the case of DEA and MAE (Kohl 1960, Bartholome 1970), or tested on the bench-scale, in the case of 1-MPZ (Freeman 2011, Chen 2011), as potential gas treating or CO_2 capture solvents. Alkalinity loss can occur through either the formation of ureas, seen in CO_2-loaded solvents, or through the formation of polyamine, seen in

147

both CO_2 and H^+ loaded solvents. The amino function of the urea and for some of the amino groups on the polyamine is too low to react with CO_2 and H_2S, which reduces the theoretical solvent capacity. This was seen with HeMAEtPZ, a polyamine degradation product suspected to be present in PZ-promoted MDEA degradation, and is shown in Figure 7.1.
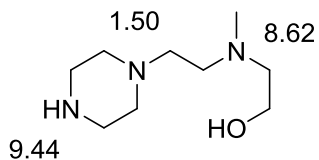
Figure 7.1: pKa values of amino functions of HeMAEtPZ, a degradation product of PZ-promoted MDEA

Solvents used in gas treating facilities can be stripped to a low loading in an effort to maximize capacity and to facilitate maximum removal of CO_2 and especially H_2S from the treated gas. Natural gas treatment facilities have a product specification of 4 ppmv H_2S (Cussler 2009) for safety reasons as H_2S is toxic, and LNG treating facilities have a product specification of 50 ppmv CO_2 to avoid formation of CO_2-hydrate as the natural gas is refrigerated (Zhou 2011, Bahadori 2014). Therefore, it is possible to treat solvent thermal degradation as a function of alkalinity loss and not as a function of amine loss if the operation of the gas treating plant is limited by amine cyclic capacity and not by absorption rate.

Alkalinity loss was measured for PZ-promoted DMAE, DMAP, DEAE, DMAEE, and MDEA using a potentiometric titrator. A first-order kinetic model was fit to the alkalinity loss data to estimate the maximum stripping temperature, or T_{MAX}, as a function of alkalinity, and is shown in Eq. 7.1; the method to extract T_{MAX} from these data is described in Chapter 4. The data are shown in Figure 7.2 and Table 7.1.

$$\frac{d[\text{Alkalinity}]}{dt} = -k_0 * [\text{Alkalinity}]$$
<div align="right">Eq. 7.1</div>

In Eq. 7.1, k_0 is the first-order rate constant for alkalinity loss, [Alkalinity] denotes the alkalinity concentration in mol/kg, and t is the time in seconds.
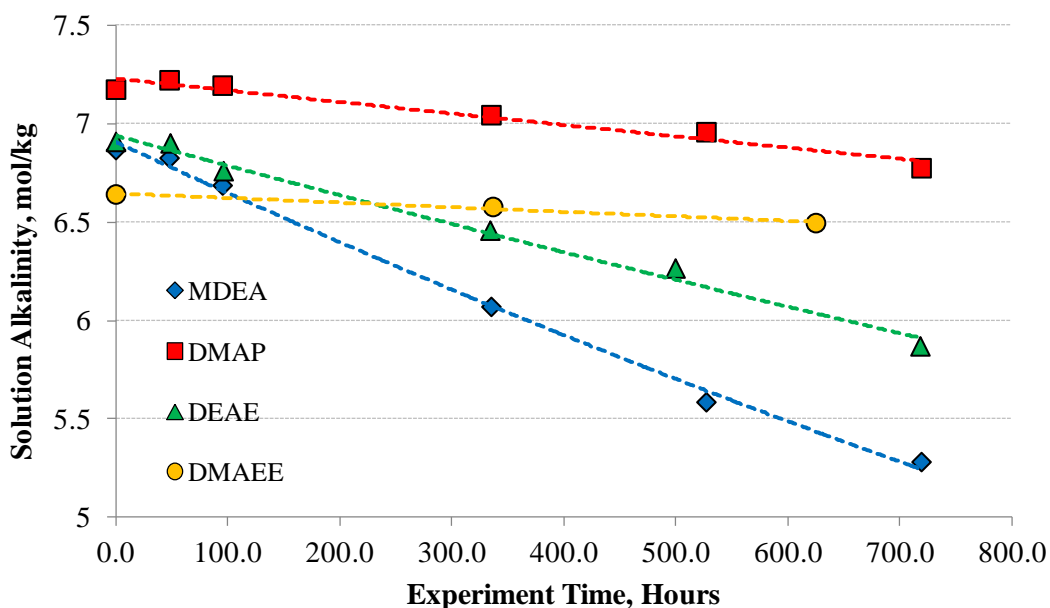
Figure 7.2: First-order alkalinity loss of PZ-promoted MDEA, DMAP, DEAE, and DMAEE, initially at 2.5 m PZ / 2.5 m Tertiary Amine, 0.23 mol CO_2/mol alkalinity, and 150 °C

All amines had a higher T_{MAX} when alkalinity was used to measure degradation rate as opposed to total amine concentration. PZ-promoted DMAP and DMAEE were the most stable solvents tested and approach the stability of PZ-promoted tertiary morpholine solvents. Both the PZ and the tertiary amine in PZ/DMAP and PZ/DMAEE degrade at nearly the same rate in the presence of CO_2, suggesting that the intermediate byproducts of PZ/DMAP and PZ/DMAEE are stable and do not readily react. MAP, the intermediate product of PZ-promoted DMAP, was found to accumulate in degraded CO_2-loaded

solutions. EAE, DEA, and MAE, degradation products of PZ-promoted DEAE, MDEA, and DMAE, were found to behave as steady-state intermediates and can react with PZ via the carbamate polymerization pathway to form polyamines, decreasing solution alkalinity.

Table 7.1: Maximum stripping temperatures of PZ-promoted tertiary amines based on alkalinity loss. Conditions: 5 m PZ / 5 m tertiary amine, 0.23 mol CO_2/mol alkalinity, 150 °C

Tertiary Amine Structure	Name / Abbreviation	First-Order Alkalinity Loss Rate $s^{*-1}*10^9$	Activation Energy ^ kJ/mol	T_{MAX} Alkalinity Parent Amine
	Dimethylaminoethoxyethanol DMAEE	9.8±15	130	163 °C 124 °C
	Dimethylaminopropanol DMAP	23±7	130	153 °C 127 °C
	Diethylaminoethanol DEAE	62±9	170	143 °C 134 °C
	Methyldiethanolamine MDEA	106±10	140	137 °C 122 °C
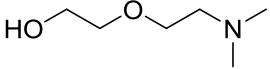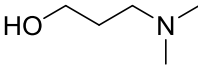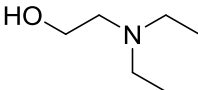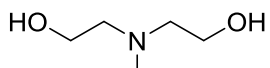
^ The activation energy of alkalinity loss is assumed to be the same as the activation energy of thermal degradation as measured in the CO_2-loaded experiments.

7.3   DEGRADATION OF PZ-PROMOTED MDEA IN THE PRESENCE OF PHYSICAL SOLVENTS

Physical solvents find use in gas-treating applications whose inlet H_2S and/or CO_2 partial pressure is greater than 1 or 5 bar, respectively. The physical solvent can absorb enough acid gas to generate a treated gas stream with a partial pressure of 70 Pa H_2S or $14*10^3$ Pa CO_2 (Nexant Inc. 2011). The solubility and cyclic capacity of physical solvents can be assumed to follow Henry's law and is essentially linear with the partial pressure of the acid gas (Chen 2013), whereas the solubility of acid gas in amine solvents

follows a logarithmic relationship (Chen 2011, Xu 2011). As the amino functions become protonated or complexed with CO_2, acid gas solubility in the amine solvent decreases, and the solvent slowly loses its ability to absorb CO_2 or H_2S. After all amino functions have been complexed, solubility decreases significantly and then becomes a function of the physical absorption of CO_2 in water. A representative figure that illustrates the trends of acid gas solubility in physical solvents and amine solvents is shown in Figure 7.3 (UOP LLC, 2009).
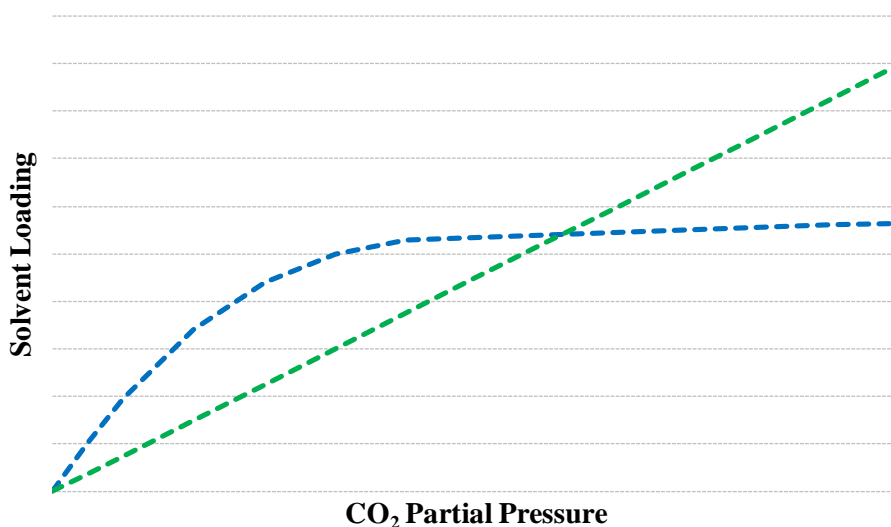
Figure 7.3: Representative CO_2 solubility curves of amine-based (blue) and physical (green) gas treating solvents (figure adapted from UOP LLC, 2009).

Hybrid solvents comprising amines, water, and a physical solvent can be used in high-pressure applications that have moderate to high acid gas pressure but very stringent removal requirements; examples include LNG treating, which require CO_2 removal to 50 ppmv, or synthesis gas treating, whose treated gas composition is dependent on downstream processing requirements. These hybrid solvents combine the high capacity

of physical solvents with the ability of the amine to generate treated gas with a low concentration of acid gas. Solutions comprising PZ, MDEA, water, and a variety of physical solvents were degraded, shown in Table 7.2. The degradation rate of PZ-promoted MDEA in the presence of a physical solvent has been estimated using first-order rate models described in Chapter 4 and is shown in Table 7.3 and Figure 7.4.

Table 7.2: List of physical solvents tested with PZ-Promoted MDEA or PZ

Physical Amine Structure	Name Abbreviation	Molecular Weight
	Polyethyleneglycol Dimethyl Ether PEGDME	Average 250^
	1-Methyl-2-pyrrolidinone NMP	99.1
	Propylene Carbonate PCAR	102.1
	Sulfolane	120.2
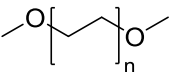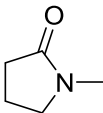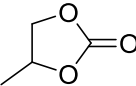
^ PEGDME in commercial applications has an average molecular weight of approximately 280 (Burr 2008).

Table 7.3: Degradation of PZ-promoted MDEA in the presence of physical solvents. Conditions: 150 °C, 20 wt% PZ, 27 wt% MDEA, 0.23 mol CO$_2$/mol alkalinity$^{\%}$ initially

Physical Solvent	Wt% H$_2$O	Wt% Physical Solvent	k_1, PZ s^{-1}*10^9	k_1, MDEA s^{-1}*10^9	$\dfrac{k_1, PZ}{k_1, MDEA}$
None	46	0	802±38	297±25	2.70
PEGDME	27	18	605±113	221±41	2.74
NMP	27	18	556±33	204±11	2.72
PCAR	27	18	1310±73	465±48	2.82

$^{\%}$ Corresponds to weight fractions of PZ and MDEA at 5 m PZ / 5 m MDEA at 0.23 mol CO$_2$/mol alkalinity
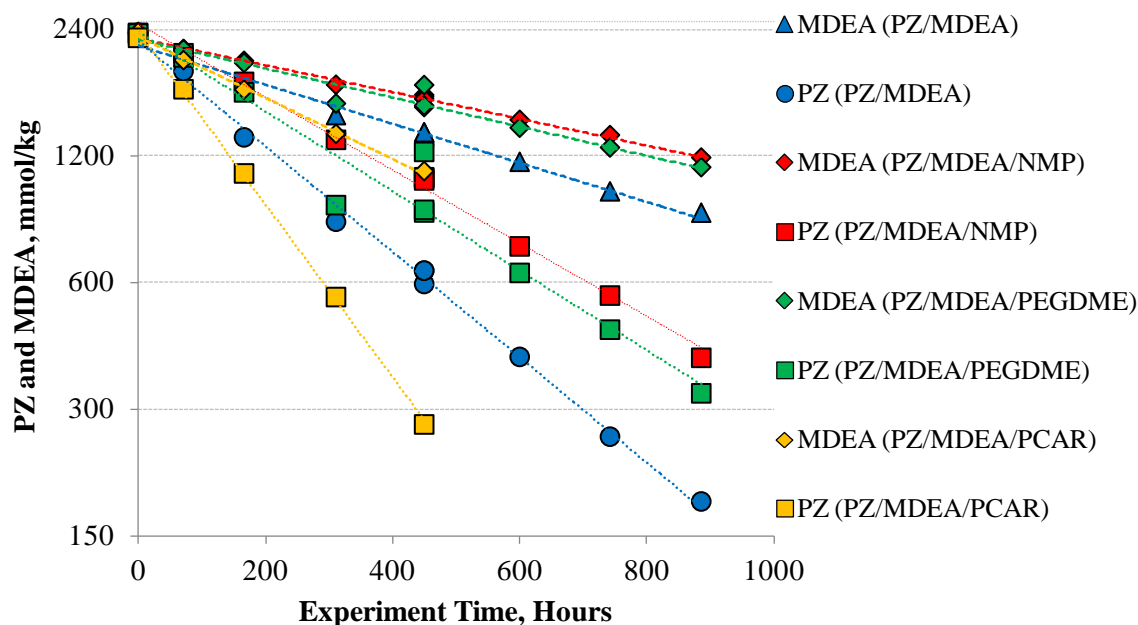
Figure 7.4: Degradation of PZ-promoted MDEA at 0.23 mol CO$_2$/mol alkalinity initially and 150 °C with and without the presence of physical solvents. Lines indicate first-order rate models fit through the data.

At ambient conditions, degraded and undegraded PZ-promoted MDEA with PEGDME phase-separated into an organic phase and an aqueous phase and had to be vigorously stirred to keep the solution as a mixed but homogenous phase before being loaded into the cylinder and also during the initial dilution step. Undegraded and degraded PZ-promoted MDEA PZ-promoted MDEA with PCAR and NMP remained as one phase at ambient conditions.

PZ-promoted MDEA with either NMP or PEGDME degrades at a lower rate than without a physical solvent present; the differences in degradation of PZ and MDEA in NMP and PZ and MDEA in PEGDME are statistically insignificant. This could be due to a variety of effects, including solvation and activity effects, but the most likely reason is

probably due to a change in speciation of CO_2 in solution due to the presence of the physical solvent, reducing the observed rate of thermal degradation.

The rate of degradation of the physical solvents was not measured. PEGDME has been reported to be stable up to 175 °C in gas-treating applications in the absence of amine (Burr 2008), and NMP, with small amounts of water added to stabilize the molecule, has been reported to be stable up to 260 °C in applications that extract aromatic hydrocarbons from mixed hydrocarbon streams (White 1979).

The ratio of the first-order rate constants of PZ degradation and MDEA degradation are about the same in solvent mixtures with and without NMP and PEGDME present. In Chapter 5, PZ was shown to be a much stronger nucleophile than MDEA when free amines reacted with the protonated tertiary amine. These two observations, coupled with the observation that the overall amine degradation rate is less in the solvent mixtures with NMP or PEGDME than without, suggests that interaction between PZ or MDEA and NMP or PEGDME is unlikely at experimental conditions.

PZ-promoted MDEA with PCAR showed a markedly higher rate of amine loss compared to PZ-promoted MDEA with or without other physical solvents. The structure of PCAR resembles an oxazolidinone; it is possible that PZ and other amines can rapidly react with PCAR. Degraded solutions of PZ-promoted MDEA with PCAR evolved gas bubbles whose quantity increased with increased degradation time when decanted from the degradation apparatus, suggesting a conversion of secondary amino functions to tertiary amino functions, decreasing CO_2 solubility. As this progresses, the tertiary amine will eventually become complexed with CO_2 as protonated amine until equilibrium is reached, increasing the rate of degradation of the tertiary amine and thus tertiary amine loss. PCAR has been reported to be stable up to 65 °C (Burr 2008) in the absence of

amine, and the degradation results presented in this study are consistent with previous observations.

Sulfolane, another physical solvent, was degraded in the presence of PZ at 175 °C. Degraded samples of 15 wt% PZ in the presence of 20 wt% sulfolane at a loading of 0.3 mol CO_2/mol alkalinity had an exceptionally strong sulfurous odor which propagated throughout the lab, which were not analyzed due to the odor. Undegraded samples had no characteristic odor, and none of the other degraded hybrid solvents had a characteristic odor. Qualitatively, these results indicate that sulfolane might not be stable and evolves volatile malodorous degradation products at elevated temperature.

7.4 SURVEY OF DEGRADATION OF UNPROMOTED TERTIARY AMINE SOLVENTS UNDER ACIDIFIED CONDITIONS

Tertiary amines require the use of a rate promoter if they are used in applications that also require CO_2 to be removed from the gas. However, they can be used without a rate promoter for H_2S removal for low and high pressure sources of gas due to the near-instantaneous reaction of amine with H_2S to form the protonated amine and bisulfide (SH^-) ion. The initial zeroth-order rate of degradation over approximately 140 hours for a variety of unpromoted tertiary amines is shown in Tables 7.5 through 7.7 and Figures 7.5 through 7.7.

The degradation behavior of all tertiary amines with at least one methyl group is similar to unpromoted MDEA degradation described in Chapter 5. The general behavior is representative of a high initial rate of degradation before reducing in rate as the tertiary amine likely approaches a kinetic equilibrium with its corresponding quaternary salt and the secondary amine byproduct. An example of this pathway – the reaction of MDEA with $MDEAH^+$ to produce quaternary amine and the corresponding secondary amine – is shown in Figure 5.2. These data are shown in Table 7.5 and Figure 7.5.

155

A second-order rate constant can be extracted from the initial degradation rate data of the tertiary amine solvents with at least one methyl group and can be estimated using the expression in Equation 7.3.

$$r = k_2 * [TA]_{t=0} * [TA^+]_{t=0} \hspace{3cm} \text{Eq. 7.3}$$

In Eq. 7.3, r is the initial rate in $mol*kg^{-1}*s^{-1}$, k_2 is the second-order rate constant in $kg*mol^{-1}*s^{-1}$, and $[TA]_{t=0}$ and $[TA^+]_{t=0}$ are the initial concentration of free and protonated tertiary amine, respectively.

Table 7.5: Degradation of unpromoted tertiary amines with at least one methyl group. Conditions: 150 °C, 5 m amine concentration, 0.2 mol H+/mol alkalinity

Tertiary Amine Structure	Name / Abbreviation	Tertiary Amine Loss Rate $mol*kg^{-1}*s^{-1}*10^7$	Second-order Rate Constant $kg*mol^{-1}*s^{-1}*10^7$
	Dimethylaminoethanol DMAE	6.6	3.8
	Dimethylaminopropanol DMAP	6.3	3.8
	Dimethylaminoethoxyethanol DMAEE	5.3	4.4
	Methyldiethanolamine MDEA	4.1	2.6
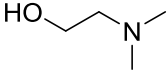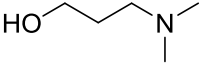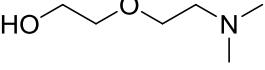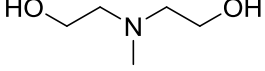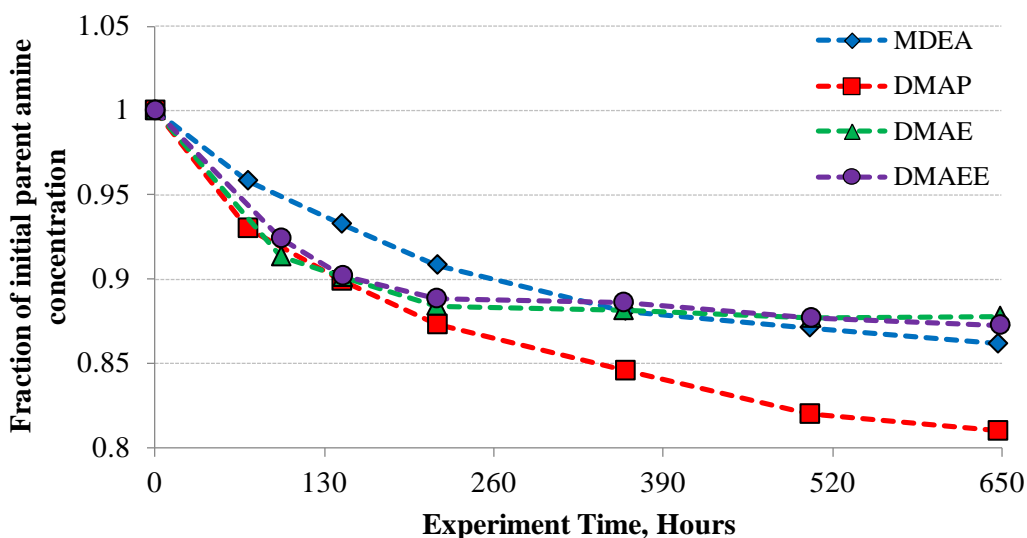
Figure 7.5: Degradation trends of unpromoted tertiary amine solvents with at least one methyl group at 150 °C and initially at 5 m tertiary amine and 0.2 mol H+/mol alkalinity

The second-order rate constant of MDEA degradation at 150 °C extracted using Eq. 7.3 is 15% less than the value predicted by the model in Chapter 5. Thus, the initial rate of degradation can be used to estimate the second-order rate constant as a function of free and protonated amine species.

The T_{MAX} for MDEA at a loading of 0.2 mol H^+/mol alkalinity is 132 °C if the activation energy of degradation is assumed to be 120 kJ/mol and a first-order model is fit through over 140 hours of degradation. Most gas treating facilities using unpromoted tertiary amine solvents typically run at a lean loading below 0.01 mol acid gas/mol alkalinity, which is significantly below the loading used in these studies, and thus the T_{MAX} analysis would not give representative results for a gas treating facility using these solvents. Primary and secondary amine solvents run at a lean loading of about 0.1 mol acid gas/mol alkalinity which, while lower than loadings encountered in CO_2 capture

157

from flue gas, is high enough for the amine to degrade by the thermal degradation pathways discussed in this work. The rich solvent loading is around 0.5 mol acid gas/mol alkalinity for most solvent systems (Fouad 2011). Thus, thermal degradation for unpromoted tertiary amine solvents likely takes place in the topmost trays or packing of the stripping column where the loading and temperature are sufficiently high enough to initiate thermal degradation of the amine.

It is also possible that other degradation reactions, such as degradation induced by corrosion, contaminants in the feed gas, or dissolved oxygen in the plant make-up water (Rennie 2006, Bosen 2010, Speight 2014) to produce heat stable salts, dominate at the lean loading conditions encountered. The literature review has indicated that at zero or near-zero loading amine loss via thermal degradation pathways is negligible.

Degradation of tertiary amines with no methyl groups was slower than tertiary amines with at least one methyl group owing to reduced rate of S_N2 substitution of ethyl and hydroxyethyl groups versus methyl groups. These data are consistent with the data presented in Chapter 6, in which S_N2 substitutions involving ethyl and hydroxyl groups were found to be 17% and 4% as fast as methyl groups with PZ as the nucleophile. Degradation products consistent with elution times of diamines were observed in the chromatograms of degraded solutions of unpromoted aliphatic tertiary amines without methyl groups, suggesting that the amino function of the tertiary amine interacts with the carbons alpha to the hydroxyl function to form diamines via a condensation reaction. The apparent concentration of diamine in degraded solution increases as the number of hydroxyl functional groups on the tertiary amine increases and is shown in Figure 7.6.

Due to the lower intrinsic rate of S_N2 substitution reactions of bulkier functional groups, the interaction between the amino function and the carbon alpha to the hydroxyl group is more significant for tertiary unpromoted aliphatic amines without methyl groups

158

than tertiary unpromoted aliphatic amines with at least one methyl group. Future studies on the degradation of unpromoted tertiary amine solvents should focus on accurately quantifying and identifying these products. These data are shown in Table 7.7 and Figure 7.7.
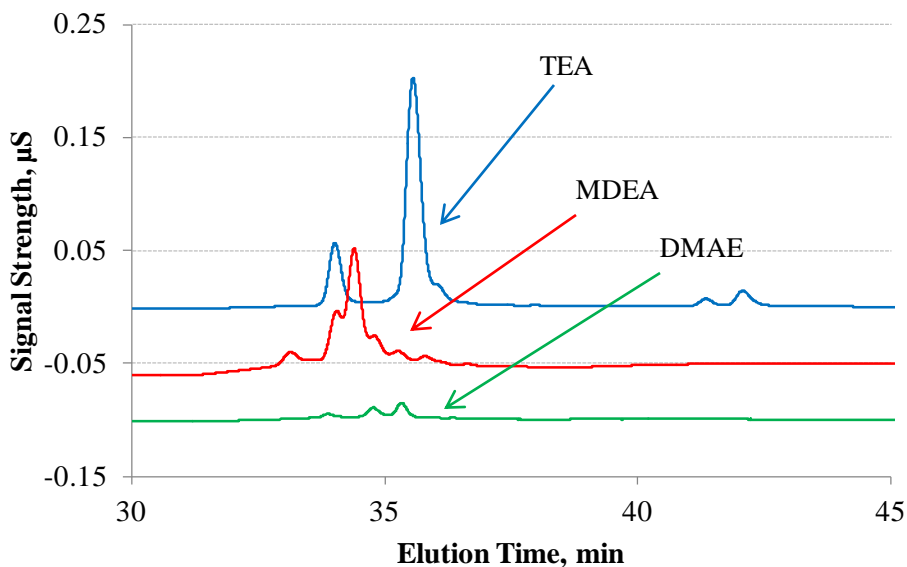
Figure 7.6: Unidentified products consistent with the elution times of diamines in degraded solutions of unpromoted TEA, MDEA, and DMAE at an initial loading of 0.2 mol H$^+$/mol alkalinity, 150 °C, and about 650 hours

Unpromoted tertiary morpholine solvents did not degrade at experimental conditions and thus a degradation rate could not be measured. These data are shown in Figure 7.8. The two solvents whose data are presented, HEM and HIPM, have low pKa values, with HEM having a pKa slightly less than 7 at ambient conditions (Tomizaki 2010). This can lead to a lower rate of reaction with H$_2$S and reduce absorption rate sufficiently that the absorption could be limited by reaction rate and not by gas-side mass transfer (Rochelle 2001, Rochelle, personal communication, 2015).

159
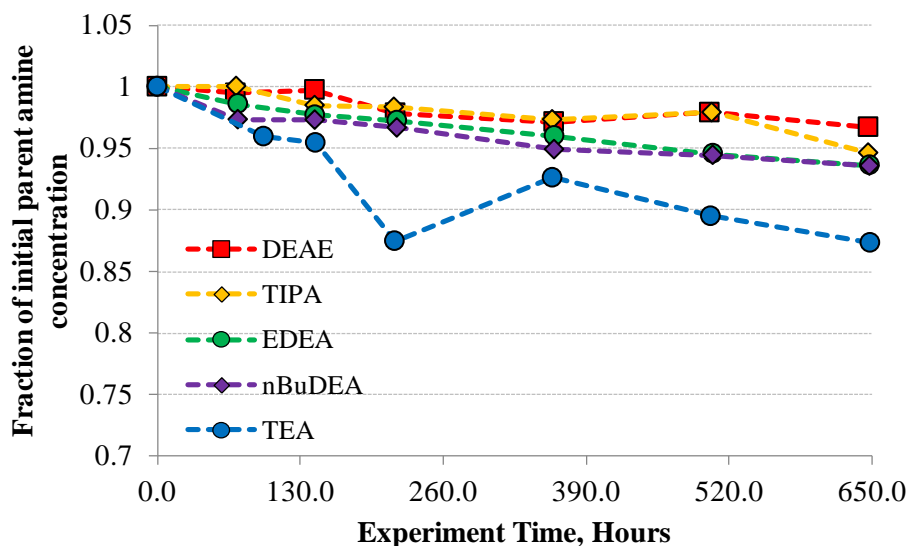
Figure 7.7: Degradation trends of unpromoted tertiary amine solvents with no methyl groups at 150 °C and initially at 5 m tertiary amine and 0.2 mol H^+/mol alkalinity
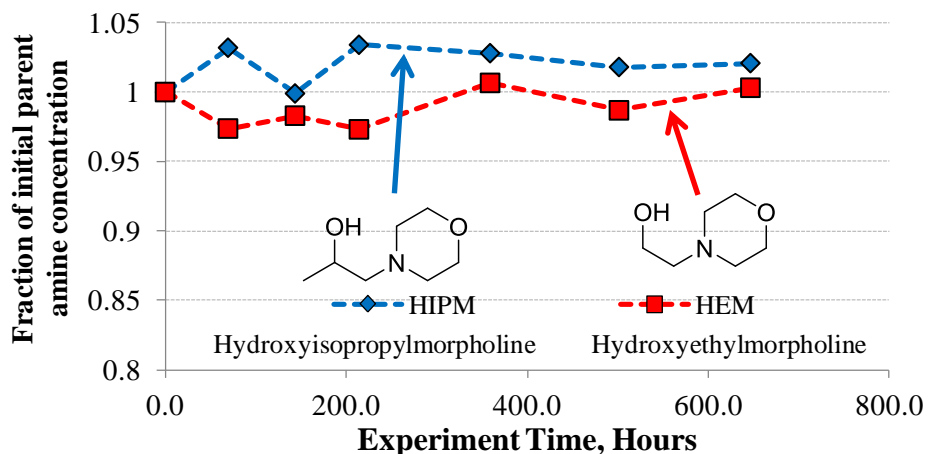
Figure 7.8: Degradation trends of unpromoted tertiary morpholine solvents with at 150 °C and initially at 5 m tertiary amine and 0.2 mol H+/mol alkalinity

Table 7.7: Degradation of unpromoted tertiary amines with no methyl groups. Conditions: 150 °C, 5 m amine concentration, 0.2 mol H+/mol alkalinity
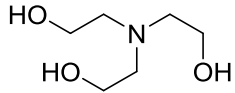
Tertiary Amine Structure	Name / Abbreviation	Tertiary Amine Loss Rate $\text{mol} \ast \text{kg}^{-1} \ast \text{s}^{-1} \ast 10^7$
	Triethanolamine TEA	2.6
	n-Butyldiethanolamine nBuDEA	1.5
	Ethyldiethanolamine EDEA	1.3
	Triisopropanolamine TIPA	0.7
	Diethylaminoethanol DEAE	0.2
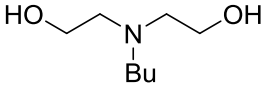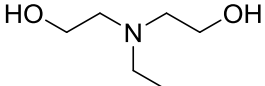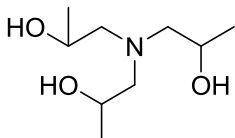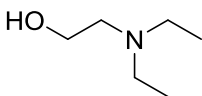
7.5 CONCLUSIONS

- Solvents whose intermediate degradation products were stable and whose initial rate of degradation was comparable, such as PZ-promoted DMAP and PZ-promoted DMAEE, show little alkalinity loss over time and can be regenerated up to 150 °C if controlling for alkalinity and not parent amine concentration.

- Degradation of PZ-promoted MDEA is reduced when mixed with NMP or PEGDME by about 30% under CO_2-loaded conditions when compared to the base case that is not mixed with a physical solvent. PZ-promoted MDEA mixed with PCAR is unstable and at a 50% greater rate than PZ-promoted MDEA in the absence of a physical solvent. Degraded PZ in the presence of sulfolane produced malodorous and volatile degradation products.

- Unpromoted tertiary amines with at least one methyl group degrade at a high rate initially and then begin to approach kinetic equilibrium with their quaternary amine salt and their corresponding secondary amine byproduct.

- Unpromoted tertiary amines with no methyl groups do not approach kinetic equilibrium and degrade at a much slower rate. Raw chromatograms suggest degradation products consistent with the elution times of diamines are present in degraded solutions of these solvents, suggesting that the amine interacts with carbons alpha to the hydroxyl functions to form diamine byproducts.

- Unpromoted tertiary morpholine solvents did not appear to degrade.

Chapter 8: Conclusions and Recommendations for Future Work

8.1. CONCLUSIONS: CO₂-LOADED PROMOTED TERTIARY AMINE DEGRADATION

- First-order rate models represent the degradation of piperazine (PZ)-promoted tertiary amines (TA) in environments in which speciation changes and the promoter has substantial interaction with other amine byproducts. In other cases, second-order rate models consistent with proposed degradation pathways can model degradation reasonably well.

- PZ-promoted tertiary amines with at least one methyl group are the least stable solvents tested and have a maximum stripping temperature between 120 and 130 °C, which is comparable to monoethanolamine (MEA).

- PZ-promoted tertiary amines with no methyl groups present have an intermediate stability and have a maximum stripping temperature between 130 and 140 °C.

- PZ-promoted tertiary morpholine solvents are the most stable amine solvents tested and have a maximum stripping temperature above 150 °C, which is comparable to concentrated PZ.

- Tertiary amines with at least one hydroxyethyl or hydroxyisopropyl functional group can form intermediate byproducts that degrade via the carbamate polymerization pathway. PZ-promoted tertiary amine solvents with these functional groups have a PZ degradation rate that is 40 to 130% greater than the tertiary amine degradation rate.

- Tertiary amines with a hydroxypropyl functional group or a five-membered functional group do not form intermediate byproducts that degrade via the

163

carbamate polymerization pathway; in these solvent systems, PZ loss is comparable to the tertiary amine loss.

- Dimethylaminobutanol (DMAB) likely degrades by a ring-closing dehydration mechanism and tert-butyl-diethanolamine likely degrades by elimination of the t-butyl functional group. These amines do not feature PZ as a part of their initial degradation mechanism and thus degrade more quickly than other tertiary amines and at the same rate as PZ.

- On a stoichometric basis and at lean loading, PZ solvents at 7 m TA / 2 m PZ degrade at a slower rate than PZ solvents at 5 m TA / 5 m PZ, likely due to the lower concentration of PZ that leads to a lower initial rate of degradation.

- Increased loading leads to significantly higher rates of degradation for most tertiary amines with at least one hydroxyethyl or hydroxyisopropyl group with the exception of PZ-promoted dimethylaminopropanol (DMAP). This is due to a higher concentration of protonated tertiary amine present in rich-loaded solutions, which increases the initial rate of degradation. The increased concentration of CO_2 in solution leads to greater PZ loss due to an increased rate of oxazolidone formation via the carbamate polymerization pathway.

- The activation energy of thermal degradation of PZ-promoted tertiary amine is correlated with the degradation rate. More stable amines have higher activation energies than less stable amines.

8.2. **CONCLUSIONS: MODELING PZ-PROMOTED METHYLDIETHANOLAMINE (MDEA) DEGRADATION**

- Degradation of PZ-promoted methyldiethanolamine (MDEA) is initiated by a S_N2 substitution involving free and protonated amine. The dominant initial degradation pathway involves free PZ attacking the methyl group of protonated MDEA, forming 1-methylpiperazine (1-MPZ) and diethanolamine (DEA). These happen to be the dominant degradation products in PZ-promoted MDEA and can account at least 60% of the mass lost by PZ and MDEA. The less dominant pathway involves MDEA attacking protonated MDEA, forming the quaternary amine salt dimethyldiethanolammonium (DMDEAm) and DEA. This pathway is the principal degradation pathway for MDEA degradation in the absence of PZ.

- Methylaminoethanol (MAE) and 1-hydroxyethylpiperazine (1-HePZ) were observed in PZ-promoted MDEA degradation; however, their estimated concentration was more than an order of magnitude less than DEA and 1-MPZ and indicates that attack on a hydroxyethyl chain is not favored. Minor degradation products include 1,4-dimethylpiperazine (1,4-DMPZ) and triamines whose structures suggest PZ attacking carbons alpha to the hydroxyl function of the MDEA and can account from 10 to 30% of the mass lost.

- DEA and DMDEAm can account for about 90% of the amine loss initially and eventually begin to approach equilibrium in MDEA degradation. Other tertiary amines, such as DMAE and TEA, and quaternary amine salts, such as THEMAm and choline, were detected on MS but were not quantified using the IC. Diamines consistent with MDEA attack on the carbon alpha to the hydroxyl were observed on MS in MDEA degradation experiments.

- The second-order rate constants predicted by the kinetic model indicate that the rate constant of PZ attacking MDEAH+ is $1.5*10^{-6}$ kg/mol/s at 150 °C and MDEA attacking MDEAH+ is $0.12*10^{-6}$ kg/mol/s in the presence of PZ. The rate of the reverse reactions to regenerate MDEA and PZ is not a significant contributor to modeling the amine losses initially.

- In the absence of PZ, the rate constant of MDEA attacking MDEAH+ is about $0.3*10^{-6}$ kg/mol/s and the reverse rate reaction to regenerate MDEA from DEA and DMDEAm is 40 times as fast as the forward reaction.

- The kinetic model is able to predict initial rates within 20% of the experimental CO_2 amine loss rates after making corrections to the kinetic model to account for additional PZ loss in the presence of CO_2 and the reactivity of the PZ carbamate. The activation energy of degradation predicted by the model is about 140 kJ/mol and is similar to the activation energy of degradation observed in CO_2-loaded experiments which ranged from 140-147 kJ/mol.

8.3.   CONCLUSIONS: MODELING PZ-PROMOTED MDEA DEGRADATION

- In PZ-promoted tertiary amines, the second-order degradation rate decreases with increased tertiary amine pKa.

- In PZ-promoted tertiary amines, the ethyl and hydroxyethyl groups are 17% and 4% as reactive as methyl groups when PZ is the nucleophile.

- Zeroth-order modeling of a range of PZ-promoted tertiary amine solvents under acidified conditions indicates that the rate of PZ loss is comparable to tertiary amine loss for the majority of the experiments.

166

- The stability of PZ-promoted solvents under acidified conditions is similar to solvents under CO_2-loaded conditions despite the additional interaction between PZ and intermediate amine byproducts in the CO_2-loaded experiments. Solvents with PZ-promoted aliphatic tertiary amines with at least one methyl group are the least stable, followed by PZ-promoted aliphatic tertiary amines with no methyl groups, and finally by PZ-promoted tertiary morpholine solvents.

- The activation energy of thermal degradation of PZ-promoted tertiary amine solvents under acidified conditions is similar to the activation energy seen in CO_2-loaded conditions, indicating that the initial degradation step does not involve CO_2 and involves PZ interacting with the tertiary amine.

8.4. CONCLUSIONS: THERMAL DEGRADATION TOPICS RELEVANT TO GAS TREATING

- Solvents whose intermediate degradation products were stable and whose initial rate of degradation was comparable, such as PZ-promoted DMAP and PZ-promoted dimethylaminoethoxyethanol (DMAEE), show little alkalinity loss over time and can be regenerated up to 150 °C if controlling for alkalinity and not parent amine concentration.

- Degradation of PZ-promoted MDEA is reduced when mixed with polyethyleneglycol dimethylether (PEGDME, trade name Selexol®) or N-Methyl-2-pyrrolidone (NMP) by about 30% under CO_2-loaded conditions when compared to the base case that is not mixed with a physical solvent. PZ-promoted MDEA mixed with propylene carbonate (PCAR) is unstable and

degrades at a 50% greater rate than PZ-promoted MDEA in the absence of a physical solvent.

- Unpromoted tertiary amines with at least one methyl group degrade at a high rate initially and then begin to approach kinetic equilibrium with their quaternary amine salt and their corresponding secondary amine byproduct.

- Unpromoted tertiary amines with no methyl groups do not approach kinetic equilibrium and degrade at a much slower rate. Raw chromatograms suggest degradation products consistent with the elution times of diamines are present in degraded solutions of these solvents, suggesting that the amine interacts with carbons alpha to the hydroxyl functions to form diamine byproducts.

- Unpromoted tertiary morpholine solvents did not appear to degrade.

8.5   RECOMMENDATIONS FOR FUTURE WORK

Extending systematic studies of PZ-promoted tertiary amines to cover oxidative degradation, corrosion, absorption rate, and thermodynamic properties.

No study exists that systematically examines the oxidation of promoted PZ tertiary amine solvents as a function of amine structure. These studies should be initiated to understand which structure is the least resistant to oxidation as oxidation represents the bulk of amine loss in CO_2 capture from flue gas.

No study exists that systematically examines the corrosion of promoted PZ tertiary amine solvents as a function of amine structure. Corrosion has a negligible effect on thermal degradation at conditions relevant to CO_2 capture from flu gas. Solvents with

low corrosivitiy will leach fewer metals; dissolved metals can function as oxidation catalysts (Voice 2013a, Sexton 2008). Carbon steel internals, instead of stainless steel internals, can be used in capture plants whose circulating solvent and corresponding degradation products are resistant to corrosion. The material change can reduce the capital cost of the capture plant significantly.

No study exists that systematically examines cyclic capacity, heat of CO_2 absorption, and CO_2 absorption rate as a function of tertiary amine structure. These data can help define an optimum pKa value of the tertiary amine to minimize the energy consumption of the plant and identify solvent properties that are amenable to maintaining good energy performance and a fast CO_2 absorption rate.

Enhance understanding of condensation reactions encountered in thermal degradation.

These reactions likely occur in PZ-promoted tertiary amine solvents based on the degradation product slate seen in PZ-promoted MDEA as well as the presence of diamine products in unpromoted tertiary amine solvents. A hypothesized degradation route to making these products is presented in Figure 8.1.
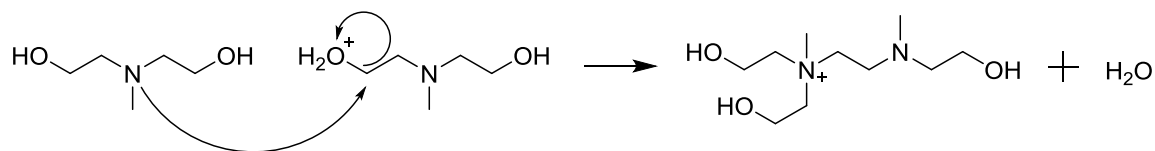
Figure 8.1: Hypothesized condensation reaction between MDEA to form a diamine

The net observed reaction rate of the condensation reactions is expected to be slow, especially considering that these products represented only up to 20% of the degradation products observed in PZ-promoted MDEA.

The rate of PZ reaction with bulky substituent groups is also slow, and condensation reactions will play a more important role in understanding the degradation product slate of promoted tertiary amines without any methyl groups present.

Understand why the PZ-promoted tertiary morpholine solvents are stable.

The PZ-promoted tertiary morpholines degrade slowly and have a thermal degradation rate comparable to concentrated PZ.

Du (Personal Communication, 2014) degraded PZ-promoted triethylenediamine (TEDA). TEDA is a PZ derivative and was hypothesized to be stable. The majority of PZ derivatives, such as 1-MPZ, 2-methylpiperazine, morpholine, and piperidine were found to be thermally stable (Freeman 2011). However, PZ-promoted TEDA was found to be thermally unstable. The degraded solution was found to be solid at room temperature whereas undegraded or mildly degraded solutions were liquid at room temperature.

Du hypothesized that PZ-promoted TEDA would initially degrade by a ring opening step in which PZ attacks a carbon alpha to a protonated amino function of TEDA to form piperazineethylpiperazine (PEP). This is analogous to the initial degradation step of concentrated PZ (Freeman 2011) to form aminoethylaminoethylpiperazine (AEAEPZ) and is shown in Figure 8.2. An analogous pathway of PZ-promoted tertiary morpholine degradation is shown in Figure 8.3 in which PZ attacks HEM to make hydroxyethylaminoethoxyethylpiperazine (HEAEEPZ).

170
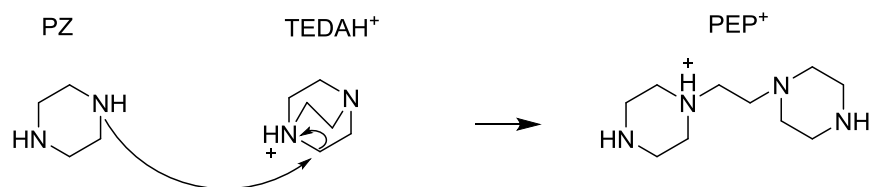
Figure 8.2: Hypothesized pathway to produce PEP from TEDA and PZ (Du 2014)
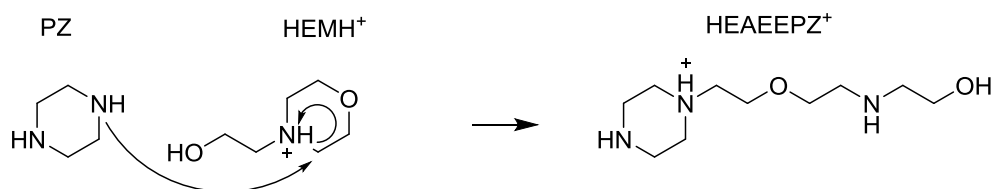
Figure 8.3: Hypothesized pathway to produce a polyamine by ring-opening of the tertiary morpholine by PZ

Freeman (2011) found that AEAEPZ was present in small quantities and only accumulated in acidified degradation. The analogous degradation product of PZ-promoted TEDA, PEP, was suspected to accumulate in degradation of PZ-promoted TEDA. Chromatograms of degraded PZ-promoted TEDA showed that a peak corresponding to the elution time of a tetramine was found to increase with increased degradation in PZ-promoted TEDA (Du 2014).

One possible reason for the stability of PZ is that the rate of AEAEPZ formation is slow. Another possibility is that AEAEPZ is unstable at elevated temperature and degrades by a ring closing step to form two molecules of PZ. This is shown in Figure 8.4.
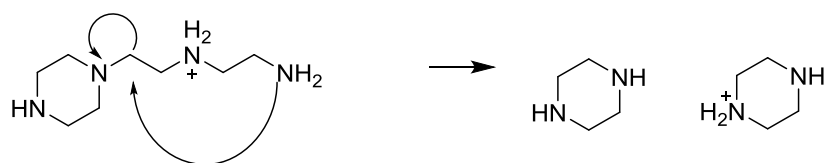
Figure 8.4: Hypothesized pathway of AEAEPZ ring closure to form two molecules of PZ

The analogous product from PZ reaction with tertiary morpholine can also ring close. PEP is more sterically hindered, which would reduce its ability to ring close and is a possible reason for its accumulation in degraded solutions of PZ-promoted TEDA.

Fundamentally understanding the stability of PZ derivatives like the tertiary morpholine solvents is important principally from the viewpoint of solvent development. If this pathway can be generalized for PZ-derivatives, it would encourage the development or screening of other PZ derivatives that maintain concentrated PZ's benefits, such as resistance to oxidation, good energy performance, and thermal stability, but without its solid solubility limitations.

Quantify the degradation of physical solvents in the presence as well as the absence of amine solvents.

The limited degradation study of PZ-promoted MDEA in the presence of physical solvent indicated that the degradation rate of amine in the presence of stable physical solvents was less than the degradation rate of the amine by itself and could be due to speciation changes that affect the observed rate of amine loss. The physical solvent ideally should be quantified as it could degrade through other pathways independently of the amine without significantly affecting speciation.

Understand formate and formamide generation in PZ-promoted tertiary amine solvents.

Closmann (2011) had found that formate salts represented less than 3% of the amine lost in degraded solutions of PZ-promoted MDEA. However, formate salts and other heat stable salts do represent a significant portion of amine loss through oxidation (Sexton 2008, Liu 2014) and were found to be significant byproducts of degradation in thermally stable amines such as PZ (Freeman 2011). Hatchell (2014) showed that an increased rate of corrosion is correlated with increased formate generation. Several sources (Stalder 1984, Sreekanth 2014) have indicated that bicarbonate can electrochemically be reduced to formate.

Formate salts were identified by Freeman (2011) to be present in CO_2-loaded solutions of concentrated PZ degraded in glass vials as well as concentrated PZ degraded in cylinders prepared in a N_2 glovebox. NMR studies of solutions degraded using CO_2 prepared from ^{13}C indicated that the formate comes from CO_2 (Freeman 2011).

In this work, 2 to 2.5 mass equivalents of 40 to 50 wt% NaOH solution were added to 1 mass equivalent of degraded solution and allowed to sit for at least 48 hours to hydrolyze any heat stable salts present in solution. The samples were then diluted in 18.2 μmho deionized water by a factor of 100 and analyzed using anion chromatography. The mechanism of base hydrolysis is shown in Figure 8.5. Raw data for all experiments is presented in Appendix B.5. The formate generation in thermally degraded PZ-promoted solvents is shown in Figures 8.6 and 8.7.

173

Anion chromatography is similar to cation chromatography. Anion chromatography columns use an ion-exchange resin that can selectively adsorb anions, and a gradient of potassium hydroxide or other base is used as the eluent instead of an acid-based eluent. The analytical method used to analyze degraded solutions for formate is identical to the one described by Freeman (2011).
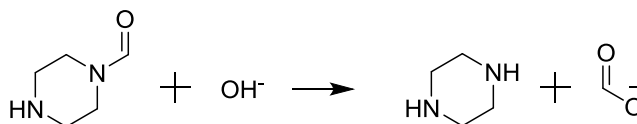
Figure 8.5: Hydrolysis of n-formyl PZ to regenerate the amine and produce formate (Freeman 2011)
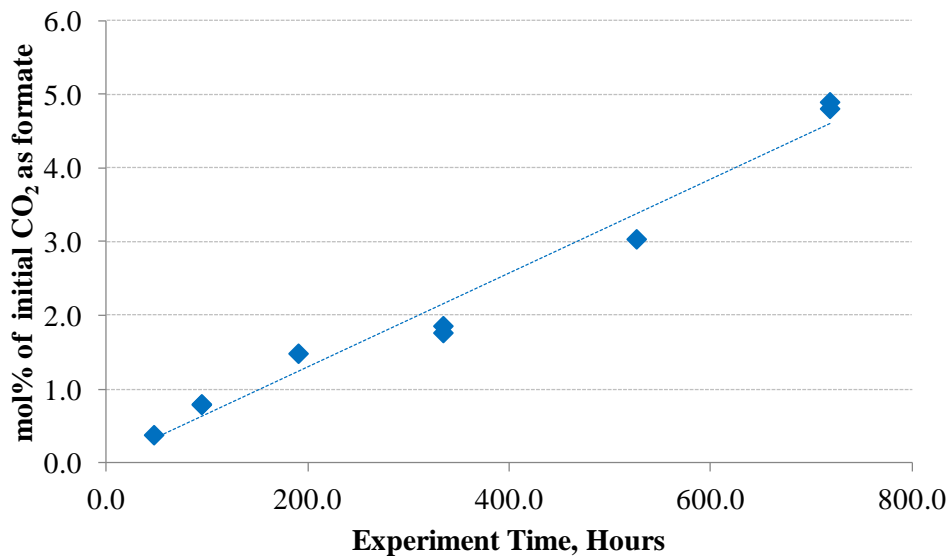
Figure 8.6: Formate generation in degraded, hydrolyzed samples of 5 m PZ / 5 m MDEA. 0.24 mol CO_2/mol alkalinity, and 150 °C
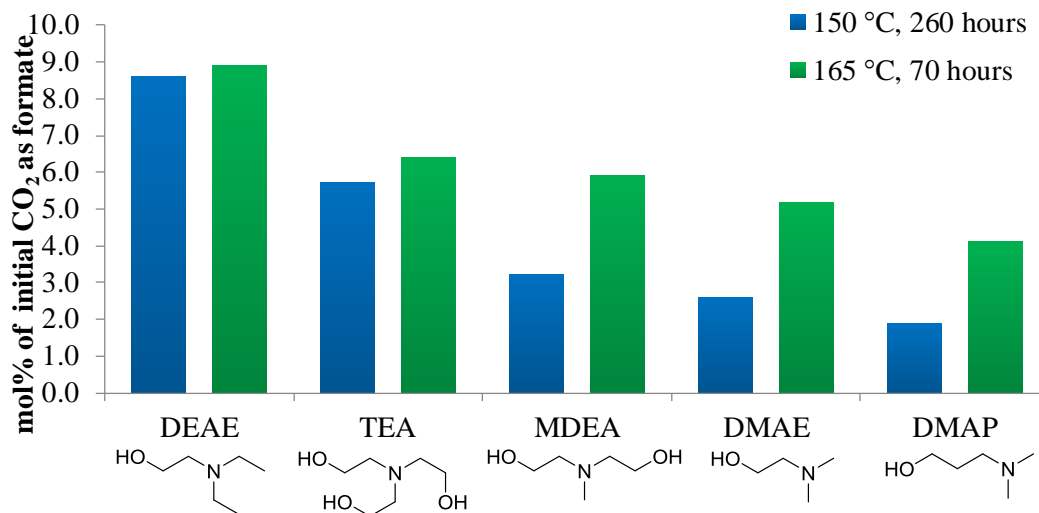
Figure 8.7: Formate production in degraded, hydrolyzed samples of 7 m TA / 2 m PZ and 0.25-0.28 mol CO₂/mol alkalinity

After 700 hours of degradation at 150 °C, about 9% of the initial CO_2 added to the solution is in the form of formate and appears to increase linearly at experimental conditions. Formate generation at 165 °C is 5 to 10 times as greater than at 150 °C. PZ-promoted DEAE had the greatest amount of total formate present in degraded solution, whereas PZ-promoted DMAP had the least amount of total formate present.

Hatchell showed that primary diamines with three carbons between the amino functional groups were resistant to corrosion and that primary diamines with two carbons between the amino functional groups were susceptible to corrosion. In particular, solutions comprising 1,3-diaminopropane (PDA) were an order of magnitude less susceptible to corrosion than ethylenediamine (EDA). The formate concentration in degraded EDA solution was five times as great as in degraded PDA solution (Hatchell 2014). It is possible that DMAP is less corrosive than the other tertiary amines with two carbons between their electron withdrawing groups.

175

Future work on understanding formate generation of PZ-promoted solvents should focus on the following items:

- Effect of corrosion on formate generation

- Effect of amine structure and properties, such as pKa, on formate generation

- Effect of process parameters, such as temperature, concentration, and CO_2 loading, on formate generation

- Effect of thermal reduction versus electrochemical (corrosion) reduction to form formate from carbamate, bicarbonate, or other forms of CO_2 present in solution

Understanding the parameters and variables that can lead to an increase or decrease in the rate of formate production can help control degradation and also aid in the process design of reclaimer units capable of removing heat-stable salts accumulating in solution (Kohl 1960). Understanding the rate of thermal reduction of CO_2 and CO_2 salts, such as amine carbamate and bicarbonate, to formate, can potentially help in developing new processes that aim to utilize CO_2 and convert it to valuable byproducts.

Appendix A – Supporting Information

A.1   Standard Operating Procedure for Thermal Cylinder Experiments

Standard Operating Procedure: Handling Swagelok® Cylinders for Thermal Degradation Experiments
Revision 4 last modified 10 July 2014 by Omkar Namjoshi

Originals by Omkar Namjoshi and Nathan Fine

Never work by yourself while preparing, tightening, or untightening cylinders. Always make sure someone else is in one of the labs.

Proper PPE must be worn while handling cylinders. This includes a lab coat, safety glasses or goggles, and nitrile gloves. Latex gloves should not be worn as latex is a poor barrier for amine solutions. Heat resistant leather gloves must be worn on top of the nitrile gloves when placing cylinders in and out of the oven.

Cylinders must be capable of handling corrosive liquids at temperatures greater than 175 °C and pressures greater than 130 barg. The 4.5 ml Swagelok cylinders are all capable of handling this rating. These cylinders are constructed from stainless steel, are about 4" long, and have end caps and nuts that are sealed at each end of the cylinder. Catastrophic failure can occur if the cylinder is not rated for this service.

Halogens can cause stress corrosion cracking in the stainless steel tubing and fittings used in the cylinder. For this reason, cylinders used to degrade solutions with known quantities of halogens must be segregated from cylinders used to degrade solutions with other solvents. The cylinders used to degrade solutions known to contain halogens must be marked as such and discarded after one year of use.

1.   Loading samples in the cylinder.
      a.   Use a 10 ml pipette and place about 4 ml of solution in the cylinder (for 4.5 ml volume cylinders) if using solutions loaded with CO2.
      b.   Load cylinders in a ventilated hood for particularly volatile, toxic, or foul-smelling solutions.

2. Torquing and tightening the cylinders.
    a. There is no set value that the cylinder needs to be torqued to – Swagelok (manufacturer of the cylinders) recommends that the cylinder be tightened between a quarter turn to half turn past hand tight. Some cylinders cannot be tightened appreciably by hand.
    b. Once the sample is loaded in the cylinder, tighten by hand as much as possible. Weigh the cylinder mass and record. Also make a note of any markings, etc., on the cap of the cylinder that was opened – this makes it easier to open the side of the cylinder that was loosened to load solvent.
    c. Put the cylinder in the vise and clamp the vise on the nut of the cylinder as tightly as possible. Use the small ratchet and, without using too much force, tighten the cylinder as tightly as you can (e.g using the palm of your hand or your pinky finger) if the cylinder cap does not smoothly thread into the nut only by hand. The cap should thread into the nut quickly and smoothly, even for old cylinders. You will notice that there will be a point at which you have to use force to tighten the cylinder further – this is the Swagelok® definition of "hand-tight."
    d. To fully tighten and seal the cylinder, use the ratchet or a large wrench to turn the cylinder nut a quarter turn past hand tight. Use the cylinder markings as a guide.
    e. Mark the cylinder (e.g. on the tube) each time it is used. Retire cylinders that have been used more than 5 times on each side.

3. Placing the cylinder in the oven.
    a. Make sure that the ventilation is drawing air from the convection oven prior to placing cylinders inside by ensuring that there is a net negative pressure at the inlet of the ventilation duct on the top of the oven.
    b. Open the oven. Slowly crack the open door away from the line of fire and check to see if any gases are escaping from the door. Caution: If there are any gases coming out, leave the door cracked slightly to allow the ventilation system to suck the ambient air through the oven so any contaminants can be vented outside. Using a leather glove, place the cylinders on one of the oven racks. Close the oven door.
    c. Keep a clear record of experiments that are being run (e.g. in a lab notebook) in a particular oven that is accessible to lab personnel as needed.

4. Removing cylinders.
   a. Using a leather glove, remove the cylinder and place it on the lab bench to cool. (For experiments with short time scales, generally less than 48 hours, cool the cylinder by quenching it in a water bath.) Record which cylinder is removed and weigh it. Use the same precautions as described in the above section when opening the oven door.

5. Opening cylinders.
   a. Caution: Before opening the cylinder, ensure that the cylinder has cooled to room temperature (25 °C) or below. If the cylinder has not cooled, its contents will be under pressure, and could result in loss of containment, spraying amine through
   b. Place the cylinder inside a vise (see Figure 1) and tighten the vise jaws to hold the cylinder securely. Slowly open the cylinder with a large wrench or the ratchet. Opening it slowly will relieve any residual pressure in the cylinder; opening it too quickly can also result in a containment loss. Cylinders that are pressured will generally make fizzling sounds and small amounts of liquid might leak from the seal; if this is the case, open the cylinder very slowly (e.g. speeds of 1 rpm and below) and away from the line of fire if the cylinder is pressurized.

Cylinder Cap
Cylinder Nut
Vise Jaws
Cylinder Tube
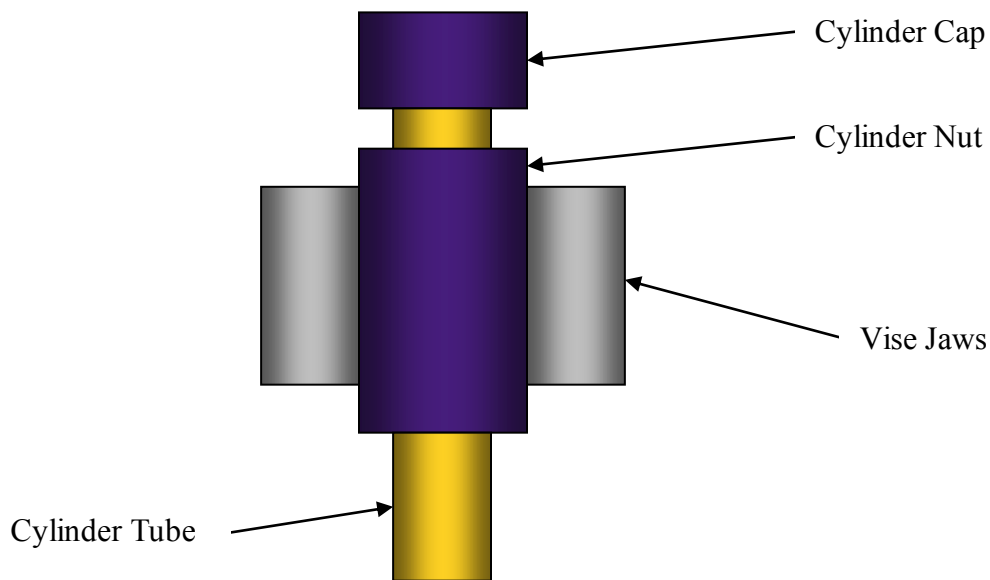
Figure 1: Schematic of Cylinder Placement in Vise

    c.   Once the cap becomes loose, use the ratchet to untighten the cylinder. After the seal has broken, the cylinder pressure will be equal to the atmospheric pressure.

    d.   If the cap does not come off (still swaged inside), use the ratchet to pry the cap off. Sometimes the seals can become stuck. The cylinder will likely not be under much pressure at this time. Consider wearing a faceshield while performing this task.

    e.   Put the cylinder contents in a vial and label it. This should be completed in the fume hood for cylinders whose contents are toxic and/or volatile.

6.   Cleaning cylinders

    a.   Ensure that the cylinder is completely free of any free liquid (I.E., has been drained).

    b.   Rinse the cylinder with DI water.

    c.   Put a small quantity of hand soap in a Nalgene PP tub and fill with DI water. Place the rinsed (and open) cylinder in the tub.

    d.   Allow the cylinder to soak in the soap solution for several days. This removes any residual water-soluble contamination from the cylinder.

    e.   After soaking, remove the cylinder and rinse with DI water a couple of times. Scrape the cylinder with a brush to remove any residue left inside and follow with at least three final DDI washes.

    f.   Dry the cylinder in an oven that is designated for cleaning equipment. Set temperature to 60 °C and place the cylinders on the rack or in the Nalgene PP tub. At these conditions, the cylinders will generally take about three days to dry out completely.

    g.   For rapid drying, set the oven temperature to 110 °C and allow the cylinders to dry for at least 24 hours. Ensure that the oven will not be used to dry plastics and other materials that cannot tolerate high temperature during this time.

    h.   Decant the liquid in the sink.

Standard Operating Procedure: Making Swagelok® Cylinders for Thermal Degradation Experiments

Never work by yourself while preparing, tightening, or untightening cylinders. Always make sure someone else is in one of the labs. Proper PPE must be worn while handling cylinders. This includes a lab coat, safety glasses or goggles, and nitrile gloves. Latex gloves should not be worn as latex is a poor barrier for amine solutions.

Cylinders must be capable of handling corrosive liquids at temperatures greater than 175 °C and pressures greater than 130 barg. The 4.5 ml Swagelok® cylinders are all capable of handling this rating. Catastrophic failure can occur if the cylinder is not rated for this service. The cylinders have an OD of 3/8" and a length of 4" and are constructed from stainless steel. ONLY USE GENUINE SWAGELOK® PARTS FOR MAKING CYLINDERS. For Swagelok® caps, ferrules, and nuts: use P/N SS-600-C. For tubing: use P/N SS-T6-S-035-20. A machine shop can cut the tubes in 4" segments.

1. Preparation of materials
   a. The Swagelok® caps come pre-assembled (the cap is already hand-tight in the nut, and the ferrule is also in the nut). Take out the assembly and hand tighten the cap to the nut as tightly as possible (in most cases, only minor adjustments need to be made, if any) and make a marking on the 12:00 side of the nut and the 9:00 side of the cap using a Sharpie marker.
   b. Turn the cap assembly upside down so the open hole (female side) of the assembly is facing upwards. Insert the tube into the female side of the assembly.
   c. Turn the cap assembly with the tube inserted right side up while holding one hand on the tube. Otherwise, the tube will fall off from the assembly.
2. Performing the initial swage
   a. With the tube/ cap assembly held right side up, place the assembly in the vise, ensuring that the nut (and not the tube) is gripped by the vise jaws. Keep your hand on the tube at all times.
   b. Using a ratchet and one hand, tighten the cylinder assembly 1.25 turns past hand-tight and take care not to allow the tube to fall to the ground.
   c. The ferrule will be swaged to the tube and a seal will be created after you have turned the assembly 1.25 turns past hand-tight. The two markings made on the cap and on the nut should be parallel to one another.
   d. To fully ensure that the cylinder is swaged properly, use the Swagelok Gauging Guide and make sure that it does not slip inside the threaded gap between the cap and the nut. If it does, tighten the cylinder enough so that the Gauging Guide doesn't slip inside the threaded gap.
   3. Repeat steps 1 and 2 to install the nut and cap on the opposite end of the cylinder.

A.2 CATION CHROMATOGRAPH PROGRAMS

The following programs have been created in Dionex Chromeleon® software to manage and run sample sequences on the Dionex ICS-2100 ion chromatograph. They are referenced in Chapter 3.

A.2.1 "Argonaut" Program

```
; Argonaut is a modification of Stpehanie3_Auto_AS wherein the
suppressor current is reduced from 77 mA to 50 mA
; the change is made to increase suppressor lifespan
; the program should be used with the CS17 column to permit quick
elution of monoamines and diamines

Sampler.AcquireExclusiveAccess
     Flush Volume = 250
     Wait  FlushState
     Pressure.LowerLimit =      200 [psi]
     Pressure.UpperLimit =      3000 [psi]
     %A.Equate =       "%A"
     CR_TC =     On
     NeedleHeight =   0 [mm]
     CutSegmentVolume =     0 [µl]
     CycleTime =      0 [min]
     SyringeSpeed =   4
         WaitForTemperature =   False
     Data_Collection_Rate =      5.0 [Hz]
     CellTemperature.Nominal =   30.0 [°C]
     ColumnTemperature.Nominal =      30.0 [°C]
     Suppressor_Type =      CSRS_4mm
     ; Pump_ECD.H2SO4 =    0.0
     ; Pump_ECD.MSA =      38.5
     ; Pump_ECD.Other eluent =  0.0
     ; Pump_ECD.Recommended Current =      57
     Suppressor_Current =  50 [mA]
     Channel_Pressure.Average = On
     Flow =     0.50 [ml/min]
     Wait  SampleReady

 0.000     Autozero
     Concentration = 5.50 [mM]
     Curve =     5
     Wait CycleTimeState
         load
     Inject
     ECD_1.AcqOn
```

182

```
        Channel_Pressure.AcqOn
        Concentration = 5.50 [mM]
        Curve =     5

 0.500     BeginOverlap

16.400     Concentration = 5.50 [mM]
        Curve =     5

16.501     Concentration = 11.00 [mM]
        Curve =     5

26.400     Concentration = 11.00 [mM]
        Curve =     5

36.400     Concentration = 38.50 [mM]
        Curve =     5

47.400     Concentration = 38.50 [mM]
        Curve =     5

47.500     Concentration = 5.50 [mM]
        Curve =     5

50.000     ECD_1.AcqOff
        Concentration = 5.50 [mM]
        Curve =     5
        Channel_Pressure.AcqOff
        End
```

A.2.2 "Nautilus_DEAMAE" Program

```
Sampler.AcquireExclusiveAccess
        Flush Volume = 250
        Wait  FlushState
        ; Nautilus - Rev0
        ; This is the first part of the Nautilus method (Nautilus
        DEAMAE) used to separate DEA from MAE. This is an isocratic
        ; method and uses a 1 mM concentration of MSA with a
        suppressor strength of 5 mA.
        ; second revision decreases flow to allow for wider
        separation
        ; by OAN
        Pressure.LowerLimit =      200 [psi]
        Pressure.UpperLimit =     3000 [psi]
        %A.Equate =       "%A"
        CR_TC =     On
        NeedleHeight =  0 [mm]
```

183

```
CutSegmentVolume =     0 [µl]
CycleTime =      0 [min]
SyringeSpeed =   4
WaitForTemperature =  False
Data_Collection_Rate =     5.0 [Hz]
CellTemperature.Nominal =  30.0 [°C]
ColumnTemperature.Nominal =     30.0 [°C]
Suppressor_Type =     CSRS_4mm
; Pump_ECD.H2SO4 =    0.0
; Pump_ECD.MSA =      38.5
; Pump_ECD.Other eluent =  0.0
; Pump_ECD.Recommended Current =     57
Suppressor_Current = 5 [mA]
Channel_Pressure.Average = On
Flow =     0.40 [ml/min]
Wait  SampleReady

0.000     Autozero
Concentration = 1.00 [mM]
Curve =     5
Wait  CycleTimeState
load
Inject
ECD_1.AcqOn
Channel_Pressure.AcqOn
Concentration = 1.00 [mM]
Curve =     5

0.500     BeginOverlap

89.900     Concentration = 1.00 [mM]
Curve =     5

90.000     ECD_1.AcqOff
Concentration = 1.00 [mM]
Curve =     5
Channel_Pressure.AcqOff
End
```

A.2.3 "Nautilus_DEAMAE_Flush" Program

```
Sampler.AcquireExclusiveAccess
     Flush      Volume = 250
     Wait       FlushState
     ; Nautilus CS19 program
     ; This is the second part of the Nautilus method
     (Nautilus DEAMAE) used to separate DEA from MAE. This
     program must be used
     ; after the DEAMAE program and on a blank DDI vial to
     scrub the diamines and triamines from the column.
     This is an isocratic
     ; method and uses a 40 mM concentration of MSA with a
     suppressor strength of 35 mA.
     ; The last 12,5  minutes uses a 1 mM concentration as
     an equilibration step to facilitate transition to the
     next sample.
     ; by OAN

     ; R1 modified 3 Aug 2013, sets suppressor strength at
     48 mA (optimized settings per CSRS manual)
     Pressure.LowerLimit =    200 [psi]
     Pressure.UpperLimit =    3000 [psi]
     %A.Equate =     "%A"
     CR_TC =    On
     NeedleHeight =       0 [mm]
     CutSegmentVolume =   0 [µl]
     CycleTime =    0 [min]
     SyringeSpeed =       4
     WaitForTemperature =     False
     Data_Collection_Rate =   5.0 [Hz]
     CellTemperature.Nominal =     30.0 [°C]
     ColumnTemperature.Nominal =   30.0 [°C]
     Suppressor_Type =   CSRS_4mm
     ; Pump_ECD.H2SO4 =  0.0
     ; Pump_ECD.MSA =     38.5
     ; Pump_ECD.Other eluent =     0.0
     ; Pump_ECD.Recommended Current =   57
     Suppressor_Current =      48 [mA]
     Channel_Pressure.Average =    On
     Flow =    0.40 [ml/min]
     Wait SampleReady

 0.000    Autozero
     Concentration =      40.00 [mM]
```

```
        Curve =    5
        Wait CycleTimeState
        load
        Inject
        ECD_1.AcqOn
        Channel_Pressure.AcqOn
        Concentration =     40.00 [mM]
        Curve =    5

 0.500    BeginOverlap

44.750    Concentration =     40.00 [mM]
        Curve =    5

45.000    Concentration =     1.00 [mM]
        Curve =    5

57.500    ECD_1.AcqOff
        Concentration =     1.00 [mM]
        Curve =    5
        Channel_Pressure.AcqOff
        End
```

A.3 ESTIMATING RATE CONSTANTS USING FINITE DIFFERENCES

Second-order rates are estimated using finite differences. This method gives similar results to Euler's method; rate constants, however, are evaluated using regression software rather than the Solver tools bundled with spreadsheeting programs. Euler's method estimates amine concentration at points in which data is not available based on the regressed rate constant. This method also estimates free and protonated amine concentration.

Depending on the complexity of the model, the rate expressions can be linearized. If the rate expression cannot be linearized, a non-linear regression package must be used to solve for the rate constants. XLSTAT 2014 (AddInSoft) was used to determine rate constants for the nonlinear models used in Chapter 5. The linear regression tools included with Excel (Microsoft Corporation) were used to determine rate constants for the linearized models used in Chapter 6.

Data from the acidified degradation of PZ-promoted MDEA, initially at 2.5 m PZ and 2.5 m MDEA, 0.14 mol H+/mol alkalinity, and 150 °C, are used in this section to show how the rate loss is calculated. These data are shown in Table A.3.1.

Table A.3.1: Concentration of total PZ and total MDEA

Time hr	PZ mol*kg^{-1}	MDEA mol*kg^{-1}	d[PZ]/dt mol*kg^{-1}*h^{-1}*10^4	d[MDEA]/dt mol*kg^{-1}*h^{-1}*10^4
0	1.581	1.563	--	--
144.75	1.485	1.480	-5.25	-4.97
288.25	1.429	1.419	-4.53	-4.43
432.75	1.355	1.353	-4.64	-4.78
577.5	1.295	1.281	-4.35	-5.04
719.25	1.229	1.207	-4.20	-4.52
864.75	1.176	1.153	--	--

The expression to calculate the rate of amine loss, $d[PZ]/dt$ or $d[MDEA]/dt$, is given in Equation A.3.1 (Fogler 2005).

$$\frac{d(C)}{dt}\bigg|_i \approx \frac{C_{i-1} - C_{i+1}}{2*(t_i - t_{i-1})}$$

Eq. A.3.1

In Eq. A.3.1, C represents the amine concentration, i denotes the experimental point, and t represents experiment time. The concentration data, which is quantified using cation chromatography, can be plugged into Eq. A.3.1 to estimate the rate of amine loss. The rate is treated as the dependent variable in the regression analysis and the concentration data are treated as independent variables. The rate constant, activation energy, and preexponential terms are all parameters that the regression software can solve for.

A.4   pKa REGRESSION AND DETERMINATION OF FREE AND PROTONATED AMINE

The reaction models used to calculate rate constants make extensive use of free and protonated amine species.   pKa data for the parent amine and byproducts are regressed and then extrapolated to the experiment temperature, and the equilibrium constants calculated from the regression are used to determine the quantity of free amine and protonated amine present in undegraded and degraded solution.

In this section, the procedure to regress pKa from experimental data is shown, and the algebraic expression used to calculate the concentration of free and protonated amine based on total amine concentration and total acid concentration is shown. The pKa data as a function of temperature of MDEA are shown in Table A.4.1 (Simond 2012).

Table A.4.1: Disassociation Constants of MDEA (Simond 2012)

Temperature Kelvin	pKa	$K*10^9$
298.15	8.54	2.88
298.15	8.53	2.95
298.15	8.53	2.95
308.15	8.35	4.47
308.15	8.35	4.47
318.15	8.18	6.61
318.15	8.18	6.61
322.76	8.08	8.32
322.76	8.07	8.51
328.15	8.00	10.0
328.15	8.00	10.0
342.48	7.71	19.5
342.48	7.77	17.0
342.48	7.75	17.8
342.48	7.74	18.2

The pKa is the negative logarithm of K, the equilibrium constant that relates the concentration of free amine and protonated amine. This is given in Equations A.4.1 and A.4.2. In Eq. A.4.2, $[H^+]$, [Free Amine], and $[Amine^+]$ denote the concentration of unbound proton, free amine, and protonated amine in solution.

$$pKa = -\log[K]$$ Eq. A.4.1

$$K = \frac{[H^+] * [Free\ Amine]}{[Amine^+]}$$ Eq. A.4.2

The relationship between K and temperature, T, is given by the Van't Hoff equation, shown in Eq. A.4.3 (Hamborg 2006):

$$\frac{d(\ln(K))}{d(1/T)} = \frac{\Delta_r H_m}{R}$$ Eq. A.4.3

In Eq. A.4.3, $\Delta_r H_m$ is the enthalpy of change of reaction and R is the gas constant. $\Delta_r H_m$ is assumed to remain constant throughout the temperature range of the experiment and can be calculated by plotting $\ln(K)$ versus $1/T$ and finding the slope. The linear relationship can be extrapolated to find the equilibrium constant corresponding to the temperature of interest. These data are shown in Figure A.4.1.
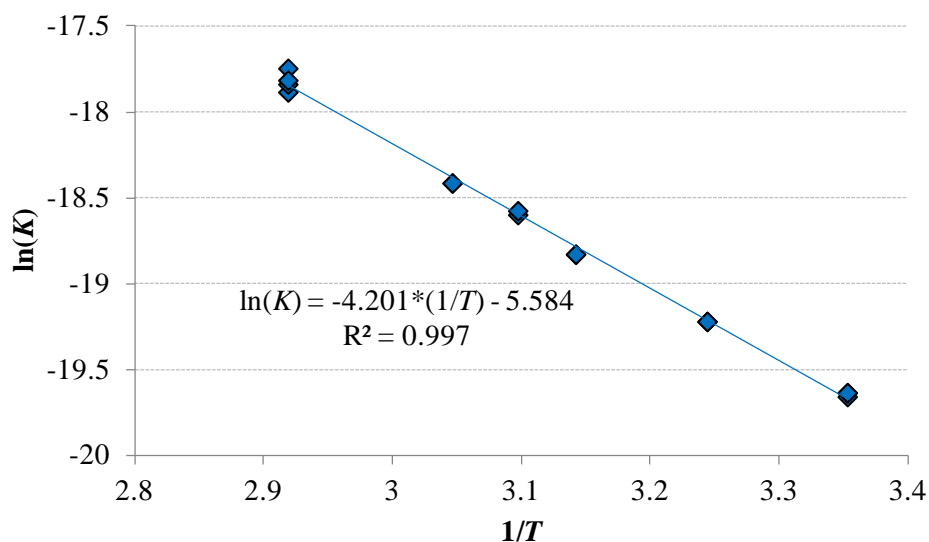
Figure A.4.1: Regression of Disassociation Constants of MDEA as a function of temperature

The extrapolated K and pKa values of PZ (Khalili 2009) and MDEA (Simond 2012), which were estimated from the linear regression, are presented in Table A.4.1.

Table A.4.2: Disassociation Constants for PZ and MDEA at 150 °C

Equilibirum Constant	PZ	MDEA
$K*10^9$	28.8	183
pKa	7.54	6.74

The extrapolated values can then be used to solve for free and protonated amine concentration in solution using the extrapolated K values, the measured total amine concentration by cation chromatography, and the gravimetric measurement of total acid added to solution. An example showing the set of equations used to calculate free and protonated PZ and MDEA in undegraded solution is presented in Equations A.4.4 through A.4.8. These equations were extended to include DEA, 1-MPZ, 1,4-DMPZ, and

191

other degradation products in degraded solutions. These equations have to be solved using either a numeric or symbolic solver.

The combined set of equations has several roots, including real and imaginary roots. The set of solutions that corresponds to the correct root is the set with only positive real roots.

$$\frac{1}{K_{\text{MDEA}}} = \frac{[\text{MDEAH}^+]}{[\text{MDEA}]*[\text{H}^+]} \qquad \text{Eq. A.4.4}$$

$$\frac{1}{K_{\text{PZ}}} = \frac{[\text{PZH}^+]}{[\text{PZ}]*[\text{H}^+]} \qquad \text{Eq. A.4.5}$$

$$[\text{MDEA}] + [\text{MDEAH}^+] = [\text{MDEA}_{\text{total}}] \qquad \text{Eq. A.4.6}$$

$$[\text{PZ}] + [\text{PZH}^+] = [\text{PZ}_{\text{total}}] \qquad \text{Eq. A.4.7}$$

$$[\text{MDEAH}^+] + [\text{PZH}^+] + [\text{H}^+] = [\text{H}^+{}_{\text{total}}] \qquad \text{Eq. A.4.8}$$

In these equations, K_{MDEA} and K_{PZ} denote the equilibrium constant of MDEA and PZ, respectively. [MDEAH$^+$], [MDEA], [PZH$^+$], [PZ], and [H$^+$] represent the concentration of protonated MDEA, free MDEA, protonated PZ, free PZ, and unbound proton in solution as calculated by the model. [MDEA$_{\text{total}}$] and [PZ$_{\text{total}}$] represent the concentration of total MDEA and PZ as measured by cation chromatography. [H$^+{}_{\text{total}}$] represents the amount of H$^+$ added to solution in the form of a strong acid. All of the concentration data have units of mol/kg.

Appendix B – Raw Data

B.1 RAW DATA FOR EXPERIMENTS PRESENTED IN CHAPTER 4

Table B.1.1: 5 m TEA / 5 m PZ, 0.22 mol CO_2/mol alkalinity, 135 °C

Time	TEA	PZ
Hour	mmol/kg	mmol/kg
0.0	2241	2343
47.8	2223	2314
98.0	2225	2285
337.6	2126	2194
528.3	2001	2126
815.0	1989	2038
0.0	2210	2344
98.0	2144	2228
190.7	2162	2182
337.6	2091	2154
815.0	1993	2016

Table B.1.2: 5 m DMAE / 5 m PZ, 0.23 mol CO_2/mol alkalinity, 135 °C

Time	DMAE	PZ
Hour	mmol/kg	mmol/kg
0.0	2479	2532
47.5	2458	2445
98.1	2471	2412
336.6	2264	2085
547.2	2115	1809
695.0	2011	1665
0.0	2488	2525
98.1	2406	2396
193.2	2357	2280
336.6	2207	2048
695.0	1967	1640

Table B.1.3: 5 m MDEA / 5 m PZ, 0.24 mol CO$_2$/mol alkalinity, 135 °C

Time	MDEA	PZ
Hour	mmol/kg	mmol/kg
0.0	2479	2285
0.0	2458	2320
47.8	2471	2192
98.0	2264	1747
98.0	2115	1922
190.7	2011	1923
337.6	2488	1771
337.6	2406	1812
528.3	2357	1628
815.0	2207	1258
815.0	1967	1308

Table B.1.4: 5 m DEAE / 5 m PZ, 0.23 mol CO$_2$/mol alkalinity, 135 °C

Time	DEAE	PZ
Hour	mmol/kg	mmol/kg
0.0	2312	2285
47.5	2182	2320
98.1	2242	2192
336.6	2259	1747
547.2	2162	1922
695.0	2141	1923
0.0	2314	1771
98.1	2221	1812
193.2	2318	1628
336.6	2232	1258
695.0	2165	1308

Table B.1.5: 5 m DMAP / 5 m PZ, 0.23 mol CO$_2$/mol alkalinity, 135 °C

Time	DMAP	PZ
Hour	mmol/kg	mmol/kg
0.0	2435	2394
47.5	2457	2431
98.1	2494	2475
336.6	2376	2350
547.2	2105	2073
695.0	2007	1968
0.0	2444	2399
98.1	2479	2468
193.2	2407	2384
336.6	2206	2184
695.0	2078	2044

Table B.1.6: 5 m TEA / 5 m PZ, 0.22 mol CO$_2$/mol alkalinity, 175 °C

Time	TEA	PZ
Hour	mmol/kg	mmol/kg
0.0	1956	2155
24.5	1513	1505
48.7	1177	951
96.1	627	206
0.0	1952	2147
24.5	1541	1555
48.7	1070	852
96.1	662	255

Table B.1.7: 5 m DMAE / 5 m PZ, 0.23 mol CO$_2$/mol alkalinity, 175 °C

Time	DMAE	PZ
Hour	mmol/kg	mmol/kg
0.0	2631	2404
24.8	1913	1561
48.4	1503	1029
96.5	881	466
0.0	2661	2499
24.8	1922	1643
48.4	1486	1030
96.5	878	489

Table B.1.8: 5 m MDEA / 5 m PZ, 0.24 mol CO$_2$/mol alkalinity, 175 °C

Time	MDEA	PZ
Hour	mmol/kg	mmol/kg
0.0	2377	2292
24.8	1580	1258
48.4	1282	698
96.5	851	212
0.0	2388	2313
24.8	1646	1398
96.5	847	215

Table B.1.9: 5 m DEAE / 5 m PZ, 0.23 mol CO$_2$/mol alkalinity, 175 °C

Time	DEAE	PZ
Hour	mmol/kg	mmol/kg
0.0	2216	2286
24.8	1794	1726
48.4	1464	1269
96.5	1074	863
0.0	2316	2294
24.8	1818	1761
48.4	1563	1417
96.5	1010	802

Table B.1.10: 5 m DMAP / 5 m PZ, 0.23 mol CO$_2$/mol alkalinity, 175 °C

Time	DMAP	PZ
Hour	mmol/kg	mmol/kg
0.0	2395	2314
23.8	1891	1907
48.7	1553	1485
96.7	1129	981
0.0	2405	2350
23.8	1892	1915
48.7	1568	1523
96.7	1137	999

Table B.1.11: 5 m TEA / 5 m PZ, 0.22 mol CO$_2$/mol alkalinity, 150 °C

Time	TEA	PZ
Hour	mmol/kg	mmol/kg
0.0	2106	2355
45.2	2252	2317
118.9	2077	2139
333.7	1799	1713
545.2	1621	1398
669.2	1493	1201
0.0	2229	2362
118.9	1907	1916
190.6	1961	1969
333.7	1834	1713
669.2	1450	1191

Table B.1.12: 5 m DMAE / 5 m PZ, 0.23 mol CO$_2$/mol alkalinity, 150 °C

Time	DMAE	PZ	MAE
Hour	mmol/kg	mmol/kg	mmol/kg
0.0	2429	2470	0
48.7	2093	2297	126
96.2	1944	2036	165
334.2	1358	1125	140
499.7	1075	796	110
718.2	782	500	82
0.0	2393	2431	
96.2	1900	2029	
192.8	1675	1639	
334.2	1370	1165	
718.2	800	524	

Table B.1.13: 5 m MDEA / 5 m PZ, 0.24 mol CO₂/mol alkalinity, 150 °C

Time Hour	MDEA mmol/kg	PZ mmol/kg	DEA mmol/kg
0.0	2294	2236	0
47.8	2180	2152	68
95.3	2070	1935	78
335.2	1633	1020	61
527.2	1310	571	52
719.3	990	330	41
0.0	2330	2272	
95.3	2129	2003	
191.3	1654	1342	
335.2	1472	920	
719.3	965	317	

Table B.1.14: 5 m DEAE / 5 m PZ, 0.23 mol CO₂/mol alkalinity, 150 °C

Time Hour	DEAE mmol/kg	PZ mmol/kg	EAE mol/kg
0.0	2612	2282	0
48.7	2540	2191	38
96.2	2494	2101	58
334.2	2134	1687	97
499.7	1943	1457	88
718.2	1699	1166	79
0.0	2564	2282	
96.2	2492	2101	
192.8	2263	1943	
334.2	2184	1689	
718.2	1660	1181	

Table B.1.15: 5 m DMAP / 5 m PZ, 0.23 mol CO$_2$/mol alkalinity, 150 °C

Time Hour	DMAP mmol/kg	PZ mmol/kg	MAP mmol/kg
0.0	2257	2176	0
47.8	2099	2211	112
95.3	2009	2120	202
335.2	1631	1669	473
527.2	1390	1385	554
719.3	1215	1174	560
0.0	2366	2320	
95.3	2093	2230	
191.3	1905	2008	
335.2	1676	1731	
719.3	1241	1201	

Table B.1.16: 5 m DMAEE / 5 m PZ, 0.23 mol CO$_2$/mol alkalinity, 150 °C

Time Hour	DMAEE mmol/kg	PZ mmol/kg
0.0	2619	2715
45.2	2527	2628
118.9	2302	2376
261.6	1906	2038
381.9	1619	1766
669.2	1187	1322
0.0	2594	2597
381.9	1582	1692
0.0	2442	2508
381.9	1490	1610

Table B.1.16: 5 m DMAB / 5 m PZ, 0.23 mol CO_2/mol alkalinity, 150 °C

Time	DMAB	PZ
Hour	mmol/kg	mmol/kg
0.0	2225	2219
49.7	1418	1700
119.2	773	1063
239.8	330	614
383.4	187	448
0.0	2226	2225
383.4	191	451
0.0	2249	2229
383.4	192	454

Table B.1.17: 5 m EDEA / 5 m PZ, 0.23 mol CO_2/mol alkalinity, 150 °C

Time	EDEA	PZ
Hour	mmol/kg	mmol/kg
0.0	1764	1832
49.7	1676	1724
119.2	1578	1592
239.8	1469	1390
383.4	1332	1164
646.4	1077	813
0.0	1710	1810
383.4	1340	1185
0.0	1743	1822
383.4	1339	1206

Table B.1.18: 5 m nBuDEA / 5 m PZ, 0.22 mol CO_2/mol alkalinity, 150 °C

Time	nBuDEA	PZ
Hour	mmol/kg	mmol/kg
0.0	2057	2011
73.3	2008	1910
168.3	1903	1744
265.9	1754	1543
358.5	1626	1366
358.5	1661	1406
358.5	1680	1427
476.3	1544	1241

Table B.1.19: 5 m tBuDEA / 5 m PZ, 0.22 mol CO$_2$/mol alkalinity, 150 °C

Time	tBuDEA	PZ	DEA
Hour	mmol/kg	mmol/kg	mmol/kg
0.0	1981	2039	0
49.5	1701	1854	127
136.3	1301	1363	143
239.8	878	835	118
384.7	479	390	76
527.3	196	178	36
527.3	230	198	42
527.3	225	196	42
766.3	71	114	-

Table B.1.20: 5 m TIPA / 5 m PZ, 0.22 mol CO$_2$/mol alkalinity, 150 °C

Time	TIPA	PZ
Hour	mmol/kg	mmol/kg
0.0	1883	1956
49.5	1871	1912
136.3	1843	1857
239.8	1770	1776
384.7	1765	1700
527.3	1685	1567
527.3	1678	1556
527.3	1689	1554
766.3	1610	1346

Table B.1.21: 5 m DMAIP / 5 m PZ, 0.22 mol CO$_2$/mol alkalinity, 150 °C

Time	DMAIP	PZ
Hour	mmol/kg	mmol/kg
0.0	2342	2430
73.5	2157	2226
167.0	1968	1995
167.1	2019	2052
289.0	1785	1762
432.0	1627	1535
599.3	1432	1283
599.3	1430	1287
599.3	1451	1299
936.1	1146	922
1104.1	1045	820

Table B.1.22: 5 m HEM / 5 m PZ, 0.22 mol CO₂/mol alkalinity, 150 °C

Time	HEM	PZ
Hour	mmol/kg	mmol/kg
0.0	2236	2248
73.5	2251	2240
167.0	2233	2254
167.1	2211	2205
289.0	2212	2188
432.0	2205	2190
599.3	2160	2131
599.3	2207	2196
599.3	2127	2098
936.1	2170	2130
1104.1	2172	2126

Table B.1.23: 5 m HEM / 5 m PZ, 0.22 mol CO₂/mol alkalinity, 150 °C

Time	HEM	PZ
Hour	mmol/kg	mmol/kg
0.0	2236	2248
73.5	2251	2240
167.0	2233	2254
167.1	2211	2205
289.0	2212	2188
432.0	2205	2190
599.3	2160	2131
599.3	2207	2196
599.3	2127	2098
936.1	2170	2130
1104.1	2172	2126

Table B.1.24: 5 m HPM / 5 m PZ, 0.22 mol CO₂/mol alkalinity, 150 °C

Time	HPM	PZ
Hour	mmol/kg	mmol/kg
0.0	2119	2180
73.5	2117	2159
167.0	2159	2197
167.1	2111	2150
289.0	2107	2142
432.0	2089	2110
599.3	2154	2143
599.3	2099	2137
599.3	2086	2126
936.1	2103	2119
1104.1	2079	2085

Table B.1.25: 5 m HIPM / 5 m PZ, 0.22 mol CO₂/mol alkalinity, 150 °C

Time	HIPM	PZ
Hour	mmol/kg	mmol/kg
0.0	2204	2196
73.5	2154	2179
167.0	2159	2160
167.1	2142	2138
289.0	1959	2107
432.0	2136	2113
599.3	2144	2113
599.3	2163	2140
599.3	2132	2108
936.1	2125	2083
1104.1	2028	2055

Table B.1.26: 5 m MDEA / 5 m HMDA, 0.24 mol CO₂/mol alkalinity, 150 °C

Time	MDEA	HMDA
Hour	mmol/kg	mmol/kg
0.0	2485	2285
45.2	2584	2136
118.9	2396	1894
333.7	2260	1607
545.2	2170	1470
669.2	2072	1420
0.0	2443	2251
118.9	2372	1885
190.6	2338	1784
333.7	2215	1585
669.2	2008	1352

Table B.1.27: 5 m MDEA / 5 m BAE, 0.23 mol CO₂/mol alkalinity, 150 °C

Time	MDEA	BAE
Hour	mmol/kg	mmol/kg
0.0	2181	2291
45.7	2055	1956
94.8	2018	1787
190.3	1856	1566
335.1	1692	1366
526.4	1506	1144
719.6	1408	1005
0.0	2122	2284
45.7	2065	1987
94.8	1992	1829
190.3	1864	1612
335.1	1698	1377
526.4	1540	1178
719.6	1336	991

Table B.1.28: 7 m TEA / 2 m PZ, 0.13 mol CO₂/mol alkalinity, 135 °C

Time Hour	TEA mmol/kg	PZ mmol/kg
0.0	2923	915
74.7	2926	900
171.4	2848	872
289.1	2871	848
453.1	2822	803
453.1	2824	804
453.1	2837	808
625.1	2816	780
816.9	2782	743

Table B.1.29: 7 m TEA / 2 m PZ, 0.13 mol CO₂/mol alkalinity, 150 °C

Time Hour	TEA mmol/kg	PZ mmol/kg
0.0	3171	932
21.9	3141	902
46.7	3189	899
71.3	3045	838
94.0	2992	810
117.9	3028	800
117.9	2849	745
142.3	2946	748
190.3	2933	708
261.6	2848	624

Table B.1.30: 7 m TEA / 2 m PZ, 0.13 mol CO₂/mol alkalinity, 175 °C

Time Hour	TEA mmol/kg	PZ mmol/kg
0.0	3089	895
26.7	2934	664
49.1	2711	450
71.8	2617	302

Table B.1.31: 7 m DMAE / 2 m PZ, 0.13 mol CO₂/mol alkalinity, 135 °C

Time	DMAE	PZ
Hour	mmol/kg	mmol/kg
0.0	3815	1102
74.7	3703	1041
171.4	3640	947
289.1	3549	834
453.1	3450	685
453.1	3443	678
453.1	3452	674
625.1	3313	532
816.9	3223	409

Table B.1.32: 7 m DMAE / 2 m PZ, 0.13 mol CO₂/mol alkalinity, 150 °C

Time	DMAE	PZ
Hour	mmol/kg	mmol/kg
0.0	3813	1144
21.9	3709	1082
46.7	3480	948
71.3	3509	882
94.0	3491	803
117.9	3361	685
117.9	3464	708
117.9	3441	715
142.3	3414	645
190.3	3260	484
261.6	3120	311

Table B.1.33: 7 m DMAE / 2 m PZ, 0.13 mol CO₂/mol alkalinity, 175 °C

Time	DMAE	PZ
Hour	mmol/kg	mmol/kg
0.0	3868	1116
24.3	3285	552
48.8	2954	211
69.8	2653	65

Table B.1.34: 7 m DMAP / 2 m PZ, 0.14 mol CO₂/mol alkalinity, 135 °C

Time	DMAP	PZ
Hour	mmol/kg	mmol/kg
0.0	3563	1031
74.7	3530	994
171.4	3450	949
289.1	3427	917
453.1	3405	870
453.1	3409	875
453.1	3407	874
625.1	3315	809
816.9	3251	737

Table B.1.35: 7 m DMAP / 2 m PZ, 0.14 mol CO₂/mol alkalinity, 150 °C

Time	DMAP	PZ
Hour	mmol/kg	mmol/kg
0.0	3547	1027
21.9	3491	986
46.7	3505	960
71.3	3420	911
94.0	3370	872
117.9	3357	840
117.9	3316	828
117.9	3266	816
142.3	3281	786
190.3	3234	723
261.6	3141	624

Table B.1.36: 7 m DMAP / 2 m PZ, 0.14 mol CO₂/mol alkalinity, 175 °C

Time	DMAP	PZ
Hour	mmol/kg	mmol/kg
0.0	3673	1062
24.3	3349	794
48.8	3060	569
69.8	2827	409

Table B.1.37: 7 m DEAE / 2 m PZ, 0.12 mol CO$_2$/mol alkalinity, 135 °C

Time	DEAE	PZ
Hour	mmol/kg	mmol/kg
0.0	3615	998
74.7	3544	965
171.4	3579	961
289.1	3540	938
453.1	3549	920
453.1	3529	915
453.1	3504	911
625.1	3487	884
816.9	3465	852

Table B.1.38: 7 m DEAE / 2 m PZ, 0.12 mol CO$_2$/mol alkalinity, 150 °C

Time	DEAE	PZ
Hour	mmol/kg	mmol/kg
0.0	3502	1017
21.9	3425	973
46.7	3435	957
71.3	3426	928
94.0	3401	900
117.9	3328	859
117.9	3353	858
117.9	3321	846
142.3	3274	815
190.3	3281	779
261.6	3214	680

Table B.1.39: 7 m DEAE / 2 m PZ, 0.12 mol CO$_2$/mol alkalinity, 175 °C

Time	DEAE	PZ
Hour	mmol/kg	mmol/kg
0.0	3600	986
24.3	3213	563
48.8	2811	255
69.8	2588	129

Table B.1.40: 7 m MDEA / 2 m PZ, 0.12 mol CO₂/mol alkalinity, 135 °C

Time	MDEA	PZ
Hour	mmol/kg	mmol/kg
0.0	3366	992
74.7	3299	937
171.4	3322	900
289.1	3251	820
453.1	3178	708
453.1	3204	717
453.1	3202	706
625.1	3128	595
816.9	3109	480

Table B.1.41: 7 m MDEA / 2 m PZ, 0.12 mol CO₂/mol alkalinity, 150 °C

Time	MDEA	PZ
Hour	mmol/kg	mmol/kg
0.0	3275	990
21.9	3242	942
46.7	3278	907
71.3	3237	846
94.0	3160	782
117.9	3137	724
117.9	3130	725
117.9	3113	716
142.3	3118	668
190.3	3084	563
261.6	2940	411

Table B.1.42: 7 m MDEA / 2 m PZ, 0.12 mol CO₂/mol alkalinity, 175 °C

Time	MDEA	PZ
Hour	mmol/kg	mmol/kg
0.0	3310	981
26.7	2932	523
49.1	2723	227
71.8	2474	54

Table B.1.43: 7 m TEA / 2 m PZ, 0.26 mol CO₂/mol alkalinity, 135 °C

Time	TEA	PZ
Hour	mmol/kg	mmol/kg
0.0	2911	846
72.8	2846	773
192.7	2767	665
289.4	2655	575
408.3	2575	486
408.3	2560	485
408.3	2569	488
575.2	2419	369
746.2	2311	271

Table B.1.44: 7 m TEA / 2 m PZ, 0.26 mol CO₂/mol alkalinity, 150 °C

Time	TEA	PZ
Hour	mmol/kg	mmol/kg
0.0	3040	841
23.4	2916	742
49.7	2775	625
73.2	2717	547
96.0	2636	471
121.3	2523	389
121.3	2534	394
121.3	2591	431
143.8	2490	346
192.2	2306	215
262.4	2119	94

Table B.1.45: 7 m TEA / 2 m PZ, 0.26 mol CO₂/mol alkalinity, 165 °C

Time	TEA	PZ
Hour	mmol/kg	mmol/kg
0.0	3142	906
13.3	2913	727
20.0	2750	622
37.4	2533	421

Table B.1.46: 7 m DMAE / 2 m PZ, 0.26 mol CO₂/mol alkalinity, 135 °C

Time	DMAE	PZ
Hour	mmol/kg	mmol/kg
0.0	3598	1023
72.8	3491	969
192.7	3316	802
289.4	3234	681
408.3	3108	546
408.3	3149	557
408.3	3139	561
575.2	2982	406
746.2	2912	327

Table B.1.47: 7 m DMAE / 2 m PZ, 0.26 mol CO₂/mol alkalinity, 150 °C

Time	DMAE	PZ	MAE
Hour	mmol/kg	mmol/kg	mmol/kg
0.0	3638	999	0
23.4	3531	942	51
49.7	3407	828	92
73.2	3303	712	126
96.0	3196	599	155
121.3	3113	498	186
121.3	3136	506	173
121.3	3104	504	172
143.8	2989	417	188
192.2	2835	275	230
262.4	2661	147	292

Table B.1.48: 7 m DMAE / 2 m PZ, 0.26 mol CO₂/mol alkalinity, 165 °C

Time	DMAE	PZ
Hour	mmol/kg	mmol/kg
0.0	3717	1062
13.3	3352	803
20.0	3286	677
37.4	2997	385

Table B.1.49: 7 m DMAP / 2 m PZ, 0.25 mol CO$_2$/mol alkalinity, 135 °C

Time	DMAP	PZ
Hour	mmol/kg	mmol/kg
0.0	3442	978
72.8	3348	933
192.7	3240	871
289.4	3172	822
408.3	3117	765
408.3	3108	768
408.3	3132	777
575.2	3082	714
746.2	3007	651

Table B.1.50: 7 m DMAP / 2 m PZ, 0.25 mol CO$_2$/mol alkalinity, 150 °C

Time	DMAP	PZ	MAP
Hour	mmol/kg	mmol/kg	mmol/kg
0.0	3484	954	0
23.4	3366	895	74
49.7	3332	861	116
73.2	3299	828	140
96.0	3231	785	151
121.3	3224	753	154
121.3	3205	759	155
121.3	3227	769	154
143.8	3188	743	153
192.2	3113	681	148
262.4	2998	587	141

Table B.1.51: 7 m DMAP / 2 m PZ, 0.25 mol CO$_2$/mol alkalinity, 165 °C

Time	DMAP	PZ
Hour	mmol/kg	mmol/kg
0.0	3415	1000
13.3	3247	875
20.0	3193	815
37.4	3023	664

Table B.1.52: 7 m DEAE / 2 m PZ, 0.28 mol CO$_2$/mol alkalinity, 135 °C

Time	DEAE	PZ
Hour	mmol/kg	mmol/kg
0.0	3255	916
72.8	3293	900
192.7	3172	824
289.4	3197	792
408.3	3122	751
408.3	3168	764
408.3	3140	760
575.2	3066	692
746.2	3011	614

Table B.1.53: 7 m DEAE / 2 m PZ, 0.28 mol CO$_2$/mol alkalinity, 150 °C

Time	DEAE	PZ
Hour	mmol/kg	mmol/kg
0.0	3287	923
23.4	3230	854
49.7	3161	780
73.2	3117	716
96.0	3022	661
121.3	3024	614
121.3	3048	625
121.3	3061	635
143.8	2959	568
192.2	2894	489
262.4	2782	369

Table B.1.54: 7 m DEAE / 2 m PZ, 0.28 mol CO$_2$/mol alkalinity, 165 °C

Time	DEAE	PZ
Hour	mmol/kg	mmol/kg
0.0	3397	938
13.3	3348	792
20.0	3196	716
37.4	3215	604

Table B.1.55: 7 m MDEA / 2 m PZ, 0.26 mol CO$_2$/mol alkalinity, 135 °C

Time	MDEA	PZ
Hour	mmol/kg	mmol/kg
0.0	3235	905
72.8	3154	835
192.7	3010	684
289.4	3207	627
408.3	2916	462
408.3	2933	466
408.3	2958	472
575.2	2832	321
746.2	2723	205

Table B.1.56: 7 m MDEA / 2 m PZ, 0.26 mol CO$_2$/mol alkalinity, 150 °C

Time	MDEA	PZ	DEA
Hour	mmol/kg	mmol/kg	mmol/kg
0.0	3271	934	0
23.4	3183	854	45
49.7	3067	726	55
73.2	3032	630	59
96.0	2926	543	56
121.3	2882	445	58
121.3	2869	448	58
121.3	2899	470	58
143.8	2846	409	56
192.2	2723	270	53
262.4	2636	161	47

Table B.1.57: 7 m MDEA / 2 m PZ, 0.26 mol CO$_2$/mol alkalinity, 165 °C

Time	MDEA	PZ
Hour	mmol/kg	mmol/kg
0.0	3269	939
13.3	3086	766
20.0	3031	675
37.4	2817	422

Table B.1.58: 7 m PZ / 2 m MEA, 0.29 mol CO_2/mol alkalinity, 150 °C

Time	MEA	PZ
Hour	mmol/kg	mmol/kg
0.0	1072	3462
90.2	818	3135
210.5	552	2919
408.2	259	2657
550.3	92	2503
0.0	1086	3452
90.2	823	3174
210.5	568	2944
408.2	278	2781
550.3	104	2610

Table B.1.59: 7 m PZ / 2 m MPA, 0.31 mol CO_2/mol alkalinity, 150 °C

Time	MPA	PZ
Hour	mmol/kg	mmol/kg
0.0	962	3427
71.3	888	3350
216.8	772	3262
336.3	646	3154
0.0	989	3455
71.3	913	3455
216.8	787	3322
544.8	503	3052

Table B.1.60: 7 m PZ / 2 m MAE, 0.30 mol CO_2/mol alkalinity, 150 °C

Time	MAE	PZ
Hour	mmol/kg	mmol/kg
0.0	934	3319
24.0	584	2940
48.4	362	2813
73.1	216	2705
0.0	999	3390
88.8	184	2656
167.1	58	2502
0.0	972	3367
167.1	60	2667

Table B.1.61: 7 m PZ / 2 m AMP, 0.30 mol CO_2/mol alkalinity, 150 °C

Time	AMP	PZ
Hour	mmol/kg	mmol/kg
0.0	1045	3615
70.2	1012	3578
167.2	951	3492
333.7	857	3380
502.4	761	3293
670.4	677	3209
837.8	591	3135
1029.7	528	3015
70.2	997	3517
167.2	961	3519
333.7	859	3385
670.4	673	3167
837.8	593	3049
1029.7	541	2994
502.4	745	3357

Table B.1.62: 7 m PZ / 2 m MIPA, 0.31 mol CO_2/mol alkalinity, 150 °C

Time	MIPA	PZ
Hour	mmol/kg	mmol/kg
0.0	1125	3405
70.4	991	3313
287.2	793	3141
454.6	663	3037
646.5	537	2906
813.4	488	2919
1173.7	410	2788
0.0	1133	3457
70.4	989	3360
287.2	790	3213
454.6	658	3077
646.5	551	2939
813.4	494	2892
1004.3	448	2896
1173.7	404	2805

Table B.1.63: 7 m PZ / 2 m DEA, 0.31 mol CO$_2$/mol alkalinity, 150 °C

Time	DEA	PZ
Hour	mmol/kg	mmol/kg
0.0	1093	3707
25.4	462	2906
49.2	226	2564
73.0	109	2364
73.0	124	2380
118.7	29	2071
216.2	0	1870

Table B.1.64: 7 m PZ / 2 m EAE, 0.31 mol CO$_2$/mol alkalinity, 150 °C

Time	EAE	PZ
Hour	mmol/kg	mmol/kg
0.0	986	3481
13.3	873	3367
20.3	816	3289
37.4	705	3206
45.4	649	3138
45.4	658	3161
45.4	660	3185
69.5	529	3045
91.8	430	2939
114.6	354	2882

B.2 RAW DATA FOR EXPERIMENTS PRESENTED IN CHAPTER 5

Table B.2.1: 2.5 m PZ / 2.5 m MDEA, 0.14 mol H$^+$/mol alkalinity, 135 °C

Time Hour	MDEA mmol/kg	PZ mmol/kg	DEA mmol/kg	1-MPZ mmol/kg	1,4-DMPZ mmol/kg	HeMAEtPZ mmol/kg	H$^+$ mmol/kg
0.0	1571	1600	0	0	0	0	664
168.3	1553	1577	28	23	0	8	664
337.3	1529	1541	50	42	0	9	664
505.1	1510	1513	77	64	0	11	664
839.5	1450	1461	118	98	3	11	664
1175.9	1406	1416	161	133	4	13	664
1847.8	1335	1340	234	196	7	18	664

Table B.2.2: 2.5 m PZ / 2.5 m MDEA, 0.14 mol H$^+$/mol alkalinity, 150 °C

Time Hour	MDEA mmol/kg	PZ mmol/kg	DEA mmol/kg	1-MPZ mmol/kg	1,4-DMPZ mmol/kg	HeMAEtPZ mmol/kg	H$^+$ mmol/kg
0.0	1563	1581	0	0	0	0	665
144.8	1480	1485	87	70	2	11	665
288.3	1419	1429	162	129	4	14	665
432.8	1353	1355	239	189	8	18	665
577.5	1281	1295	296	233	11	22	665
719.3	1207	1229	375	296	18	27	665
864.8	1153	1176	406	320	21	29	665

Table B.2.3: 2.5 m PZ / 2.5 m MDEA, 0.14 mol H$^+$/mol alkalinity, 165 °C

Time Hour	MDEA mmol/kg	PZ mmol/kg	DEA mmol/kg	1-MPZ mmol/kg	1,4-DMPZ mmol/kg	HeMAEtPZ mmol/kg	H$^+$ mmol/kg
0.0	1595	1610	0	0	0	0	665
24.2	1526	1526	70	57	2	12	665
48.3	1477	1480	130	109	4	16	665
72.5	1395	1399	175	145	5	19	665
96.8	1337	1346	242	199	8	24	665
121.0	1302	1313	280	228	11	28	665
144.1	1256	1272	372	278	16	34	665

Table B.2.4: 2 m PZ / 7 m MDEA, 0.09 mol H$^+$/mol alkalinity, 150 °C

| Time | MDEA | PZ | DEA | 1-MPZ | 1,4-DMPZ | HeMAEtPZ | H$^+$ |
Hour	mmol/kg	mmol/kg	mmol/kg	mmol/kg	mmol/kg	mmol/kg	mmol/kg
0.0	3302	944	0	0	0	0	503
143.5	3177	822	116	90	5	14	503
288.3	3108	726	230	165	11	25	503
427.1	3004	622	358	245	26	32	503
577.5	2838	508	504	316	50	43	503
719.8	2812	461	567	339	62	37	503
863.3	2718	393	664	368	83	41	503

Table B.2.5: 3.7 m PZ / 7 m MDEA, 0.07 mol H$^+$/mol alkalinity, 165 °C

| Time | MDEA | PZ | DEA | 1-MPZ | 1,4-DMPZ | HeMAEtPZ | H$^+$ |
Hour	mmol/kg	mmol/kg	mmol/kg	mmol/kg	mmol/kg	mmol/kg	mmol/kg
0.0	3232	1673	0	0	0	0	443
25.2	3147	1586	84	64	3	21	443
49.1	3036	1471	207	170	6	30	443
73.2	3026	1465	221	181	6	31	443
112.7	2753	1225	455	367	21	49	443
146.2	2733	1205	479	388	23	51	443
187.0	2653	1123	584	462	36	61	443

Table B.2.6: 2 m PZ / 7 m MDEA, 0.09 mol H$^+$/mol alkalinity, 165 °C

| Time | MDEA | PZ | DEA | 1-MPZ | 1,4-DMPZ | HeMAEtPZ | H$^+$ |
Hour	mmol/kg	mmol/kg	mmol/kg	mmol/kg	mmol/kg	mmol/kg	mmol/kg
0.0	3501	999	0	0	0	0	474
25.2	3361	899	83	60	4	23	474
49.1	3350	857	145	111	6	30	474
73.2	3312	804	207	160	8	34	474
112.7	3181	716	293	221	15	40	474
146.2	3152	661	360	267	22	46	474
187.0	3032	592	436	310	32	53	474

Table B.2.7: 0.75 m PZ / 7 m MDEA, 0.12 mol H⁺/mol alkalinity, 165 °C

Time	MDEA	PZ	DEA	1-MPZ	H⁺
Hour	mmol/kg	mmol/kg	mmol/kg	mmol/kg	mmol/kg
0.0	3623	391	0	0	501
25.2	3547	328	77	41	497
49.1	3460	260	142	81	496
73.2	3380	203	208	113	495
112.7	3271	142	289	136	494
146.2	3237	111	345	144	494
187.0	3127	64	416	133	493

Time	1,4-DMPZ	HeMAEtPZ	HeMAEtMPZ	DMDEAm	
Hour	mmol/kg	mmol/kg	mmol/kg	mmol/kg	
0.0	0	0	0	0	
25.2	4	24	24	4	
49.1	7	31	16	5	
73.2	15	38	15	6	
112.7	30	40	19	7	
146.2	44	43	20	7	
187.0	68	49	27	7	

Table B.2.8: 2.5 m PZ / 2.5 m MDEA, 0.14 mol H⁺/mol alkalinity, 165 °C

Time	MDEA	PZ	DEA	1-MPZ	1,4-DMPZ	HeMAEtPZ	H⁺
Hour	mmol/kg	mmol/kg	mmol/kg	mmol/kg	mmol/kg	mmol/kg	mmol/kg
0.0	1640	1629	0	0	0	0	686
23.7	1573	1551	62	52	0	13	686
47.3	1525	1507	117	100	3	17	686
71.1	1460	1447	176	153	4	21	686
94.7	1425	1409	217	191	6	25	686
120.2	1373	1363	276	240	10	31	686
143.8	1312	1307	327	281	14	36	686

Table B.2.9: 2.5 m PZ / 2.5 m MDEA, 0.15 mol H⁺/mol alkalinity as HCl, 165 °C

Time	MDEA	PZ	DEA	1-MPZ	1,4-DMPZ	HeMAEtPZ	H$^+$
Hour	mmol/kg	mmol/kg	mmol/kg	mmol/kg	mmol/kg	mmol/kg	mmol/kg
0.0	1652	1645	0	0	0	0	697
23.7	1555	1552	84	72	0	11	697
47.3	1474	1471	169	148	4	15	697
71.1	1405	1402	236	205	7	19	697
94.7	1359	1354	298	260	10	23	697
120.2	1262	1265	398	338	18	29	697
143.8	1185	1198	451	384	24	39	697

Table B.2.10: 5 m MDEA, 0.20 mol H⁺/mol alkalinity, 135 °C

Time	MDEA	DEA	DMDEAm	H$^+$
Hour	mmol/kg	mmol/kg	mmol/kg	mmol/kg
0.0	3074	0	0	599
170.1	3028	42	32	567
339.1	2906	62	56	543
676.1	2853	90	92	507
1011.0	2774	110	117	481
1346.1	2747	118	132	467
2019.8	2681	122	145	454

Table B.2.11: 5 m MDEA, 0.20 mol H⁺/mol alkalinity, 150 °C

Time	MDEA	DEA	DMDEAm	H$^+$
Hour	mmol/kg	mmol/kg	mmol/kg	mmol/kg
0.0	3067	0	0	602
71.3	2963	55	46	556
143.3	2888	81	77	524
216.7	2808	102	104	497
360.9	2714	123	133	469
502.5	2668	132	146	456
646.9	2667	122	146	456

Table B.2.12: 5 m MDEA, 0.20 mol H⁺/mol alkalinity, 165 °C

Time	MDEA	DEA	DMDEAm	H⁺
Hour	mmol/kg	mmol/kg	mmol/kg	mmol/kg
0.0	3076	0	0	599
24.4	2949	46	43	556
48.1	2842	70	76	523
72.0	2794	92	106	494
96.4	2759	105	126	473
119.9	2690	116	139	460
144.3	2659	121	147	452

Full view, showing parent amines and major byproducts

Zoomed-in view, showing all products present
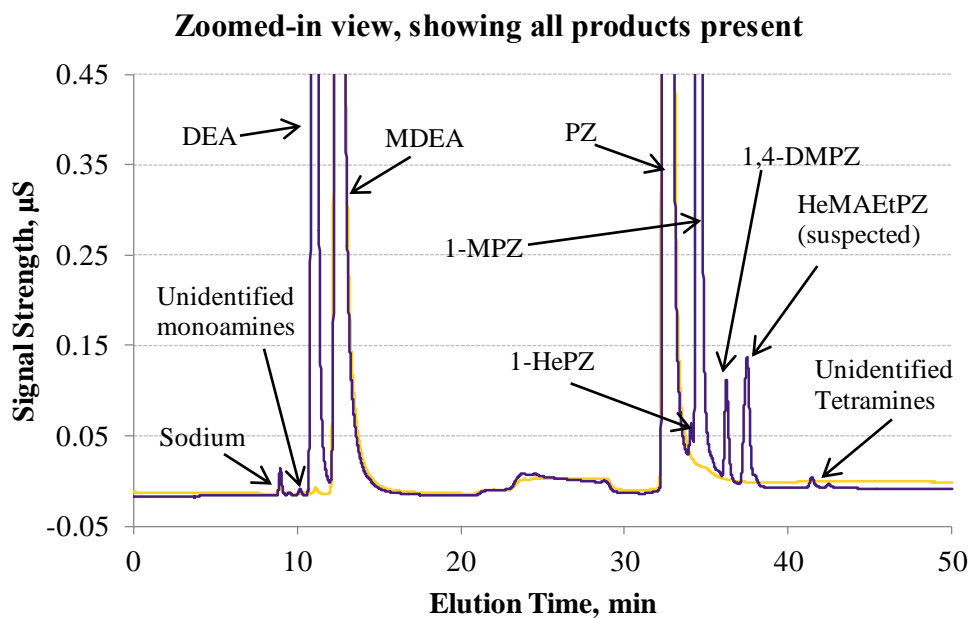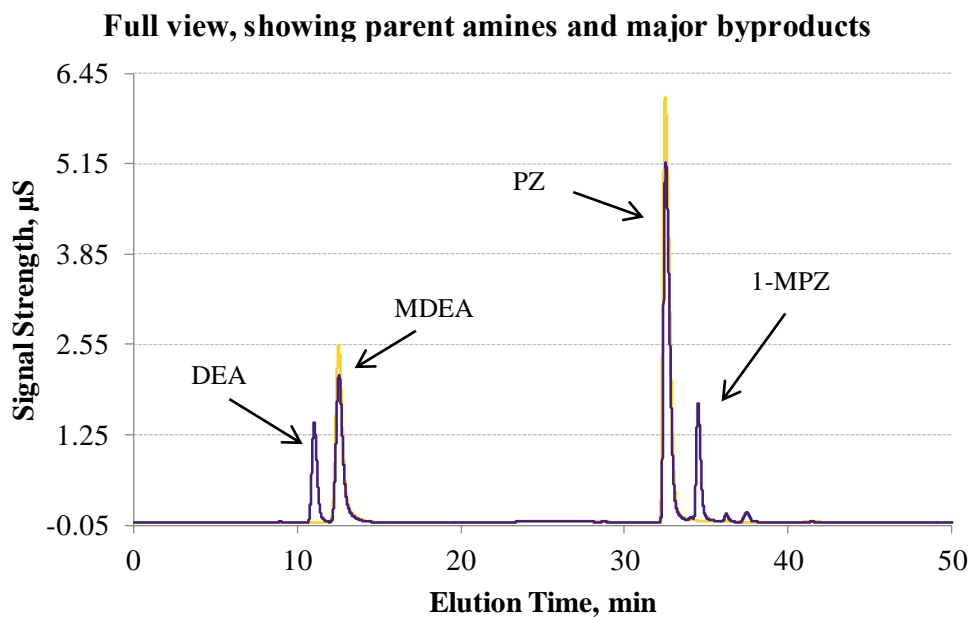
Figure B.2.1: Cation Chromatogram of undegraded (gold) and degraded (purple) 2.5 m PZ / 2.5 m MDEA at 0.14 mol H+/mol alkalinity, 150 °C, and after 865 hours using the CG17/CS17 column set and "Argonaut" program
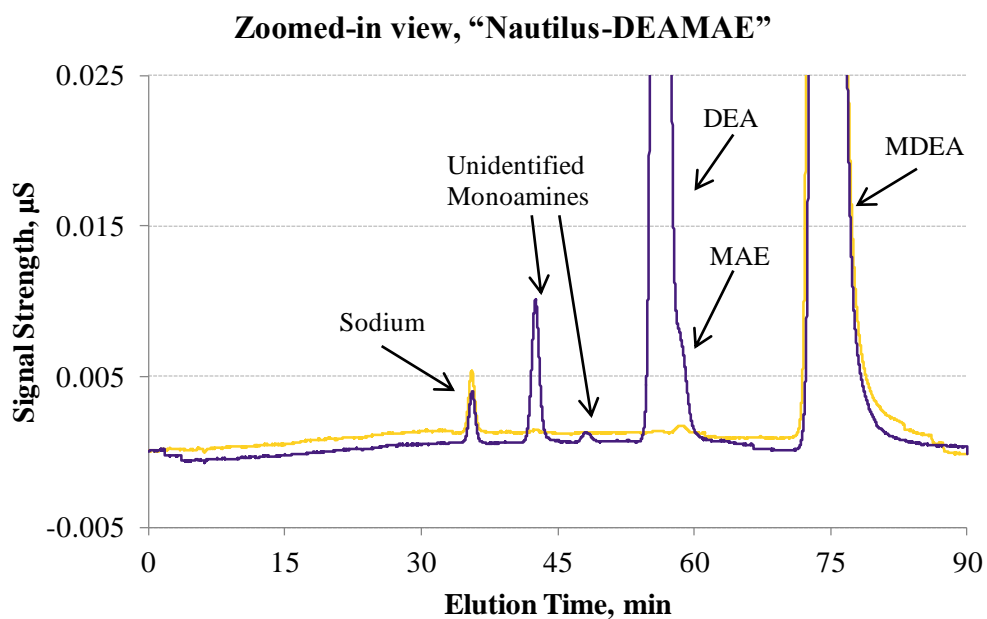
Figure B.2.2: Cation Chromatogram of undegraded (gold) and degraded (purple) 2.5 m PZ / 2.5 m MDEA at 0.14 mol H+/mol alkalinity, 150 °C, and after 865 hours using the CG19/CS19 column set and "Nautilus" programs (zoomed-in views)
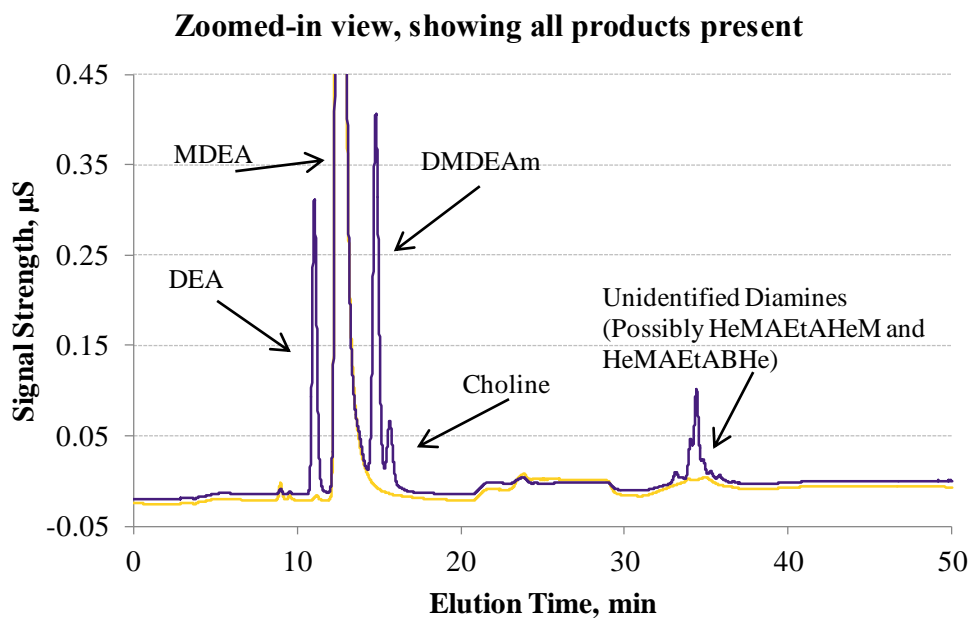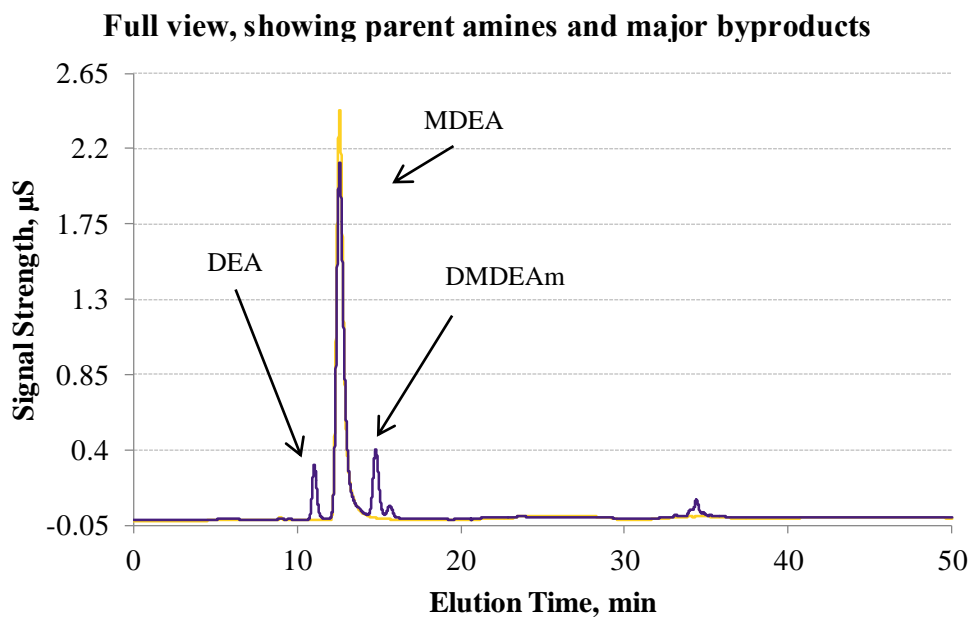
Figure B.2.3: Cation Chromatogram of undegraded (gold) and degraded (purple) 5 m MDEA at 0.20 mol H+/mol alkalinity, 150 °C, and after 647 hours using the CG17/CS17 column set and "Argonaut" program

225
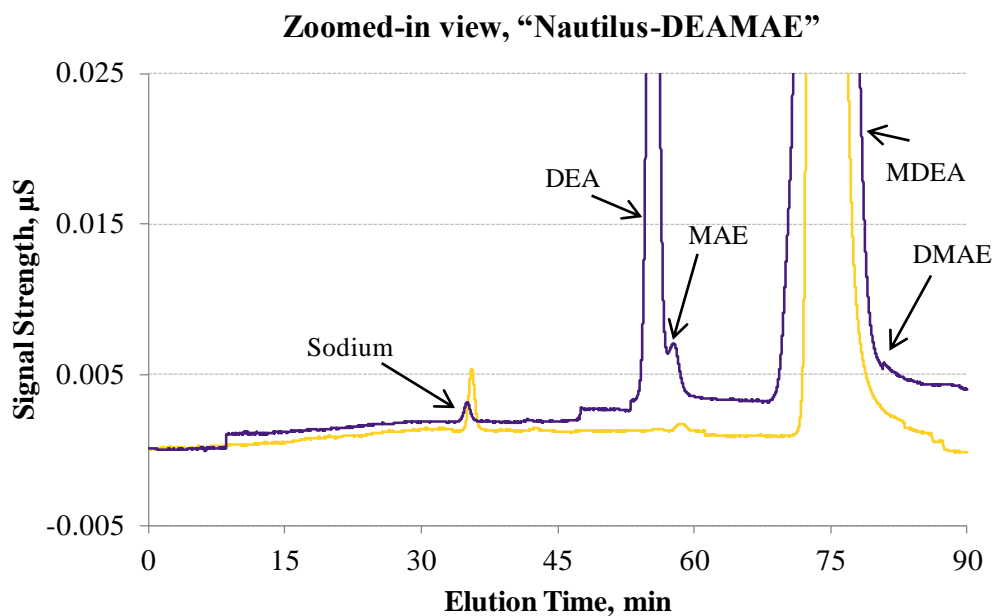
Figure B.2.4: Cation Chromatogram of undegraded (gold) and degraded (purple) 5 m MDEA at 0.20 mol H+/mol alkalinity, 150 °C, and after 647 hours using the CG19/CS19 column set and "Nautilus" programs (zoomed-in views)

226
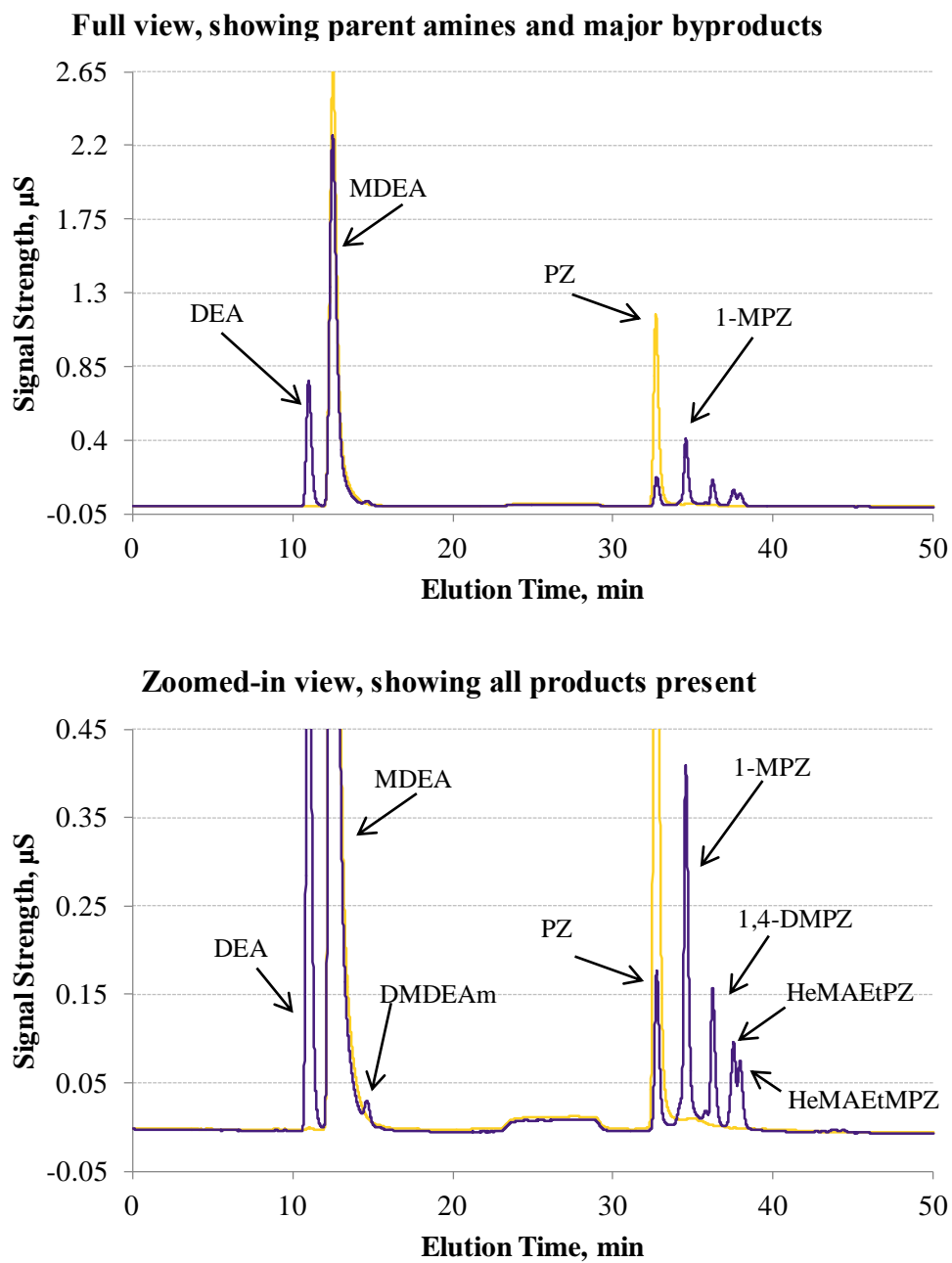
Figure B.2.5: Cation Chromatogram of undegraded (gold) and degraded (purple) 0.75 m PZ / 7 m MDEA at 0.12 mol H+/mol alkalinity, 165 °C, and after 187 hours using the CG17/CS17 column set and "Argonaut" program
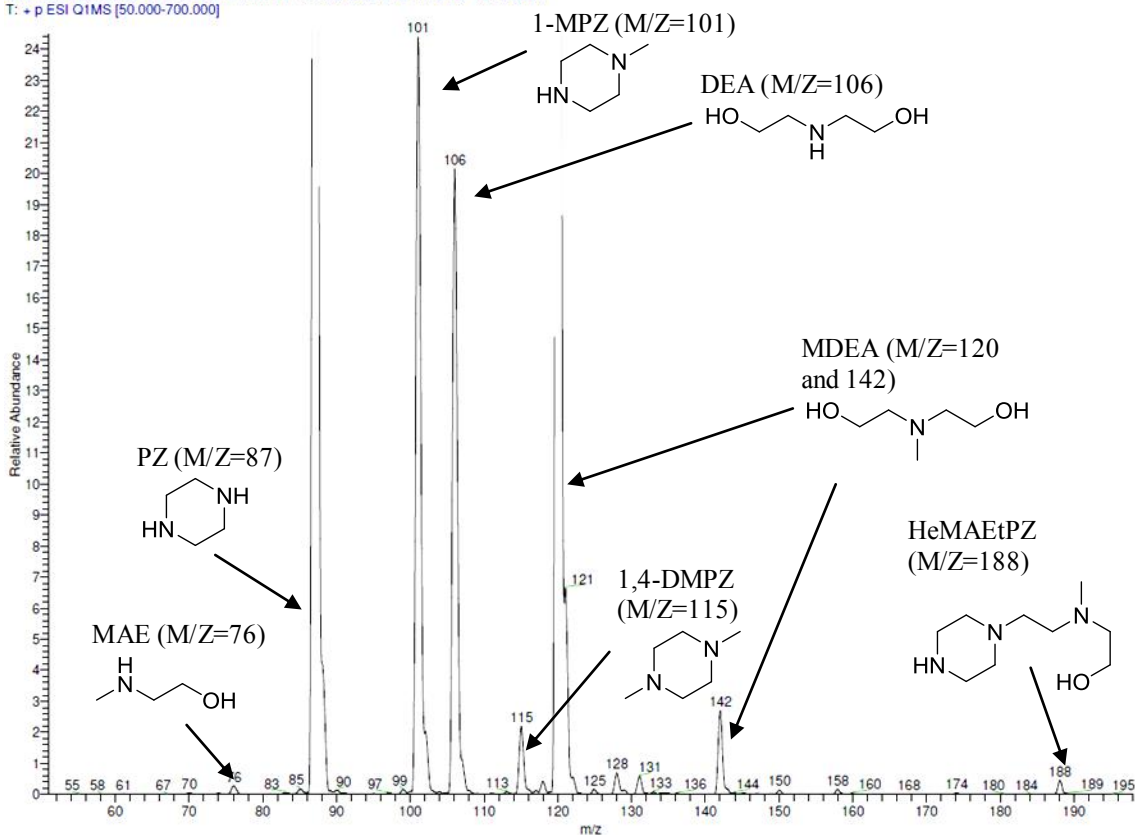
Figure B.2.6: Low Resolution Mass Spectra of 2.5 m PZ / 2.5 m MDEA and 0.14 mol H⁺/mol alkalinity degraded at 150 °C after 865 hours
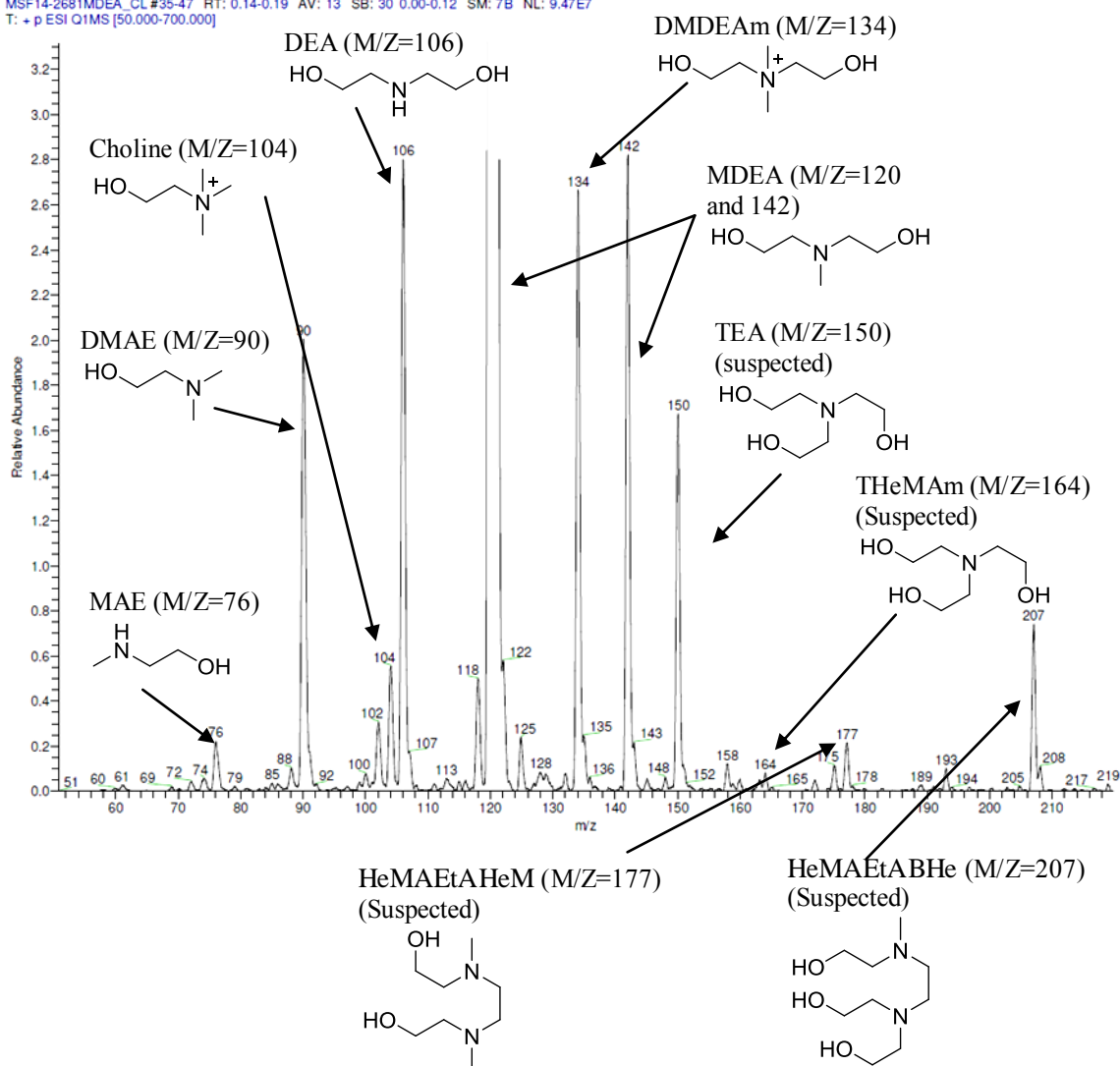
Figure B.2.7: Low Resolution Mass Spectra of 5 m MDEA and 0.20 mol H$^+$/mol alkalinity degraded at 150 °C after 647 hours

B.3 RAW DATA FOR EXPERIMENTS PRESENTED IN CHAPTER 6

Table B.3.1: 2.5 m PZ / 2.5 m DMAE, 0.14 mol H^+/mol alkalinity, 135 °C

Time Hour	DMAE mmol/kg	PZ mmol/kg	MAE mmol/kg	1-MPZ mmol/kg	1,4-DMPZ mmol/kg	H^+ mmol/kg
0.0	1642	1671	0	0	0	697
168.3	1597	1627	41	46	0	697
337.3	1548	1583	76	80	0	697
505.1	1487	1522	121	122	5	697
839.5	1411	1442	186	189	9	697
1175.9	1350	1382	237	244	12	697
1847.8	1213	1257	341	355	26	697

Table B.3.2: 2.5 m PZ / 2.5 m DMAE, 0.14 mol H^+/mol alkalinity, 150 °C

Time Hour	DMAE mmol/kg	PZ mmol/kg	MAE mmol/kg	1-MPZ mmol/kg	1,4-DMPZ mmol/kg	H^+ mmol/kg
0.0	1670	1682	0	0	0	699
144.8	1545	1551	127	103	3	699
288.3	1450	1453	227	197	7	699
432.8	1390	1395	291	261	12	699
577.5	1347	1348	337	309	16	699
719.3	1269	1267	398	372	23	699
864.8	1233	1229	443	419	29	699

Table B.3.3: 2.5 m PZ / 2.5 m DMAE, 0.14 mol H^+/mol alkalinity, 165 °C

Time Hour	DMAE mmol/kg	PZ mmol/kg	MAE mmol/kg	1-MPZ mmol/kg	1,4-DMPZ mmol/kg	H^+ mmol/kg
0.0	1657	1672	0	0	0	697
24.2	1556	1568	108	88	2	697
48.3	1490	1498	194	166	6	697
72.5	1423	1422	265	232	10	697
96.8	1345	1352	335	304	16	697
121.0	1294	1298	394	364	22	697
144.1	1246	1247	437	411	28	697

Table B.3.4: 2.5 m PZ / 2.5 m DMAP, 0.14 mol H$^+$/mol alkalinity, 135 °C

Time	DMAP	PZ	MAP	1-MPZ	1,4-DMPZ	H$^+$
Hour	mmol/kg	mmol/kg	mmol/kg	mmol/kg	mmol/kg	mmol/kg
0.0	1635	1642	0	0	0	681
168.3	1590	1570	33	42	0	681
337.3	1565	1548	60	65	0	681
505.1	1520	1503	82	85	0	681
839.5	1482	1465	133	133	0	681
1175.9	1439	1425	163	161	5	681
1847.8	1374	1362	234	233	10	681

Table B.3.5: 2.5 m PZ / 2.5 m DMAP, 0.14 mol H$^+$/mol alkalinity, 150 °C

Time	DMAP	PZ	MAP	1-MPZ	1,4-DMPZ	H$^+$
Hour	mmol/kg	mmol/kg	mmol/kg	mmol/kg	mmol/kg	mmol/kg
0.0	1660	1647	0	0	0	681
144.0	1542	1508	110	107	3	681
288.3	1429	1391	196	191	7	681
433.3	1358	1323	276	276	13	681
576.9	1294	1262	323	329	18	681
719.9	1254	1230	362	374	23	681
865.1	1223	1197	388	403	27	681

Table B.3.6: 2.5 m PZ / 2.5 m DMAP, 0.14 mol H$^+$/mol alkalinity, 165 °C

Time	DMAP	PZ	MAP	1-MPZ	1,4-DMPZ	H$^+$
Hour	mmol/kg	mmol/kg	mmol/kg	mmol/kg	mmol/kg	mmol/kg
0.0	1654	1656	0	0	0	681
24.2	1547	1528	73	75	2	681
48.3	1489	1471	127	122	2	681
72.5	1444	1425	182	174	6	681
96.8	1376	1358	244	236	10	681
121.0	1337	1320	300	289	15	681
144.1	1299	1280	318	312	17	681

Table B.3.7: 2.5 m PZ / 2.5 m DEAE, 0.14 mol H$^+$/mol alkalinity, 135 °C

Time	DMAP	PZ
Hour	mmol/kg	mmol/kg
0.0	1603	1594
168.3	1583	1585
337.3	1569	1574
505.1	1574	1566
839.5	1562	1557
1175.9	1551	1557
1847.8	1541	1542

Table B.3.8: 2.5 m PZ / 2.5 m DEAE, 0.14 mol H$^+$/mol alkalinity, 150 °C

Time	DEAE	PZ	EAE	1-EPZ
Hour	mmol/kg	mmol/kg	mmol/kg	mmol/kg
0.0	1577	1579	0	0
144.3	1604	1551	18	16
288.2	1575	1562	29	26
432.4	1585	1537	41	38
576.4	1552	1516	49	46
721.7	1440	1410	52	50
865.6	1496	1488	65	62

Table B.3.9: 2.5 m PZ / 2.5 m DEAE, 0.14 mol H$^+$/mol alkalinity, 165 °C

Time	DEAE	PZ
Hour	mmol/kg	mmol/kg
0.0	1616	1642
24.2	1514	1555
48.3	1501	1539
72.5	1506	1542
96.8	1489	1520
121.0	1476	1513
144.1	1482	1522

Table B.3.10: 2.5 m PZ / 2.5 m TEA, 0.14 mol H⁺/mol alkalinity, 135 °C

Time	TEA	PZ
Hour	mmol/kg	mmol/kg
0.0	1585	1520
168.3	1555	1504
337.3	1564	1505
505.1	1560	1496
839.5	1550	1490
1175.9	1554	1490
1847.8	1549	1478

Table B.3.11: 2.5 m PZ / 2.5 m TEA, 0.14 mol H⁺/mol alkalinity, 150 °C

Time	TEA	PZ	DEA
Hour	mmol/kg	mmol/kg	mmol/kg
0.0	1608	1516	11
144.3	1595	1495	15
288.2	1582	1487	17
432.4	1534	1443	18
576.4	1550	1457	22
721.7	1533	1443	25
865.6	1523	1420	28

Table B.3.12: 2.5 m PZ / 2.5 m TEA, 0.14 mol H⁺/mol alkalinity, 165 °C

Time	TEA	PZ
Hour	mmol/kg	mmol/kg
0.0	1611	1542
24.2	1597	1522
48.3	1566	1489
72.5	1584	1491
96.8	1552	1472
121.0	1561	1481
144.1	1529	1448

Table B.3.13: 2.5 m PZ / 2.5 m EDEA, 0.14 mol H$^+$/mol alkalinity, 150 °C

Time	EDEA	PZ	EAE	1-HePZ	DEA	1-EPZ
Hour	mmol/kg	mmol/kg	mmol/kg	mmol/kg	mmol/kg	mmol/kg
0.0	1590	1554	11	0	10	0
144.3	1546	1508	18	2	20	8
288.2	1552	1505	20	4	26	16
432.4	1534	1483	22	5	32	23
576.4	1513	1467	24	6	36	29
721.7	1487	1434	26	8	45	34
865.6	1460	1410	28	9	47	41

Table B.3.14: 2.5 m PZ / 2.5 m DMAIP, 0.14 mol H$^+$/mol alkalinity, 150 °C

Time	DMAIP	PZ
Hour	mmol/kg	mmol/kg
0.0	1640	1649
144.0	1510	1515
288.3	1428	1432
433.3	1323	1324
576.9	1253	1260
719.9	1193	1197
865.1	1128	1129

Table B.3.15: 2.5 m PZ / 2.5 m DMAEE, 0.14 mol H$^+$/mol alkalinity, 150 °C

Time	DMAEE	PZ
Hour	mmol/kg	mmol/kg
0.0	1552	1548
144.3	1413	1405
288.2	1314	1308
432.4	1221	1216
576.4	1132	1128
721.7	1067	1067
865.6	961	963

Table B.3.16: 2.5 m PZ / 2.5 m nBuDEA, 0.14 mol H$^+$/mol alkalinity, 150 °C

Time	nBuDEA	PZ
Hour	mmol/kg	mmol/kg
0.0	1474	1479
144.3	1462	1468
288.2	1449	1454
432.4	1427	1431
576.4	1442	1443
721.7	1425	1428
865.6	1404	1406

Table B.3.17: 2.5 m PZ / 2.5 m TIPA, 0.14 mol H$^+$/mol alkalinity, 150 °C

Time	TIPA	PZ
Hour	mmol/kg	mmol/kg
0.0	1444	1402
144.3	1446	1399
288.2	1409	1366
432.4	1400	1351
576.4	1396	1349
721.7	1406	1347
865.6	1295	1311

Table B.3.18: 2.5 m PZ / 2.5 m DMAB, 0.14 mol H$^+$/mol alkalinity, 150 °C

Time	DMAB	PZ
Hour	mmol/kg	mmol/kg
0.0	1887	1593
144.3	1638	1364
288.2	1426	1180
432.4	1236	1005
576.4	1086	870
721.7	1018	810
865.6	978	778

Table B.3.19: 2.5 m PZ / 2.5 m HEM, 0.14 mol H$^+$/mol alkalinity, 150 °C

Time	HEM	PZ
Hour	mmol/kg	mmol/kg
0.0	1667	1605
144.8	1634	1560
289.0	1657	1567
432.0	1655	1569
575.3	1610	1574
720.9	1668	1576
889.2	1643	1572

Table B.3.20: 2.5 m PZ / 2.5 m HIPM, 0.14 mol H$^+$/mol alkalinity, 150 °C

Time	HIPM	PZ
Hour	mmol/kg	mmol/kg
0.0	1673	1610
144.8	1633	1587
289.0	1636	1575
432.0	1635	1566
575.3	1648	1581
720.9	1635	1571
889.2	1615	1553

Table B.3.21: 2.5 m PZ / 2.5 m HPM, 0.14 mol H$^+$/mol alkalinity, 150 °C

Time	HPM	PZ
Hour	mmol/kg	mmol/kg
0.0	1592	1550
144.8	1569	1522
289.0	1571	1526
575.3	1617	1532
720.9	1588	1545
889.2	1576	1531

Full view, showing parent amines and major byproducts

Zoomed-in view, showing all products present
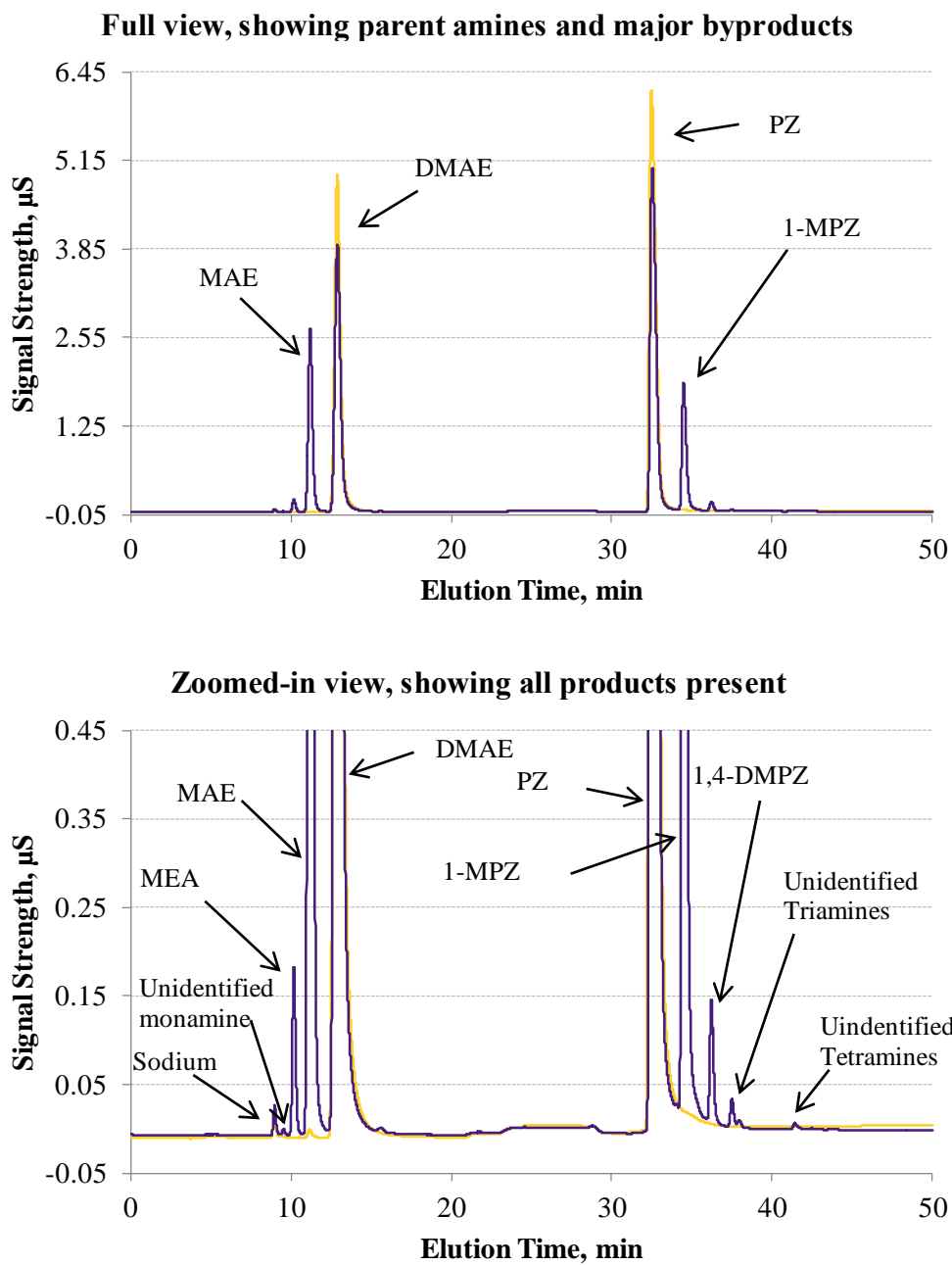
Figure B.3.1: Cation Chromatogram of undegraded (gold) and degraded (purple) 2.5 m PZ / 2.5 m DMAE at 0.14 mol H+/mol alkalinity, 150 °C, and after 865 hours using the CG17/CS17 column set and "Argonaut" program

237

Full view, showing parent amines and major byproducts

Zoomed-in view, showing all products present
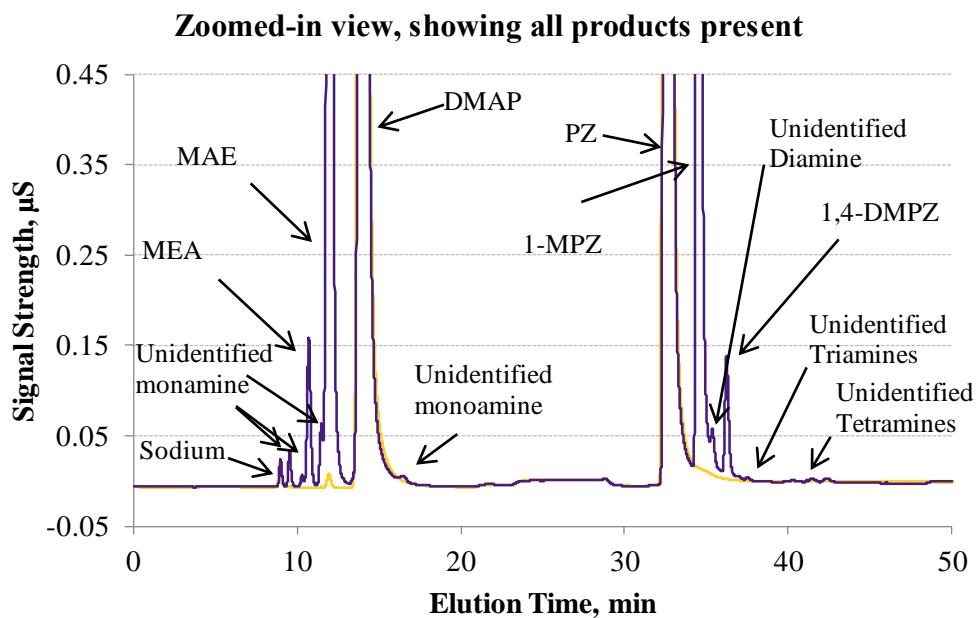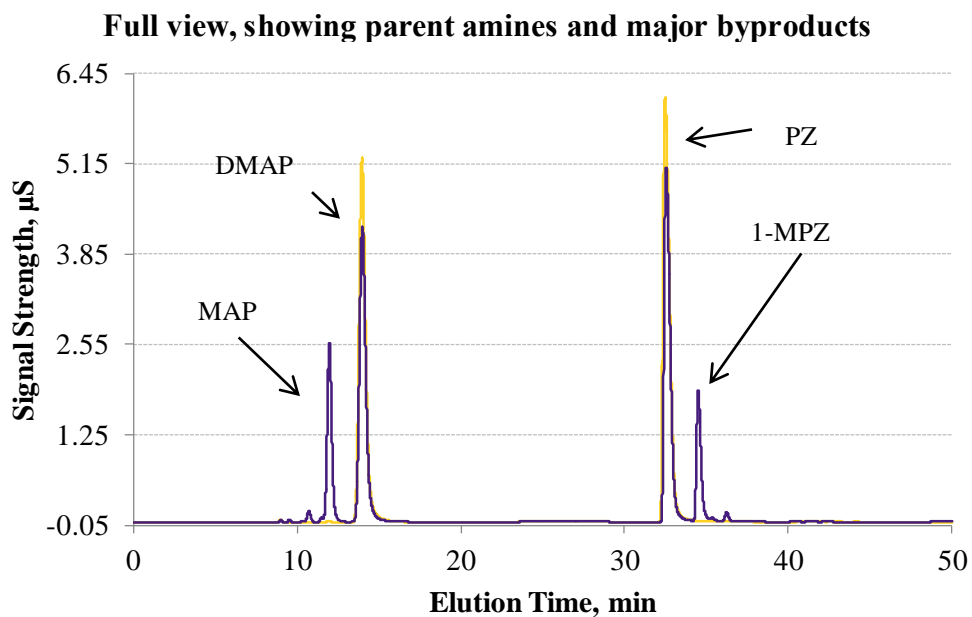
Figure B.3.2: Cation Chromatogram of undegraded (gold) and degraded (purple) 2.5 m PZ / 2.5 m DMAP at 0.14 mol H+/mol alkalinity, 150 °C, and after 865 hours using the CG17/CS17 column set and "Argonaut" program

238
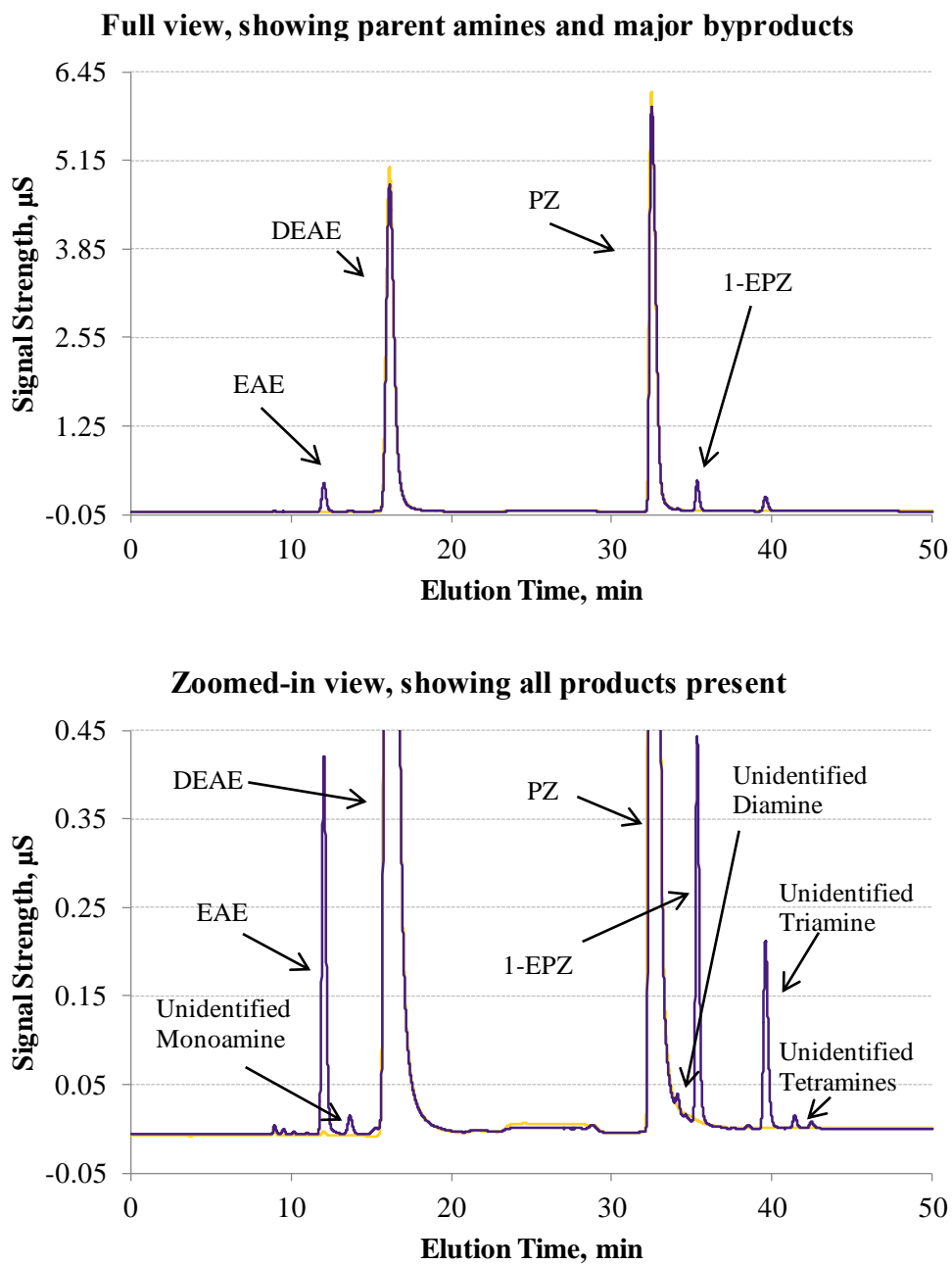
Figure B.3.3: Cation Chromatogram of undegraded (gold) and degraded (purple) 2.5 m PZ / 2.5 m DEAE at 0.14 mol H+/mol alkalinity, 150 °C, and after 865 hours using the CG17/CS17 column set and "Argonaut" program
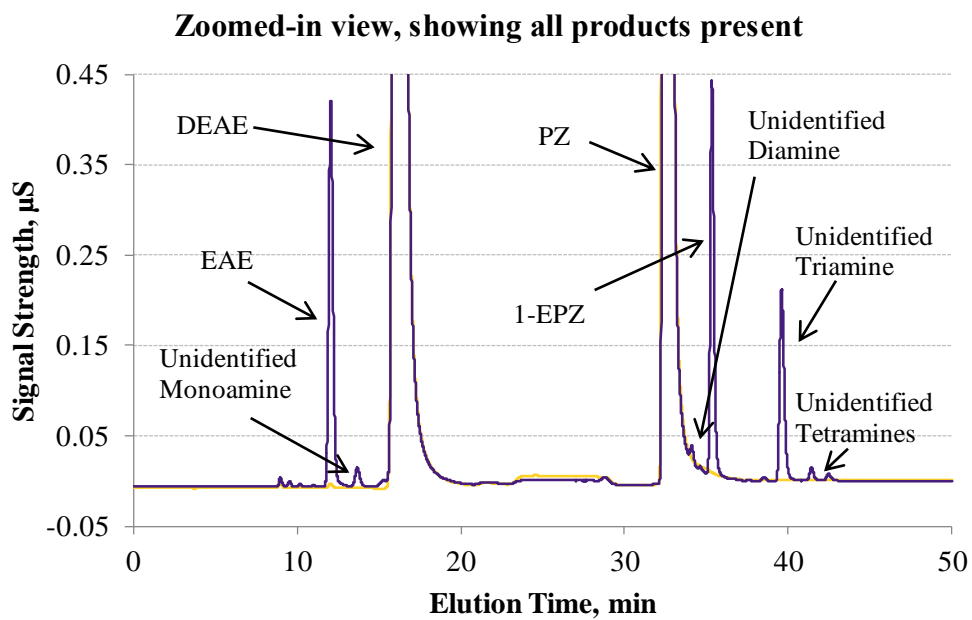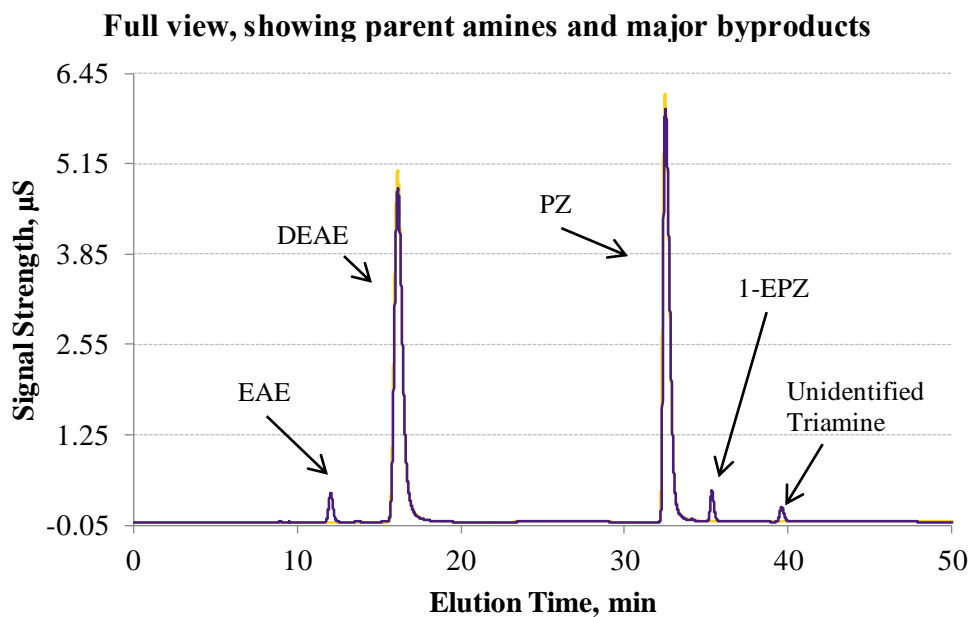
Figure B.3.3: Cation Chromatogram of undegraded (gold) and degraded (purple) 2.5 m PZ / 2.5 m DEAE at 0.14 mol H+/mol alkalinity, 150 °C, and after 866 hours using the CG17/CS17 column set and "Argonaut" program
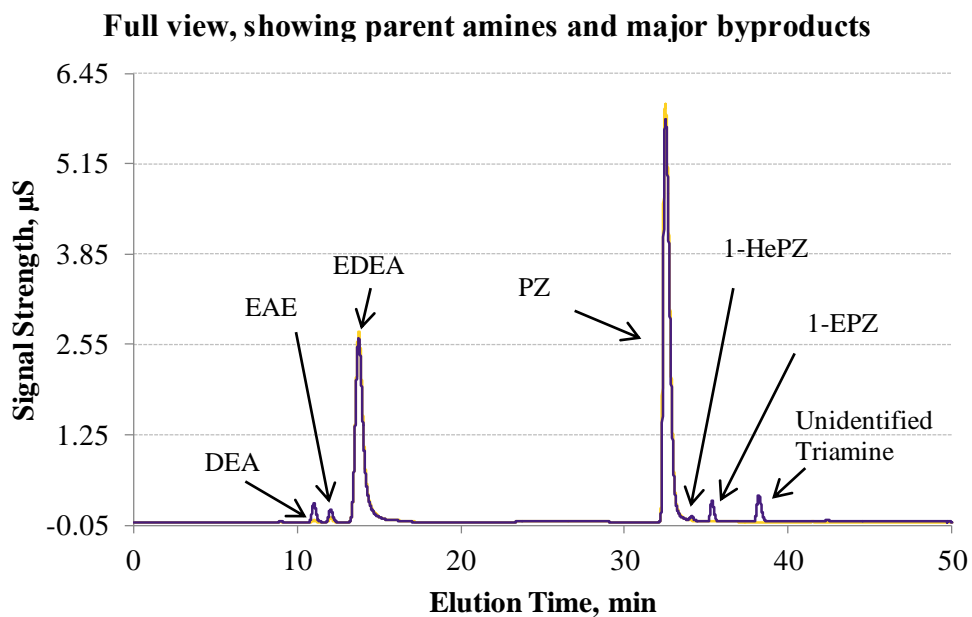
Figure B.3.4: Cation Chromatogram of undegraded (gold) and degraded (purple) 2.5 m PZ / 2.5 m EDEA at 0.14 mol H+/mol alkalinity, 150 °C, and after 866 hours using the CG17/CS17 column set and "Argonaut" program
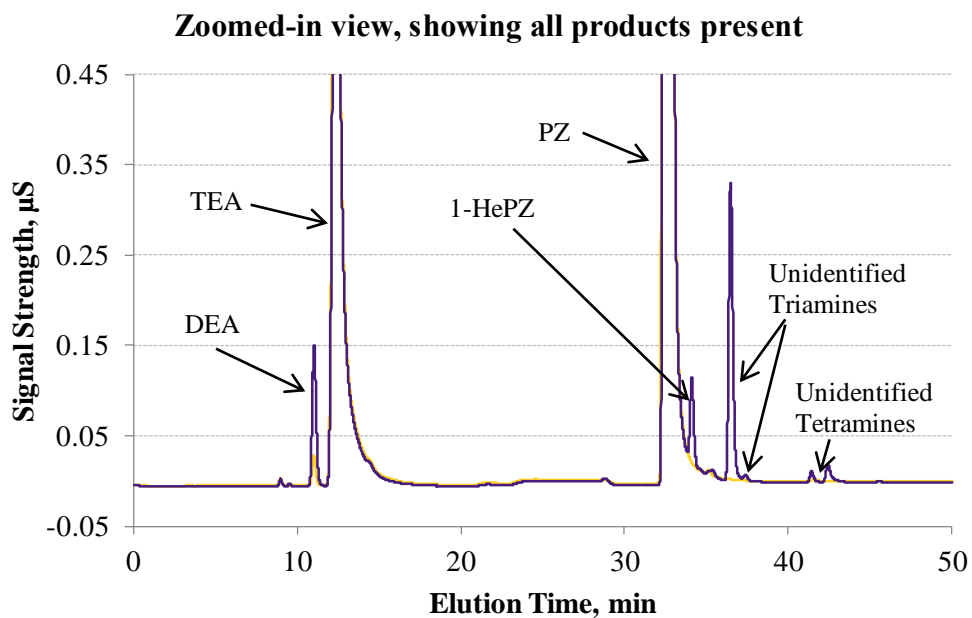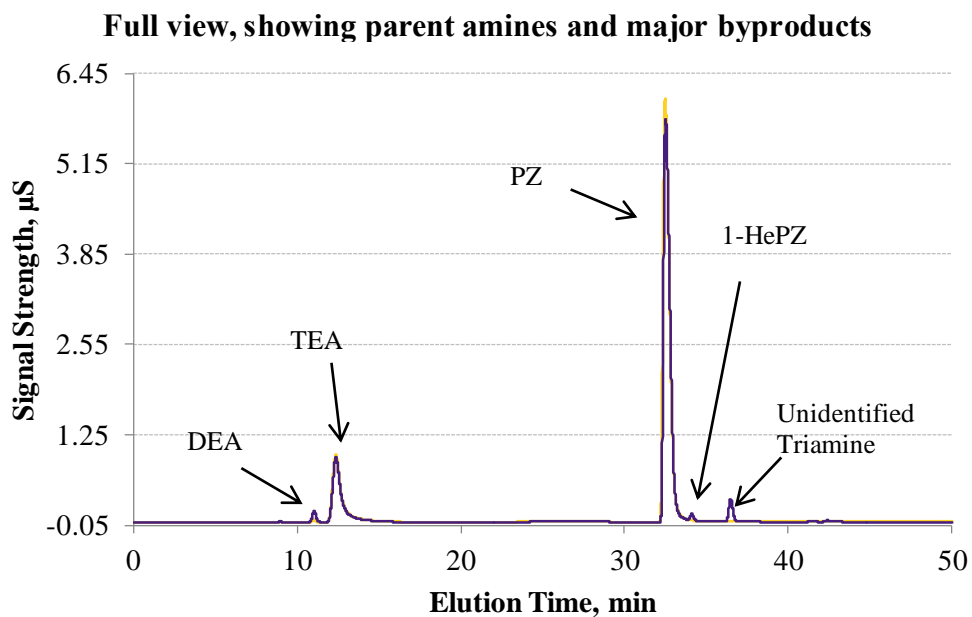
Figure B.3.5: Cation Chromatogram of undegraded (gold) and degraded (purple) 2.5 m PZ / 2.5 m TEA at 0.14 mol H+/mol alkalinity, 150 °C, and after 866 hours using the CG17/CS17 column set and "Argonaut" program
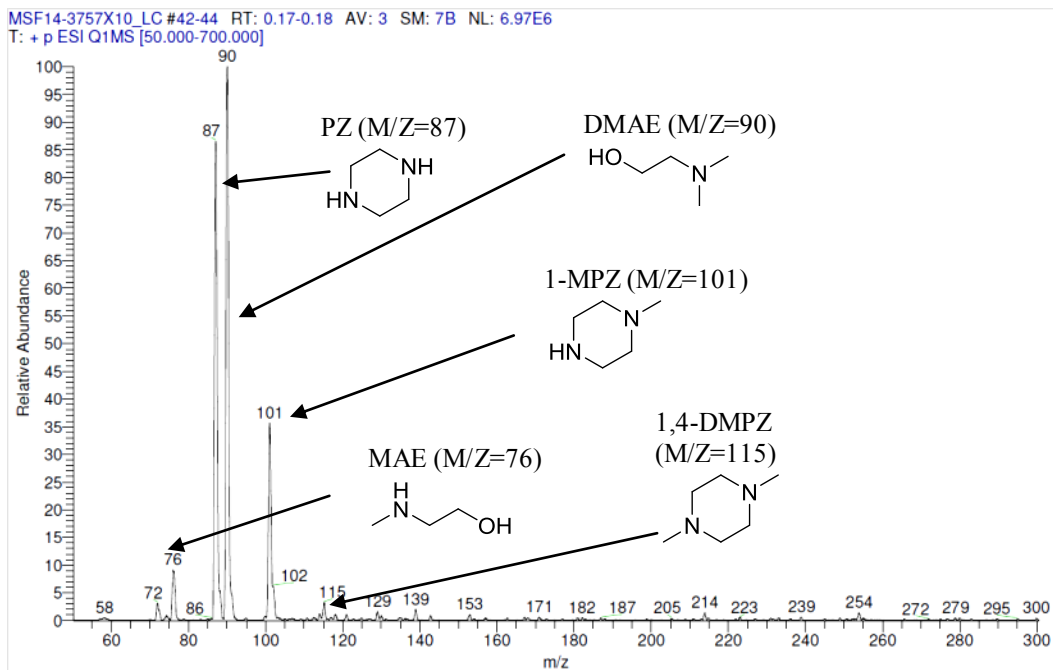
Figure B.3.6: Low Resolution Mass Spectra of 2.5 m PZ / 2.5 m DMAE and 0.14 mol H⁺/mol alkalinity degraded at 150 °C after 865 hours
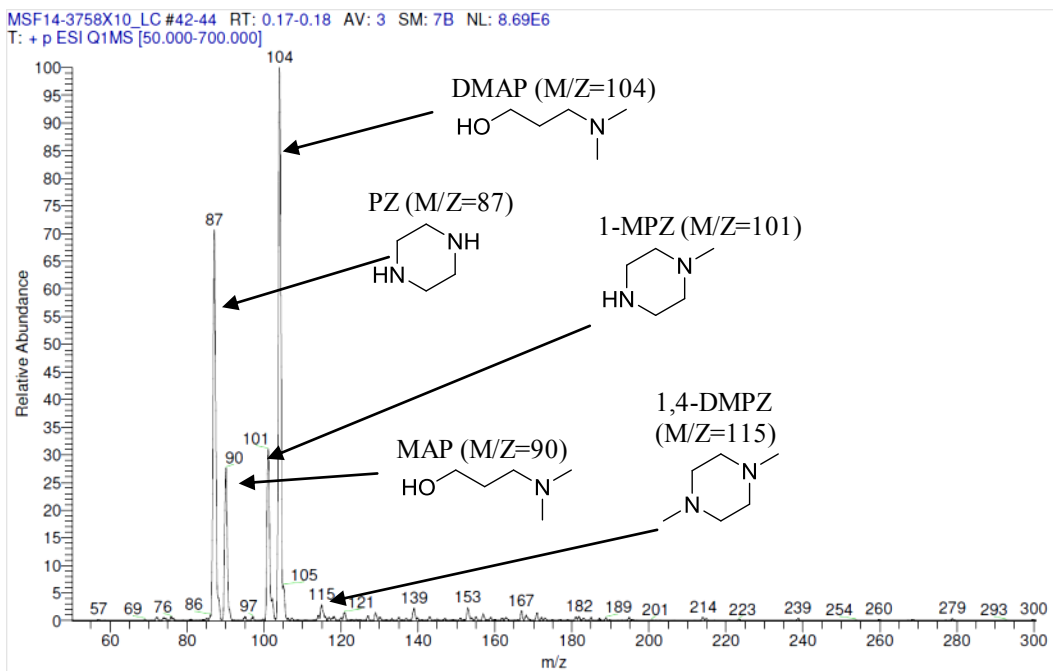
Figure B.3.7: Low Resolution Mass Spectra of 2.5 m PZ / 2.5 m DMAP and 0.14 mol H⁺/mol alkalinity degraded at 150 °C after 865 hours

243
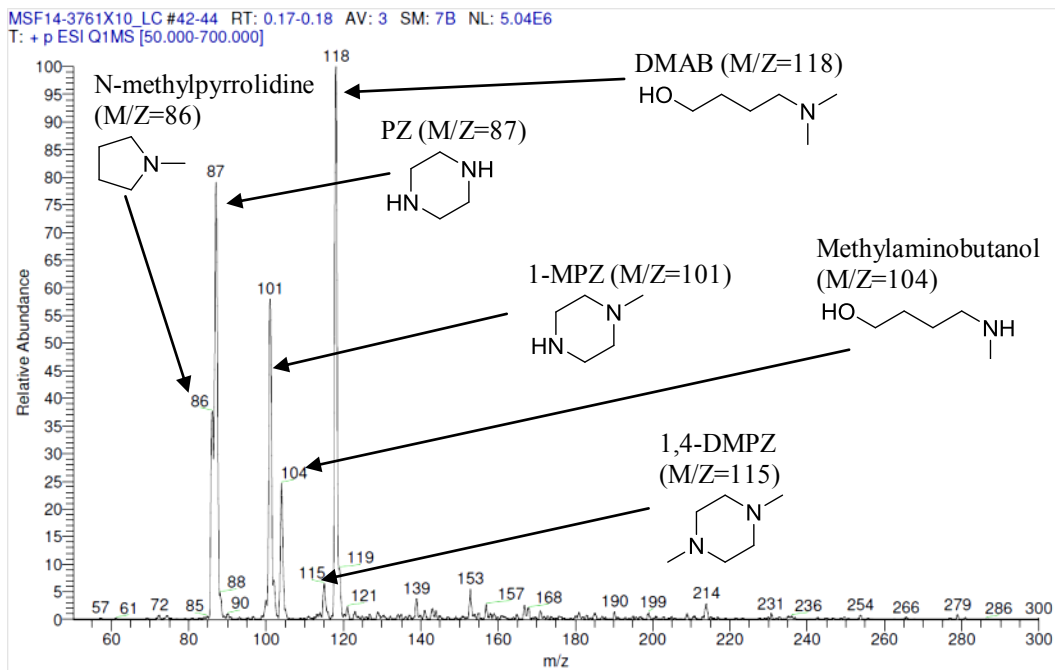
Figure B.3.8: Low Resolution Mass Spectra of 2.5 m PZ / 2.5 m DMAB and 0.14 mol H$^+$/mol alkalinity degraded at 150 °C after 866 hours

B.4 RAW DATA FOR EXPERIMENTS PRESENTED IN CHAPTER 7

Table B.4.1: 5 m MDEA / 5 m PZ, 0.24 mol CO_2/mol alkalinity, 150 °C (Alkalinity)

Time	Alkalinity
Hour	mmol/kg
0.0	6867
47.8	6826
95.3	6686
335.2	6070
527.2	5585
719.3	5281

Table B.4.2: 5 m DEAE / 5 m PZ, 0.23 mol CO_2/mol alkalinity, 150 °C (Alkalinity)

Time	Alkalinity
Hour	mmol/kg
0.0	6908
48.7	6901
96.2	6759
334.2	6457
499.7	6265
718.2	5869

Table B.4.3: 5 m DMAP / 5 m PZ, 0.23 mol CO_2/mol alkalinity, 150 °C (Alkalinity)

Time	Alkalinity
Hour	mmol/kg
0.0	7174
47.8	7221
95.3	7194
335.2	7044
527.2	6957
719.3	6774

Table B.4.4: 5 m DMAEE / 5 m PZ, 0.23 mol CO_2/mol alkalinity, 150 °C (Alkalinity)

Time	Alkalinity
Hour	mmol/kg
0.0	6641
336.8	6577
625	6495

Table B.4.5: 20 wt% PZ / 27 wt% MDEA, 0.22 mol CO₂/mol alkalinity, 150 °C

Time	MDEA	PZ
Hour	mmol/kg	mmol/kg
0.0	2327	2349
71.6	2051	1902
166.9	1766	1324
311.7	1496	834
450.5	1334	593
450.5	1361	638
450.5	1362	638
600.9	1158	398
743.1	985	257
886.7	876	180

Table B.4.6: 20 wt% PZ / 27 wt% MDEA and 18 wt% PEGDME, 0.22 mol CO₂/mol alkalinity, 150 °C

Time	MDEA	PZ
Hour	mmol/kg	mmol/kg
0.0	2345	2338
71.6	2144	2052
166.9	1991	1694
311.7	1764	1223
450.5	1563	877
450.5	1576	890
450.5	1594	913
600.9	1396	630
743.1	1253	462
886.7	1124	326

Table B.4.7: 20 wt% PZ / 27 wt% MDEA and 18 wt% PCAR, 0.22 mol CO₂/mol alkalinity, 150 °C

Time	MDEA	PZ
Hour	mmol/kg	mmol/kg
0.0	2355	2284
71.6	2021	1723
166.9	1720	1086
311.7	1350	552
450.5	1100	275

246

Table B.4.8: 20 wt% PZ / 27 wt% MDEA and 18 wt% NMP, 0.22 mol CO$_2$/mol alkalinity, 150 °C

Time	MDEA	PZ
Hour	mmol/kg	mmol/kg
0.0	2322	2347
71.6	2149	2099
166.9	2014	1794
311.7	1670	1059
450.5	1655	1064
450.5	1634	1046
450.5	1767	1306
600.9	1457	728
743.1	1341	557
886.7	1185	396

Table B.4.9: 5 m DMAE, 0.20 mol H$^+$/mol alkalinity, 150 °C

Time	DMAE
Hour	mmol/kg
0.0	3311
96.8	3024
144.0	2983
216.0	2927
359.5	2918
503.5	2903
648.6	2906

Table B.4.10: 5 m MDEA, 0.20 mol H$^+$/mol alkalinity, 150 °C

Time	MDEA
Hour	mmol/kg
0.0	3127
71.3	2997
143.3	2917
216.7	2841
360.9	2755
502.5	2724
646.9	2694

Table B.4.11: 5 m DMAEE, 0.20 mol H$^+$/mol alkalinity, 150 °C

Time	DMAEE
Hour	mmol/kg
0.0	2746
96.8	2538
144.0	2477
216.0	2440
359.5	2434
503.5	2408
648.6	2397

Table B.4.12: 5 m DMAP, 0.20 mol H$^+$/mol alkalinity, 150 °C

Time	DMAP
Hour	mmol/kg
0.0	3214
71.3	2989
143.3	2889
216.7	2806
360.9	2718
502.5	2635
646.9	2603

Table B.4.13: 5 m TEA, 0.20 mol H$^+$/mol alkalinity, 150 °C

Time	TEA
Hour	mmol/kg
0.0	2832
96.8	2718
144.0	2703
216.0	2477
359.5	2623
503.5	2535
648.6	2473

Table B.4.14: 5 m nBuDEA, 0.20 mol H⁺/mol alkalinity, 150 °C

Time	nBuDEA
Hour	mmol/kg
0.0	2743
73.5	2669
143.5	2668
218.2	2651
361.3	2603
505.6	2590
648.2	2566

Table B.4.15: 5 m EDEA, 0.20 mol H⁺/mol alkalinity, 150 °C

Time	EDEA
Hour	mmol/kg
0.0	2961
73.5	2919
143.5	2892
218.2	2879
361.3	2843
505.6	2800
648.2	2772

Table B.4.16: 5 m TIPA, 0.20 mol H⁺/mol alkalinity, 150 °C

Time	TIPA
Hour	mmol/kg
0.0	2425
72.0	2425
143.4	2388
215.5	2384
359.5	2360
504.6	2374
647.0	2294

Table B.4.17: 5 m DEAE, 0.20 mol H⁺/mol alkalinity, 150 °C

Time	DEAE
Hour	mmol/kg
0.0	3076
71.3	3060
143.3	3068
216.7	3010
360.9	2988
502.5	3012
646.9	2975

Table B.4.18: 5 m HEM, 0.20 mol H⁺/mol alkalinity, 150 °C

Time	HEM
Hour	mmol/kg
0.0	3161
69.6	3078
143.7	3107
214.3	3076
359.3	3182
501.8	3120
647.2	3171

Table B.4.19: 5 m HIPM, 0.20 mol H⁺/mol alkalinity, 150 °C

Time	HIPM
Hour	mmol/kg
0.0	2862
69.6	2954
143.7	2859
214.3	2960
359.3	2942
501.8	2914
647.2	2922

Full view, showing parent amines and major byproducts

Zoomed-in view, showing all products present
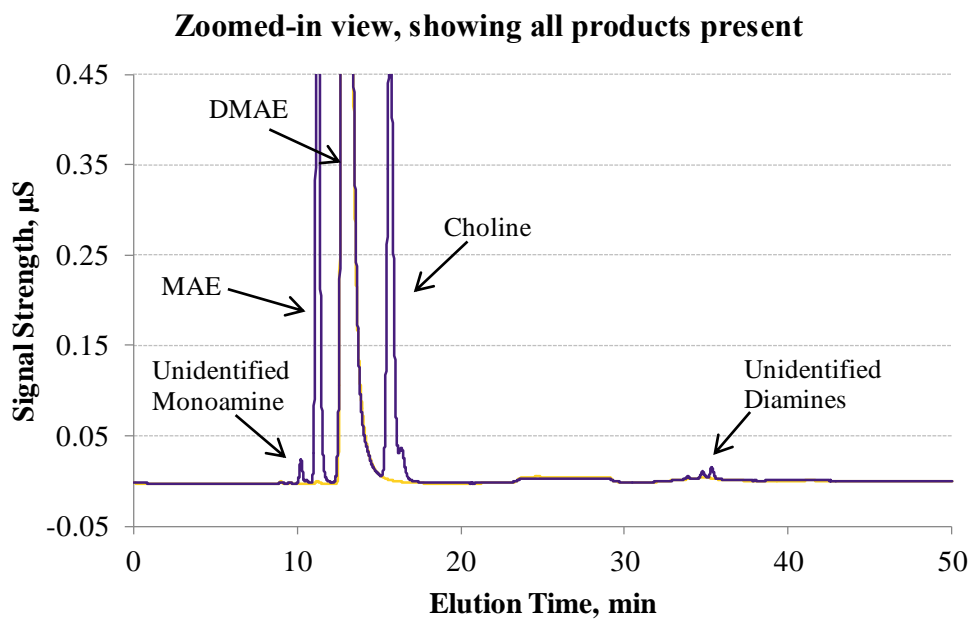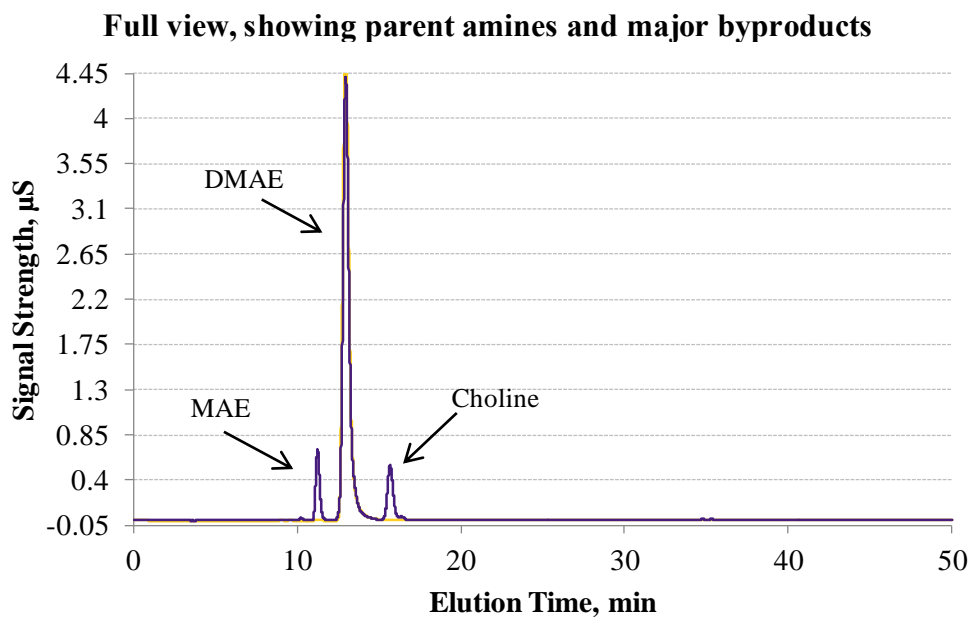
Figure B.4.1: Cation Chromatogram of undegraded (gold) and degraded (purple) 5 m DMAE at 0.20 mol H+/mol alkalinity, 150 °C, and after 649 hours using the CG17/CS17 column set and "Argonaut" program
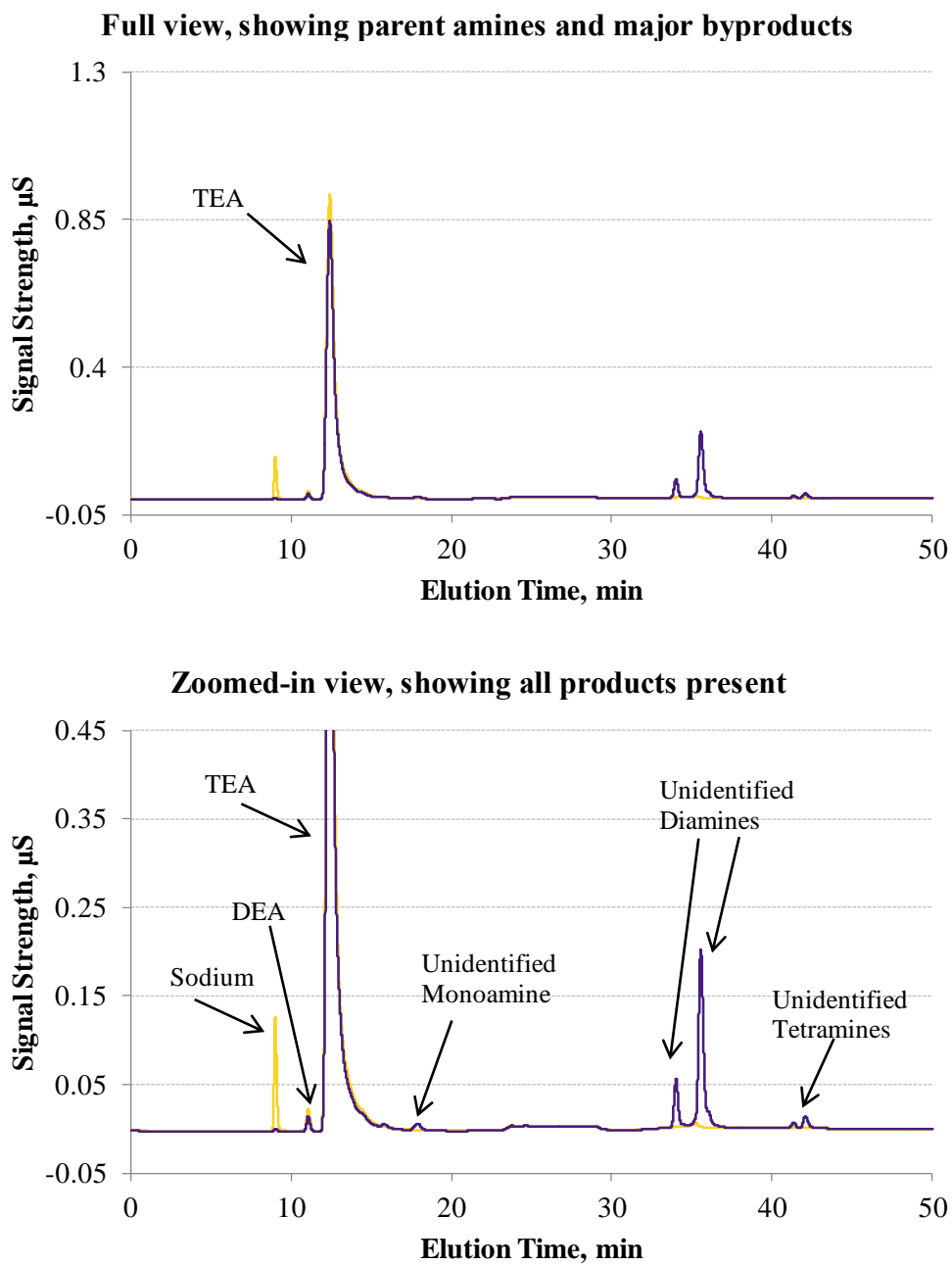
Figure B.4.1: Cation Chromatogram of undegraded (gold) and degraded (purple) 5 m TEA at 0.20 mol H+/mol alkalinity, 150 °C, and after 647 hours using the CG17/CS17 column set and "Argonaut" program

252

B.5 RAW DATA FOR EXPERIMENTS PRESENTED IN CHAPTER 8

Table B.5.1: 5 m MDEA / 5 m PZ, 0.24 mol CO_2/mol alkalinity, 150 °C (Hydrolyzed samples for formate analysis)

Time Hour	Formate mmol/kg
47.8	6.2
95.3	13.0
95.3	13.1
191.3	24.3
335.2	28.9
335.2	30.4
527.2	49.7
719.3	78.7
719.3	80.2

Table B.5.2: 7 m TA / 2 m PZ, 0.25-0.28 mol CO_2/mol alkalinity, 150 °C (Hydrolyzed samples for formate analysis after approximately 260 hours)

Amine	CO_2 Loading mol CO_2/mol alk	Formate mmol/kg
DEAE	0.28	123
TEA	0.26	70
MDEA	0.26	43
DMAE	0.26	38
DMAP	0.25	25

Table B.5.3: 7 m TA / 2 m PZ, 0.25-0.28 mol CO_2/mol alkalinity, 165 °C (Hydrolyzed samples for formate analysis after approximately 70 hours)

Amine	CO_2 Loading mol CO_2/mol alk	Formate mmol/kg
DEAE	0.28	131
TEA	0.26	85
MDEA	0.26	78
DMAE	0.26	76
DMAP	0.25	56

Appendix C – Summary of Maximum Stripping Temperature (T_{MAX}) Results for a Range of Amine Solvents

The maximum stripping temperature (T_{MAX}) analysis for a range of solvents for CO_2 capture is presented in this section. Data are grouped by amine structure and solvent category. The T_{MAX} values have been calculated using the procedure outlined in Chapter 4 and in Freeman (2011). Many of these results are summarized from other sources and referenced where appropriate.

T_{MAX} is defined as the temperature at which the first-order degradation rate constant of the parent amine is equal to $2.91*10^{-8}$ s^{-1}, which corresponds to an amine loss of 2% / week. The sum of the concentration of the parent amines, such has the PZ-promoted solvents, is used to determine the T_{MAX} of blended solvent systems. The activation energy of thermal degradation are calculated if enough experimental data are available or, if not calculated, estimated based on the similarity of the amine structure and measured degradation rate to other amines whose activation energy data are available.

Results from single-point experiments, such as those from Lepaumier (2009) and Eide-Hagumo (2011), are not tabulated as initial rate measurements cannot be reliably extracted from single-point experiments. As examples, MDEA was found to approach equilibrium with its quaternary salt and secondary amine byproduct in this work, diisopropanolamine was found by Kim (1988) to form an equilibrium with its corresponding oxazolidone degradation product, and ethylenediamine was found by Hatchell (2014) to form an equilibrium with its corresponding cyclic urea.

Table C.1: T_{MAX} of Piperazine (PZ) and its derivatives

Amine Name (Abbreviation)	Structure	Concentration (molality) Loading (mol CO_2/mol alk)	T_{MAX} (°C)	Source(s)
Piperidine (PD)		8 m 0.3	170	1
Morpholine (Mor)		8 m 0.3	166	1
Piperazine (PZ)		8 m 0.3	163	1
2-Methylpiperazine (2-MPZ)		8 m 0.3	151	1
1-Methylpiperazine (1-MPZ)		8 m 0.3	148	1
Pyrrolidine (Pyr)		8 m 0.3	142	1
Homopiperazine (HomoPZ)		8 m 0.3	140	1
Hexamethylene-imine (HMI)		8 m 0.3	131	1
1-Hydroxyethyl-piperazine(1-HePZ)		7 m 0.4	130	1, 2
2-Piperidine-ethanol (2-PE)		8 m 0.4	127	1, 3
Aminoethyl-piperazine (AEP)		2.33 m 0.4	121	1, 2
2-Piperidine-methanol (2-PM)		7 m 0.4	109	1, 2
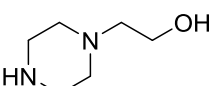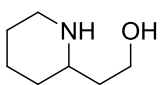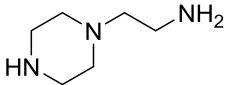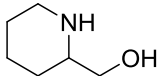
Table C.2: T_{MAX} of PZ-promoted hindered amine or tertiary amine solvents whose hindered amine or tertiary amine is a PZ derivative

Amine Name (Abbreviation)	Structure of PZ derivative in blended solvent	Concentration (molality) Loading (mol CO_2/mol alk)	T_{MAX} (°C)	Source(s)
PZ / Hydroxypropyl-morpholine (HPM)		5 m PZ / 5 m HPM 0.22	161	This work
PZ / Hydroxyisopropyl-morpholine (HIPM)		5 m PZ / 5 m HIPM 0.22	157	This work
PZ / 1-MPZ		4 m PZ / 4 m 1-MPZ 0.3	156	1
PZ / Hydroxyethyl-morpholine (HEM)		5 m PZ / 5 m HEM 0.22	156	This work
PZ / 2-MPZ		4 m PZ / 4 m 2-MPZ 0.3	155	1
PZ / Triethylene-diamine (TEDA)		2.5 m PZ / 2.5 m TEDA 0.2	135	4
PZ / 2-PE		1.33 m PZ / 2.67 m 2-PE 0.23	127	5
PZ / 2-PM		1.33 m PZ / 2.67 m 2-PM 0.23	97	5
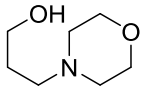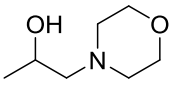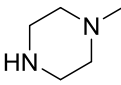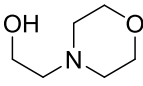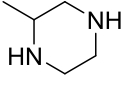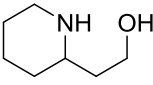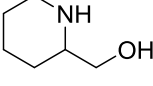
Table C.3: T_{MAX} of PZ-promoted aliphatic tertiary amine solvents

Amine Name (Abbreviation)	Structure of Tertiary Amine in Blend	Concentration (molality) Loading (mol CO$_2$/mol alk)	T_{MAX} (°C)	Source(s)
PZ / Triisopropanol-amine (TIPA)		5 m PZ / 5 m TIPA 0.22	140	This work
PZ / diethylamino-ethanol (DEAE)		2 m PZ / 7 m DEAE 0.12	137	This work
PZ / Triethanolamine (TEA)		5 m PZ / 5 m TEA 0.22	134	This work
PZ / DEAE		5 m PZ / 5 m DEAE 0.23	134	This work
PZ / n-Butyldiethanol-amine (nBuDEA)		5 m PZ / 5 m nBuDEA 0.22	133	This work
PZ / Ethyldiethanol-amine (EDEA)		5 m PZ / 5 m EDEA 0.23	132	This work
PZ / TEA		2 m PZ / 7 m TEA 0.13	131	This work
PZ / dimethylamino-propanol (DMAP)		2 m PZ / 7 m DMAP 0.14	128	This work
PZ / Dimethylaminoiso-propanol (DMAIP)		5 m PZ / 5 m DMAIP 0.22	127	This work
PZ / DMAP		5 m PZ / 5 m DMAP 0.23	127	This work
PZ / Methyldiethanol-amine (MDEA)		2 m PZ / 7 m MDEA 0.13	127	This work
PZ / Dimethylamino-ethoxyethanol (DMAEE)		5 m PZ /5 m DMAEE 0.23	124	This work
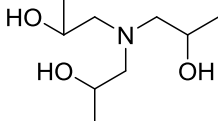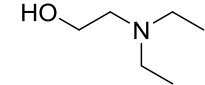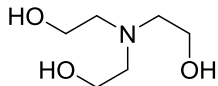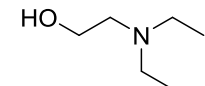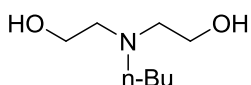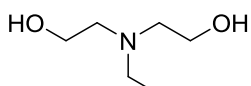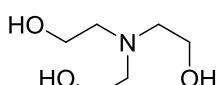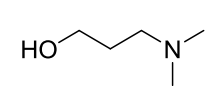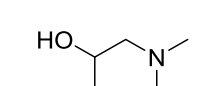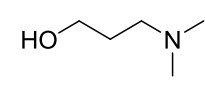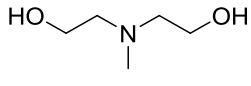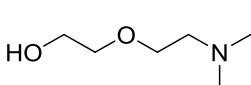
Table C.3: T$_{MAX}$ of PZ-promoted aliphatic tertiary amine solvents (continued)

Amine Name (Abbreviation)	Structure of Tertiary Amine in Blend	Concentration (molality) Loading (mol CO$_2$/mol alk)	T$_{MAX}$ (°C)	Source(s)
PZ / MDEA		5 m PZ / 5 m MDEA 0.24	122	This work
PZ / Dimethylamino-ethanol (DMAE)		2 m PZ / 7 m DMAE 0.13	121	This work
PZ / DMAE		5 m PZ / 5 m DMAE 0.23	120	This work
PZ / Tert-butyl-diethanolamine (tBuDEA)		5 m PZ / 5 m tBuDEA 0.22	111	This work
PZ / Dimethylamino-butanol (DMAB)		5 m PZ / 5 m DMAB 0.22	108	This work

Table C.4: T$_{MAX}$ of PZ-promoted aliphatic hindered amines

Amine Name (Abbreviation)	Structure of Hindered Amine in Blend	Concentration (molality) Loading (mol CO$_2$/mol alk)	T$_{MAX}$ (°C)	Source(s)
PZ / Tert-butyl-aminoethanol (TBAE)		1.33 m PZ / 2.67 m TBAE 0.23	147	4
PZ / 2-amino-2-methyl-1-propanol (AMP)		1.33 m PZ / 2.67 m AMP 0.23	141	4
PZ / 2-Amino-2-Methyl-1,3-Propanoediol (AMPD)		1.33 m PZ / 2.67 m AMPD 0.23	131	4
PZ / Tris(hydroxymethyl)-aminomethane (Tris)		1.33 m PZ / 2.67 m TRIS 0.23	128	4

Table C.5: T_MAX of promoted methyldiethanoalmine (MDEA) amine solvents

Amine Name (Abbreviation)	Structure of Promoter Used in Blend	Concentration (molality) Loading (mol CO_2/mol alk)	T_{MAX} (°C)	Source(s)
Hexamethylene-diamine (HMDA) / MDEA	H₂N⌒⌒⌒NH₂	5 m HMDA / 5 m MDEA 0.24	135	This work
Bis(aminoethyl)-ether (BAE) / MDEA	H₂N⌒O⌒NH₂	5 m BAE / 5 m MDEA 0.23	129	This work
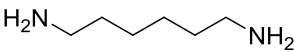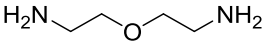
Table C.6: T_MAX of aliphatic diamine solvents

Amine Name (Abbreviation)	Structure	Concentration (molality) Loading (mol CO_2/mol alk)	T_{MAX} (°C)	Source(s)
HMDA	H₂N⌒⌒⌒NH₂	2.5 m 0.4	145	5
BAE	H₂N⌒O⌒NH₂	5 m 0.4	137	5
1,4-diaminobutane (DAB)	H₂N⌒⌒NH₂	5 m 0.4	133	5
1,3-diaminopropane (PDA)	H₂N⌒⌒NH₂	5 m 0.4	133	5
Ethylenediamine (EDA)	H₂N⌒NH₂	5 m 0.4	128	5
Methylaminopropyl-amine (MAPA)	H₂N⌒⌒N(H)⌒	9 m 0.4	114	1, 6
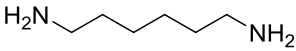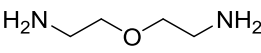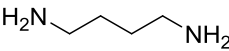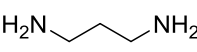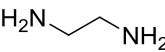
259
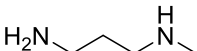
Table C.7: T_{MAX} of aliphatic alkanolamine solvents

Amine Name (Abbreviation)	Structure	Concentration (molality) Loading (mol CO_2/mol alk)	T_{MAX} (°C)	Source(s)
Pentanolamine (MPtA)	HO~~~~NH₂	7 m 0.4	145	1, 2
AMP	HO—C(CH₃)₂—NH₂	7 m 0.4	137	1, 2
Butanolamine (MBuA)	HO~~~NH₂	7 m 0.4	133	1, 2
MDEA	HO~N(CH₃)~OH	5 m 0.2 (as H⁺)	132	This work
Propanolamine (MPA)	H₂N~~OH	10 m 0.4	128	5
Diglycolamine® DGA	HO~O~NH₂	10 m 0.4	126	5
Ethanolamine (MEA)	H₂N~OH	**7 m 0.4**	**121**	**1, 2**
Hexanolamine (MHxA)	HO~~~~~NH₂	7 m 0.4	117	1, 2
Isopropanolamine (MIPA)	H₂N~CH(CH₃)OH	7 m 0.4	114	1, 2
MEA	H₂N~OH	10 m 0.4	113	5
Methylamino-ethanol (MAE)	CH₃-NH~OH	5.7 m 0.5	90	7
Diethanolamine (DEA)	HO~NH~OH	5.5 m 0.38	86	8
Diisopropanol-amine (DIPA)	HO~CH(CH₃)~NH~CH(CH₃)~OH	6.5 m 0.45	78	9

Table C.8: T_{MAX} of PZ / primary or secondary aliphatic amine solvent blends

Amine Name (Abbreviation)	Structure of other amine in PZ blend	Concentration (molality) Loading (mol CO₂/mol alk)	T_{MAX} (°C)	Source(s)
PZ / BAE	H₂N～～O～～NH₂	6 m PZ / 2 m BAE 0.35	162	10
PZ / HMDA	H₂N～～～～NH₂	6 m PZ / 2 m HMDA 0.4	161	10
PZ / DAB	H₂N～～～NH₂	6 m PZ / 2 m DAB 0.4	156	10
PZ / MEA	H₂N～OH	2 m PZ / 7 m MEA	104	1, 2
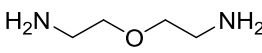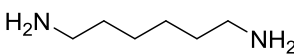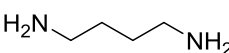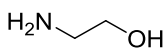
Table C.9: T_{MAX} of amino acid solvents activated with NaOH

Amine Name (Abbreviation)	Structure	Concentration (molarity) Loading (mol CO₂/mol alk)	T_{MAX} (°C)	Source(s)
Sarcosine (Sar)		2.5 M 0.4	108	11
Alanine (Ala)		2.5 M 0.4	92	11
Glycine (Gly)		2.5 M 0.4	89	11
β-Alanine (B-Ala)		2.5 M 0.4	48	11
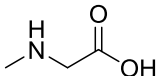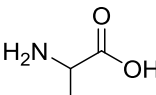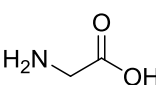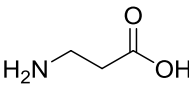
Sources:
1. Freeman (2011)
2. Davis (2009)
3. Rochelle (2010)
4. Namjoshi (2014)
5. Hatchell (2014)
6. Voice (2013b)
7. Lepaumier (2011)
8. Kim (1984)
9. Kim (1988)
10. Namjoshi (2013)
11. Hwang (2014)

References

Addinsoft (2014). XLSTAT-Pro core statistical software [Software].

Anslyn, E.V., & Dougherty, D.A. (2006). *Modern Physical Organic Chemistry.* Sausalito, CA, USA: University Science Books.

Appl, M., Wagner, U., Henrici, H.J., Kuessner, K., Volkamer, K., Fuerst, E. (1982, June 22). U.S. Patent No. 4,336,233. Washington, DC, USA: U.S. Patent and Trademark Office. Retrieved from http://worldwide.espacenet.com

Artanto, Y., Jansen, J., Pearson, P., Do, T., Cottrell, A., Meuleman, E., & Feron, P. (2012, February 22). Performance of MEA and amine-blends in the CSIRO PCC pilot plant at Loy Yang Power in Australia. *Fuel, 101.* Retrieved from http://dx.doi.org/10.1016/j.fuel.2012.02.023

Aspen Techology Inc (AspenTech) (2011, May). Aspen Plus Process Simulator 7.3. [Software].

Bahadori, A. (2014). *Natural Gas Processing: Technology and Engineering Design.* Waltham, MA, USA: Gulf Professional Publishing.

Bartholome, E., Schmidt, H.W., & Friebe, J. (1970, August 13). German. Patent No. 1,904,428. Munich, Germany: Deutsches Patentamt. Retrieved from http://worldwide.espacenet.com

Bedell, S.A., Worley, C.M., Sadek Al-Horr, R., & McCrery, D.A. (2010, July 12). Quaternaries as Intermediates in the Thermal and Oxidative Degradation of Alkanolamines. *Ind. Eng. Chem. Res., 49.* Retrieved from http://dx.doi.org/10.1021/ie100938e

Bedell, S.A., Worley, C.M., Darst, K., & Simmons, K. (2011 May). Thermal and oxidative disproportionation in amine degradation – O_2 stoichoimetry and mechanistic implications. *Int. J. Greenhouse Gas Control, 5.* Retrieved from http://dx.doi.org/10.1016/j.ijggc.2010.03.005

Billo, E.J. (2001). *Excel for Chemists: A Comprehensive Guide* (Second Edition). New York, NY, USA: John Wiley & Sons.

Bishnoi, S., & Rochelle, G.T. (2000, October 26). Absorption of carbon dioxide into aqueous piperazine: reaction kinetics, mass transfer and solubility. *Chem. Eng. Sci., 55.* Retrieved from http://dx.doi.org/10.1016/S0009-2509(00)00182-2

Bishnoi, S., & Rochelle, G.T. (2002, December). Absorption of Carbon Dioxide in Aqueous Piperazine/Methyldiethanolamine. *AICHE J., 48.* Retrieved from http://dx.doi.org/ 10.1002/aic.690481208

Böttinger, W., Maiwald, M., & Hasse, H. Online NMR Spectroscopic Study of Species Distribution in MDEA-H_2O-CO_2 and MDEA-PIP-H_2O-CO_2. *Ind. Eng. Chem. Res., 47*. Retrieved from http://dx.doi.org/ 10.1021/ie800914m

Bosch, C., & Meiser, W. (1922, September 19). U.S. Patent No. 1,429,483. Washington, DC, USA: U.S. Patent and Trademark Office. Retrieved from http://worldwide.espacenet.com

Bosen, S.F. (2010, November 20). *Causes of Amine Plant Corrosion- Design Considerations.* Retrieved from http://www.dow.com/gastreating/solution/ngp_lngt.htm

Bottoms, R. (1933, September 26). U.S. Patent No. 1,783,901, Reissue 18,958. Washington, DC, USA: U.S. Patent and Trademark Office. Retrieved from http://worldwide.espacenet.com

Brok, T.J., Groenen, R.J.M, Klinkenbijl, J.M., & Knapp, M.C. (2003, 17 July). International Patent Publication No. WO 03/057348 A1. Geneva, Switzerland: World Intellectual Property Organization. Retrieved from http://worldwide.espacenet.com

Bruckner, R. (2002). *Advanced Organic Chemistry: Reaction Mechanisms*. Burlington, MA, USA: Harcourt/Academic Press.

Burfiend, B., Multhaupt, H., Brehm, A., Hofmann, J., Mikow, U. Degradation rate and degradation kinetics of activated and non-activated aqueous N-Methyldiethanolamine (MDEA) absorption solutions. *Int. J. Sci. Eng. Res., 6*, 1204-11.

Burr, B. & Lyddon, L. (2008). *A Comparison of Physical Solvents for Acid Gas Removal.* Retrieved from http://www.bre.com

Cohen, S.M. (2012). *A Techno-Economic Plant and Grid-Level Assessment of Flexible CO_2 Capture* (Ph.D Dissertation). The University of Texas at Austin, Austin, Texas, USA. Retrieved from http://repositories.lib.utexas.edu

Chakma, A. (1987). *Studies on DEA and MDEA Degradation* (PhD Dissertation). The University of British Columbia, Canada.

Chakma, A., & Meisen, A. (1997, October). Methyl-Diethanolamine Degradation – Mechanism and Kinetics. *Can. J. Chem. Engr., 75*. Retrieved from http://dx.doi.org/10.1002/cjce.5450750506

ChemAxon. Chemicalize.org Properties Viewer [Software]. Available from http://www.chemicalize.org

Chen, E. (2014, January 30). *UT Pilot Plant Results & Plans*. Presented at the 2nd UT-Austin Carbon Capture and Sequestration Meeting, Austin, Texas, USA.

263

Chen, W-H., Chen, S-M., & Hung, C-I. (2013, May 18). Carbon dioxide capture by single droplet using Selexol, Rectisol and water as absorbents: A theoretical approach. *Appl. Energy, 111*. Retrieved from http://dx.doi.org/10.1016/j.apenergy.2013.05.051

Chen, X. (2011). *Carbon Dioxide Thermodynamics, Kinetics, and Mass Transfer in Aqueous Piperazine Derivatives and Other Amines* (Ph.D Dissertation). The University of Texas at Austin, Austin, Texas, USA. Retrieved from http://repositories.lib.utexas.edu

Closmann, F.B. (2011). *Oxidation and thermal degradation of methyldiethanolamine/piperazine in CO_2 Capture* (Ph.D Dissertation). The University of Texas at Austin, Austin, Texas, USA. Retrieved from http://repositories.lib.utexas.edu

Critchfield, J.E., Su, W-Y., Kenney, T.J., & Holub, P.E. (1999, January 19). U.S. Patent No. 5,861,051. Washington, DC, USA: U.S. Patent and Trademark Office. Retrieved from http://worldwide.espacenet.com

Cousins, A., Huang, S., Cottrell, A., Feron, P.H.M., Chen, E., & Rochelle, G.T. (2014, August 24). Pilot-scale parametric evaluation of concentrated piperazine for CO_2 capture at an Australian coal-fired power station. *Greenhouse Gas. Sci. Tech., 5*. Accessible from http://dx.doi.org/10.1002/ghg.1462

Cussler, E.L. (2009). *Diffusion: mass transfer in fluid systems* (Third Edition). New York, NY, USA: Cambridge University Press.

da Silva, E.F., Lepaumier, H., Grimstvedt, A., Vevelstad, S.J., Einbu, A., Vernstad, K., Svendsen, H.F., & Zahlsen, K. (2012, September 19). Understanding 2-Ethanolamine Degradation in Postcombustion CO_2 Capture. *Ind. Eng. Chem. Res., 51*. Retrieved from http://dx.doi.org/10.1021/ie300718a

Daptardar, S.D., Mahajani, V.V., Chopra, S.J., Sen, P.K., & Sridhar, S. (1994). On degradation of chemical solvents for bulk removal of CO_2. *Gas. Sep. Purif., 8*. Retrieved from http://dx.doi.org/10.1016/0950-4214(94)80018-9

Davis, J.D. (2009). *Thermal Degradation of Aqueous Amines Used for Carbon Dioxide Capture* (Ph.D Dissertation). The University of Texas at Austin, Austin, Texas, USA. Retrieved from http://repositories.lib.utexas.edu

Dawodu, O.F., & Meisen, A. (1996, December). Degradation of Alkanolamine Blends by Carbon Dioxide. *Can. J. Chem. Engr., 72*. Retrieved from http://dx.doi.org/10.1002/cjce.5450740620

Derks, P.W. (2006). *Carbon Dioxide Absorption in Piperazine-Activated N-methyldiethanolamine* (Ph.D Dissertation). Universiteit Twente, Enschede, The Netherlands. Retrieved from http://doc.utwente.nl

Dugas, R.E. (2009). *Carbon Dioxide Absorption, Desorption, and Diffusion in Aqueous Piperazine and Monoethanolamine* (Ph.D Dissertation). The University of Texas at Austin, Austin, Texas, USA. Retrieved from http://repositories.lib.utexas.edu

Dutchover, D. (2005). International Patent Publication No. WO 2005/069965 A3. Geneva, Switzerland: World Intellectual Property Organization. Retrieved from http://worldwide.espacenet.com

Eide-Hagumo, I. (2011). *Environmental impacts and aspects of absorbents used for CO_2 Capture* (Ph.D Dissertation). Norges teknisk-naturvitenskapelige universitet, Trondheim, Norway.

Erga, O., Juliussen, O., & Lidal, H. (1995). Carbon Dioxide Recovery by Means of Aqueous Amines. *Energy Convers. Mgmt., 36.* Retrieved from http://dx.doi.org/10.1016/0196-8904(95)00027-B

Fine, N.A, & Rochelle, G.T. (2013). Thermal Decomposition of N-nitrosopiperazine *Energy Procedia., 37.* Retrieved from http://dx.doi.org/10.1016/j.egypro.2013.06.043

Fine, N.A., Nielsen, P.T., & Rochelle, G.T. (2014, April 14). Decomposition of Nitrosamines in CO_2 Capture by Aqueous Piperazine or Monoethanolamine. *Environ. Sci. Technol., 48.* Retrieved from http://dx.doi.org/10.1021/es404949v

Fisher, K.S., Searcy, K., Rochelle, G.T., Ziaii, S., & Schubert, C. *Advanced Amine Solvent Formulations and Process Integration for Near-Term CO_2 Capture Success*. Retrieved from http://www.trimeric.com

Fogler, H.S, & Gürmen, M.N. (2008). *Elements of Chemical Reaction Engineering Website – Summary Notes to Accompany Chapter 5, Collection and Analysis of Rate Data*. Retrieved from http://www.umich.edu/~elements/course/lectures/five/

Fouad, W.A., Berrouk, A.S., & Peters, C.J. (2011, November 7). Mixing MDEA, TEA shows benefit for gas-sweetening operations. *Oil Gas J.,* 112-118. Retrieved from http://www.lexisnexis.com

Fountain, H. (2014, October 2). First Carbon Capture Plant Opens in Canada. *The New York Times*. Retrieved from http://www.nytimes.com

Frailie, P.T. & Rochelle, G.R. (2011, June 16). *Modeling Energy Performance of Aqueous MDEA/PZ for CO_2 Capture*. Presented at the 6th Trondheim CCS Conference, Trondheim, Norway.

Frailie, P.T. (2014). *Modeling of Carbon Dioxide Absorption/Stripping by Aqueous Methyldiethanolamine/Piperazine* (Ph.D Dissertation). The University of Texas at Austin, Austin, Texas, USA. Retrieved from http://repositories.lib.utexas.edu

Frazier, H.D., & Kohl, A.L. (1950, November). Selective Absorption of Hydrogen Sulfide from Gas Streams. *Ind. Eng. Chem., 42.* Retrieved from http://dx.doi.org/10.1021/ie50491a032

Freeman, S.A. (2011). *Thermal Degradation and Oxidation of Aqueous Piperazine for Carbon Dioxide Capture* (Ph.D Dissertation). The University of Texas at Austin, Austin, Texas, USA. Retrieved from http://repositories.lib.utexas.edu

Global CCS Institute (2014, October 7). *Status of CCS Project Database*. Retrieved from http://www.globalccsinstitute.com/projects/large-scale-ccs-projects

Goldman, M.J., Fine, N.A., & Rochelle, G.T. (2013, February 25). Kinetics of N-Nitrosopiperazine Formation from Nitrite and Piperazine in CO_2 Capture. *Environ. Sci. Technol., 47*. Retrieved from http://dx.doi.org/10.1021/es304640f

Gouedard, C., Picq, D., Launay, F., & Carrette, P-L. (17 July 2012). Amine degradation in CO_2 capture. I. A review. *Int. J. Greenhouse Gas Control, 10*. Retrieved from http://dx.doi.org/10.1016/j.ijggc.2012.06.015

Grossmann, C., & Asprion, N. (2004, August 26). International Patent Publication No. WO 2004/071624 A1. Geneva, Switzerland: World Intellectual Property Organization. Retrieved from http://worldwide.espacenet.com

Hamborg, E.S., & Versteeg, G.F. (2009 February). Dissociation constants and thermodynamic properties of alkanolamines. *Energy Procedia, 1*. Retrieved from http://dx.doi.org/10.1016/j.egypro.2009.01.159

Hatchell, D., Namjoshi, O., Fischer, K., & Rochelle, G.T. (2014). Thermal Degradation of Linear Amines for CO_2 Capture. *Energy Procedia, 63*. Retrieved from http://dx.doi.org/10.1016/j.egypro.2014.11.165

Haynes, W.M. (2014). *CRC Handbook of Chemistry and Physics* (95th Edition). Boca Raton, FL, USA: CRC Press.

Herzog, H, & Golumb, D. (2004). *Carbon Capture and Storage from Fossil Use*. Encyclopedia of Energy. C.J. Cutler (Ed.). Amsterdam, The Netherlands: Elsevier. Retrieved from https://sequestration.mit.edu/pdf/enclyclopedia_of_energy_PROOF.pdf

Hsu, C.S. & Kim, C.J. (1985, December). Diethanolamine (DEA) Degradation under Gas-Treating Conditions. *Ind. Eng. Chem. Prod. Res. Dev., 24*. Retrieved from http://dx.doi.org/ 10.1021/i300020a025

Huang, Q., Bhatnagar, S., Remias, J.E., Selegue, J.P., & Liu, K. (2013, October 4). Thermal degradation of amino acid salts in CO_2 capture. *Int. J. Greenhouse Gas Control, 19*. Retrieved from http://dx.doi.org/10.1016/j.ijggc.2013.09.003

Inderwildi, O, & King, D. (2009, March 5). Quo Vadis Biofuels? *Energy Environ. Sci., 2*. Retrieved from http://dx.doi.org/10.1039/B822951C

International Energy Agency (IEA). (2010, November 15). *World Energy Outlook 2010: Executive Summary*. Retrieved from http://www.worldenergyoutlook.org/media/weowebsite/2010/WEO2010_es_english.pdf

International Energy Agency Environmental Projects Ltd. (IEAGHG). *Evaluation of Reclaimer Sludge Disposal from Post-Combustion CO$_2$ Capture.* Retrieved from http://ieaghg.org/exco_docs/2014-02.pdf

Just, P., Ouimet, M.A., & Hakka, L.E. (2010, July 14). International Patent Publication No. WO 2011/009195 A1. Geneva, Switzerland: World Intellectual Property Organization. Retrieved from http://worldwide.espacenet.com

Keitz, B.K., Bouffard, J., Bertrand, G., & Grubbs, R.H. Protonolysis of a Ruthenium-Carbene Bond and Applications in Olefin Metathesis. *J. Am. Chem. Soc., 133.* Retrieved from http://dx.doi.org/10.1021/ja203070r

Kennard, M.L., & Meisen, A. (1985, May). Mechanisms and Kinetics of Diethanolamine Degradation. *Ind. Eng. Chem. Fundamen., 24.* Retrieved from http://dx.doi.org/10.1021/i100018a002

Khalili, F., Henni, A., & East, A. (2009, July 15). pKa Values of Some Piperazines at (298, 303, 313, and 323) K. *J. Chem. Engr. Data, 54.* Retrieved from http://dx.doi.org/10.1021/je900005c

Kim, C.J., & Sartori, G. (1984, March). Kinetics and Mechanism of Diethanolamine Degradation in Aqueous Solutions Containing Carbon Dioxide. *Int. J. Chem. Kinet., 16.* Retrieved from http://dx.doi.org/10.1002/kin.550161008

Kim, C.J. (1988, January). Degradation of Alkanolamines in Gas-Treating Solutions: Kinetics of Di-2-propanolamine Degradation in Aqueous Solutions Containing Carbon Dioxide. *Ind. Eng. Chem. Res., 27.* Retrieved from http://dx.doi.org/10.1021/ie00073a001

Kim, I., Grimstvedt, A., & da Silva, E.F. (2011). Thermodynamics of protonation of alkanolamines in aqueous solutions. *Energy Procedia, 4.* Retrieved from http://dx.doi.org/10.1021/je9000069

Kohl, A.L, & Riesenfeld, F. (1960). *Gas Purification.* New York, USA: McGraw-Hill Book Company, Inc.

Knudsen, J.N., Jensen, J.N., Vilhelmsen, P-J., Biede, O. (2007 September). First year operation experience with a 1 t/h CO2 absorption pilot plant at Esbjerg coal-fired power plant. *Proceedings of the European Congress of Chemical Engineering.* Retrieved from http://www.nt.ntnu.no/users/skoge/prost/proceedings/ecce6_sep07/upload/3356

Krase, N.W., & Gaddy, V.L. (1922, July). Synthesis of Urea from Ammonia and Carbon Dioxide. *J. Ind. Eng. Chem., 14.* Retrieved from http://dx.doi.org/10.1021/ie50151a009

Lagas, J.A. (2000). Survey of H$_2$S and SO$_2$ Removal Processes. In P.N.L. Lens & L. Hulshoff (Eds.), *Environmental Technologies to Treat Sulfur Pollution:*

Principles and Engineering (237-264). London, United Kingdom: IWA Publishing.

Lazo, A. (2014, September 28). How Cap-and-Trade Is Working in California. *The Wall Street Journal.* Retrieved from http://online.wsj.com

Lepaumier, H., Picq, D., & Carrette, P-L. (2009, October 21). New Amines for CO_2 Capture. I. Mechanisms of Amine Degradation in the Presence of CO_2. *Ind. Eng. Chem. Res.*, 48. Retrieved from http://dx.doi.org/10.1021/ie900472x

Lepaumier, H., Martin, S., Picq, D., Delfort, B., & Carrette, P-L. (2010, April 12). New Amines for CO_2 Capture. III. Effect of Alkyl Chain Length between Amine Functions on Polyamines Degradation. *Ind. Eng. Chem. Res.*, 49. Retrieved from http://dx.doi.org/10.1021/ie902006a

Lepaumier, H., Grimstvedt, A., Vernstad, K., Zahlsen, K., Svendsen, H.F. (2011, August 1). Degradation of MMEA at absorber and stripper conditions. *Chem. Eng. Sci.*, *66*. Retrieved from http://dx.doi.org/10.1016/j.ces.2011.04.007

Li, J.J. (2006). *Name Reactions: A Collection of Detailed Reaction Mechanisms.* Berling, Germany: Springer-Verlag GmbH.

Li, L. (2014, October 3). *Solvent Screening at UT-Austin* [GHGT-12 Handout]. The University of Texas at Austin, Austin, TX, USA.

Liu, H., Namjoshi, O., & Rochelle, G.T. (2014). Oxidative Degradation of Amine Solvents for CO_2 Capture. *Energy Procedia, 63*. Retrieved from http://dx.doi.org/10.1016/j.egypro.2014.11.164

Lichtfers, U., Asprion, N., Claessen, M., Umino, H., & Tanaka, K. (2007, June 21). International Patent Publication No. WO 2007/068695 A1. Geneva, Switzerland: World Intellectual Property Organization. Retrieved from http://worldwide.espacenet.com

Lindberg, V. (2000, July 1). *Uncertainties and Error Propagation.* Retrieved from http://people.rit.edu/vwlsps/

Loudon, G.M. (2002). *Organic Chemistry* (Fourth Edition). New York, NY, USA: Oxford University Press.

Mathews, A.P (1916). *Physiological Chemistry: A Text-Book and Manual for Students* (Second Edition). New York, NY, USA: William Wood and Company. Retrieved from http://books.google.com

Mokhatab, S., Poe, W.A., & Speight, J.E. (2006). *Handbook of Natural Gas Transmission and Processing.* Burlington, MA, USA: Gulf Professional Publishing

Mokhatab, S., & Poe, W.A. (2012). *Handbook of Natural Gas Transmission and Processing* (Second Edition). Waltham, MA, USA: Gulf Professional Publishing

Moser, P., Schmidt, S., Sieder, G., Garcia, H., Stoffregen, T. (2011, May 31). Performance of MEA in a long-term test at the post-combustion capture plant in Niederaussem. *Int. J. Greenhouse Gas Control, 5.* Retrieved from http://dx.doi.org/10.1016/j.ijggc.2011.05.011

Muhammad, A., Abdul Mutalib, M.I., Murugesan T., & Shafeeq A. (2009, May 11). Thermophysical Properties of Aqueous Piperazine and Aqueous (N-Methyldiethanolamine + Piperazine) Solutions at Temperatures (298.15 to 338.15) K. *J. Chem. Eng. Data, 54.* Retrieved from http://dx.doi.org/10.1021/je9000069

Namjoshi, O., Li L., Du Y., & Rochelle, G.T. (2013). Thermal Degradation of Piperazine Blends with Diamines. *Energy Procedia, 37.* Retrieved from http://dx.doi.org/10.1016/j.egypro.2013.06.071

Namjoshi, O., Du Y., Closmann F., Hatchell D., Liu H., & Rochelle, G.T. (2014, October 9). Thermal *degradation of piperazine blends with tertiary amines and hindered amines for CO_2 capture.* Presented at the 12th International Conference on Greenhouse Gas Control Technologies (GHGT), Austin, TX, USA.

Nexant Inc (2009, September). *Survey and Down Selection of Acid Gas Removal Systems for the Thermochemical Conversion of Biomass to Ethanol with a Detailed Analysis of an MDEA System.* National Renewable Energy Laboratory Subcontract Report NREL/SR-5 100-50482. Retrieved from http://www.nrel.gov/docs/fy11osti/50482.pdf

Nielsen, P.T. (2013, September 18). *Piperazine and Nitrosamine Degradation in Pilot Plants.* Presented at the 2nd Post Combustion Capture Conference, Bergen, Norway.

Nguyen, T. (2013). *Amine Volatility in CO_2 Capture* (PhD Dissertation). Retrieved from http://repositories.lib.utexas.edu

Nguyen, T., Hilliard, M.D., & Rochelle, G.T. (2010 September). Amine volatility in CO_2 capture. *Int. J. Greenhouse Gas Control, 5.* Retrieved from http://dx.doi.org/10.1016/j.ijggc.2010.06.003

NRG Energy. (2014, July 15). *World's Largest Post-Combustion Carbon Capture-Enhanced Oil Recovery Project to be built by NRG Energy and JX Nippon Oil & Gas Exploration* [Press Release]. Retrieved from http://investors.nrg.com

Perrin, D.D. (1964). The effect of temperature on pK values of organic bases. *Aus. J. Chem., 17.* Retrieved from http://dx.doi.org/10.1071/CH9640484

Purich, D.L., & Allison, R.D. (2000). *Handbook of Biochemical Kinetics.* San Diego, CA, USA: Academic Press.

Rayer, A.V., Sumon, K.Z., Jaffari, L., & Henni, A. Dissociation Constants (pKa) of Tertiary and Cyclic Amines: Structural and Temperature Dependences. *J. Chem. Eng. Data, 59*. Retrieved from http://dx.doi.org/10.1021/je500680q

Rennie, S. (2006). Corrosion and Materials Selection for Amine Service. *Materials Forum, 30,* 126-120. Retrieved from http://www.materialsaustralia.com.au/lib/pdf/Mats.%20Forum%20page%20126_130.pdf

Rochelle, G.T., Bishnoi, S., Chi, S., Dang, H., & Santos, J. (2001, January 17). *Research Needs for CO_2 Capture from Flue Gas by Aqueous Absorption/Stripping*. Final report for U.S. Department of Energy P.O. No.DE-AF26-9 9FT01029.

Rochelle, G.T. (2009, September 25). Amine Scrubbing for CO_2 Capture. *Science, 325*. Retrieved from http://dx.doi.org/ 10.1126/science.1176731

Rochelle, G.T. (2010, January 31). *CO2 Capture by Aqueous Absorption: Summary of 4th Quarterly Progress Reports 2009*. Retrieved from http://www.che.utexas.edu/rochelle_group/Pubs/4th_quarterly_report_2009.pdf

Rochelle, G.T., & Hilliard, M.D. (2011a, May 10). U.S. Patent No. 7,938,887 B2. Washington, DC, USA: U.S. Patent and Trademark Office. Retrieved from http://worldwide.espacenet.com

Rochelle, G.T., Chen, E., Freeman, S.A., Van Wagener, D., Xu, Q., & Voice, A.K. (2011b, July 15). Aqueous piperazine as the new standard for CO_2 capture technology. *Chem. Eng. J., 171*. Retrieved from http://dx/doi.org/ 10.1016/j.cej.2011.02.011

Rochelle, G.T. (2012, March 26). *Energy for CO_2 capture with thermal regeneration: Why amine scrubbing is hard to beat*. Presented at the 243rd ACS National Meeting & Exposition, San Diego, California, USA.

Rochelle, G.T., Ashouripashaki, M., Voice, A.K., Namjoshi, O., & Fulk, S. (2013, July 18). International Patent Publication No. WO 2013/106831 A1. Geneva, Switzerland: World Intellectual Property Organization. Retrieved from http://worldwide.espacenet.com

Rochelle, G.T., Du, Y., & Namjoshi, O. (2014 June). U.S. Provisional Patent Application 62/006,627. Washington, DC, USA: U.S. Patent and Trademark Office.

Sartori, G., & Savage, D.W. (1983, May). Sterically Hindered Amines for CO_2 Removal from Gases. *Ind. Eng. Chem. Fundamen., 22*. Retrieved from http://dx.doi.org/ 10.1021/i100010a016

Saskpower. (2015, February 11). *CCS Performance Data Exceeding Expectations* [Press Release]. Retrieved from http://saskpowerccs.com/newsandmedia/

Schubert, C.N., Forte, P., & Dean, J.W. (2000, 9 November). International Patent Publication No. WO 00/66249. Geneva, Switzerland: World Intellectual Property Organization. Retrieved from http://worldwide.espacenet.com

Sexton, A.J. (2008). *Amine Oxidation in CO$_2$ Capture Processes* (Ph.D Dissertation). The University of Texas at Austin, Austin, Texas, USA. Retrieved from http://repositories.lib.utexas.edu

Shih, I-H., & Been, M.D. (13 February 2001). Involvement of a cytosine side chain in proton transfer in the rate-determining step of ribozyme self-cleavage. *PNAS., 98.* Retrieved from http://dx.doi.org/10.1073/pnas.98.4.1489

Simond, M.R., Ballerat-Busserolles, K., Coulier, Y., Rodier, L., & Coxam, J.Y. (2012, January 11). Dissociation Constants of Protonated Amines in Water at Temperatures from 293.15 K to 343.15 K. *J. Solution Chem., 41.* Retrieved from http://dx.doi.org/10.1007/s10953-011-9790-3

Song, C., & Ma, X. (2010). Desulfurization Technologies. In K. Liu, C. Song, and V. Subramani (Eds.), *Hydrogen and Syngas Production and Purification Technologies* (211-310). Hoboken, NJ, USA: Wiley.

Speight, J.G. (2014). *Oil and Gas Corrosion Prevention: From Surface Facilities to Refineries.* Waltham, MA, USA: Gulf Professional Publishing.

Sreekanth, N., & Phani, K.L. (2014, July 30). Selective reduction of CO$_2$ to formate through bicarbonate reduction on metal electrodes: new insights gained from SG/TC mode of SECM. *Chem. Comm., 50.* Retrieved from http://dx.doi.org/10.1039/C4CC03099K

Stalder, C.J., Chao, S., & Wrighton, M.S. (1984, February). Electrochemical Reduction of Aqueous Bicarbonate to Formate with High Current Efficiency Near the Thermodynamic Potential at Chemically Derivatized Electrodes. *J. Am. Chem. Soc., 106.* Retrieved from http://dx.doi.org/10.1021/ja00324a046

Talley, I. (2009, February 23). EPA Set to Move Toward Carbon-Dioxide Regulation; Climate Czar Says Agency Will Determine That Greenhouse Gas Endangers Public, Propose New Emissions Rules. *The Wall Street Journal.* Retrieved from http://online.wsj.com

The Economist (2012, March 3). Energy Storage: Packing Some Power. *The Economist: Technology Quarterly.* Retrieved from http://www.economist.com

The MathWorks, Inc (MathWorks) (2013). Matlab Release R2013a. [Software].

Tomozaki, K-Y., Shimizu S., Onoda M., Fujioka Y. (2008, April 5). An Acid Dissociation Constant (pKa)-based Screening of Chemical Absorbents that Preferably Capture and Release Pressurized Carbon Dioxide for Greenhouse Gas Control. *Chem. Lett., 37.* Retrieved from http;

United States Energy Information Administration (EIA). (2013, April). *Updated Capital Cost Estimates for Utility Scale Electricity Generating Plants*. Retrieved from http://www.eia.gov/totalenergy/data/monthly/pdf/sec7_5.pdf

United States Energy Information Administration (EIA). (2015, February). *Monthly Energy Review 2015*. Retrieved from http://www.eia.gov/forecasts/capitalcost/pdf/updated_capcost.pdf

United States Environmental Protection Agency (EPA). (2014, July 2). *Sources of Greenhouse Gas Emissions*. Retrieved from http://www.epa.gov/climatechange/ghgemissions/sources/electricity.html

United States Environmental Protection Agency (EPA). (2015, January 7). *Fact Sheet: Clean Power Plan & Carbon Pollution Standards Key Dates*. Retrieved from http://www2.epa.gov/carbon-pollution-standards/fact-sheet-clean-power-plan-carbon-pollution-standards-key-dates

UOP LLC. (2009). UOP *Selexol™ Technology for Acid Gas Removal*. Retrieved from http://www.uop.com/tech-library/

Vaidya, P.D., & Kenig, E.Y. (2007, October 26). CO_2-Alkanolamine Reaction Kinetics: A Review of Recent Studies. *Chem. Eng. Technol.*, 30. Retrieved from http://dx.doi.org/10.1002/ceat.200700268

van Riel, N. (2014). *Euler's method in Excel to simulate simple differential equation models*. Retrieved from http://bmi.bmt.tue.nl/sysbio/

Van Wagener, D. (2011). *Stripper Modeling for CO_2 Removal Using Monoethanolamine and Piperazine Solvents* (Ph.D Dissertation). The University of Texas at Austin, Austin, Texas, USA. Retrieved from http://repositories.lib.utexas.edu

Voice, A.K. (2013a). *Amine Oxidation in Carbon Dioxide Capture by Aqueous Scrubbing* (Ph.D Dissertation). The University of Texas at Austin, Austin, Texas, USA.

Voice, A.K., Vevelstad, S.J., Chen, X., Nguyen, T., & Rochelle, G.T (2013b, March 5). Aqueous 3-(methylamino)propylamine for CO_2 capture. *Int. J. Greenhouse Gas Control, 15*. Retrieved from http://dx.doi.org/10.1016/j.ijggc.2013.01.045

Wagner, E.D, Osiol, J., Mitch, W.A., & Plewa, M.J. (2014, July 15). Comparative in vitro toxicity of nitrosamines and nitramines associated with amine-based carbon capture and storage.? *Environ. Sci. Tech.*, 48. Retrieved from http://dx.doi.org/10.1021/es5018009

White, A.M., & Sankey, B.M. (1979). U.S. Patent No. 4,168,226. Washington, DC, USA: U.S. Patent and Trademark Office. Retrieved from http://worldwide.espacenet.com

White, L. (2010). Evolution of Natural Gas Treatment with Membrane Systems. In B. Freeman & Y. Yampolskii (Eds.), *Membrane Gas Separation*. Available from http://www.wiley.com

Xu, Q. (2011). *Thermodynamics of CO_2 Loaded Aqueous Amines* (Ph.D Dissertation). The University of Texas at Austin, Austin, Texas, USA. Retrieved from http://repositories.lib.utexas.edu

Zhou, L., & Wen, X. (2011, December 1). International Patent Publication No. WO 2011/149660 A3. Geneva, Switzerland: World Intellectual Property Organization. Retrieved from http://worldwide.espacenet.com

Vita

Omkar Namjoshi graduated from Louisiana State University in Baton Rouge with a bachelor's degree in Chemical Engineering in May 2008. He took employment as an engineer with ExxonMobil Chemical in Baton Rouge following graduation. In January 2010, he was accepted to the PhD program in Chemical Engineering at The University of Texas at Austin. In July 2010, he went on an educational leave of absence from ExxonMobil to attend UT.

Permanent email address: omkar.namjoshi@utexas.edu

This dissertation was typed by the author.